Diagnostic and Prognostic Methodology for Monitoring Silk Fade in a Museum Environment

ADITI RAWAL

School of Computing and Mathematical Sciences
University of Greenwich
London, UK

A thesis submitted in partial fulfilment of the requirements of the University of Greenwich for the Degree of Doctor of Philosophy

November 2020

DECLARATION

I certify that the work contained in this thesis, or any part of it, has not been accepted in substance for any previous degree awarded to me or any other person, and is not concurrently being submitted for any other degree other than that of the Doctor of Philosophy which has been studied at the University of Greenwich, London, UK.

I also declare that the work contained in this thesis is the result of my own investigations, except where otherwise identified and acknowledged by references. I further declare that no aspects of the contents of this thesis are the outcome of any form of research misconduct.

I declare any personal, sensitive, or confidential information/data has been removed or participants have been anonymised. I further declare that where any questionnaires, survey answers or other qualitative responses of participants are recorded/included in the appendices, all personal information has been removed or anonymised. Where University forms (such as those from the Research Ethics Committee) have been included in appendices, all handwritten/scanned signatures have been removed.

Student Name: Aditi Rawal
Student Signature:

Date: 23rd November 2020

First Supervisor's Name: Professor Chris Bailey

First Supervisor's Signature:

Date: 23rd November 2020

Second Supervisor's Name: Dr. Stoyan Stoyanov
Second Supervisor's Signature:

Date: 23rd November 2020

ACKNOWLEDGEMENTS

My sincere gratitude goes first to my Professor Chris Bailey, who expertly guided me throughout my research with trust, enthusiasm, and unwavering support. Secondly, I would like to thank Dr. Stoyan Stoyanov for his patience, encouragement and mentoring throughout my research exploring the data modelling and mathematical discussions. Thirdly, I would like to also thank Visiting Professor, Peter Mason, for his early insights into the model development and for his continual encouragement and insightful discussions about condition-based modelling.

I would also like to express my deepest gratitude to Jurgen Huber, Senior Furniture Conservator at The Wallace Collection, for providing and permitting the use of sensor data and condition-data. This thesis would not have been possible without his expert opinions and valuable input for data gathering. I would also like to thank, The Wallace Collection, for providing access to the museum premises, silk artefacts, and to object archives throughout my research.

I am deeply thankful to the University of Greenwich for providing this opportunity and for funding this PhD research project. I would like to extend my gratitude to my Head of the Department, Professor Marc Cavazza, for his continual sponsorship and support. I am also indebted to many of my colleagues, especially Maria and Keeran for their invaluable support and encouragement throughout my years of study.

I would like to thank my family for their unfailing support and encouragement, without whom I would not have been able to reach this far. My husband, Pri, for his steadfast and unwavering love and support throughout, my daughters Nalini and Anya, for being my forever champions, always ready with encouragement and positivity, my sister Gayatri, for her advice, unshakeable support and providing a vital, and healthy competition, as we both undertook our PhD journeys together, and to my loving parents, Vikram and Manjula, to whom I owe everything, and to my in-laws, Kushal and Krishna, for their abiding love and support. Lastly, I would like to thank Milli, my four-legged friend, who sat at my feet for many long hours of research, with complete faith and loyalty.

ABSTRACT

Amongst the natural fibres found in museums, silk is reported to be the most vulnerable to damage, especially because of photodegradation of silk dyes. Deterioration of silk, on open display in museums, cannot be prevented, and this degradation often results in complete or partial loss of the silk fabric, requiring expensive interventive restorations. Research conducted, so far, in this field, has utilised methods that expose sensitive and sometimes rare fabric to a destructive process of analysis.

The aim of this research is to develop a non-invasive and non-destructive methodology that can predict the remaining useful life (RUL) of silk within the controlled museum environment. The benefit arising from this research is to improve the decision-making process, relating specifically to the conservation of silk, through the application of this novel methodology and prognostic model.

The prognostic and health management methodology developed in this work is applied and demonstrated on three chairs, originally made between 1768 to 1770, and re-upholstered with historically authentic silk in 1956. These chairs form part of the *Shrewsbury Set* displayed in the Great Gallery, at The Wallace Collection in London.

This research develops upon the widely researched Prognostic and Health Management (PHM) approach of engineering systems, used in aerospace and for structural monitoring of built environments, including heritage structures. To achieve this, a new mathematical fade model is postulated, to predict the fading, (colour degradation) of the silk that is a function of the exposure to its environmental conditions, such as, temperature, light levels, and relative humidity. This is the first time such a model has been presented that seeks to combine these factors. A relatively inexpensive portable instrument was used to take in situ measurements of silk samples, from the chairs displayed in the museum environment. The data driven diagnostic technique adopted the international colour standard, such as CIE XYZ, with Euclidian distance analysis to identify the colour condition of the silk. Statistical data-driven prognostic techniques have been utilised to model cumulative degradation of the colorimetric condition data of the silk and to predict its remaining useful life. The diagnostic and prognostic tools presented in this research are validated though numerical optimisation and through demonstration examples.

Based on this research, the brand-new colour condition of the silk was determined to be 376.12 and it was found that the brand-new silk would have a life of 55 years, based on the typically maintained museum environmental conditions. This new prognostic methodology for the silk colour condition in situ can be used to predict the cumulative degradation to silk fabric over different time horizons and under different museum environmental conditions. Sensitivity analysis scenarios are proposed that enable the prediction of the Remaining Useful Life (RUL) of the silk samples that are currently on display at the Wallace Collection.

This novel non-invasive and non-destructive, data driven PHM methodology for the conservation of silk encourages timely and optimal actions based on the diagnostic and prognostic outputs for cumulative fade of silk in situ. This methodology can be further extended to other silk samples, as well as to other textiles.

NOMENCLATURE

Abbreviations	Definition
α	Model Constant
A	Constant
AICCM	Australian Institute for the Conservation of Cultural Material
ATR - IR	Attenuated Total Reflectance Infrared Spectroscopy
ASHRAE	The American Society of Heating, Refrigerating and Air-Conditioning Engineers
b	Constant
B	Constant
BW	Blue Wool
C	Colour condition at time t
C_0	Colour of silk at time 0
$C^{(k)}$	Model predicted value silk colour with the chromometer, for silk exposed to environmental degradation condition $^{(k)}$ for model validation
CBM	Condition-based maintenance
CCD	Charge coupled device
CIE	Commission Internationale de l'Eclairage
CIPM	Certificate in Investment Performance Measurement
CM	Condition monitoring
D	Degradation
DET	Distance evaluation techniques
DMTA	Dynamic mechanical thermal analysis
Ea	Activation energy
ECCO	European Confederation of Conservator-Restorer' Organisation
EDET	Euclidean Distance Evaluation Technique
EDX	Energy dispersive X-ray
EDXRF	Energy dispersive X-ray fluorescence
FIR	Far infrared
FPA	Focal plane array
FT	Fourier transform
FTIR	Fourier transform infrared spectroscopy
GC-MS	Gas chromatography-Mass spectrometry
γ	Model Constant
GVA	Gross Value Added
HPLC	High-performance liquid chromatography
HPSEC	High performance size exclusion chromatography
HSE	Health and Safety Executive
HVAC	Heating, ventilation, and air conditioning
IEC	International Electrotechnical Commission
IR	Infrared
ISO	International Standards Association

$^{(k)}$	Super script of k is a model parameter to indicate association of parameter value with each sample environmental condition
k	The reaction rate represented with the Arrhenius constant k
l	Constant
m	Constant
$M^{(k)}$	The measured value for silk color with the chromometer, for silk exposed to environmental degradation condition $^{(k)}$ for model validation
MS	Mass spectrometry
MGC	Museums and Galleries Commission
n	Linearised expression of the temperature effect
NEDCC	Northeast document conservation centre
NIR	Near infrared
NPS	National Park Service
PAL	Positron Annihilation Lifetime
PHM	Prognostic Health Management
PoF	Physics of Failure
POL- ATR	Polarised attenuated total reflectance
RGB	Red, Green, Blue
RH	Relative humidity
RNA	Ribonucleic acid
RP	Reverse Phase
RP-HPLC	Reverse Phase High Pressure Liquid Chromatography
RUL	Remaining useful life
S1	Cumulative degradation values, product of linearised temp and RH
S2	Cumulative degradation values, product of visible light and RH
SDS - PAGE	Sodium dodecyl sulphate polyacrylamide gel electrophoresis
SEM	Scanning electron microscopy
SEM-EDX	Scanning electron microscopy with energy- dispersive X-ray spectroscopy
SHM	Structural Health Monitoring
T	Temperature in Kelvin
TBM	Time-based maintenance
TFSWT	Two-stage feature selection and weighting technique
Tr	Room Temperature
TWPI	Time-Weighted Preservation Index
UV	Ultraviolet
v	Visible light
WCCS	Wiltshire County Conservation Service
WDXRF	Wavelength dispersive X-ray fluorescence
X, Y, Z	Tristimulus values
XRF	X-ray fluorescence

CONTENTS

FIGURES

TABLES

1. INTRODUCTION

1.1. Overview

Silk is one of most widely found organic materials in museum collections and is amongst the most vulnerable of materials, prone to continual degradation in the museum environment. This is often despite museums maintaining and using extensively engineered and expensive environmental monitoring systems. The cost of restoring or repairing silk to its historically accurate state is high and interventive repairs may lead to a loss of the authentic intrinsic value of the silk fabric. Cost effective conservation is a growing challenge for many organisations in the museum sector. This research project seeks to develop a cost-effective Prognostic and Health Management (PHM) methodology for determining the Remaining Useful Life (RUL) of silk kept under museum display conditions. The developed methodology gathers the condition data of the silk and existing environmental museum sensor data, (with extrapolated assumptions made where data is not available), to advance a cost effective and predictive modelling capability. It seeks to aid the conservator's decision-making relating to silk conservation, enabling the prolongation of the RUL of samples under study. This introduction sets out the main aim and objectives, highlights current silk studies and the critical gaps in the field. The motivation for undertaking this research is also outlined, as well as the key contributions provided by this research. An outline of the thesis structure is also detailed.

1.1.1. Fading of silk textile

Museums have the challenging responsibility of safeguarding cultural and historical artefacts in their care. They own and host a variety of material categories in their collections, ranging from organic to inorganic materials. Silk is an organic material composed of cellulose and protein derived from the silkworm. Like all organic materials, silk is prone to deterioration due to natural aging. Silk-based artefacts form a significant proportion of a museum's collection. These artefacts are found in the form of upholstery, costumes, tapestry, silk paintings, etc. Studies have indicated silk deterioration can occur in many forms, but the most common indication of deterioration is photodegradation, otherwise more commonly known as 'fading' (Liu et al., 2019). Some of key reasons for the deterioration process are a combination of environmental factors and usage constraints, for example, exposure to temperature, light, water, oxygen, pollution, bacteria, fungi, chemicals, accidental spills, moisture, and pests (Smith and Thomson, 2017) (Muge and Suat, 2016). Museums and Galleries Scotland

(2020b) further state the main environmental factors that affect the fabric in museums are uncontrolled temperatures; uncontrolled relative humidity levels; light levels exposure and UV level exposure. A recent study, done on organic objects such as textile and wood in the Tutankhamun collection, housed at the Giza Museum in Egypt identified the agents of degradation for organic objects such as textile and wood to be abnormal environmental conditions such as light over exposure, pests, poor air quality, and physical forces (Kamal et al., 2018). The fading of silk is mainly because of the degradation of the molecules of dyes used in the silk, in varying degrees, which often leads to a brittleness of the silk fabric. Both natural and artificial light found in museums cause significant harm to textile artefacts (Liu et al., 2019). Light is seen to cause cumulative damage to silk causing it to lose flexibility, making it fragile and resulting in shredding. Further exposure can compound the fragmentation of the silk fibre, eventually rendered it to a powdered state. This gradual process of degradation is accompanied by discoloration, fading, or yellowing of the fabric, which is usually a useful indicator of the object's deterioration state (Smith and Thomson, 2017) (Vilaplana et al., 2014). The degradation of textiles is usually a combination of various factors and not in isolation (Smith and Thomson, 2017). Besides, light-induced damage, fluctuating humidity levels, and high temperature also affects the degradation of silk. Commonly used pigments in the dyes demonstrate increased light-induced change with increasing Relative Humidity (RH), (Saunders and Kirby, 2004). The extent of deterioration occurring in silk can also be dependent on factors such as the initial condition of the fabric, dye, pigment used, glues used to bind the fabric together, and display and storage conditions (Smith and Thomson, 2017). Previous studies in silk conservation have mainly concentrated on accelerated aging methods, which has its limitations, requiring samples to be subjected to extreme conditions, thus damaging the silk sample fabric used in the experimentation (Luxford et al. (2009). Further, there is limited study in this area to conclusively show a correlation in the properties between accelerated aged and conventionally aged samples (Vilapana et al., 2014) (Ahn et al., 2014). A detailed review of the current silk studies is provided in Chapter 2.

Historical collections of silk are most monitored and managed by conservators, through a process of visual inspection and by maintaining the display environment to established museum standards. These standards are maintained and regulated by deploying expensive heating, ventilation, and air conditioning (HVAC) systems and wireless sensors. These sensors provide the numerical data and are checked against the museum's documented standards defined according to the categorisation of the collections. These standards provide an acceptable range for the environmental conditions, within which the collection should be stored and displayed. However, there is active debate within the conservation science community about the effectiveness of applying these strict standards (Bennet 2019). It has been suggested that the conditions need to be determined less generally, but more specifically, according to the specific needs of the artefact (Sharif and Esmaeli, 2017). It has also been suggested that the local climate of the geographic region should also be taken into consideration. The standards provide generic guidance but are not informative about specific artefacts, their condition, or their geographical location recommendations (Kamal et. al., 2018). Boersma, et al. (2018), have criticised environmental standards for collections based on being a "one-size fits all" standards that are often unattainable or not based on evidence. Additionally, the high energy consumption costs of restricted and controlled environments are a major concern for the museums (Sharif-Askari and Abu-Hijleh, 2018). A detailed review of the current museum standards and their limitations is provided in Chapter 2.

The use of a Prognostic and Health Management (PHM) approach, as used in the electronics, aerospace, and manufacturing industry, can assist in determining the condition of silk at the present time and predict the future condition (Li et al., 2020) (Fink et al.,2020). PHM has been adopted in the maintenance and care of heritage buildings, where either a condition-based monitoring or structural health management approach has been used to determine the current "health" of the structure and a prognostic method used to forecast the structure's Remaining Useful Life (RUL). Statistical modelling and predictive algorithms have been utilised to interpret historical and current condition data, to facilitate meaningful decisions for taking preventative action and for gaining future insights for the future point of failure (Edwards, 2019).

A challenge for the PHM approach is in gathering adequate knowledge, in terms of historical data on the condition of the object that is being analysed. Most of the studies in silk predictive modelling use accelerated aging methods to extrapolate to normal conditions. These are not directly comparable to data relating to the natural aging of the silk in the ambient museum environmental conditions. The data and knowledge for current diagnostic and prognostic analysis is mainly based on accelerated aging techniques. There is a limited knowledgebase of studies relating to the natural aging of silk in regulated museum environmental conditions (Luxford et al., 2009) (Li et al., 2020). These studies highlight a need to undertake further research into the studying of the natural aging of silk.

This research represents the development of a novel Prognostic and Health Management (PHM), methodology to determine the impact of the museum's controlled environmental conditions on silk colour fade. This methodology is used to determine the rate of colour fade of the silk fabric upholstered on the chairs on display in the museum, and to predict the time until a predefined colour fade threshold is reached. This is achieved by studying the cumulative damage caused by environmental conditions over a period and by collecting and analysing environmental sensor data, representing light levels, relative humidity, and temperature. The novel empirical exponential degradation model postulated helps in correlating the sensor data to the primary colorimetric condition-data of silk.

This approach can aid museums by enabling the assessment of object-specific colour degradation in situ. The modelling predictions can be used for informed decision-making to prolong the RUL of silk. Thus, minimising costly reactive interventive restorations. The silk sample measured in situ, is part of the heritage Shrewsbury Set, housed and displayed at The Wallace Collection in London, UK. The developed methodology and novel degradation model can be further applied, practically, in the field of conservation to develop targeted condition-based methodologies for silk and by extension other artefacts.

1.2. Research Motivation

Museums have an indispensable position in heritage tourism. They provide a positive cultural experience for visitors, be they domestic or international, and add to the economic welfare of the communities that host them. According to Historic England, (2019), the heritage sector contributes £31 billion to the UK economy, and provides over 464,000 jobs. About 35% of UK citizens cite cultural heritage as the leading influencer for their holiday choices, and in 2018 £17 billion was spent on heritage related visits and trips. Libraries, Archives, Museums, and other cultural activities accounted for £2.5billion in gross value added (GVA) of the total heritage related revenue. Therefore, maintaining the cultural significance of the museum's artefacts is an important factor in the development and growth of tourism, be it local or international, which in turn attracts investment in local economies, increases employment, and helps regenerate local areas (Historic England, 2019). Museums are unique spaces for interdisciplinary research and educational innovation. Through extensive exhibits and educational programmes, they provide integration of science and discovery as well as a locus of community engagement (Bakker, F. T. *et al.* 2020).

Restorations are a form of interventive approach to the maintenance of artefacts and are commonly associated with significant cost. In the case of the 12 silk chairs that form the basis of this study, known as the Shrewsbury Set, the cost of replacing the existing silk fabric is estimated to be approximately £180,000. Therefore, in the case of this Collection specifically, (though equally applicable more generally), it is important when planning for a more cost-effective and less interventive approach to conservation, to study the impact of the museum's environmental conditions on the ongoing degradation of the silk that is being exhibited.

According to Luxford and Thickett (2011), identifying the critical factors facilitating deterioration, and studying the natural aging processes under real conditions and timescales is difficult. According to the literature reviewed on silk degradation (Ahn et al., 2014), most of the studies conducted so far have used accelerated ageing methods. These methods expose the historical fabric to extreme experimental conditions, which may not be able to extrapolate to the real environmental conditions that the fabric is exposed to in a museum (Luxford et al. 2009). The impact of the indoor environment that many organic artefacts are exposed to, needs to be evaluated (Dahlin, 1995). Further studies to understand the impact of the museum environment on the condition of the object in their ambient display conditions, using environmental sensor data is required (Valach et al., 2015) (Klein et al., 2017). Kozlowski (2018) has called for a more customised approach, taking into consideration the different environments for artefacts in storage, on display, as well as individual sensitivities to certain conditions to which the artefacts have been exposed to in their local environment. There remains an acute gap in the conservation literature of thoroughly documented reports on the effect of climate control on actual objects in museum. The emerging methodology linking collection analysis and numerical studies to better understand climate induced damage of specific objects has mainly focused on fine decorative art predominantly made from wood. Computer modelling can provide a quantitative assessment of museum climate-induced damage, based on visual observations and object-based data, offering a direct measure of hazard through the evaluation of climate parameters. Thus, enabling evidence-based decision-making (Kozlowski, 2018).

1.3. Aims and objectives of the Research

1.3.1. Aim

The aim of this research is to develop a prognostic and health management methodology that gathers environmental sensor data, including, light, temperature, relative humidity, and colourimetry data, together with a novel mathematical model, which is used to predict and minimise cumulative colour degradation of silk artefacts on display in a museum environment.

1.3.2 Objectives

The aim of the research project will be realised by addressing the following objectives:

1. Review and document state-of-the-art studies into conservation approaches used in museums, including current standards for managing textile collections. – Chapter 2
2. Methodology – Develop a methodology that correlates environment sensor data and colourimeter data to develop a diagnostic and prognostic model of colour degradation. – Chapter 3
3. Data Gathering – Working with The Wallace Collection, gather environmental sensor data and colourimeter primary data of the silk fabric. – Chapter 4
4. Results – Exhibit the usefulness of the developed model using sensitivity analysis demonstration scenarios to predict the remaining useful life of the silk in the museum environmental conditions. – Chapter 5
5. Museum Implementation – Document recommendations for implementing the methodology as part of a decision-making process for prolonging the life of the silk fabric. – Chapter 6
6. Document research findings in peer-review publications. Journal paper submitted for publication in the Journal Cultural Heritage, Elsevier, is currently in revision.

1.4. Contributions

The following are the key contributions of this research:

1. Reviewed and commented on 92 published articles for silk conservation approaches, techniques, and instrumentation, including identification of fundamental gaps for silk conservation. Also reviewed and commented upon the preventative conservation approach for museum collections and five leading museum standards, their recommendations, and limitations. - Chapter 2

2. Developing knowledge in the form of a prognostic and health management methodology that incorporates a mathematical model to determine the Remaining Useful Life (RUL) of silk samples in-situ. Chapter 3

3. Gathered and analysed environmental data from museum historical records. For example, archived records for care and restoration, hygrothermographs data, visual inspections data record and museum environmental sensor data. Non-invasive, non-destructive measurements of colour fade of silk samples in ambient museum conditions with a portable colorimeter used in situ to measure primary colorimetric data (Direct condition data). - Chapter 4

4. Validation of the developed data-driven exponential colour degradation model. The model can help capture the cumulative damage of the silk fabric fade in ambient conditions. Using optimisation, the error between the model predictions and the measured values for these three conditions is minimised. - Chapter 5

5. The derived exponential model can help determine the cumulative degradation of the colour of silk by performing sensitivity analysis. The study goes on to forecast the remaining life of the fabric as per the current environmental conditions, as well as hypothesised future conditions. The prognostics regarding the colour degradation can potentially help museums mitigate the risk of ongoing degradation. - Chapter 5 and Chapter 6

6. Submission of the findings of the research in a peer-reviewed journal paper. The journal paper is submitted for publication in the Journal Cultural Heritage, (Elsevier), and is currently in revision.

1.5. Thesis Structure

The thesis is structured in the following chapters:

Chapter 2 reviews conservation approaches within the museum sector. The museum standards for preventative conservation are detailed along with the limitations and issues found. An overview of the textile conservation is documented, followed by a detailed discussion of current studies in silk degradation and fade. The causal factors and indicators of fade are also discussed, relevant instruments reviewed, and current state of the art techniques and approaches to measure silk deterioration are detailed, followed by their issues and limitations.

Chapter 3 details the methodology and standards that have informed the development the diagnostic and prognostic health management methodology to aiding decision-making within The Wallace Collection. The detailed mathematical model correlating the environmental factors to the silk condition with the help of a linearised Arrhenius and Euclidean distance model are discussed. The data-driven cumulative colour degradation model is detailed and discussed.

Chapter 4 describes the data collected from the Wallace Collection. It includes the raw environmental sensor data, environmental data from museum's archived historical records such as hygrothermographs data, and visual inspection data records. It also details archived records for care and restoration of the artefact, as well as the process adopted for measuring colorimetric data. The refined indirect and direct condition data is detailed and discussed.

Chapter 5 discusses the application of the data driven prognostic model and the results. It illustrates the examples set up to demonstrate the sensitivity of the silk to the environment. The different scenarios developed to determine the impact of ambient conditions over time are developed and discussed. The predictions of fade for future scenarios and sensitivity analysis are detailed. Also included are the set of assumptions and limitations of the research undertaken.

Chapter 6 discusses the steps involved in the Prognostic and Health Management (PHM) methodology, both as specifically applied in the context of the Wallace Collection, as well as generalised for adoption more broadly within the conservation community. Further recommendations and future work are also detailed and discussed.

Chapter 7 concludes the thesis with the summary of the research work undertaken for The Wallace Collection.

2. LITERATURE REVIEW

This chapter discusses conservation approaches for museum collections, including museum controlled environmental standards; and then goes on to review current silk conservation studies. The current state of art techniques and methods to measure and monitor silk fade in museum environments are also discussed.

2.1. Introduction

Museums have a significant responsibility for managing various historical, as well as near historical, artefacts within their collections for current, as well as future generations. Museums are culturally and economically significant to the UK, as they attract tourism, which is a significant driver for economic growth (Heritage, 2019). Museums contribute to education and learning as platforms for interdisciplinary research focussed on the past, present and the future (Bakker et al, 2020). Socially, museums are an expression of community and civic pride (Keene, 2002). The artefacts and collections that museums are responsible for are in a process of continual change, caused by numerous factors ranging from natural ageing processes to the damage caused by display, storage, handling, and transportation.

Conservation is the method of managing these artefacts and collections by adopting various techniques to sustain their intrinsic value, integrity, and aesthetics for the present as well as future generations (Depcinski, 2014). The Burra Charter (ICOMOS, 2013), which focuses on sites and built heritage, refers to conservation as, looking after a place to retain its cultural significance. Although the Burra Charter focuses on monuments and sites, it is applicable to artefacts and objects as well. The updated charter goes on to clarify that cultural significance can seem to apply to objects or places that offer aesthetic, historic, scientific, social, or spiritual value for the past, present or future generations. According to De la Torre (2013), conservation encompasses any action that is designed to maintain the significance of a heritage object or place. It is a process that is initiated the moment an object or a place is attributed to be significant, in terms of its cultural values are singled out for protection. Conservation can be achieved through an understanding of the significance of the artefact and taking action to ensure it retains its near authentic state. Timely action must be taken to counter the harmful effects of natural degradation, or to minimise the chance of damage. This must be proportionate to the severity and likelihood of the known consequences otherwise the impact would be a loss of historical authenticity for generations to come (Drury and McPherson, 2008). Conservation is the process that involves taking direct action on an artefact or a collection to try to stabilise its condition and attempt to mitigate further deterioration or damage caused. Avrami, E et al, (2000), describe conservation as a process that is recreating consistently its product, for example, its cultural heritage, by accumulating the marks of the passing generations on it and trying to preserve authenticity. Restorative, preventative, or corrective efforts are undertaken to reinstate the artefact, as near as possible to the original (Atakul, Thaheem and De Marco, 2015).

The International Council of Museums Committee for Conservation (ICOMCC, 2008) defines conservation as, "*all the measures and actions aimed at safeguarding tangible cultural heritage, while ensuring its accessibility to present and future generations. Conservation embraces preventative conservation, remedial conservation, and restoration. All measures and actions should respect the significance and the physical priorities of the cultural heritage item*."

ICOM-CC (2008) further adopted and defined the following types of conservation of tangible cultural heritage:

- Preventative Conservation – all efforts to try to avoid and minimise future loss or degradation. This type of conservation does not alter the appearance but aims to modify the conditions the artefacts are exposed to.
- Remedial Conservation – all efforts aimed at stopping current detrimental procedures or strengthening the constitution. These efforts would be carried out only when the condition is very fragile or is decaying at a very fast rate and could be lost in a relatively short time. These measures occasionally alter the appearance of the artefact or the collection of artefacts.
- Restoration – all efforts are targeted at a single item to stabilise it. The artefact may have had substantial loss or damage. These efforts are aimed at trying to recreate, as close as is possible to the original aesthetics of the impacted artefact.

However, these measures do not maintain a strict separation, as there are times when these conservation activities serve more than one aim and can overlap; for example, removal of varnish can be both a remedial action as well as restoration. Figure 2-1 provides an overview of areas of conservation.

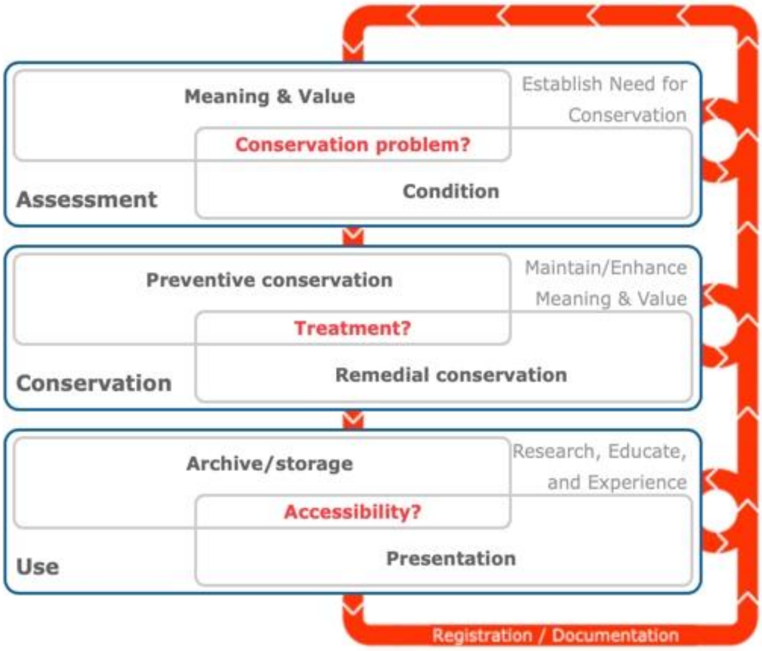

Figure 2-1: Conservation Overview

(Source ICOM-CC, 2008)

The European Network for Conservation Education (2002) has documented the following conservation approaches to preserve collections:

- Diagnostic Approach – these are mainly techniques that identify, detect and assess any decay in the condition of the artefact(s) and then set-in motion conservation plans for treatment. These also include the evaluation of the causal agents that have caused the decay and any remedial plans for the artefact.

- Preventative Conservation – the aim of preventative conservation is to try and reduce any anticipated damage to the artefact(s) and to minimise the decay or deterioration caused naturally or through any other casual agents in the environment by optimising conditions for preservation. It also encompasses the production of replicas to preserve the original artefact. Preventative conservation has a wide remit which involves enabling the appropriate handling, storage and display conditions, usage as well as any transportation.

- Restoration – The restoration process involves taking direct action to reduce the damage caused by causal agents and try to repair the artefact, returning it as closely as possible, to the original. Extra care is taken to maintain authenticity as far as is possible. The objective is to recondition the historical, artistic, and material properties to the original artefact to maintain a near-authentic experience.

- Documentation – The aim of this process is to maintain a record of the method followed to restore or repair the artefact, along with the reasoning for carrying out the procedure. The documentation process also archives the diagnostics, handlings, and any necessities for specific storage and display conditions. These documents can be both pictorials as well as written records.

2.1.1. Preventative Conservation in Museums

Meister, (2019) defines, "*preventative conservation as a holistic methodology that includes holistic policies, plans, procedures to mitigate deterioration and damage to objects*." The scope of the definition also includes any documentation and digital data management of the data that is produced in the process of managing the collections. Preventative conservation is the strategy used to provision the appropriate environmental safeguarding against known causes of deterioration of museum specimens and works of art (ICOM,1991 cited in Dahlin, 1995, p.57). According to Ruga et al. (2019), preventive conservation plays a crucial role in preserving cultural heritage, as it permits the continuous control of the state of the artwork. Preventative conservation, according to Caple (2012), learns and utilises the concepts and inventions from other industry practices and applies it to museum artefacts and its collections, to help preserve them. The main aim of preventative conservation is to retain the authenticity and have a minimal intervention approach (Forster and Kayan, 2009). Caple (2012) has collated a series of research studies and goes on to mention how preventative conservation in the museum sector has taken on ideas from other disciplines. For example, the method of oxygen-free storage of artefacts, is taken from the food preservation industry. The storage of artefacts in bubble wrap has been taken from the packaging industry; heating, ventilation and air conditioning (HVAC) from the building industry, and environmental sensors from the electronics industry. However, the cost of implementing these approaches has to be considered, as the museum and the heritage sector have restricted financial reserves.

Schlanger et al. (2015), state that current issues in museum collection conservation relate to data-driven problems, going on to state that modern conservation is a data management crisis. Museum's collections are creating data in greater detail and greater volume, and there are very few effective ways of sharing, managing, analysing, or archiving generated data. Environmental conditions play a significant role in controlling the deterioration processes to which materials are susceptible to degradation (Bradley, 1994). Both indoor and outdoor environments have an impact on the collections. The aim of environmental management is to minimise the rate of degradation of an artefact, whilst not unintentionally compromising access to them (Ashley-Smith, 2018). Museum conservators are particularly interested in the impact of these environmental conditions on organic objects, predominantly because organic materials are among the most vulnerable to deterioration (Dahlin, 1995).

According to The Benchmark in Collection Care for Museums, Archives and Libraries (2006a), a self-assessment checklist, "*Preventive conservation consists of indirect action to retard deterioration and prevent damage by creating conditions optimal for the preservation of cultural heritage as far as is compatible with its social use. Preventive conservation also encompasses correct handling, transport, use, storage, and display. It may also involve the issue of the production of facsimiles for the purpose of preserving the original.*" (European Confederation of Conservator-Restorer' Organisation (ECCO) Professional Guidelines, 2002 cited in The Council for Museums, Libraries and Archives, 2002, factsheet 4)

In most of the cases, the decline in the condition of the artefact is inevitable. And as such the main aim of the conservator is to slow the rate of deterioration as much as possible. The aim of preventative conservation is to decrease the deterioration and decay to the artefacts by improving and refining the environment they are kept in (The Field Museum, 2020).

There are various well-established standards and guidelines for museums to manage their collections to the best of their ability. These benchmarks are available to museums to adopt as recommended standards or guidelines and it is exclusively up to the museums to adopt these guidelines.

2.1.2. Deterioration Factors in the Environment of Museum Collections

The following section provides an overview of the causal factors of decay in the objects within the museum environment. There are several factors that can cause decay and deterioration in museum collections. Understanding the impact of these plays a key role in determining the long-term conservation plan for the artefacts in the museum environment. The presence, of artefacts of cultural, social, and historical significance makes the museum environment very different from other built environments as museums carry the responsibility for the preservation of the artefacts under its stewardship (Sharif-Askari and Abu-Hijleh, 2018).

Based upon research undertaken by several prominent museums and research studies, internationally (CCI, 2017) (Smithsonian Postal Museum) (Kamal, et. al, 2018) (Dahlin, 1995), the following agents can cause deterioration in the museum collections:

- Light and UV light damage – Light damage occurs when there is excessive exposure of the objects to natural or artificial light.
- Incorrect humidity – Excessive humidity may cause damage; indeed, studies establish the potential for more damage to occur because of humidity then from temperature.
- Incorrect temperature – Very high or low temperatures can have a detrimental effect on artefacts, according to the material, especially so for organic materials such as silk. Temperature shifts of a large magnitude may also have an adverse effect on the artefacts and collections.
- Pollutants – These can be in the form of natural or synthetic liquids, gases, dust, etc that can accelerate the deterioration of the objects.
- Water damage – This can occur from natural incidents, accidents, mechanical failures of equipment. Rainwater and floods are the most common form of water damage.
- Pest infestation – These can cause significant damage to artefacts and can be found in the shape of insects, rodents, and microorganisms.
- Fire damage – Damage from fire can destroy the whole artefact(s) and is considered the most significant, hence it is given an extremely high priority.
- Neglect – This occurs when the artefacts are not provided appropriate conservation and care.
- Visitors – The presence of humans may alter the conditions of temperature and humidity in the air and therefore impact the objects inadvertently.

2.1.3. Standards and Guidelines in Museum Care

Standards and guidelines provide best practise to museum professionals for various categories such as collections management, object acquisition, documentation of collections, security, personnel management, and environmental management (International Council of Museums, 2020)

According to Wiltshire County Conservation Service's signposts to collection care (WCCS 2006a), the various areas of preventative conservation are intertwined, and if constructive actions are taken in one area, it has a knock-on effect on other areas. The main areas for preventative conservation guidelines are listed as below:

- Buildings
- Storage
- Housekeeping
- Handling of collection
- Objects on Display
- Environmental Monitoring and Control
    - Relative humidity (RH)
    - Temperature
    - Light (including ultra-violet)
    - Air Pollution
    - Pests
- Emergency Planning

Wiltshire County Council's (2006a) guidelines are based on the Museums and Galleries Commission's standards in the Museum Care of Archaeological Collections (1992) and BS5454:2000 recommendations for the exhibition and storage of archival documents. These recommendations state, that for textiles, paper, drawings, manuscripts and photographs, the illumination exposure should be set at 50 lux maximum and 75μ maximum for UV radiation. The temperature should be set at 18℃ and relative humidity (RH) at 50-60% for textiles. The allowance for fluctuations must not be more than 2℃ and 2% from the level fixed within the range. These guidelines by the WCCS are an updated version of the earlier standard provided by the Museums and Galleries Commission (1992), which detailed recommendations for museums to adopt to protect their collections. It states, that if collections were to be preserved, the museums had to reach the set attainable standards. The standard also defines the documentation process for recording details of the artefact's preservation, including citing different conservation approaches; establishing approaches for examining the material's condition; guidelines relating to the security of the museum building and details about the storage of artefacts. The Museums and Galleries Commission's (1992) Standards into the Museum Care of Archaeological Collections provides a series of standards pertaining to two broad categories, a) managing collections and, b) protecting collections. Under the protecting collections category, a specific standard 14 for Protection Against Damage Through Poor Internal Environmental Conditions is detailed in Table 2-1 and Table 2-2. These guidelines are recommendations for the museums to adopt, for their storage and display environments, and refer to median set points.

Material	Ambient Temperature	Ambient Relative Humidity	Decay Indicators
Metals (non-ferrous)	18°C (Min 10°C – Max 25°C)	50% (for part of mixed collection) 35% (for dedicated mixed collection)	- Tarnish on polished surfaces - Powdering
Metals (ferrous)	18°C (Min 10°C – Max 25°C)	50% (for part of mixed collection) 35% (for dedicated mixed collection)	- Fresh Corrosion - Weeping - Cracking
Organic Materials (Bones, wood, leather, cotton, wool, silk, etc)	18°C (Min 10°C – Max 25°C)	50% (for part of mixed collection)	- Mould & Fungus - Cracks - Warping - Flaking - Shredding
Inorganic Material (Pottery, Stone, glass, etc)	18°C (Min 10°C – Max 25°C)	50% (for part of mixed collection)	- Stone Efflorescence (Salts coming out) - Glass Weeping (Wet surface) - Crizzling- Fine cracks, glass becoming opaque - Powdering Fabric
Waterlogged or wet store materials	10°C Cooler and darker is better but always above freezing	Not applicable	- Shrinkage - Embrittlement o Drying out and breakdown of adhesives - Fading and bleaching

Table 2-1: MGC Standard for RH and Temperature in Display and Storage

(Source: Museums and Galleries Commission, 1992)

Materials	Maximum Illuminance	Maximum UV radiation
Paper (prints, watercolours, drawings, manuscripts, photographs)	50 lux	75μ W/Lumens
Textiles	50 lux	75μ W/Lumens
Dyes, and inks on any support materials	200 lux	75μ W/Lumens
Undyed organic materials (leather, horn, bone, ivory, wood)	200 lux	75μ W/Lumens
Inorganic materials (stone, metals, glass, ceramics, jewellery) enamels – all undyed)	300 lux	75μ W/Lumens
Waterlogged materials	Total Darkness	Not applicable

Table 2-2: MGC Standard for Illuminance and UV for archaeological materials
(Source: Museums and Galleries Commission 1992)

Environmental condition guidelines have used these RH and Temperature set points with strict fluctuation allowances. Sharif-Askari and Abu-Hijleh (2018) have highlighted the challenges presented by these prescribed standards recommending set points. Maintaining these standards, can result in high energy costs for the museum, depending on their local climatic conditions.

The Australian Institute for the Conservation of Cultural Material (2018) recommends set ranges for temperature and RH instead of median set-points, to improve heating, ventilation, and air conditioning (HVAC) energy efficiency (Sharif-Askari and Abu-Hijleh, 2018). Additionally, AICCM environmental guidelines for Australian Cultural Heritage collections (2018), support sustainable practices within the cultural heritage profession by promoting low energy technology to reduce environmental impact. AICCM recommends that RH should remain within set ranges of 45-55% for most of the time. They state that RH below 40% would adversely affect organic materials.

Table 2-4 compares the different international standards of acceptable ranges for temperature and relative humidity.

	T °C	T (24 h)	T Seasonal	RH %	RH (24 h)	RH Seasonal
AICCM 2014	15C–25C	± 4C	–	45–55%	± 5%	40–60%
UK standard 2012	18C–24C	± 4 °C		50%	± 10%	
ASHRAE AA 2011	15C–25C	± 2 °C	Up 5 °C 5 °C Down	50%	± 5%	No change
ASHRAE A 2011	15C–25C	± 2 °C	Up 5 °C Down 10 °C	50%	± 5%	Up 10% Down 10%
ASHRAE A 2011	15C–25C	± 2 °C	Up 5 °C Down 10 °C	50%	± 10%	No change
ASHRAE B 2011	15C–25C	± 5 °C	Up 10 °C (but not above 30 °C) Down as low as necessary to maintain RH control	50%	± 10%	Up 10% Down 10%
ASHRAE C 2011	Rarely over 30 °C, usually below 25 °C	–	–	Within range 25–75% RH Year round.	–	–
ASHRAE D 2011	–	–	–	Reliably below 75% RH	–	–
HCC (Hot Humid) 2002	22C–28C Daily	–	10% acceptable 20% dangerous 40% Destructive	55% – 70% Daily	–	Not to exceed 70% Not below 40%
HCC (Hot Dry) 2002	22C–28C Daily	–		40%–60% Daily	–	
HCC (Temperate) 2002	14C–24C Daily	–		45%–65% Daily	–	

Table 2-3: Museum's indoor environments by different standards

(Source: Sharif-Askari and Abu-Hijleh, 2018)

However, short term ($\leq 24\ hours$) fluctuations of $\pm 5\%$ from the outer limits of the RH ranges are acceptable. They state that temperature should remain within $15℃ - 25℃$ with an allowance for short-term fluctuations of no greater than 4℃, from the stated temperature range, for ≤ 24 hours duration.

This temporary allowance of some flexibility in the temperature and relative humidity dead bands, allows for an improvement in the resultant energy consumption and therefore the energy efficiency of the HVAC systems. 'Dead band' is a term defined as the range around a set target point. For example, to achieve environmental conditions of 50% RH ± 10, 50% RH is the target point and the deadband is up to 60% and down to 40%. Further energy efficiency can be achieved using the set range as the target, instead of the median point. This may require smaller and fewer climate corrections and may therefore consume less HVAC energy (Pagliarino, 2019). Table 2-4 differentiates the standards for illumination and UV limits for indoor museum environments, ranging from very sensitive to insensitive objects.

	Very Sensitive Objects		Sensitive		Insensitive	
	Lux lumen/ m^2	UV µwatt/ lumen	Lux lumen/ m^2	UV µwatt/ lumen	Lux lumen/ m^2	UV µwatt/ lumen
UK Standard 2012	50		200		300	
HCC 2002	50	30	200	75	300	200
ASHARE	50–80	0–75	200–250	0–75	Can be higher but not recommended	0–75
Havells Sylvania 2015	50		100		300	
IESNA Museum and Art Gallery Lighting 1996 p14	50	0	200	0	Depending on the exhibition	0

Table 2.4: Comparison of Illuminance and UV standards

(Source: Sharif-Askari and Abu-Hijleh, 2018)

The UK Standard 2012 recommends temperature range between minimum 18℃ to maximum 24℃, allowing ±4℃ change during the 24 hours. Relative humidity between an average of 50% with allowance of ±10% change during the 24 hours. The light levels for very sensitive materials such as textiles, water colours, drawings, prints, manuscripts, and ethnographic objects at 50 lux. Sensitive materials such as oil paintings undyed leather, horn, and lacquer at 200 lux. Insensitive material such as metal, stone, jewellery, ceramics, and glass at 300 lux (Sharif-Askari and Abu-Hijleh, 2018). For the very sensitive category, which includes silk, the illuminance levels are consistent across all standards, excluding ASHRAE (The American Society of Heating, Refrigerating and Air-Conditioning Engineers). Although UV levels are varied and the UK standard 2012 does not indicate a value or range.

MGC's standard has been updated by the Society for Museum Archaeology (Boyle and Rawden, 2020) by identifying additional materials such as composite objects, botanical materials etc. The standard they document has added individual factsheets for the museums about these materials. For textiles, the standard recommended is as follows:

- Temperature Below $10°C$

- Relative Humidity $45\% - 65\%$
- Illuminance 50 lux maximum
- Ultraviolet radiation $0 - 10$ microwatts per lumen ($75\ \mu$ W/Lumens maximum)

2.1.3.1. Current Issues and Limitations of the adopting Museum Standards

Managing artefacts and collections is usually reactive process and are cost intensive, hence these decisions are constantly being debated. Maintenance department budgets are seen as a cost centre and are being decreased. The argument put forward is that maintenance activities are costly, however it is proposed that the lack of maintenance ultimately costs more (Salonen and Deleryd, 2011). There is an absence of accessible and rigorous literature aimed at targeted maintenance in conservation (Dann and Cantell, 2007 cited in Forster and Kayan, 2009, p. 215). There is an increasing awareness about the relationship between maintenance and the ability to retain cultural significance, however, this does not seem to have been mirrored in the form of effective action. Policies need to be developed by organisations that would link the aims of proactive conservation with monitoring activities (Forster and Kayan, 2009).

According to the Image Permanence Institute (2019), "*Monitoring and controlling temperature and relative humidity (RH) in collection spaces is essential to providing adequate preservation conditions for collections. In many museums there has been a shift in thinking from static environmental management in cultural institutions – that is one in which institutions aim to achieve the same temperature and RH levels in collections spaces year-round – to dynamic environmental management in which conditions are allowed to vary within safe ranges, particularly seasonally*."

The Image Permanence Institute (2019) further mentions the significance of museums monitoring their collections and basing their preservation approach, accordingly, stating it will not only improve the environment for preservation but also improve the longevity of museums' collections. They also state that museum environmental management should include analysis and interpretation of the recorded museum environmental conditions. Utilising the knowledge gained by monitoring the museum environment can assist in making improvements to the environmental conditions. It recommends continual monitoring and analysis of the data to enable informed decision making regarding its artefacts. Thereby describing a dynamic approach that can reduce decay as well as lowering energy costs.

High energy consumption costs of maintaining the restricted and controlled environment is a significant concern for museums (Sharif-Askari and Abu-Hijleh, 2018).

Further criticism of the museum standards, that recommend a strict range of relative humidity of $50 \pm 5\%$ and for temperature within the museums-controlled range at $20°C - 21°C \pm 2°C$ for the object collections, are made by (Atkinson, 2014) (Alcántara, 2002) (Sharif-Askari and Abu-Hijleh, 2018), stating:

- The energy consumption and impact on the museum's carbon footprint is high if strict environmental conditions are maintained. Economic considerations are challenging, as the cost-effectiveness and affordability can be a significant obstacle for institutions that feel that the existing standards are too far out of reach. Climate control to a standard is at the forefront of the criticism, as it is perceived to be biased in favour of "rich museums." Rising energy costs have meant that even well-to-do museums have pressed for a relaxing of the recommended values.

- Additionally, there has been a tendency to make the standards an end in themselves, instead of a means to inform and improve the preservation of collections.

- The need to balance conservation temperature ranges of the recommended standards with workplace environment for staff has to be carefully balanced as its the duty of the employers to provide a reasonable work environment. Workplace (Health, Safety and Welfare) Regulations (HSE, 1992) suggests $16°C$ as the acceptable reasonable temperature for staff in the workplace, whereas the updated standard by the Society for Museum Archaeology is for textile's to be maintained in an environment below $10°C$ (Boyle and Rawden, 2020).

- It has been suggested that the conditions need to be determined by the needs of the artefact(s). It has also been suggested that the local climate of the region should be taken into consideration in establishing standards.

Kamal et. al., (2018), Sharif and Esmaeli (2017) have critiqued current museum standards for organic based artefacts category as being too wide a range and have proposed the development of a more customised approach that involves a targeted monitoring of organic-based artefacts to choose the best-suited combination of environmental conditions for the artefact's condition. Further, Boersma, et al, (2018), too have criticised the general "one size fits all" approach to environmental specifications for collections. The authors state that these standards need to be based on evidence and are quite possibly unnecessary. There is active debate about standards, particularly for artefacts that have multi component aspects. For example, artefacts that comprise of part-metal and part-textile may have different preservation requirements. Maintaining the recommended internal climatic conditions for collection care has been questioned for its efficacy, particularly for multi components artefacts (Kamal et. al., 2018).

A study by Atkinson (2014) provided a detailed review of strict museums environmental standards. It found that stable environments benefit artefacts particularly those composed of hygroscopic materials. However, the study also found that similar materials did not seem to suffer, when acclimatised to local environments and fluctuating conditions. The study recommended further research into the understanding of individual artefact behaviour, when kept in strict climatic conditions, to determine the impact.

2.2. Textile Conservation Studies in Museum Environment

2.2.1. Introduction

Objects curated in museum collections are constituted from a broad range of materials, including inorganic material such as pottery, stone, glass, as well as organic materials such as textile, paper, leather, and wood (Museums and Galleries Commission, 1992). Textiles form a specifically significant portion of heritage assets in museums (Dahlin, 1995) and are most found in collections of upholstery, tapestry, costumes, and paintings.

The factors significant to the deterioration of textiles, as discussed in section 2.2.2.1, are relevant to consider further.

2.2.2. Degradation of textiles

Many studies have been conducted to understand the causes of deterioration in textile-based artefacts. According to Smith and Thomson (2017) the types of textiles can be defined in three distinct groups; natural, restored (treated), or man-made. The physical structure and the chemical composition of each vary, and hence, the degradation, when exposed to factors previously discussed, can also be seen to vary. The deterioration of textiles is because of the continuing breakdown of their long chain fibre molecules into shorter chain, manifesting itself in a brittleness of the textile, and associated loss of strength and sometimes decolourisation of the material. Other manifestations of degradation are seen in a flattening of the material fibres, shredding, and sometimes fragmentation of the fabric, seen as tearing of the material (Smith and Thomson, 2017a) (National Park Service, 2002).

The degradation of textile is usually a combination of various factors and not one in isolation. Environmental factors are significant in the deterioration process, for example, heat, light, bacteria, fungi, chemicals, accidental spills, water, moisture, and pollution (Smith and Thomson, 2017a). According to the Museums and Galleries Scotland (2020b), some of the main environmental factors that affect fabric in museums are uncontrolled temperatures; uncontrolled relative humidity levels; exposure to light; UV exposure; footfall and pests.

2.2.2.1. Pathways of Degradation in Textile

The main forms of degradation pathways (National Park Service, 2002) (Smith and Thomson, 2017), (Vilaplana et al., 2014) (Brzozowska et al. 2018) are detailed here:

- Hydrolysis – The chemical breakdown of a compound due to reaction with water.

- Oxidation – The presence of oxygen naturally degrades textiles, resulting in overall brownish discolouration on white- or natural-coloured textiles

- Photodegradation – This involves the alteration of the textile by light. Light exposure can cause dyes to fade and undyed textiles to either bleach or darken. The degradation process involves oxidation and hydrolysis to alter the state of the material and therefore requires sunlight or any artificial light along with water to enable the degradation. Light damage is cumulative and irreversible (National Park Service, 2002b).

- Biodegradation – This is the decomposition of the material by bacteria, fungi, or other living organisms. As the material ages, the process of oxidization, (principally, a change in the chemistry of the material), takes place causing an increase in the sources of carbon, nitrogen, and other elements that are attractive nutrients for microorganisms. Factors responsible for the rise of microorganisms in a textile, relate to its chemical nature, environmental conditions, light intensity, and favourable humidity.

- Abrasion – The loss of material by the process of scraping or wearing it away.

- Shredding – The loss of fabric by tearing or fragmentation as result of a loss of the materials elasticity.

2.2.2.2. Environmental Agents of Damage and their Impact

To identify damage in textiles, it is important to understand the fundamental causes of the environmental factors mentioned in section 2.3.2. and to be able to identify the indicators of damage (Wiltshire County Council Conservation Service, 2006) as follows:

- *Light Damage* - It has been seen that both natural and artificial light found in museums cause the most harm to the textile artefacts as light enables the photodegradation process to activate.

    - As a result, the colours in the textile become pale and dull and over time become fragile, shredding easily. The colours blue, green, and purple of the nineteenth-century textiles seem to be extra suspectable to fade. Fading or discolouration is most identifiable result of over exposure to light. Discolouration or yellowing of the fabric usually a useful indicator of the object's deterioration and may result in structural damage to the fabric in the long-term (Museums and Galleries Commission,1992) (Dahlin, 1995).

    - Damage caused by light in textiles happens progressively. The objects tend to lose flexibility, reduce strength, and then become fragile leading to shredding and fragmentation and eventually powder. (Museums Galleries Scotland, 2009b) (Dahlin, 1995).

- *Temperature and Relative Humidity* – These environmental factors can cause significant damage to textiles, specifically if there are extreme fluctuations in the museum environment the objects are housed. Some of the textiles in the museums are dyed or are covered with coatings on their fibres. These coatings can expand and reduce due to extreme conditions of heat and moisture, resulting in damage.

- If the objects are exposed to high humidity in the environment, mould and mildew growth can grow on the textiles.

- If the objects are exposed to low humidity in the environment, it can cause the drying of the fabric, resulting in brittleness, splitting and other alterations. Materials that are made of a thicker consistency dry out faster from their surface causing distortions.

- If the objects are exposed to fluctuating temperatures in the museum environment, it can cause textiles to fray, shred, and fracture (Carter and Walker 1991).

- Mould are micro-fungi that tend to thrive in humid environments and can cause permanent staining and decay of textiles. Once moulds are found on the fabric, they can quite swiftly break down the fabric strength (Museums Galleries Scotland, 2009).

- *Dust, Dirt, and other Pollutants* – These agents of deterioration are in particulate or gaseous form and can cause breakage of the threads of the fabric by lodging between the fibres.
  - Dust disfigures, dulls, and stains textiles. Dirt and dust also contain a high proportion of silica. The sharp surfaces of silica can cut and abrade textile fibres, especially when the fibres expand and contract in response to RH fluctuations (National Park Service, 2002).
  - Dust has been seen to exert a grinding (friction) force on the fibres of the textiles. It has also been seen to attract pests.
  - Sulphur dioxide bleaches, discolours and embrittles textiles and hydrogen sulphide can lead to a darkening of the pigments in the presence of water. Formaldehyde in paints, carpets and varnishes can adversely affect dyes in textiles (National Park Service, 2002). Ozone, sulphur dioxide and nitrogen as the most hazardous chemical and gaseous pollutants (Sharif-Askari and Abu-Hijleh, 2018).

- *Materials in contact with the textiles* – Harm can also come from materials which come in close contact with other materials such as chemicals used in varnishes, dyes, paints, inks, etc.
  - The impact of incompatible materials on the textiles, can result degradation. For example, certain metals that may contain iron could react with moisture in museum air and cause rust. This rust could in turn stain the fabric and eventually damage it

permanently. Further, poor quality material in contact with textiles can cause damage because of their causing chemical reactions, resulting in the textiles becoming discoloured, dull and embrittled (Museums Galleries Scotland, 2009).

Stabilising the artefacts in their care, is the primary objective of the conservation process. Such stabilisation is made harder, as the deterioration process can be inherently unpredictable, for example, slowing until it reaches a threshold where the deterioration equilibrium is disturbed, and the deterioration reaction gathers momentum. Temperature and moisture affect the rate at which these reactions proceed, hence environmental factors play a crucial part in regulating the degradation mechanisms to which the artefacts are susceptible (Bradley, 1994).

2.3. Silk Conservation Studies

Textiles, in the form of silk, are found in numerable objects such as paintings, upholstery, tapestry and costumes.

Silk is an organic material produced by silk moths belonging to the *Bombycidae* family, the most significant of which, to the production of silk is the *Bombyx mori*, a domesticated silkworm (May and Jones, 2006). As silk fabric is a natural material made of protein, it is susceptible to damage by heat, light, microorganisms, pollutants, and chemicals (Muge and Suat, 2016). As such, silk remains prone to the impact of the textile degradation factors discussed in section 2.3.2. and the further subsections 2.3.2.1. - 2.3.1.2.

There have been multiple studies on the degradation of silk, at the molecular and macroscopic level, deliberating on the structural and molecular level breakdown of the silk fabric. Other studies have focused on photodegradation and the alteration of silk material by light. Further research has investigated the fading of dyes and pigments found in silk samples, because of the exposure to environmental conditions. These studies have mainly adopted accelerated aging techniques to identify degradation (Vilaplana et al., 2014). Duxbury (1994) detailed the following factors that govern the fading of dye,
(a) the ability of the substrate, or residual solvent within the substrate, to donate electrons or hydrogen atoms to the dye and (b) the degree of dye aggression (c) the physical and chemical structure of the substrate.

2.3.1. Molecular and Structural Silk Studies

Muge and Suat, (2016), have studied silk degradation at a molecular level by use of 'proteomics'. Proteomics is an interdisciplinary study of proteins and is used to examine protein degradation in silk at a molecular level. This technique uses proteomic tools such as mass spectrometry to study protein oxidation. Similarly, Li et al., (2019) studied the changes in the structure of silk protein by thermally aging silk and modern silk samples to observe the degradation process by ATR-FTIR and SDS-PAGE. The proteomic method requires the preparing of silk proteins by a process of destructive analysis. This research found that the solubility of silk proteins varied between ancient and modern silk, finding the former's solubility to be much higher than that of ancient silk. Other silk studies such as Cao and Wang (2009) have focused on the structural and molecular weight of the silk fibroins to discover its degradation behaviour for medical usage such as biodegradable sutures. Ramgopal et al., (1997) used the positron annihilation lifetime technique (PAL), an invasive approach to study the effect of ultra-violet (UV) irradiation on the microstructure of the most found bivoltine, an Indian silk fibre. Lifetime results in the early stages of UV irradiation found that the chain scission led to free radical formations. Longer irradiation led to crosslinking and the study concluded bivoltine silk type I changes into more ordered silk II on longer irradiation. Thus, successfully probing structural modifications in the silk fibres under thermal treatment.

Brzozowska et al., (2018) tried to address the need for greater in-depth microbial study of historical textiles. The study conducted investigations on the impact of airflow on the microbial diversity for several silk and velvet masterpieces, on display at the Palace of Wilanow, in Poland. The study utilised a sequencing of 16SrRNA amplicons and found that this method did not have the discriminatory capability to provide a comprehensive analysis of the biodegradation of the museum objects. The study found the historical silks to be resistant to conservation procedures. Gutarowska et al., (2017), investigates the biodeterioration of historical material resultant from their chemical composition. The study reviews the current techniques of analysing the mechanical properties of textiles. Natural fibres are made up of plant cellulose or animal protein and are susceptible to microbial degradation if exposed to high humidity. It is unfortunately the case that most pre-described analytical methods are invasive by nature, requiring a sizeable sample piece of the textile. The study identifies a need for non-invasive techniques for biodeterioration analysis. Ruga et al., (2019) researched the impact of fungal particles on historical assets and utilised aerobiological volumetric monitoring. The research analysed fungal spores, which are most frequent and commonly associated with biodeterioration of organic and inorganic artefacts in museum. The study provided knowledge about the high-risk environment based on the volumetric sampling and qualitative analysis of the airflows in the museum.

Liu et al., 2019, studied photodegradation of silk fibres by examining the interactions between sericin and fibroin. FTIR spectroscopy analysed the breakdown of the peptide bond in the silk fibres, when irradiated with UV light, with one sample immersed in water at $38°C$ and one without. The mechanical properties were analysed using tensile stress strain curves. The study concluded that, as the aging time increased, the rate of degradation increased in the sample immersed in water, compared to fibres irradiated without water.

2.3.2. Photodegradation Studies on Dyes and Pigments

Dyes are variable in their behaviour and their lightfastness depends on the depth of dyeing and on the environmental factors (Padfield and Landi,1996). Light fastness of dyes greatly depends upon the mordant and the fibre to which it is applied, as well as how heavily it is applied. If it is lightly applied to give a pale tint, it fades much faster. The authors further recommend colorimetry as a very accurate method of fade measurement and recommend that the exact colour of dyes should be recorded before being displayed (Padfield and Landi, 1966). The loss of colour in silk is mainly because of degradation of the dye molecules to varying degrees. Ahn et al (2014) have studied the fading of three different natural silk dyes with accelerated techniques of thermal heating, through the exposure of the silk material to high temperatures (of 100°C). The study found that certain dyes such as alizarin and purpurin were more resistant to degradation possibly due to the large deposits of chemical aggregates. The result was verified by the CIE colour difference measurement (ΔE) of the artificially degraded silk dyes with individual dye solutions.

Colombini et al., (2007) stated that identifying dyes in old textiles is a difficult task because of the complexity of the degradation processes undergone by the organic molecules of dyes. The research describes an analytical procedure based on gas chromatography and mass spectrometric detectors (GC-MS), to identify the material used in natural dyes of tapestry dated around the mid to the late 19th century. The method is based on solvent extraction of the yellow dyes from raw materials of aged and not aged samples for comparison. Reverse Phase High Pressure Liquid Chromatography

(RP-HPLC) has been combined with a spectrophotometric UV-Vis detector to recognise patterns of changes in the dye structures. GC-MS requires samples and is a destructive analytical technique.

Studies done on understanding the effect of varying levels of relative humidity on pigments used in historical fabrics, have indicated that the higher the relative humidity levels, the greater the degree of colour change observed in pigments found in the dyed fabric, for a given light exposure level (Giles et al. 1988 cited Saunders and Kirby, 2004, p.64). Figure 2-2 below indicates the general trend of the cumulative damage on the pigments of the fabric, as the light and RH are increased, the fade increased monotonically.

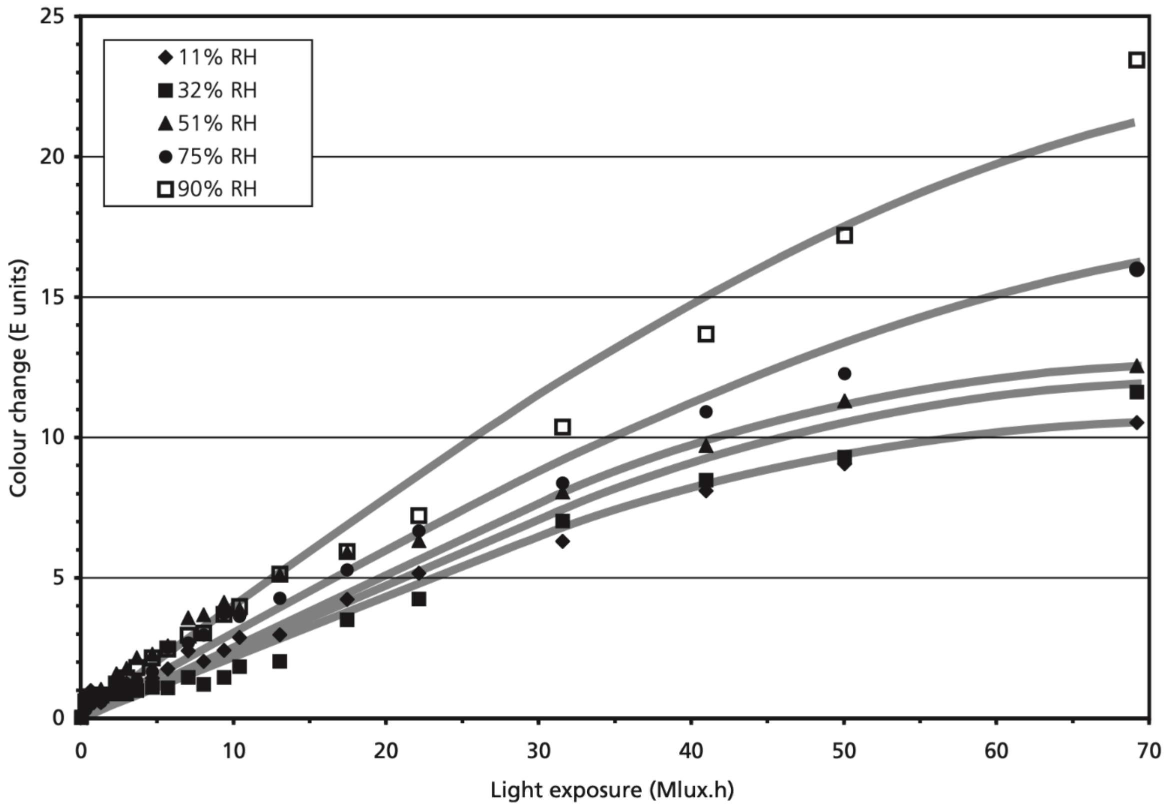

Figure 2-2: Cumulative damage on artist pigments

(Source: Saunders and Kirby 2004)

It was also noted that the dyed silks kept in the dark were mostly unaffected. Supporting this, evidence in previous studies on kermes and cochineal-dyed silks, also indicated that the degree of fading is directly proportional to the increase in relative humidity (Giles et al. 1988 cited Saunders and Kirby, 2004, p.64). Commonly used pigments in the dyes demonstrate increased light-induced change with increasing RH. The research also found that some pigments are not affected by the increase in relative humidity and similarly others were also less vulnerable to light induced degradation. Besides high RH, there are other degradation changes that take place and are dependent on the presence of water, the passage of dissolved salts or conditions of unusually high pH found especially in certain wall paintings particles (Saunders and Kirby, 2004). Bradley (1994) states that all organic materials such as silk, paper, and wood are significantly affected by fluctuations in relative humidity and temperature. This fluctuation causes them to expand and contract, thus putting a strain on the fibre causing warping, flaking, and structural deterioration. Silk also suffers structural deterioration from UV and visible light. Some of the pigments fade on exposure, and some undergo a chemical change. Vasileiado et al., (2019) studied the effects of UV-induced degradation of wool and silk dyed with shellfish purple. The UV induced changes to the molecular structure of the sample with resultant chemical changes was evaluated using colorimetry, HPLC-DAD, scanning electron microscopy (SEM) and FTIR spectroscopy. The study found that upon exposure to intensive UV light, the dye changed structural, chemical, and visually. The study observed rapid decrease in the shellfish compounds in the early stages of exposure, whereas longer exposure had minor effect.

2.3.3. Accelerated Aging Silk Studies

As previously described, historical studies conducted into silk degradation have, for the most part, used destructive analytical methods for studying deterioration of silk samples. Examples of these destructive methods are viscometry, high performance size exclusion chromatography (HPSEC), dynamic mechanical thermal analysis (DMTA), and sodium dodecyl sulphate polyacrylamide gel electrophoresis (SDS-PAGE) (Wang &Wong, 2019). Luxford et al. (2009) have also used accelerated aging to determine the effects of relative humidity and temperature on historic silk by examining the mechanical properties and molecular weight with the Arrhenius equation. Their findings, extrapolated from the accelerated aging, is that light (excluding UV) is not a critical factor, but high elevated temperatures, combined with relative humidity, results in a significant deterioration in the silk textile.

Zhang and Yuan (2010) artificially degraded modern cultivated silk through accelerated light, heat, and hydrolysis experimentation. The study assessed the potential for viscometry for quantitative assessment for silk degradation by comparing it with tensile strength testing. The study concluded that this was useful technique to detect small changes in silk molecular weight due to degradation. However, the study further highlighted tensile strength testing required sampling and preferentially

large samples. This was found to be unsuitable for ancient silk textiles. On the other hand, viscometry was seen to be effective and less destructive as it required a smaller sample size.
Zhang et al., (2011) studied the tensile strength of the silk fabric by subjecting the samples to artificial heat and moisture by means of amino acid analysis. The research studied the tyrosine content to assess the condition of the silk by artificially aging the raw silk. These studies done in silk degradation have used accelerated aging methods to study the silk deterioration, requiring samples to be subjected to extreme conditions, thus damaging the silk sample fabric for experimentation. del Hoyo-Meléndez et al., (2012) utilised micro-fading spectrometry, which combines visible reflectance spectroscopy and accelerated light aging, to study the light fastness behaviour of dyes. The study also assessed the use of BW standard reference scale as an alternative to light ageing assessment. Koperska et al., (2014) (2015) also studied silk degradation by artificially aging the samples to a temperature of $150°C$, while exposing them to various environments of oxygen, volatile organic products, and water vapour respectively. This study examined the oxidation process in silk. The study indicated water vapour and oxygen as having the most significant impact on silk degradation in the artificially aging experiment, in both photo and thermo-oxidation. For this study, ATR-FTIR spectroscopy was used for monitoring structural damage.

Luxford and Thickett (2011), conducted accelerated aging experimentation to study critical environmental factors causing deterioration of heritage silks on open display in historic properties. The environmental parameters such as light, relative humidity, temperature and UV light, and their extrapolation to real museum data was demonstrated. The Arrhenius approach was adapted to apply to solid material, informed by its use in paper and photographic conservation studies. The deterioration caused by accelerated aging can be relayed to an equivalent display time, under the same relative humidity. The study proposed an accelerated aging methodology for preventative conservation for silk. Furthermore, they questioned the validity of the inference linking accelerated aging data to natural aging conditions. Additionally, they highlighted the complexity of the large number of variables to extrapolate the magnitude of the change. They called for further studies to consider the impact of museum environmental conditions for samples on open display. Accelerated aging experiments are useful to understand the degradation mechanism of the samples, but their influence must be considered with precaution (Vilaplana et al., 2015).

2.3.4. Non -invasive Silk Studies

Using non-invasive analysis is key to silk conservation and developing a better understanding of materials and methods is central to advancing the conservation of textile artifacts (Thomson et al., 2017). The majority of analytical techniques require mounting or embedding samples. This is problematic when since many silk artefacts are on display, and sampling in this way causes damage to the original artefact and may require it to be taken out of display.

Some of the key analytical techniques as detailed in Figure 2.3 indicate the optical and chemical analysis undertaken for textiles.

Method/Technique	Preparation	Ease of Use	Information Gained
Visual examination	Flat surface and good illumination	Basic to skilled	Overall picture & surface detail
Staining and solubility tests	Loose or embedded samples	Basic to skilled	Identification of materials classes & fibres
Low level microscopy	Flat surface and good illumination	Basic microscope	Overall picture, surface detail & magnified ×10
High level microscopy (Polarised, ultra-violet)	Small sample sometimes embedded	Skilled	Detail of structure magnified ×1000
			Detail down to around 1 μm
SEM	Sample mounted or embedded	Highly skilled	Detail of structure to around 1nm
SEM-EDX	Sample mounted or embedded	Highly skilled	Identification of elements

Figure 2-3: Optical and chemical analytical techniques for textile conservation

(Source: Thomson et al., 2017)

Thomson et al, 2017 provided a detailed review of the analytical techniques and their ease of use. Wang and Wong (2019), tried to move away from destructive invasive methods by using scanning electron microscopy (SEM) coupled with energy- dispersive X-ray spectroscopy

(SEM-EDX) to analyse silk and adhesive samples taken from the Stein Collection of the British Library. Although accelerated aging of the samples was done using minor silk samples, the study suggests the use of a combination of invasive and non-invasive techniques to help contribute to the long-term conservation of silk. SEM produces images by detecting secondary electrons which are emitted from the surface due to excitation by the primary electron beam. The drawbacks are that firstly, this technique requires an expert to be able to generate the raster images and to interpret them effectively and secondly, that SEM is costly to purchase and use (Thomson et al., 2017b). Further review of the analytical techniques by Smith et al., 2017 provides a detailed insight into vibrational, X-ray spectroscopic and chromatographic analytical techniques.

Del Hoyo-Melendez and Mecklenburg (2012) used micro-fading spectrometry, which combines accelerated light aging with visible reflectance spectroscopy to study the effect on dyes used in silk. This technique was found to generate quicker results when compared to traditional techniques, which required longer exposure to light. The lightfastness was compared to a standard reference Blue wool scale standard. This research used a micro-fading spectrometer, consisting of a reflectance spectrophotometer coupled to an accelerated light fading micro tester. Clementi et al., (2006) used non-invasive techniques to study natural dyes that occur in silk and wool artefacts. Laboratory samples of silk and wool were analysed with a portable non-destructive instrument to measure fluorescence spectra in the orcein-dyed silk tapestry. For the chromatographic analysis the original tapestry threads from the reverse of the tapestry were used to extract the dye for comparison.

Figure 2-3 illustrates organic dyes are markedly dependant on the microenvironment and both the thread and the dye are photodegradable, and the extent of the photodegradation is dependent on dyes of different substrates.

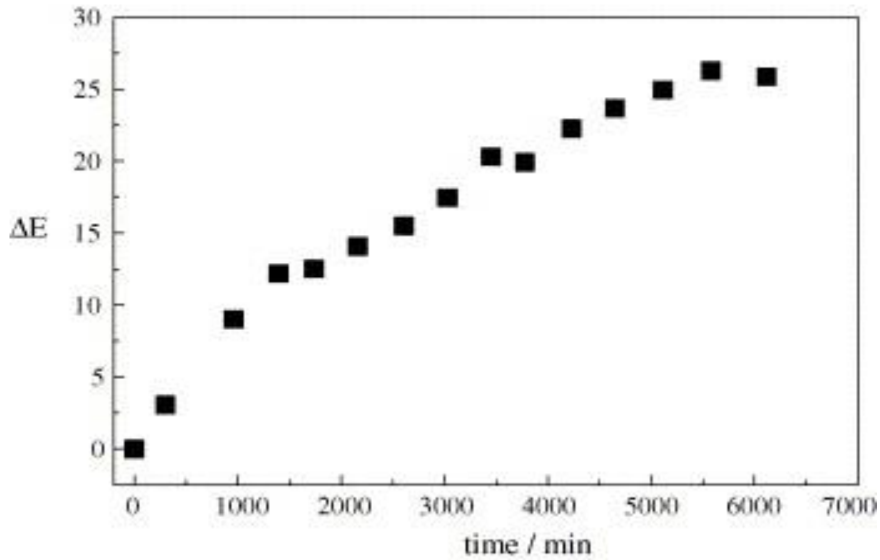

Figure 2-4: Colorimetric ΔE as a function of the irradiation time for an orcein-dyed silk

(Source: Clementi et al, 2006)

The results of spectrophotometry and fluorimetry are reliable but needed to be integrated with complementary experimental approaches. This approach had a limitation when the colour of the threads was mixed and the colours could not be isolated (Clementi et al., 2006). Sharif and Esmaeili (2017), studied the chemical effects of improper temperature and relative humidity on Buyid silk for degradation using Time-Weighted Preservation Index (TWPI). The findings presented did not mention an exact number of years in the permanence of the life of the object, but a comparative measure between different storage conditions and various combinations of temperature and relative humidity. The study found the permanence of the silk object is more sensitive to temperature than relative humidity. The results of the sensitivity analysis show that a decrease in 1°C increases the permanence by 11 years, but a decrease of 1% in relative humidity had an increase of only 2 years.

May and Jones (2006) indicated the sensitivity of silk to a variety of environmentally induced degradative processes and Vilaplana et al., (2014) further discussed the need to understand the environmental causal factors and the deterioration level in the silk fabric, to help in decision-making for the preservation of silk. It was important to understand the impact on silk through aging and to find dependable diagnostic indicators for monitoring the degree of degradation of the silk fabric. These diagnostic indicators could help museums to assess the condition of the silk artefacts, whether they should continue to be exhibited or choose other preservation options.

This is also confirmed by Muge and Suat (2016), who found that silk textiles in museum collections undergo continual photodegradation even after careful attention is paid to the display museum environment, and textiles rarely survive their useful lifetime. Wang and Wong (2019), also reiterated in their conclusion the importance of preventative conservation approach rather than remedial approach for long term conservation of silk. A practical example, of the application of these findings can be seen by Kamal et al (2019), in their recent review of the collection of King Tutankhamen at the Grand Egyptian Museum, where they deployed a targeted object-based preventative conservation approach for object display.

2.3.5. Limitations of current silk aging studies

Although the above studies for silk have focussed on accelerated ageing methods to study degradation and have provided valuable insight to the field of textile conservation, these methods require available samples. Frequently, this approach is not practical or possible where rare, valuable, historical artefacts are concerned. Often it is impossible to extract a sample from historical furniture, without damaging the fabric (Zhang &Yuan, 2010). Erhardt & Mecklenburg (1995) highlighted the issue of accelerated aging and its implications when compared to natural aging. They conclude that the results from the accelerated aging method do not necessarily simulate natural aging, and that it is not always valid to compare aging conditions.

Saunders and Kirby (2004) point out that aging experiments are usually of short duration as compared with the natural aging of most silk materials, and therefore the degradation seen in the accelerated aging sample of silk, is not necessarily comparable to that seen in the natural aging of silk. The silk dyes and pigments vary significantly from sample to sample with the result that the make-up of the original silk samples does not necessarily correspond to the samples used as surrogates for experiments. The changes seen in the accelerated experimental samples arise from a different chemical reaction. The authors stress the importance of not relying too much on results of these accelerated experiments. Luxford and Thicket (2011), reiterate that there isn't a standardised universal method for accelerated aging to compare the various silk studies. They go on to question whether accelerated ageing conditions can be extrapolated to the aging process which occurs naturally and go onto question the validity of as these short-accelerated research studies, as compared to studying natural ageing of silk in real time.

A recent study done by Shahid, et al., (2019) researching dye analysis for historical textiles, has reiterated the need for minimally invasive or non-destructive techniques in the cultural heritage community, which is in accordance with preservation principles of historical objects; thus, looking to limit destructive analysis sampling. Luxford et al., (2019) highlight the need for a balance between care of the artefacts on display and the use of material for sampling, and therefore state that the need for large samples to be tested in laboratory conditions is counterproductive. They see micro-sampling, (the use of minimal samples of fabric – for example, using silk fibres as opposed to larger samples of material), as an acceptable alternative, but state that more research into non-destructive techniques for analysing in situ is required. Gutarowska et al. (2017), explain that most of the applied analytical techniques and methods are destructive and invasive; thus, unsuitable for historical objects. The most important requirement for analysis in this area is non-invasiveness.

Masciotta et al., (2019) presented a sustainable conservation strategy for protecting cultural heritage. The protocol recommended is as detailed in Figure 2-4 and Figure 2-5

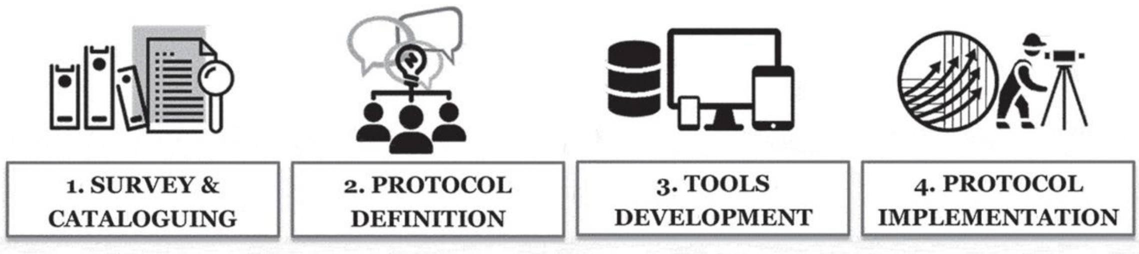

Figure 2-5: Four Phases of the HeritageCare Methodological approach

Source: Masciotta et al., (2019)

This methodology focuses on heritage buildings and architectural asset categories as the research revealed a lack of a uniform and standardised method for documentation and management of cultural heritage. The protocol is defined as follows.

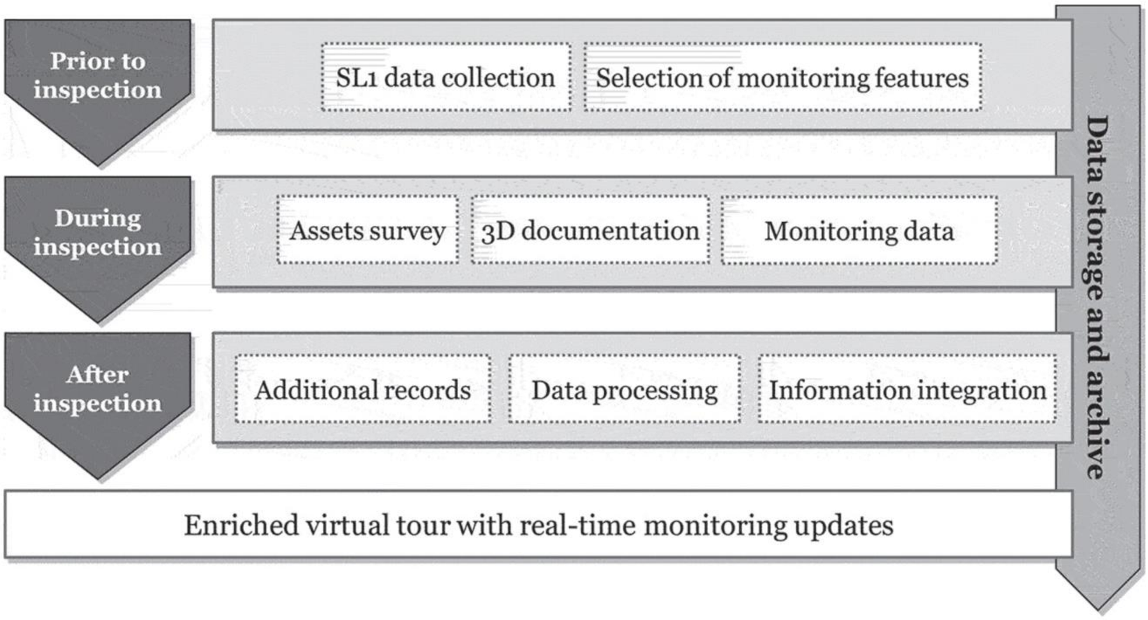

Figure 2-6: HeritageCare Protocol

Source: Masciotta et al., (2019)

For the heritage asset being monitored, the Protocol applies a 4-point rating system, which initially assesses the severity of observed damages, how these damages are measured, and the causal factors. A final grade is computed from the weighted sum of the assessed damage. The output of the Protocol is a scored condition and risk index for the asset, allowing conservation to be prioritised. To obtain high resolution information digital tools such as laser scanners, 3D data modelling, web enabled platforms and a mobile-based application are recommended.

2.4. Instruments Used for Silk Studies

The key techniques currently being used for silk conservation are reviewed in this section.

2.4.1. Colourimeter

A colourimeter is an instrument designed to measure, capture, and communicate colour (Choudhary 2014). It provides data such as the tristimulus values X, Y, Z or CIE values for standard illuminants. A colourimeter mimics the human eye-brain perception to perform a psychophysical sample analysis using a set illuminant. The tristimulus filter isolates a band of wavelengths of the objective's colour data. It can facilitate further comparison to a reference or standard to determine acceptability. Colorimeters are extremely precise in colour measurement and are ideal for identifying colour difference, colour fastness as well as routine comparisons of similar colours (Ramanathan, 2016). Tristimulus values XYZ are typically used to report the spectral response of a sample measured by a colorimeter or a spectrophotometer.

The use of colour measuring instruments allows for colour specification and communication by means of international standards such as the CIE XYZ, CIELAB, etc. (Gilchrist and Nobbs, 2000). The Commission Internationale de l'Eclairage (CIE) is an independent non-profit organisation, recognised by ISO, IEC and CIPM, as a body dedicated to global cooperation and exchange of knowledge on all matters relating to art and science of light, lighting, colour and vision, image technology and photobiology (CIE, 2020). CIE has recommended the colour standards theory, such CIE XYZ, CIE Luv, CIE Lab, and CIE UVW. Colour space is a method by which colour can be specified, created, and visualised. Colour is specified using three co-ordinates, or parameters. These parameters describe the position of the colour within the colour space being used CIE XYZ (1931) system is at the root of all colorimetry (Ford and Roberts, 1998). The CIE X, Y, Z system of colour specification is closely based on the RGB system of colour perception. The key advantage of the XYZ system is that it is an improvement over the RGB system as it eliminates negative numbers in colour specification. The key difference between the two is that R, G, and B are real light sources of known specifications, whereas X, Y, and Z are based on theoretical sources that are more saturated and allow matching of any real colour using positive amounts of three primary sources. The X, Y, Z tristimulus values represent all real visible colours having the widest possible range of values. The X value represents a red more saturated in the spectral red; Y represents a green more saturated than any spectral green, and Z represents blue more saturated than any spectral blue (Gilchrist and Nobbs, 2000).

The three-dimensional colour space produced by plotting CIE tristimulus values is not visually uniform, hence the CIE have proposed the use of simple Euclidean distances to identify the relative magnitude of colour differences (CIE, 2020C).

The key advantages of a colourimeter are (Patil, 2019):

- Fast and convenient to use due to its portability
- Easily optimised for automation
- User friendly and does not require complex technical knowledge

- Allows for computational, quantitative analysis.
- Allows for cost effective analysis

Examples of portable instruments are, TES 136 Chroma Meter, CL-200A and CR-400, which are a range of handheld portable instruments that can measure colour on various surfaces for numerous applications. These instruments are used to determine the spectral response of colour stimuli of an object in the form of tristimulus values. The colour stimulus function requires measurement intervals of 5nm or less, in a wavelength range of at least 360nm to 830nm to be CIE standard compliant (CIE, 2020D). These instruments can help in identifying colour difference, illuminance, and provide the potential to be used in quality assurance tests to ascertain if the sample meets the defined standard. The CR-400 range is more expensive than the TES 136 Chroma Meter and offers higher quality control colour measurement with 8mm and 50mm measuring apertures. The CR 400 can also detect minimal colour variations and can measure samples with smoother surface conditions in situ (Konica Minolta, 2020A) (TES 2014) (Pro-Light Technologies 2020). These instruments have also been used for colour quality control in production, and inspection stages of manufacturing, as well as being applied to the analysis of food quality in the food and meats industry (Ramanathan 2016) (Cąkici, 2015). They are additionally used for assessing the quality of paints (Karlsson et al. 2019), in the printing industry for measuring the quality of printed graphic images (Simpson and Jansen, 1991), for measuring plant colours in biotechnology (Kasajima, 2019) as well as in conservation science where they are used for the purpose of measuring colour change in historic textiles (Ford, 1992). Colorimetric properties of four pigments (red, blue, yellow and green) found in thermal woven textiles have been studied by Zhao and Li (2019). Xu (2010) used colorimetry to grade cotton which had, prior to this, been a problematic process due to subjective biases in visual human inspections and interpretations. This method became the official US cotton colour grading classing system. Chu et al., (2010) have used colorimeter, spectrophotometer and imaging systems for measurement, analysis and quality control of tooth colour. The study goes on to recommend combining instrumental and visual colour matching methods as these were found to be complementary to each other, resulting in a successfully predictable colour mapping outcome. Koussoulou (1999) utilises the Minolta Chromameter to calculate the colour difference of heritage silk fibres and dyes to study the mechanisms of deterioration. This research study proposed the application of light stabilizers directly to the fabric, as a new method of fabric protection. Recently, Tamburini and Dyer (2019), have jointly utilised colorimetry, spectroscopy, and digital imagery to provide insights into the signature behaviour of Dunhuang silk textiles, (from ancient China), housed at the British Museum. Colourimetry was used before and after artificially aging the dyes used in the fabric. The CIE colour difference formula was applied to analyse colour difference between the two sample sets with the help multispectral images. The information, obtained non-invasively, complemented further molecular analysis using High Pressure Liquid Chromatography Mass Spectrometry (HPLC-MS).

Some key limitations of colourimeters are (Patil 2019):

- The inability to measure colourless samples.
- Wavelength limitations

And, as measurements are not based on the visual appreciation of colour, the visual colour difference between two samples is not linearly related to the difference in the XYZ values (Gilchrist and Nobbs, 2000).

2.4.2. Spectrophotometer

While a colorimeter may contain as few as three sensors, one for red, green, and blue, or X, Y, Z, a spectrophotometer can report the entire range of the spectral response, measured every 10nms (Colourphil, 2020). Spectrophotometers measure reflectance, transmittance, or absorbance of various wavelengths in the spectrum. The main components of this instrument are a light source, a method of separation or dispersion, and a detection system. Most devices have a microprocessor for data handling and computations (Randall 1997). A spectrophotometer, as defined by Craic Technologies (2019), *"is an optical instrument for measuring the intensity of light relative to wavelength"*. The top-end instruments measure the electromagnetic energy, ultraviolet, visible, and near infrared regions. The Konica Minolta CM -3610A can be used for textile colour measurement as well as paper, powder and pigment and is suitable for non-contact measurements (Konica Minolta, 2020C). A recent study conducted by Tamburini and Dyer (2019), utilised the Konica Minolta CM-2600d spectrophotometer equipped with a 52 mm barium sulphate integrating sphere, dual-beam geometry, di:8°, a 360–740 nm wavelength range with 10 nm measurement intervals, was used in the analysis of ancient textiles in the British Museum.

Advantages (Konica Minolta 2019B) (Geisler, 2015):

- Increased precision
- Increased versatility

- Can measure spectral reflectance at each wavelength
- Can be combined with other instrumental analysis techniques as well as multivariate datasets to have more robust analysis of the samples.

Spectrophotometers have been widely used in numerous industries and have had success in determining the condition or colour of an object. Specific applications of this method have been in dentistry (Chu et al, 2010); determining environmental contaminants (Sargazi & Kaykhaii, 2020); measuring sunscreen efficiency (Couteau 2018), and in the application to buildings and the material industry, as seen in the absorption performance between cement and emulsified asphalt (Wang et al, 2017). Spectrophotometers have been used in the preservation of medieval plasterwork (Martínez, 2020), and the use of spectrophotometric methods for qualitative and quantitative analysis of substances in the study of composition and structure of various compounds is widespread (Zinchenko et al, 2020). Tamburini and Dyer (2019) have recently analysed Chinese textiles from 7th -10th century AD with reflectance spectroscopy to identify ancient colourants, pigments, and dyes non-invasively.

Limitations (Konica Minolta 2019B) (Geisler, 2015):

- Spectrophotometers are more expensive than colorimeters.
- Another critique relates to the selectivity of these instruments; they have been noted to not discriminate between the sample of study and any contaminant that absorbs the same wavelength.
- Broadband detectors used in these devices respond to all light that reaches them, which may result in erroneous readings. Stray light has known to cause a decrease in absorbency thus reducing the linearity range of the instrument.
- The results can be influenced by pH, impurities, temperature, and any contaminants in the sample leading to errors in the readings.

The main advantage of the techniques discussed in this section are that they can be combined with other instrumental analysis approaches to achieve a more robust analysis. Some of the current spectroscopic analytical techniques used for conservation are further detailed subsequently.

2.4.2.1. Raman spectroscopy

Raman spectroscopy is a vibrational spectroscopic method that allows for analysis and the characterisation of compounds, providing the possibility for the identification of the characteristic of the spectra molecular vibrations (Xu et. al, 2019). Walthius et al., (1999) have defined Raman spectroscopy as "*an optical, vibrational spectroscopic technique that provides detailed information about molecular composition and molecular structure*." Raman spectroscopy has evolved with the rapid development of optical instrumentation such as CCD detectors that are sensitive to near-infrared spectral region, fibre optic probes, high power, narrow-band lasers, and high-quality notch-filters. The advancement in fibre optic probes enables in vivo Raman spectroscopy which is important in the biomedical field. A Raman spectrometer and a micro-Raman spectrometer are designed to measure Raman spectra of microscopic samples or microscopic areas of larger objects. These instruments are built and optimised for micro spectroscopy and can measure microscopic samples (Craic technologies, 2019).

Klisińska-Kopacz (2019) have used Raman spectroscopy to identify polymers used in cast sculptures, from museum collections, and understand their degradation process. This non-destructive technique is based on applying the laser in the visible, near infrared, or near ultraviolet range to illuminate a cell or compound, which can be tagged by radioactive staining or fluorescence (Minakshi et al., 2019). Recent studies have proved its usefulness in conservation of Maori textiles, by understanding the properties and behaviour of degradation (Samanali, et.al., 2020).

2.4.2.2. Fourier-transform infrared spectroscopy (FTIR)

Fourier-transform infrared spectroscopy (FTIR) is a technique based on infrared light absorption in the wavelength range of 2.5-25 μm by the material under investigation. This technique enables mechanical motion of different forms of the molecules or the compound atoms. Slight energy differences resulting from the vibrational and rotational states in different compounds are the basis of FTIR analysis for organic matter (Nasrazadani and Hassani, 2016).

Fourier-transform infrared spectroscopy (FTIR) is one of the most used analytical techniques as it is non-destructive and capable of in situ analysis. Xu et al., (2019) has used FTIR coupled with Raman imaging for identification and quantification of microplastics from different environmental samples. Thus, allowing a comparison of the characterisation of the polymeric chemical structure and identification by comparing it to a known reference spectrum.

Kirkland (2009) uses Fourier transform infrared spectroscopy with attenuated total reflectance sampling (ATR-FTIR) to examine the changes in the chemical nature of the archaeological and modern samples upon plasma treatment. Textile samples were treated with destructive wet chemicals and compared with plasma treated samples to demonstrate plasma treatment efficacy for alternative sample preparation for radiocarbon dating. Similarly, Peets et. al. (2019) has used FT-IR micro spectrometer Thermo Scientific Nicolet iN10 MX Integrated FT-IR microscope, both in reflectance and ATR modes for textile analysis. FTIR spectrometers can be combined with accessories such as the ATR, Reflectance and Transmission.

2.4.2.2.1. Attenuated total reflectance infrared spectroscopy (ATR-IR)

This technique has been used for determining the spectra of sample silk fibres with a low non-damaging and reproducible pressure on the fibre. The Golden Gate single-reflection ATR accessory uses a diamond as an ATR element and a highly focused beam. The silk samples can be rotated while maintaining constant infrared radiation penetration depth (Boulet-Audet et al., 2008). Garside et al., (2005) developed a micro destructive methodology for studying physical degradation of weighted silk derived with FTIR-ATR and high-performance liquid chromatography (HPLC) micro sampling analysis. This study was extended to also include the POL-ATR technique to calculate the correlation between the breaking strength of the aged and fibroin polymers within the fibres.

2.4.2.2.2. Reflectance-FT-IR (r-FT-IR) spectroscopy

Peets et al., (2019) used reflectance FT-IR (r-FT-IR) spectroscopy to compare and compile textiles such as wool, silk and polyamide fibres spectra collection for the use of further research. Their study found the technique useful and comparable if not slightly better than ATR-FT-IR spectroscopy. r-FT-IR was more effective in differentiating between the amide-based fibres, wool, silk and polyamide. The two instruments used were FT-IR micro spectrometer with ATR mode (mATR-FT-IR) and ATR-FT-IR spectrometer. The instruments used for this study were the Thermo Scientific 6700 FT-IR spectrometer with Smart Orbit micro-ATR accessory and FT-IR micro spectrometer Thermo Scientific Nicolet iN10 MX Integrated FT-IR microscope both in reflectance mode.

Tamburini and Dyer (2019), used reflectance spectroscopy to analyse dye in Dunhuang fabrics, a specific type of heritage textile curated at the British Museum. Due to their fragility, rarity and value, samples for destructive analysis could not be attained. Hence, a non-invasive technique combining multi spectral imaging and fibre optic reflectance spectroscopy was applied.

2.4.2.2.3. Near-Infrared (NIR) spectroscopy

NIR spectra can be acquired on a FT-IR spectrometer extended to the NIR region, a UV-visible-NIR absorption spectrometer or a dedicated NIR spectrometer. In the NIR region, absorption bands come from overtones, combinations of overtones and/or combinations of fundamental vibrational motions. The overtone bands and combination bands are much less intense and are broader than the corresponding fundamental absorption bands (Le Pevelen & Tranter, 2017).

One of the key advantages of NIR spectroscopy is that it requires little or in some cases no sample preparation. It allows for differentiation between polymorphs, which the mid-IR is not able to do. The sample is treated in a manner like the r-FT-IR technique. However, the spectra captured is not as easy to interpret and requires chemometric tools for analysis in the mid-IR region (Le Pevelen & Tranter, 2017).

Zhang and Wyeth (2007) use NIR spectroscopy as a non-invasive approach for characterisation of silk fabrics and to determine the moisture content of silk as a potential age-related marker. Current conservation studies have used the Fourier Transform Infrared (FTIR) spectroscopy for demonstrating the efficiency of reflectance with a Focal plane array detector (FPA µ-FTIR) to study silk protein structures at the micron scale for a rigorous, non-invasive study on large datasets of silk samples. South American historical textiles have been studied with FTIR coupled with multivariate statistical analysis to correlate the colour of the samples, the structural alterations of the protein samples with the age and the chemical nature of the dye present (Badillo-Sanchez et. Al., 2019).

2.4.2.3. X-ray fluorescence (XRF)

This technique can help in determining the chemical composition of samples varying from solids, liquids, slurries, and powders. It can also be used to determine thickness and composition of coatings and layers. XRF is an atomic emission method that measures the wavelength and intensity of light emitted by energised atoms in the sample. In this technique X-ray irradiation from an X-ray tube, creates an emission of fluorescent X-rays with the distinct characteristic of the energies of the elements present in the sample (Malvern Panalytical, 2020). Conservation studies done on the Huashan Rock paintings have demonstrated its usefulness in analysing the structural features and the composition of the rock as well as the paint pigment used (Agnew, 2010).

There are two types of devices, wavelength dispersive (WDXRF) and energy dispersive (EDXRF). The main difference between the two is found in the detection systems. The basis of all spectrometers is a source of radiation, a sample, and a detection system. WDXRF uses an X-ray tube as a source to irradiate a sample, and the fluorescence from the sample is measured by the detection systems, in this case, wavelength dispersion. EDXRF uses the same system, with just a difference in the detector type used to measure the energy dispersed from the sample. It can separate the radiation from the sample into the constituent radiation spectra of its different elements (Malvern Panalytical, 2020). The ARTAX 400 instrument has been used in several studies to measure heritage metal objects (Pospíšilová et al., 2016) as well as coins (Bolewski et al., 2020).

2.4.3. Limitations of the analytical techniques and instruments

Some of the relevant instruments, ranging from colourimeters to spectrophotometers, and the techniques for determining colour, physical, and molecular condition of samples has been previously discussed in section 2.4. As with any instrument, there are benefits and drawbacks, and to consider these instruments and techniques, there needs to be a clear understanding of how the technology relates to the needs and the expectations of the user (Chu et al., 2010).

It has been critiqued that instrument such as colorimeter do not fully take account of the minimally perceptible differences in colour discrimination based on aspects of photoreception and are affected by background noise (Forester et al., 2016). A limited range of wavelengths are measured, and these measurements are not based on the visual appreciation of colour. In particular, the visual colour difference between two samples is not linearly related to the difference in the XYZ values (Gilchrist and Nobbs, 2000). While colorimeters can produce accurate colour measurements, they are not able to identify metamerism or colour strength and cannot be used under variable illuminant (Ranganathan, 2016), the same colours from interfering material can sometimes create errors in the results (Patil, 2019).

Sophisticated spectrophotometers for high-end applications can be very costly ranging from £3000 - £10,000 (Fisher Scientific, 2020) and XRF fluorescence systems can range from £18,000 to £80,000 (Eastern Applied, 2018). Broadband detectors used in these devices respond to all light that reaches them, which may result in erroneous readings. A decrease in absorbency caused by stray light can reduce the linearity range of the instrument. PH impurities, temperature, and any contaminants can influence the sample, leading to errors in the readings (Geisler 2015) (Konica Minolta 2019B).

Certain techniques such as Raman spectroscopy, and polarised attenuated total reflectance infrared spectroscopy (pol-ATR) require micro samples for measurement, typically less than 1mg. Most of these techniques are not strictly non-destructive. Few of the instruments utilising these techniques can be used on site (Luxford and Thickett, 2011). According to Walthius et al., (1999) high-quality fibreoptic probes provide an advantage to in vivo Raman spectroscopy for the visible and NIR regions as compared to IR spectroscopy of 3- 12 ~tm IR-region. Although Raman spectroscopy is extensively used in heritage analysis, it has limitations in identifying textile fibres, due to the dyes found in these textiles. It has been noted that most of the Raman bands are derived from the dyes and represent only a small portion of the textile fibres repository. This significantly hinders its use in studying dyed textiles (Peets et al., 2019).

Badillo-Sanchez et.al (2019) have critiqued the *ATR-IR* technique and identified that when pressure is applied to the silk fibres, it may induce changes in the fibre structure, thus producing spectra that is similar for both new and aged fibre samples. ATR-FT-IR spectroscopy is the other most acknowledged analytical technique used for textiles. However, similarly to ATR-IR, its main limitation lies in the necessity to apply pressure to the sample textile, potentially causing damage to the sample. In rare and historically significant samples, this can be significantly limiting and sometimes unacceptable. To have a non-invasive contactless approach, reflectance mode can be used instead of ATR. By means of reflectance FT-IR (r-FT-IR) with micro spectrometer. Here, smaller portions of a larger object in situ can be analysed by controlling the position from where the spectra are measured. Multiple spectra can be collected in situ, of the surface of the sample, for spectral mapping. Despite these possibilities, r-FT-IR has been mainly considered for flat surfaces and has been overlooked for fibre identification (Peets et al., 2019).

Techniques that are progressively becoming more widely acceptable are X-ray fluorescence (XRF) and near-infrared (NIR) spectroscopy for their non-destructive and non-invasive ability to be able to be utilised for in situ analysis (Luxford and Thickett, 2011). Although XRF systems can be cost-intensive, near-infrared (NIR) spectroscopy has gained popularity by maintaining a balance between cost, time, and analytical performance across a range of materials (Beć and Huck, 2019).

2.5. Chapter Summary

This chapter has provided an overview of the standards of conservation in museums, and the analytical techniques and instruments prevalent in textile conservation. The current museum standards and guidelines, which come under the umbrella of preventative conservation, have been discussed along with their issues and limitations. This includes standards and guidelines such as MGC's Standard for Museum Care of Archaeological Collections (1992), Standard by the Society for Museum Archaeology, UK Standard 2012 and AICCM 2014. The research indicates that the current guidelines, although relevant, need to be reviewed on a collection-by-collection basis rather than an overall band category. Recently, it has been observed that museums that have maintained a loose interpretation of the grade boundaries for environmental monitoring recommendations, for their collections, have had issues with continued degradation, and a case for object-specific or case-in-case specific environmental conservation approach is favoured. Efficient condition management approaches are essential towards extending the life of the objects to avoid the need for potentially expensive and disruptive repair works, which may damage the heritage value of the object. (Idris et all, 2010). There is a need to determine the full extent of material susceptibilities, within the context of the museum's' environmental conditions, and to understand the associated degradation mechanisms for promoting preventative conservation (Ashley-Smith, 2018).

Textiles form a large portion of museum collections, and the pathways of degradation are discussed. Silk conservation studies have been reviewed, along with the current limitations of the accelerated aging techniques. It has been found that most of the published work reviewed for silk conservation has used accelerated aging methods to determine degradation, with limited comprehensive studies into non-invasive and non-destructive in situ techniques. Most of the discussed techniques have proved their effectiveness in laboratory tests, however these have invariably still required the use of micro samples, such as fibres in most studies. This is not necessarily a practical and efficient approach when dealing with artefacts, for example, upholstery and textiles such as tapestries, which are not easily moved from the location of their display for analysis. For such artifacts a non-invasive, non-destructive approach that can analyse the objects in museum conditions is sought. Efficient condition management approaches are essential to extending the life of the objects to avoid the need for potentially expensive and disruptive repair work, which may damage the heritage value of the object. (Idris et all, 2010). There is a need to determine the full extent of material susceptibilities to degradation in their given environment, and to understand mechanisms of change for preventative conservation (Ashley-Smith, 2018). Masciotta et al., (2019) present a conservation strategy aimed at standardisation of inspections procedures, documentation, and classification criteria based on a unified rating system for condition and risk assessment but mainly for protecting cultural heritage buildings and architectural asset categories.

The latter section of the chapter provides an overview of the state-of-the-art instruments used for silk conservation studies. The analytical techniques and methods used are also reviewed. The instrumentation used in most of the reviewed silk conservation studies, has broadly varied between different types of colourimeters and spectrophotometer. Although, spectrophotometers are more sophisticated and have wider spectral range, they are far more expensive and, in the main are not handheld, thus having limited portability. Consequently, they require samples to be sent to laboratories, which has been the most significant criticism of these non-portable instruments. Current techniques such as XRF and near-infrared (NIR) spectroscopy are increasingly becoming portable. However, NIR spectroscopy requires a suitable reference dataset for comparison. Whereas, Colourimeters have proven to be accessible, portable, and affordable to measure colour in situ. These measurements can be applied to the CIE international standards of colour spaces to determine colour of the samples. Recently published studies have successfully combined colorimetric data with statistical modelling, as well as graphical image modelling to study degradation in silk. The next chapter will detail the methodology developed with the colorimetric instrumentation and analytical techniques used to help in decision-making for silk condition monitoring in museum conditions.

3. DIAGNOSTIC AND PROGNOSTIC HEALTH MANAGEMENT METHODOLOGY

The following chapter introduces Prognostic, and Health Management (PHM) widely used in medicine, electronics, nuclear energy and building maintenance. It is applied, to the development of a non-invasive, non-destructive, data-driven methodology for silk conservation. An exponential decay model is adopted to determine the rate of silk degradation, based on the environmental conditions that the Shrewsbury Set, is displayed and stored under. These predictions can be used to inform decision-making relating to the prolongation of the remaining useful life (RUL) of the silk, thus minimising the need for costly, reactive interventive restorations. The protocol addresses the problem definition, data collection, data analysis, and the derivation of a postulated diagnostic and prognostic colour degradation model.

3.1. Overview of Prognostic and Health Management

Prognostic and Health Management (PHM) is a methodology that aids in the monitoring of the health of a system, in real-time, by dynamically updating the reliability function (hazard rates) based on in-situ measurements and bespoke evolution models obtained from historical data (Tsui et al., 2015). The terms 'diagnostics' and 'prognostics', are used to describe the broad range of processes, which aim to determine the material's condition at the present time as well as at a later pre-determined time (Rosunally, 2012). Diagnostics relates to the detection and isolation of faults or failures (Pecht, 2008) to determine the state of an item to perform its function (Hoffman 2007). Prognostics is the method of predicting a future state by basing it on the current and historical conditions (Pecht, 2008). In (Baraldi et al., 2013), prognostics is described as the process of providing reliable predictions about the RUL of a system or component undergoing degradation. The phrase 'Health Management', as is typically applied, relates to the ability to make appropriate decisions in advance, about the operational use of a system, where the maintenance of that system is based on the diagnostic and prognostic information available from the system and its environment (Hoffman, 2007) (Rezaeianjouybari and Shang, 2020). With these three elements defined, PHM is a methodology for the evaluation of a system, to predict and mitigate failures (Sun et al., 2010). PHM provides actionable information that aids decision support (Vogl et al., 2019) and is seen to produce economic benefits for owners, operators, and society (Rezaeianjouybari and Shang, 2020). In industry, the aim of PHM has been to provide an approach and tools necessary to design optimal maintenance policies for a specific useful asset (as an example), in the context of its distinct operating and degradation conditions. The result is to operate the asset at high availability, and at minimal costs. In practice, PHM as seen in this example of an industrial asset, would consider the fault diagnostics, in terms of the of the type of fault, its origin, and the conditions under which the fault occurred. It would then apply prognostics, to predict the RUL of the asset. Finally, the PHM model considers the health management of the asset, supporting contextualised decision-making relating to its operation, the availability of resources to fix and maintain it, and the financial cost benefit of doing so (Fink et al., 2020). Therefore, in summary, the outcome of an effective PHM model is to provide an ability to monitor the progression of the fault and to help in making assessment decisions (Rezaeianjouybari and Shang, 2020).

As previously discussed, degradation modelling, is part of the PHM model, and attempts to probabilistically characterise the evolution of the physical degradation processes (Gebraeel et al., 2009). The preservation of a system or a product through its lifecycle is the key objective for most maintenance approaches. Traditional approaches are, in the main, reactive resulting in issues such as unscheduled downtime, significant damage to the product or system, and higher inherent costs to remedy the problem. Maintenance processes have evolved from this reactive approach to those based on time-based maintenance (TBM), and subsequently to reliability-based techniques. The development in machine diagnostic techniques has led to the concept of condition-based maintenance (CBM), which relies on detected symptoms of failure to enable preventative actions. PHM goes beyond CBM by providing predictions of the future condition of an object to enable actions to be taken to avoid failure (Vogl et al., 2019).

The critical objectives of PHM include (Pecht, 2008) (Zhang et al., 2008):

- Providing early warning of fault or failures
- Providing guidance to extend the useful life
- Allowing reduction in unscheduled maintenance or repair
- Reduction in costly inspections and down time of product or system
- Improving design, qualification, and logistical support of fielded and future systems
- Supporting business and regulatory decisions

A viable PHM methodology provides an early detection and isolation capability, together with effective tools to monitor the progression of the fault. Furthermore, it aids assessment decisions and maintenance schedules (Rezaeianjouybari and Shang, 2020). Figure 3-1 provides an overview of the general and essential PHM methodology.

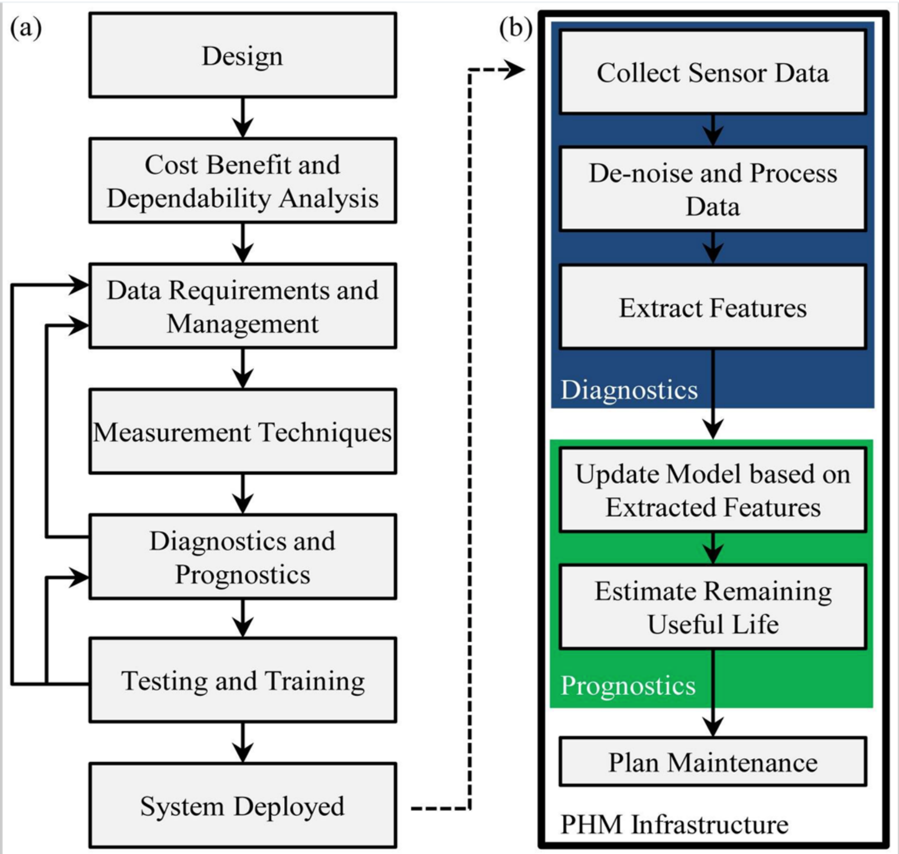

Figure 3-1: a) General PHM and b) Essential PHM

(Source: Vogl et al., 2019)

Diagnostics are based on observed data, fault detection, knowledge about the current operational and environmental system. Prognosis is dependent on historical health condition, current health, previous maintenance history and expected use in the future (Goh et al., 2006). Even though diagnostics and prognostics each have a separate goal, they are tightly coupled methods. Furthermore, health management utilises the diagnostic and prognostic information to provide the capability to make informed decision-making (Kumar and Pecht, 2010).

There are many mathematical models used for diagnostics and prognostics. These are based on statistical reliability, life cycle load, state estimation, and feature extraction (Kumar and Pecht, 2010). Figure 3-2 provides a general overview of the types of prognostic approaches.

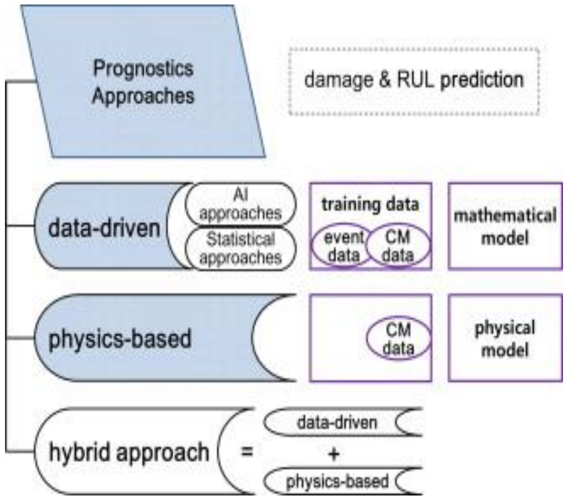

Figure 3-2: Categorisation of Prognostic Approaches

(Source: An et al., 2015)

The general methods for using prognostic and health management are as follows:

- Data-Driven – Data-driven methods are derived from the pattern recognition theory based on statistical and routinely monitored system operating data (Goh et al., 2006). This method allows for the usage of derived measures of data for estimating the current and future health of the system. Data-driven methods rely on the availability of observations collected during the degradation process relating to the target object or similar objects from which RUL predictions can be directly or indirectly derived (Baraldi et al., 2015). Data driven prognostics can be conducted via algorithms modelling and reasoning (Zhang et al., 2009). The requirement of datasets and good training data are essential for the data-driven approach. Data-driven prognostics employ degradation models, as well as measured information to achieve better accuracy for predictions such as artificial neural networks (ANN) and similarity-based regression techniques (Hu et al., 2012) (Baraldi et al., 2015). They provide an informative estimation of the entire degradation path, which can be checked against expert opinion to verify consistency (Baraldi et al., 2015).

- Model-Driven - Model-based prediction technology relies on combining the operating mechanism and the physical failure model. Insufficient modelling information and changes in physical behaviour or environmental conditions may limit its prediction accuracy (Fan and Zhao, 2017).

Physics of failure methodology and underlying system degradation models are the basis for the model-based prognostic approach (Hu et.al 2012). The main limitation of Physics-of-Failure models is the inability to capture real-life conditions in the remaining useful life predictions (Rosunally et al., 2011) and they require a good understanding of the failure mechanisms involved to define the relationship which may not be accurate for real-time applications (Kumar and Pecht, 2010). Model based methods assume that a mathematical model of the degradation process is available. This approach requires detailed knowledge of the degradation mechanisms and their interaction. Furthermore, these models require explicit account of uncertainty in the evolution of degradation (Baraldi et al., 2015).

- Hybrid - Hybrid approach combines both the data-driven and model-driven approaches. They address the problem of limited data associated with the data-driven approach. This provides greater stability as the degradation model does not change, as compared to fluctuations of predictions in the statistical approach. However, the statistical information is only used to update the physical model parameters and not for reliability prediction. In the case of an inaccurate physical model the hybrid approach would increase computational cost and not improve the predictive accuracy (Hu et.al 2012) (Fang and Zhao, 2017).

With the growing pervasiveness of sensor data and powerful computing, PHM has been successfully adopted across various industries such as aerospace, smart manufacturing, transportation, and the energy sector. Common across these fields, is the ability for PHM to transform raw data into information that can be actioned to assist safeguarding decision making (Lee et al., 2017) (Rezaeianjouybari and Shang, 2020). PHM has emerged as a vital method for gaining competitive advantage through an improvement in reliability, maintainability, safety, and affordability. Vogl et al., (2019) review the current capabilities and best practices of diagnostic and prognostic approaches in manufacturing and indicate that PHM is still an area emerging, with the significant portion of published research being limited in scope. Developments in mechanical engineering, electrical engineering, and statistical science have helped in the development of PHM concepts and components (Tsui et al., 2015). The aerospace industry has adopted systems prognostics for systems health inspections on spacecraft and aircrafts. Most of the metrics have focused on monitoring condition of the aircraft structures, avionics, wiring, propulsion systems, power supplies, maintenance scheduling and asset purchasing systems (Saxena et al., 2008).

Diagnostic and prognostics have had a long tradition in medicine. The historic use of prognostic indicators has been to aid decision-making in the identifying of metrics for blood pressure, cholesterol levels (Saxena et al., 2008) and cancer survival rates (Lu et al., 2020). Recently studies conducted for COVID-19 modelling have adopted prognostics approaches. Prognostic predictors are being used for detecting elevated cardiac biomarkers such as creatine kinase isoenzyme (CK-MB), myoglobin and troponin I for COVID-19 patients. The study utilises LASSO regression analysis to study 357 patients divided into non-recovery group and recovery group. The study concluded that COVID-19 patients with elevated CK-MB and myoglobin on admission may be effective predictors for adverse outcomes and the combined use of CK-MB and myoglobin had a better performance for predictions (Yang et al., 2019). Jain et al., (2020) studied COVID-19 related neuroimaging findings for thromboembolic complications to determine the prognostic marker of poor outcomes.

Increasing energy demand has advanced the diagnostics and prognostics to study the feasibility of extending the life of the nuclear reactors, the average life of which is 20-30 years. Data records like overall plant operating efficiency and maintenance, and machinery repair records are used to derive cost-benefit analysis for prognosis. Most metrics developed so far have been to establish a profitable business case rather than maturing prognostics itself (Saxena et al., 2008). Recent study Kim et al., (2018) have utilised PHM to predict the future degradation states of nuclear power plants (NPP). The authors presented an application of particle filtering for the prediction of degradation in steam generator tubes. Baraldi et al., (2015) utilised the Gaussian process regression (GPR) to build a stochastic model of the equipment degradation of nuclear components. GPR is a probabilistic technique for non-linear parametric regression that estimates the distribution of the future equipment degradation states by constraining a prior distribution to fit the available training data, based on Bayesian inference. The study was promising in its modelling of the degradation of ferritic steel exposed to high stress and in modelling the clogging of sea water filters, used in the heat exchangers of boiling water reactor (BWR) condensers. Training data was taken from sequences of degradation collected from a set of similar historical equipment which had undergone a similar degradation process.

The diagnostic and prognostic health monitoring system for structures such as bridges, and buildings, is also often referred to as Structural Health Monitoring (SHM). SHM can provide accurate feedback on the health of a structure and aid in discovering and preventing performance degradation or even failure (Yao et al., 2019). SHM is a non-destructive technique that involves analysing natural frequencies of structures with the help of sensors (Mahmud et al., 2018). Cost-effective conservation of historical material is a growing concern for many organisations in the heritage sector. Salonen &

Deleryd (2011) state that maintenance is often a reactive operation and maintenance departments are often considered cost centres, that are required to constantly debate the maintenance of their budgets for conservation. According to a survey, Kayan and Forster (2009), despite a general recognition that the protection and maintenance of historic buildings should, as a matter of best practice, adopt proactive maintenance, it is often not adopted or implemented, although reactive maintenance is more costly when measured against expenditure for proactive (preventative) maintenance. This is represented in the relationship graph in Figure 3-3, illustrating the cost between planned and unplanned maintenance.

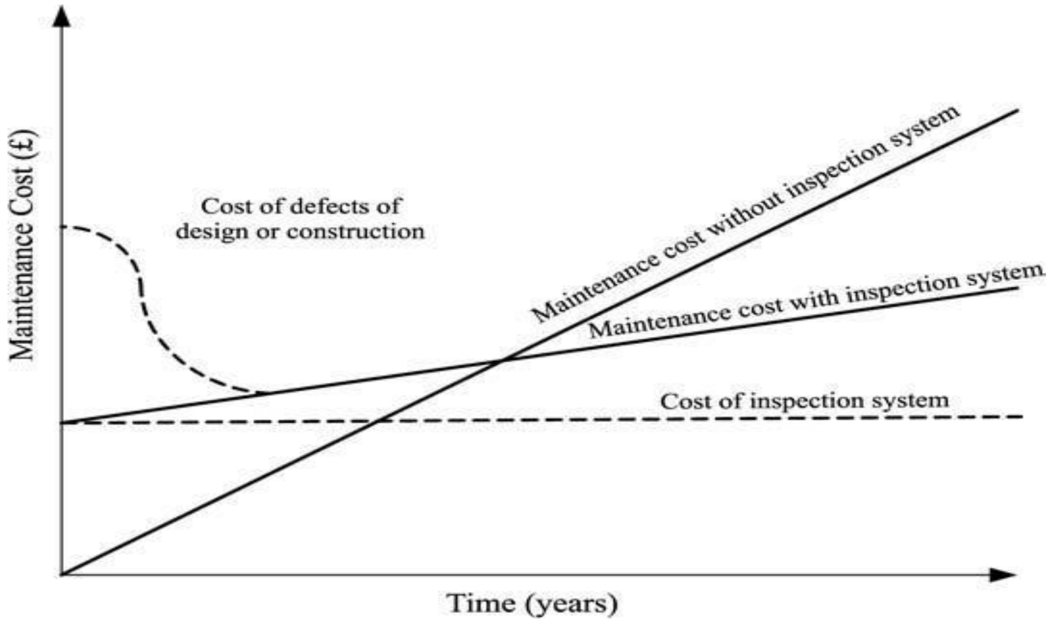

Figure 3-3: Planned and unplanned maintenance cost

(Source: Kayan and Forster, 2009)

Kayan and Forster (2009) further distinguish between repair and maintenance stating that while repair work is effective in prolonging the life of the element, it also involves damage to the fabric by reconstruction. The minimum intervention approach is recommended as it inflicts the least harm to the fabric of the object, thus potentially maintaining the historic object's authenticity. Like all objects, heritage objects are also exposed to factors that cause its deterioration and require continuous care and protection to limit its impact. Efficient maintenance management is essential in extending the life of the objects to avoid the need for potentially expensive and disruptive repair works, which may damage the heritage value of the object (Idris et al., 2010).

The use of the PHM framework in conservation science, to determine the deterioration of historical artefacts is documented in study by Rosunally et al., (2011). The research developed a prognostic framework to monitor the health of the iron-structure and fabric of the Victorian ship, the Cutty Sark, to conserve it, with an allowance for minor deterioration. The PHM framework encompassed canary and parrot devices, physics-of-failure (PoF) models, precursor monitoring, data trend analysis and Bayesian networks to develop a fusion approach to determine the ‘Health” of the iron structures of the Cutty Sark. In a study to determine the structural health of historic Duomo of Parma in Italy, Garziera et al., (2007), used non-destructive and non-invasive sensors. Laser Doppler Vibrometry was used to detect the structural degradation dynamically. This allowed for the identification of the frequency spectrum of the structure by modal responses and the computation of the damage.

Figure 3-4 illustrates the typical PHM workflow.

- *Fault diagnosis* - is the first task in the workflow to identify and diagnose the root causes of the system failure. This forms the basis for the prognostic model accuracy.

- *Prognostics* –the second task takes the processed data and the existing system models or failure mode analysis as the input to predict failure and degradation of the system by utilising the developed library of prognosis algorithms.

- *Condition-based maintenance* – is the third task that utilises the prognosis results in the form of RUL and enables preventative decision-making with different maintenance actions to minimise operating costs and risks. The key significance is that the three tasks need to be executed dynamically and in real-time.

Typically, in the current data-rich environment, large sets of data are gathered automatically within short time periods, and this amount of data poses new challenges in data management, analysis, and interpretation. Thus, data pre-processing and feature extraction have become standard to enable better analysis of data by reducing complexities and noise. The prognosis and diagnostic algorithms can also be developed offline, if need be, to cater for special signals and systems properties. Statistical algorithms can also be used with new sensing signals to compute the distribution of RUL and find root causes of abnormalities (Tsui et al., 2015).

Fault diagnosis, prognostics, and condition-based maintenance are the three significant dynamic tasks and the remaining tasks in Figure 3.4 can be prepared at timely intervals or offline.

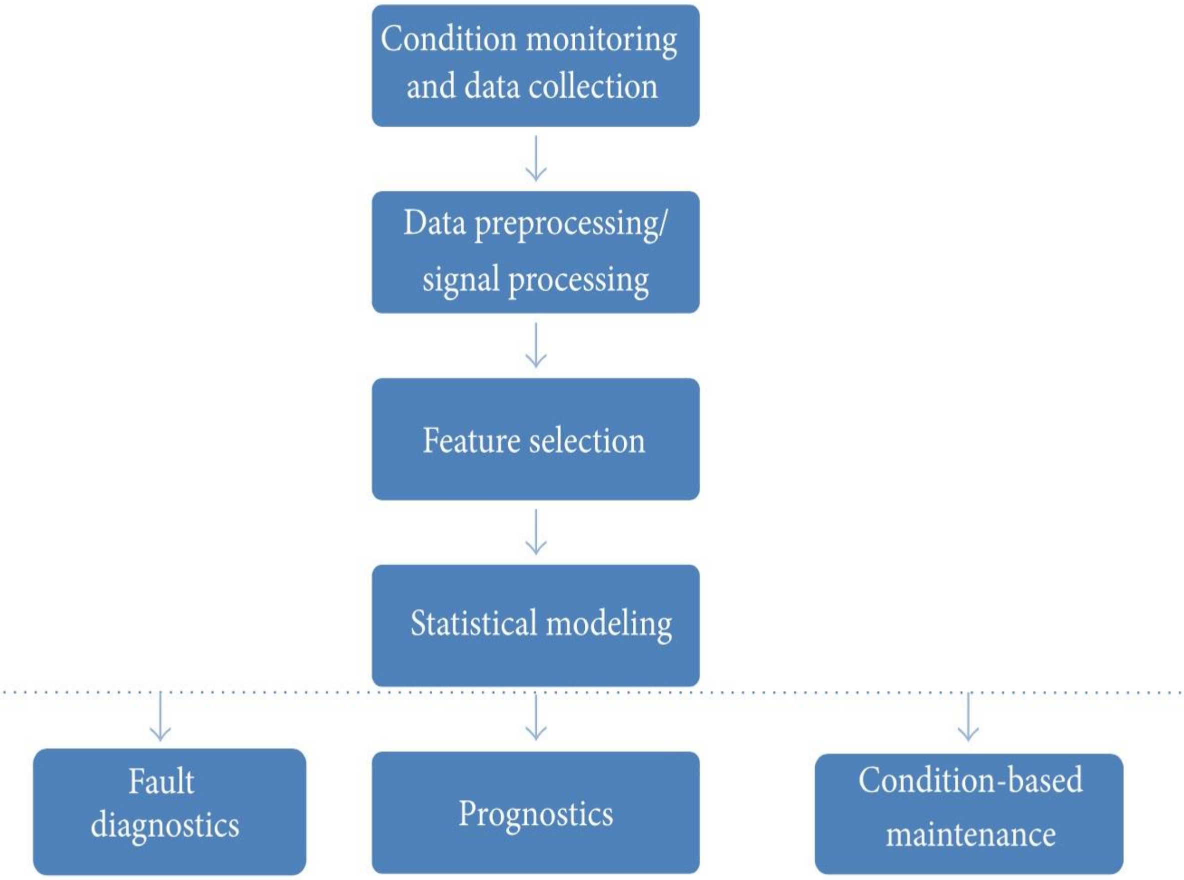

Figure 3-4: Overview of PHM workflow system

(Source: Tsui et al.,2015)

Data-driven models can be used, where PoF models are not available or where there is limited knowledge about the physics of the object being analysed. Data driven approaches can be utilised to detect changes in object parameters because of aging or gradual degradation. The parameter data collected around the time of occurrence of intermittent faults as the object ages and aids the prediction and assessment of the object's health. The prognostic is not developed as diagnostics, but is feasible through modelling with Markov chains, stochastic processes, and time series analysis. These help in predicting the future state with the help of historical data. The accuracy is continually updated and associated with predictable variation although it is reliant on sufficient and reliable data. There is also a lack of a standard approach in defining thresholds through which precursors and faults can be detected or predicted (Kumar and Pecht, 2010).

Statistical data-driven approaches for RUL are better suited to model situations with limited data and for systems with no observed failure data and where no CM information exists. Remaining useful life is the useful life left of an object at a particular time of operation. RUL is random and unknown and is obtained from condition and health monitoring techniques. There is no universally ideal approach due to its complicated relationship with observable health information. Statistical data-driven models rely on past observed data and statistical models and are broadly seen in two types: those that rely on the direct observed state of the object and those that use indirect parameters (Si et al., 2011). Figure 3-5 details some of the condition data for statistical data-driven approaches.

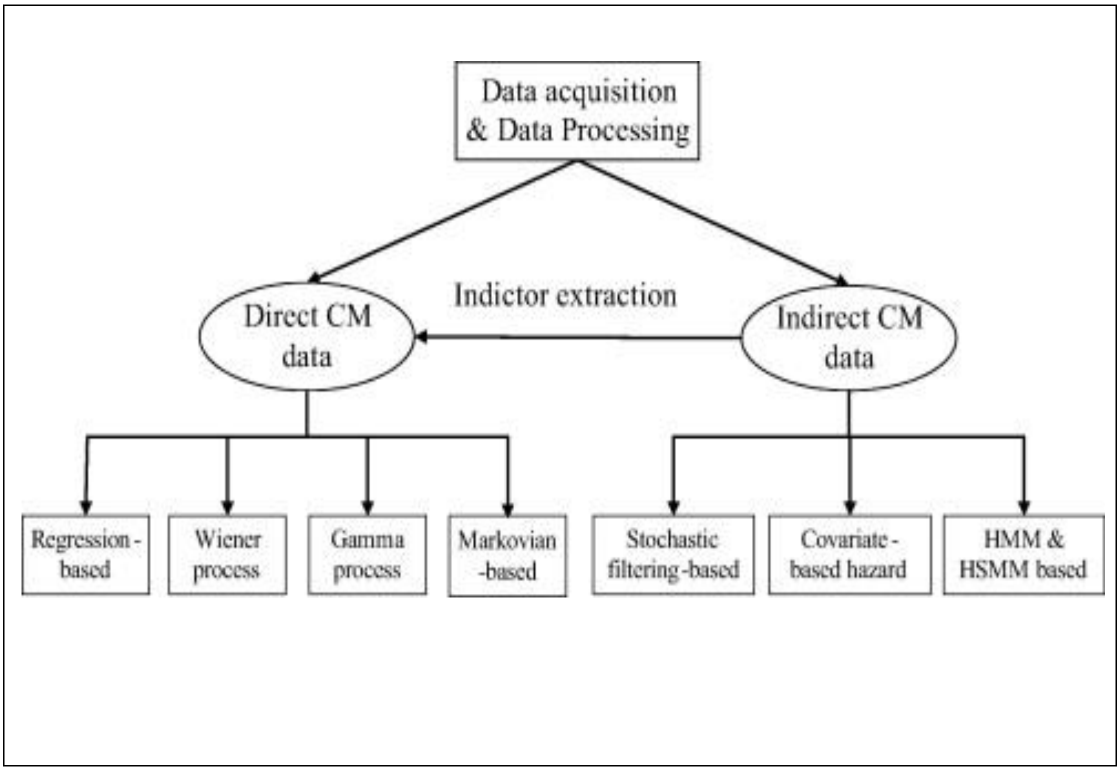

Figure 3-5: Classification of statistical data driven approaches for RUL estimation

(Source: Si et al., 2011)

Direct condition measurement is sometimes not possible, or CM data may be scarce given that some assets are not allowed to run to failure. For such instances, PHM must be flexible enough to use sensors and parameters to infer degradation information (Hess, 2005 cited in Vogl et al., 2019, p.91).

Most of the existing published work train their models using public data, collected under laboratory conditions (Rezaeianjouybari and Shang, 2020). Natural ageing is very difficult to simulate as the history of a textile is generally difficult to determine. Thus, available public data is derived mainly from newly woven silk and not on historic silk. The direct correlation of the newly woven silk samples to historic silk has proven to be inconsistent (Tamburini and Dyer 2019). Therefore, it is necessary to study physical attributes as well as environmental data and to develop evaluating techniques which analyse the interactive effects of these deteriorating agents. Therefore, offering a more accurate estimation of the silk's permanence (Sharif and Esmaeli, 2017). More work on domain adaptation is required to reach superior domain generalisation ability, which can create feasible models in practice.

The evolution of smart sensors and IoT technologies has eased some of the industrial data scarcity issue. Nonetheless, more data means more noise and uncertainty associated with the operating environment, various data sources and data transmission, all of which needs to be addressed. Real-world data comes from various sensors and are mostly non-structured, multimodal, and heterogeneous, which makes the task more complex. New generative models that create temporal dependencies and create valid time-series data in time and frequency domain can be utilised to address the gap of real data (Rezaeianjouybari and Shang, 2020).

3.2. Developing the PHM Methodology

Methodology is a collection of procedures, techniques, tools and documentation. It consists of phases to plan, manage, control, and evaluate projects to address a problem situation with the help of data analysis and data modelling (Evison et al., 1992). The data driven PHM methodology as discussed in 3.1, is developed for the diagnosis and prognosis for determining the health or "colour condition" of the Shrewsbury Set silk, part of the Wallace Collection.

The overall PHM workflow adopted uses a diagnostic and prognostic approach to predict the RUL of the silk as depicted in Figure 3-6.

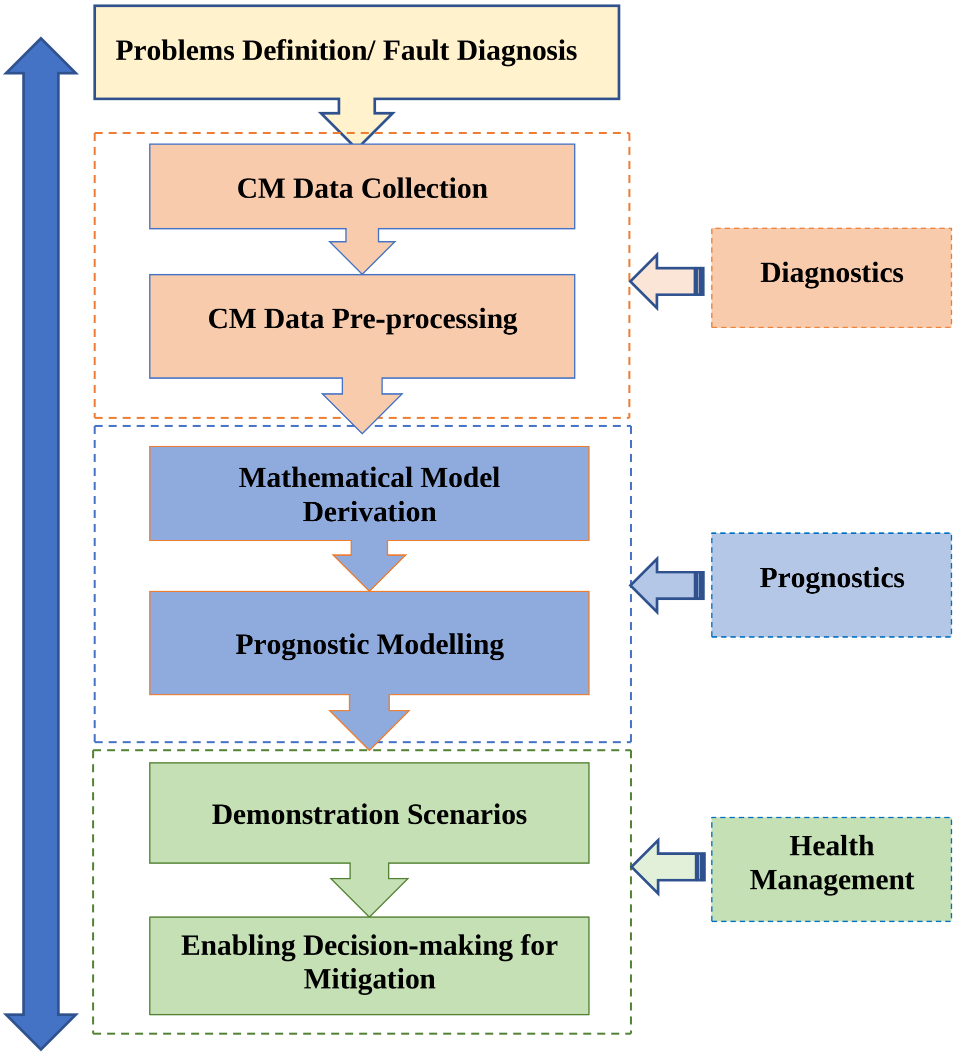

Figure 3-6: PHM Protocol adopted

The essential PHM protocol identified in Figure 3.1 has been fully adopted to develop a discretised data-driven model for determining silk degradation in its ambient museum environmental conditions. However, only certain protocols from the Figure 3.1 (a), the general approach, have been utilised for this methodology. For example, data requirements and management has been adapted to include the problem definition. Measurement techniques have been adapted as CM data collection. Diagnostic and Prognostics, which is one phase in the general protocol, has been split into their own sub phases. Testing and training phase in Figure 3.1 has been combined as, prognostic modelling.

3.2.1. Problem Definition/Fault Diagnosis

The Problem Definition or Fault Diagnosis, as detailed in this section, adapts the cost benefit and dependability analysis of the PHM general protocol, as seen in Figure 3.1 (a), to identify the existing fault. Fault detection is defined to be the task of determining if a system or asset is experiencing problems (Tsui et al., 2014). Health assessment of the asset involves estimating its health by analysing collected data, and if failure data is unavailable, then degradation monitoring or fault detection for abrupt faults can be used (Lee et al., 2017). The data can be objective or subjective, depending on the nature of the data and the collections method (Si et al., 2011). The determination of the problem definition for this research was established through a combination of analysis techniques for capturing requirements, such as structured open-ended interviews with museum subject matter experts, observation of their existing systems, environmental monitoring sensor data and the use of archived documents relating to the object collection and care of the silk, as provided in the Appendix 8.1 and 8.2. For the scope of this project, the subject matter experts' opinion was taken into consideration with the help of visual inspections initially, to identify the lowest acceptable threshold or point of failure of the silk sample on display in the museum's Great Gallery. For example, in the case of the silk in the collection, this related to an unacceptable level of increased fading of the colour of the silk and loss of material in the form of fraying. Such a point of failure represented the point at which the silk had deteriorated to such an extent that it would have been taken away from display in the Great Gallery, to undertake costly restoration.

3.2.2. Data Collection

This section reuses the measurements techniques of the PHM general protocol of Figure 3.1 (a), to gather condition data. Observed health information through constant inspection is often referred to as condition monitoring (CM) data. It can be directly related or indirectly related to the asset health status and can be viewed as its health indicator (Tsui et al., 2015). For the scope of this research, both direct and indirect CM data have been considered. The direct CM data was collected by measuring the silk with a colorimeter to determine the colour condition of the silk using the CIE XYZ colour theory, as discussed in section 2.4.1. To determining the colour fade, the International Commission of Illumination (CIE) 1931 CIE XYZ colour system has been applied. This colour system is the standard for the quantitative expression of colours seen by the human eye and represents the colours as tristimulus values *XYZ* (Murata et al, 2018).

The CM data may be insufficient; hence any degradation information such as environmental information, sensors, temperature, moisture, relative humidity, light levels can be used to estimate the health (Si et al., 2011). For the scope of this research, the environmental sensor data of light levels, relative humidity, and temperature have been included, as indirect CM data. The sensor data was collected in the form of readings in TimeDate variable format. These Timestamps are the most common example of TimeDate variables, and they vary in their specificity ranging from 10 minutes to approximately 30 minutes. The sensor readings of the temperature, light, and relative humidity maintained were collected from the available sensors. Further details of the data collected are discussed in Chapter 4. Figure 3-7 illustrates the condition data inputs.

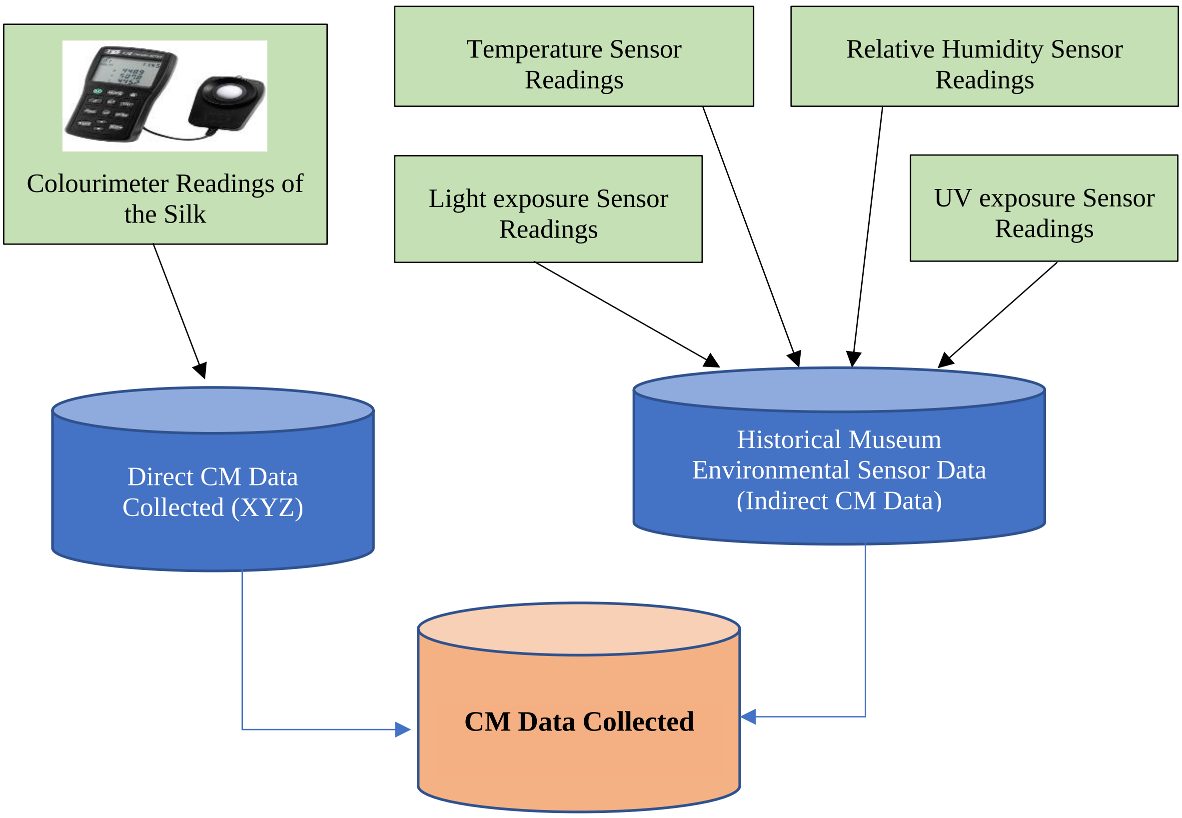

Figure 3-7: Condition Monitoring Data Collected

3.2.3. Data Analysis

This section uses diagnostics in Figure 3.1 (a) to observe data, identify the fault and acquire knowledge about the environmental system. Data pre-processing or feature extraction includes data cleaning, data quality evaluation, and segmentation. It is an important part of the PHM approach as it helps in identifying valuable parts of data whilst increasing the efficiency of data analysis by removing unwanted segments and redundancy (Tsui et al., 2014) (Lee et al., 2017). The data analysis techniques for data pre-processing or signal processing can be generally classified as statistical methods and engineering knowledge-based methods. Some of these techniques, such as distance evaluation techniques (DET) in its various versions, can be applied such as the Euclidean distance evaluation technique (EDET), two-stage feature selection and weighting technique (TFSWT). For the prognostic analysis conditional data can be summarised into the following categories (Tsui et al., 2015):

- Value type - for example temperature, humidity, pressure, etc.
- Waveform type – for example vibrational data, spectral, etc.
- Multidimensional type – for example image data, X-ray images, etc.

Both the forms of CM data gathered, direct and indirect, were collected and analysed statistically to remove redundancies and improve data efficiency as discussed below.

The direct CM data was derived by measuring the silk with the colorimeter, the TES 136 Chroma Meter. The waveform type of data was measured in the form of XYZ ratios of CIE colour theory. The instrument used was a portable device that could measure in situ and provide tristimulus values XYZ. To maintain the consistency of readings, equidistant multiple readings were taken of a pre-selected area of the silk. The XYZ values were then treated with Euclidean distance formula to determine the colour condition of the silk, based as shown, in the following equation (1) (McLaren, 1983 cited in Roy Choudhary 2015, pg. 3):

$$\Delta E = \sqrt{X^2 + Y^2 + Z^2} \tag{1}$$

ΔE was calculated for all the data points of the silk and was derived from the measurement obtained with the colourimeter tristimulus values XYZ, to provide the colour condition C of the same silk object in various instances of the silk's display and storage within the museum environment. Total colour difference, 'E' stands for "Emfundung,' the German term for sensations. The XYZ colour space is not visually uniform, and the visual non-uniformity can be reduced by linear or non-linear mathematical transformations (Choudhary, 2015).

The indirect CM value type of data was collected in the form of sensor readings of the museum environment. The sensor data included light levels, UV, relative humidity, and temperature, each collected in TimeDate variable format. Any gaps or missing values in the four environmental parameter readings were removed. UV readings were found to be capturing null readings by museum sensors and hence were excluded from the modelling. The rest of the environmental parameters were utilised. Time-domain statistical techniques such as the mean were calculated, to understand the environmental pattern of the museum environment in the Great Gallery. Although daily readings were being generated by the sensors, it is the long-term historical environmental pattern that is useful. Hence, the museum's monthly and yearly mean temperature was calculated. The same was done for all the environmental factors, such as the annual average relative humidity and annual average light level.

3.2.4. Mathematical Model Derivation

This section is an addition to the general process identified in Figure 3.1 to derive the prognostic model. Studies reviewed in Chapter 2 state that the degradation and fade of dyes in silk is a complex process. Chakraborty (2015) indicates that silk degradation is dependent on Temperature, Humidity, Ultraviolet *(uv)* and Visible light (v). Koperska et al. (2015) and Vasileiadou et.al., (2019) state that visible light and UV light induces damage to dyed silk visually, structurally, and chemically. A study by Kirby and Saunders (2004) indicates the degradation of dye in silk reveals monotonic rates of degradation in the presence of both Relative Humidity (RH) and light. As the light increases the RH increases and higher RH results in greater colour change, and it was observed that dyed silks kept in the dark were not affected. It has been further noted by Nishimura (2011) and Padfield (2004), that degradation, in general, is proportional to relative humidity (RH) and Arrhenius Constant (k.) Based on the published studies on silk dye fade degradation, it can be postulated that the rate of change with time of the silk degradation, *D*, is defined in terms of colour fade. Relative humidity, temperature, and light are the key environmental factors that affect the rate of reaction monotonically.

Thus, the rate of degradation in respect to time increases monotonically with the increase in relative humidity:

$$\frac{dD}{dt} \text{ } increases\ monotonically\ with\ (RH) \qquad (2)$$

The rate of a reaction depends upon several factors, including absolute temperature and activation energy. This may be expressed in the Arrhenius equation, k = $Ae^{\frac{-E_a}{RT}}$ (Arrhenius Constant). Arrhenius is written in terms of the energy to drive a reaction and to see the effect of temperature, so it is the reaction rate. The known universal gas constant *R* and activation energy E_a are the unknowns. They can be transformed (bundled) into the formulated unknown model parameters. The universal gas constants and activation energy are not relevant for this model development. Thus, the rate of degradation in respect to time increases monotonically with the increase in Arrhenius constant k:

$$\frac{dD}{dt}\ increases\ monotonically\ with\ (k) \tag{3}$$

$$\frac{dD}{dt}\ increases\ monotonically\ with\ (lv + UV) \tag{4}$$

Where, v = Visible light (Illuminance) (in *lx*), UV = Ultraviolet exposure (in *mW/cm2*), *RH* = Relative humidity (in %), l = a constant.

The fading of the colours in textiles is due to the degradation of dyes in the fabric, which results in different degrees of loss of intact dye molecules (Ahn et al., 2017) (Liu et. al., 2019). This degradation process has been denoted as D. If C denotes the silk colour condition or state (for example, a colour measurement over an area), and dye molecules are converted from colour to non-colour by the process of degradation D, the rate of degradation depends on how much colour is left in an area. Hence it can be postulated that,

$$\frac{dD}{dt} \propto C \tag{5}$$

The extent of deterioration occurring in silk can also be dependent on factors such as condition of the fabric, dye, pigment used in the fabric, any glues used to bind the fabric together, display, and storage conditions. Besides light-induced damage, fluctuating humidity levels, as well as temperature, affect the degradation of silk (Vilapana et al., 2014). Gutarowska (2017), studied biodeterioration of silk fibres and found that these materials are more vulnerable to high humidity due to their chemical composition of cellulose and protein. Light damage is seen to cause cumulative damage to silk as the silk tends to lose flexibility, becoming fragile and leading to shredding, fragmentation, and eventually to the deterioration to the state of a powder. This gradual process is accompanied by discolouration, fading, or yellowing of the fabric, usually a useful indicator of the object's deterioration (Smith and Thomson, 2017), (Vilaplana et al., 2014). The artefacts deteriorate in the light as it enables photodegradation process to activate with RH (Wiltshire County Council Conservation Service, 2006). It can be assumed that temperature and light are both sources of energy, which could be additive in their effect and relative humidity enables the photodegradation to occur chemically.

Integrating terms (2) - (5) it can be postulated that:

$$\frac{dD}{\alpha t} \propto k(RH) + (lv)RH \ \cdot C \tag{6}$$

where k is the reaction rate that is represented with the Arrhenius constant k

Now the Arrhenius equation $k = Ae^{\frac{-E_a}{RT}}$ can re-arranged and written as:

$$k \ = \ A(e^{\frac{E_a}{R}}) \ (e^{\frac{-1}{T}}) \tag{7}$$

$$k \ = \ A\left(e^{\frac{E_a}{R}}\right)^{-1/T} \tag{8}$$

$$\text{Now, } \ e^{\frac{E_a}{R}} = \text{Constant B} \tag{9}$$

$$\text{Therefore } k \ = A \cdot B^{-1/T} \tag{10}$$

Hence equation (6) can be written as,

$$\frac{dD}{dt} \propto \left(A \frac{1}{B^{1/T}} (RH) + (lv)RH\right) C \tag{11}$$

Figure 3-8 illustrates an exponential decay model adopted to determine the rate of silk degradation D.

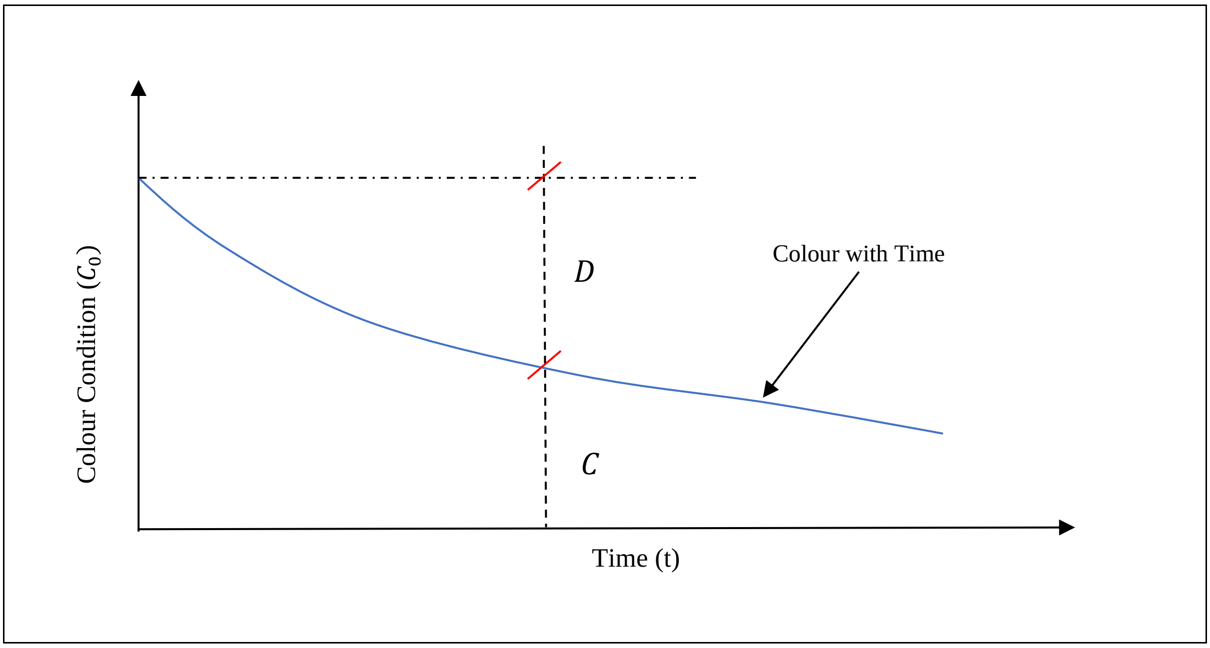

Figure 3-8: Exponential Colour Fade Model

Where C is the colour of silk at time t, C_0 is the colour of silk fabric at time 0.

From the degradation curve above, $C = C_0 - D$ *(12)*

$$\text{and } \frac{d}{dt}C = \frac{d}{dt}(C_0 - D) \tag{13}$$

$$\frac{dC}{dt} = 0 - \frac{dD}{dt} \tag{14}$$

$$\frac{dC}{dt} = \frac{-dD}{dt} \tag{15}$$

From equation 11, put $a = \left(A\frac{1}{B^{1/T}}(RH) + (lv)RH\right)$ (16)

Therefore, $$\frac{dD}{dt} = aC \qquad (17)$$

From equation (15), $$\frac{dC}{dt} = -aC \qquad (18)$$

Eq. (18) is an ordinary differential equation and is widely used for growth and decay rate.

The solution of this equation in terms of C can be derived as follows:

$$\frac{1}{C}\frac{dC}{dt} = -aC.\frac{1}{C}.\frac{dC}{dt} \qquad (19)$$

$$\int \frac{1}{C}\, dC = \int \quad -a\, .dt \qquad (20)$$

$$\ln|C| = e^{-at}\, e^{c} \qquad (21)$$

$$|C| = e^{-at+C} \qquad (22)$$

$$C = Ce^{-at} \qquad (23)$$

$$C = C_0 e^{-at} \qquad (24)$$

Temperature and light are both sources of energy, which could be additive in their effect, and Arrhenius constant k is written in terms of energy to drive a reaction and that RH facilitates a reaction. The Arrhenius constant can be linearised as the temperature values of the museum are consistent, thus resulting in a modified expression of the equation (Nishimura, 2011). The Arrhenius constant can be linearised as the temperature values of the museum are consistent, thus resulting in a modified expression of equation (16). Hence, it is postulated that:

$$a = [\alpha(n) + \gamma v]RH \qquad (25)$$

where α *and* γ = constants which must be solved for, and n is linearised expression of the temperature effect. The Arrhenius equation has been adapted to include the effect of temperature and utilised the rule of thumb to linearize the response over a sensible temperature range; for most reactions, the reaction rate doubles for each 10°C rise in room temperature. The rule proposed is for the rate to double, as room temperature goes from 18°C to 28°C (Clark, 2018), as illustrated in Figure 3-9:

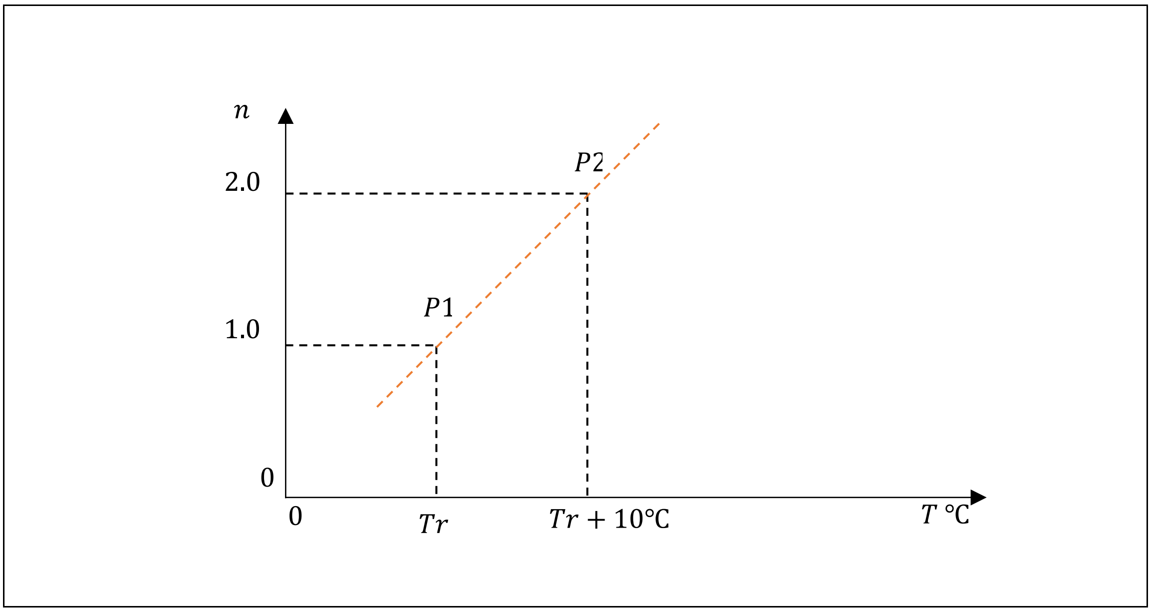

Figure 3-9: Linearisation of temperature effect

The linearised equation for the reaction rate *n* is expressed as

$$n = mT + b \tag{26}$$

where, T is temperature in Kelvin, m and b are constants.

At room temperature (Tr), i.e., at $P1$, $1.0 = mTr + b$ *(27)*

And at $P2$, $2.0 = m(Tr + 10) + b$ *(28)*

Eq. *(27)* and Eq. *(28)* gives, $1.0 = m10$ *(29)*

$$m = 0.1 \tag{30}$$

Substituting in Eq. *(26)* gives,

$$1.0 = 0.1Tr + b \tag{31}$$

$$b = 1 - 0.1Tr \tag{32}$$

Hence, the reaction rate n can be expressed as,

$$n = 0.1T - (0.1Tr - 1) \tag{33}$$

If $Tr = 21°\text{C} = 294K$ then, $n = 0.1T - 28.7$ *(34)*

If $Tr = 18°\text{C} = 291K$ then, $n = 0.1T - 28.1$ *(35)*

The minimum temperature of the room taken at $18°\text{C}$ which in Kelvin is $291K$; hence, it can be postulated that Eq. (25) can be re-written by integrating Eq. (33) as follows:

$$a = [\alpha(0.1T - 28.7) + \gamma v]RH \tag{36}$$

Where a = a constant which is a function of mean temperature TK linearised, Relative Humidity (RH), light levels (*lx*) over time *t*.

Therefore, integrating the values of equation 24 and 36, the fade model to be used is:

$$\therefore C_0 e^{-at} = C_0 e^{-[\alpha(0.1T - 28.7) + \gamma v]RH]t} \tag{37}$$

Thus, the final colour degradation model can be extrapolated as follows:

$$C(t,T,RH,v) = C_0 e^{-\alpha(T,RH,v)t} \quad (38)$$

Discretised $C = C_0 e^{\sum_{i=1}^{n}(-\alpha(0.1T_i-28.7)RH_i\Delta t_i-\gamma(v_i RH_{i)}\Delta t_i)}$ *(39)*

where $\sum_{i=1}^{n} \Delta t_i = t$ (forecasting time horizon in unit of years)

T_i, RH_i, Lv_i = Averaged values of temperature (in Kelvin), humidity (in %), and light (in lux) for the time period Δt_i

C = condition at time t

C_0 : the condition at time $t = 0$

$\alpha,\ \gamma$ = unknown model constants

Time intervals are in the unit of years, but can also be in the unit of months, weeks, or days. The data points which link colour condition to time are limited. Hence, the reference to causal information to published silk studies, as well as, to subject matter experts in the museums, helps to inform the model. Thus, the simplest empirical exponential decay model is derived as an optimal fit for the silk fade.

The constant C_0 is the new silk condition and as a parameter this should be known. In the case of historic silk, where the new condition is not possible to measure, C_0 can be treated also as an unknown parameter and be estimated along with $\alpha\ and\ \gamma$. These unknowns are solved using the measured data in silk conditions by minimising the model prediction error for the model expression (equation 39).

3.2.5. Prognostic Colour Degradation Model

This section uses the prognostics process identified in Figure 3.1 to identify the prognostic model for determining cumulative colour degradation. The data-driven prognostic model utilises the diagnostic information gathered through directly measured data of the colour condition C and the indirectly related CM sensor data of the environmental conditions, as inputs for developing the prognostic fade model by adapting the linearised Arrhenius reaction rate and CIE colour theory. The aim of the prognostic model is to predict the health condition of an object (Lee et al., 2017). According to Tsui et al., (2015), PHM underpins the assumption that the object is subject to stochastic deterioration. The forecast modelling for the different museum scenarios can provide information for mitigation.

Preventative conservation decisions can be based upon the specific conditions of the silk being studied. PHM model can be referred to as an optimising model, that enhances the efficiency of the data collected to arrive at the best possible forecast about the remaining life of the silk sample, within the model parameters established. This novel non-invasive, non-destructive data-driven modelling methodology for the conservation of silk fabrics in-situ, utilises Prognostic and Health Management (PHM) of engineering systems. PHM can help determine the "health" of an object under specified environmental conditions and to predict the remaining useful life (RUL) of the object. The originality of the proposed methodology is to predict silk fade that is a function of environmental conditions such as lighting conditions, temperature, and relative humidity.

Figure 3-10 provides a detailed illustration of the protocol, documenting the process of data collection, analysis, mathematical model derivation, exponential decay modelling for silk colour degradation, and finally, the forecasting of RUL.

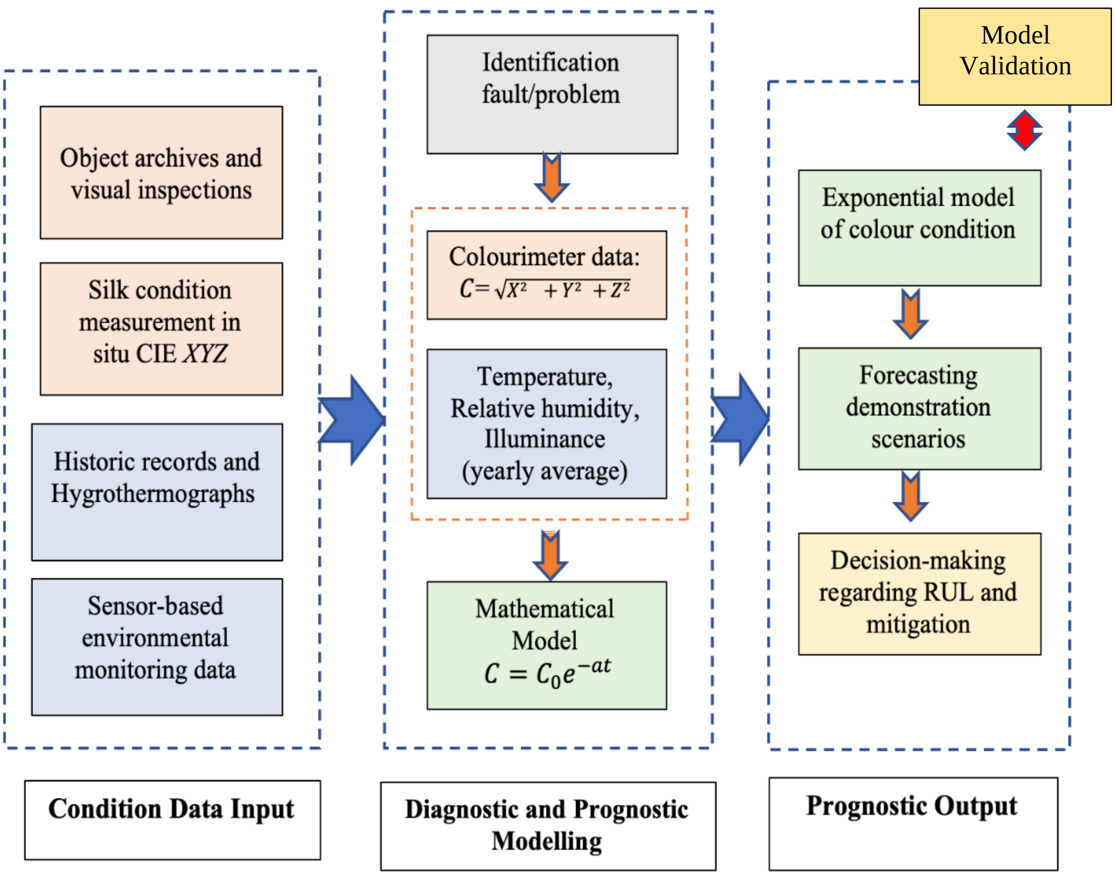

Figure 3-10: Protocol of the Data-driven Diagnostic and Prognostic Methodology

This is the first time that such a model has been presented that combines three of the environmental factors and condition data of the silk artefacts in ambient conditions. The PHM methodology developed in this work is applied and demonstrated for silk on historic chairs displayed in the Great Gallery at the Wallace Collection to aid decision-making. The model output can then be used to conduct sensitivity analysis based upon different environmental conditions under which the silk could be displayed, thereby allowing the museum staff to use predictive modelling methods to determine the cumulative colour degradation of the silk-based on these conditions.

3.3. Chapter Summary

This chapter provides an overview of the PHM methodology developed for studying colour fade. The growing prevalence of sensor data and powerful computing has enabled PHM to be successfully adopted across various industries such as aerospace, smart manufacturing, transportation, and the energy sector. Prognostic and Health Management (PHM) has been adapted to be used in museums to help determine the "health" of an object under specified environmental conditions. Diagnostics are based on observed data, knowledge about the current operation and environmental system. Prognostics, on the other hand, are based on historical data, knowledge of the system, use in the future, and future environmental conditions. Prognostics involve the assessment of the product or systems actual health, followed by modelling health degradation, prediction of performance and remaining useful life. Even though each has a separate goal, they are tightly coupled, as prognostics are built on diagnostic methods. PHM goes beyond condition-based maintenance (CBM) by enabling decision-making using future predictions.

A significant portion of published research into the development of PHM concepts and the framework applied in this study, has come from the fields of mechanical engineering, electrical engineering, medicine, and statistical science. Data-driven PHM models can be used, where physics of failure (PoF) models are not available or where there is limited knowledge about the physics of the product. Data-driven approaches can be utilised to detect changes in product parameters because of aging or gradual degradation. Statistical data-driven approaches for remaining useful life are better suited to model situations with limited condition data. PHM can use sensors and parameters that are placed for other functional purposes to infer degradation information. The development of the methodology based on an exponential decay model is documented, ranging from problem definition, data collection, data analysis, and data modelling approach.

The chapter details how the parameters in the mathematical model can be estimated, through measured data, and how the model can be used to predict the remaining useful life of silk artefacts. This is a new mathematical model for predicting silk fade that is a function of environmental conditions such as illumination, temperature, and relative humidity. It is the first time that such a model has been presented that combines all the factors. The chapter also details how the parameters in the mathematical model can be estimated, through measured data, and how the model can be used to predict remaining useful life of silk artefacts. The exponential decay model derived adapts linearised Arrhenius reaction rate and CIE XYZ colour theory to develop a predictive fade model for silk. The last section provides the detailed mathematical derivation of postulated data driven PHM model used to predict the cumulative damage to the silk on historic chairs displayed in the museum.

The next chapter details the data gathering carried out to develop the diagnostic and prognostic approach for silk colour fade in the Shrewsbury Set exhibited at the Great Gallery as part of the Wallace Collection.

4. DATA GATHERED FROM THE WALLACE COLLECTION

The following chapter details and documents the primary data collected for this research. A portable colourimeter is used to analyse silks in situ and is combined with environmental sensor data, to provide the inputs into the previously described prognostic model, as discussed in Chapter 3.

4.1. Data Description – Shrewsbury Set

The Wallace Collection is amongst the most distinguished cultural institutions in the United Kingdom. It houses a collection of art and artefacts, assembled from the private collections of the 4th Marquesses of Hertford and Sir Richard Wallace. The entire collection and the building, Hertford House, located in London's Manchester Square, was bequeathed to the nation by Lady Wallace in 1897 and opened to the public as a museum in 1900. The museum houses some of the finest collections of eighteenth-century French art, seventeenth and nineteenth-century paintings, medieval and Renaissance works of art and one of the finest collections of princely arms and armour in Britain (Wallace Collection, 2020).

The silk sample, at the centre of this research study, was provided by the Wallace Collection and is known as the Shrewsbury Set. It is estimated to date to c.1768-c.1770. The collection comprises of a set of two sofas and twelve armchairs with carved and gilded walnut frames, upholstered in silk, with a design of floral silk lampas. The design is representative of styles during the transition period, between Louis XV and Louis XVI, with straight legs and richly carved classical motifs of the latter period, and the lingering curves of the Rococo period (The Wallace Collection, 2020). The collection suffered damage over the years and some of the chairs were re-upholstered in the late 18th century using historically accurate silk to maintain authenticity to the original. Subsequently, the three chairs upon which this study is focused, were restored and re-upholstered, again using historically accurate silk, though this time woven and produced in 1956. The chairs were then displayed in the Great Gallery, the main exhibition hall in the museum. The silk on the chair as shown in the Figure 4.1. reveals some of the damage and colour fade, resulting from the continual display of the Shrewsbury Set since 1956. With close inspection, it is visible to the naked eye that the fabric at the front lower edge of the chair is faded and frayed.

Figure 4-1: Shrewsbury Set Silk 1956 sample analysed in situ

In addition to the 1956 restoration, two other chairs, as shown in Figure 4-2, also forming part of this research, were restored and re upholstered, one being restored in 1991 and the other in 1993, using the surplus silk fabric that was woven for the 1956 restoration.

Figure 4-2: Shrewsbury Set Silk samples 1991 and 1993 analysed in-situ

This surplus piece is seen in Figure 4-3. Prior to restoration, the historically accurate silk used, as seen in Figure 4-3, was kept in storage in an environmentally controlled room under $50\ \pm 10\%$ RH and temperature $16°\text{C} - 20°\text{C} \pm\ 2°\text{C}$, without any exposure to light.

Figure 4-3: 1956 Surplus silk sample in storage used for restoration

4.2. Colourimeter Readings of Silk Sample

Silk samples from the museum display were used to measure the colour condition of the fabric and to determine any damage caused by the environment in which they were kept, over the years of their display. Four samples were considered. Sample 1 was the silk sample reference, from the chair that had been on continuous display in the Great Gallery since it's restoration in 1956. Museum restoration records suggest that the silk had not been removed from the chair since its restoration. This reference sample had been exposed for the longest period to the open display conditions of the museum. Sample 2 was the silk sample reference, from the chair that had been restored with historically accurate silk, as seen previously in Figure 4.2, in 1991. Up until its use in the restoration, the silk, made in 1956, was kept in storage in an environmentally controlled room under $50\ \pm\ 10\%$ RH and temperature $16°C\ or\ 20°C\ \pm\ 2°C$, without any exposure to light. From the point of restoration in 1991, the chair was displayed in the museum. Sample 3 was the silk sample reference of the surplus silk kept in storage conditions. This was an offcut from the historically accurate silk fabric roll, and unlike the previous samples, that had been upholstered and put on display, this sample had been kept in storage throughout with a covering protecting it from any exposure to light and under controlled environmental conditions. The conditions of this storage were, as previously detailed, set at temperature range $16^{\circ}C - 20^{\circ}C$, relative humidity $50\% \; RH \pm 10\%$, and minimal exposure to light. Sample 4 was the silk sample reference, from the chair that had been restored in 1993. Prior to this restoration the silk had been kept in storage, under the same conditions as sample 3, and from the point of its restoration was maintained under the display conditions of sample 2.

A summary of these Samples is referenced in Table 4-1:

Silk Sample Reference	**Sample Environmental Conditions [k]**
Sample Reference 1	Silk fabric on display since 1956
Sample Reference 2	Silk fabric on display since 1991
Sample Reference 3	Surplus silk fabric kept in storage conditions
Sample Reference 4	Silk fabric on display since 1993

Table 4-1: Sample reference of the silk fabric

To determine the colour condition of the silk sample, the Chromameter TES 136 was utilised, as shown in Figure 4-3. This is a digital precision handheld instrument, which can measure colour coordinates such as tristimulus values XYZ, as well as the illuminance of light sources. This instrument meets the CIE standard of photopic spectral response. The photosensor used is a Silicon photocell that has a measuring rate of 1 sample per second and can measure up to an accuracy level of xy ± 0.02. The repeatability of each measurement has an accuracy of xy ± 0.003, Standard Illuminant A measured (TES, 2014). CIE standard Illuminant A is used in photometry and colorimetry as primary reference spectrum for the calibration of the photometric and colorimetric devices (CIE, 2020B).

Figure 4-4: Instrument used to measure colour condition

(Source: TES Electrical Electronic Corp. 2014)

For the purpose of this research, the tristimulus values (XYZ) were measured to determine the initial colour of the fabric. To measure the extent of the colour fade, the International Commission of Illumination (CIE) 1931 CIE XYZ colour system was used. As discussed in section 2.4.1, this colour system is the standard for quantitative expression of colours seen by the human eye and represents the colours as tristimulus values *XYZ* (Murata et al, 2018). Figure 4-5 and 4-6 show that the specific area of measurement was the silk flower motif, (also known as the Lampas). This section of the sample was taken as it contained all the colours of the silk threads in that particular area. The one area was measured multiple times to maintain consistency of measurement. The multiple readings can be found in the Appendix 8.3. For positioning, the readings were taken in situ, using a stabilising accessory to hold the Instrument in place, at a precise and repeatable distance of 10cm from the surface of the sample to minimise sampling errors and a provide consistency between the different samples.

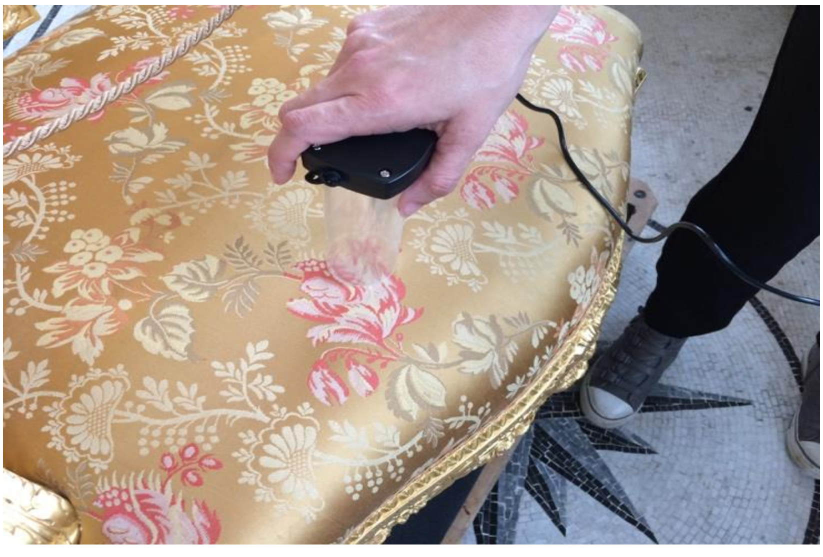

Figure 4-5: Measurements taken at an equidistance for all the samples

The use of the instrument, as seen in Figure 4-6, provides an advantage over traditional accelerated aging methods as it facilitates the taking of multiple measurements thereby reducing the chance of errant measurements, and doesn't involve any movement of the samples from their display location to laboratories for measurement.

Figure 4-6: Instrument being used in situ to measure colour condition

The diameter of the sample taken was 5cm. To test reproducibility of the results, three measurements were taken of the same sample, as documented in Appendix 8.3. Table 4-2 details the mean values of the colorimetric tristimulus (XYZ) values measured in situ.

Silk Sample Reference	Sample Environmental Conditions (k))	X	Y	Z
Sample Reference 1	Silk on display since 1956	190.5	178.6	105.1
Sample Reference 2	Silk on display since 1991	224.9	215.0	115.2
Sample Reference 3	Silk kept in storage conditions	241.7	231.3	139.1
Sample Reference 4	Silk on display since 1993	227.7	213.6	119.3

Table 4-2: Colourimeter Data (XYX) Readings Measured

The assumption has been made that the historically accurate replica silk fabric was kept in one of two states, either on display, or in the museum storage environment. Therefore, exposure to any other, (not documented external environmental conditions), cannot be fully accounted for while determining the fade rate of the silk.

4.3. Raw environmental data

The Wallace Collection provided the museum environmental sensor data used in this study, consisting of temperature, light, and relative humidity.

4.3.1. Temperature data

The temperature data was gathered from the Meaco sensors (Meaco, 2020) placed in the great gallery in 2012 to monitor the environmental conditions of the museum display. The data recorded was from recent years, mainly 2012 onwards. For the years prior to 2012, some data was available from the historical records of the museum, but where it wasn't, it was complemented with best estimates of gap periods were based on the statistical average of the actual historical records. The temperature sensor readings were gathered in timestamps in the Time Date variable format. Whilst the temperature sensors were implemented in 2012, the monitoring of the temperature before that time was in the format of Min/max hygrothermographs. Hygrothermograph is a recording instrument that can provide a continuous measurement of the highest and lowest temperature, as well the humidity on a rotating chart for durations such as one day, one week, one month or two months. The instrument utilises a hygroscopic RH sensor and bimetal temperature sensor. (NPS, 1993) (NEDCC, 2020).

The primary data collected, as seen in Table 4-3, shows a sample of the temperature readings, taken over a two-day period in 2012. Dynamic temperature measurements recorded were every half hour period with the Meaco Sensors.

Timestamp	Temperature - Reading
31/03/2012 01:00	20.6
31/03/2012 01:30	20.6
31/03/2012 02:00	20.6
31/03/2012 02:30	20.6
31/03/2012 03:00	20.7
31/03/2012 03:30	20.6
31/03/2012 04:00	20.6
31/03/2012 04:30	20.6
31/03/2012 05:00	20.6
31/03/2012 05:30	20.6
31/03/2012 06:00	20.6
31/03/2012 06:30	20.6
31/03/2012 07:00	20.6
31/03/2012 07:30	20.6
31/03/2012 08:00	20.6
31/03/2012 08:30	20.7
31/03/2012 09:00	20.7
31/03/2012 09:30	20.6
31/03/2012 10:00	20.6
31/03/2012 10:30	20.6
31/03/2012 11:00	20.4
31/03/2012 11:30	20.3
31/03/2012 12:00	20.3
31/03/2012 12:30	20.3
31/03/2012 13:00	20.2

Timestamp	Temperature - Reading
31/03/2012 13:30	20.2
31/03/2012 14:00	20.2
31/03/2012 14:30	20.2
31/03/2012 15:00	20.2
31/03/2012 15:30	20.2
31/03/2012 16:00	20.2
31/03/2012 16:30	20.2
31/03/2012 17:00	20.2
31/03/2012 17:30	20.2
31/03/2012 18:00	20.2
31/03/2012 18:30	19.9
31/03/2012 19:00	20.2
31/03/2012 19:30	20.2
31/03/2012 20:00	20.5
31/03/2012 20:30	20.6
31/03/2012 21:00	20.6
31/03/2012 21:30	20.6
31/03/2012 22:00	20.6
31/03/2012 22:30	20.6
31/03/2012 23:00	20.6
31/03/2012 23:30	20.7
01/04/2012 00:00	20.7
01/04/2012 00:30	20.7
01/04/2012 01:00	20.6
01/04/2012 01:30	20.3

Table 4-3: Meaco Sensor Readings Sample for Temperature

4.3.2. Relative Humidity Data

Similarly, the relative humidity present in the Great Gallery of the museum was also monitored. The sensors gathered the relative humidity from 2012 onwards, and before that, data was captured with the help of hygrothermographs and best estimates. However, the humidity measurements tended to be accurate only to about ±5% (at mid-range temperatures, accuracy may be less at temperature extremes), so these instruments could provide a broad outline of environmental conditions.

The Table 4-4 below documents a sample of the relative humidity, of a two-day period, as captured by the Meaco Sensors.

Timestamp	WC - Great Gallery West - Wallace Collection – Relative Humidity
15/11/2014 01:19	53.4
15/11/2014 01:29	53.8
15/11/2014 01:39	53.9
15/11/2014 03:59	53.9
15/11/2014 05:29	55.7
15/11/2014 20:55	54.6
15/11/2014 22:05	54.9
15/11/2014 22:55	54.8
15/11/2014 23:15	55
16/11/2014 00:24	55.8
16/11/2014 00:54	55.2
16/11/2014 01:04	55.5
16/11/2014 01:24	55.4
16/11/2014 03:44	54.7
16/11/2014 05:34	54.1
16/11/2014 05:44	54.1

Table 4-4: Meaco Sensor Readings Sample for Relative Humidity

4.3.3. Illuminance (Light) Data

The sensor readings capture the illuminance data, as in Table 4-5.

Timestamp	WC - Great Gallery West (Wallace Collection - Illuminance - Reading
14/11/2014 15:27	153
14/11/2014 15:37	149
14/11/2014 15:47	149
14/11/2014 15:57	149
14/11/2014 16:16	149
14/11/2014 16:26	149
14/11/2014 16:36	149
14/11/2014 16:46	149
14/11/2014 16:56	149
14/11/2014 17:06	20
14/11/2014 17:16	20
14/11/2014 17:35	20
14/11/2014 17:45	20
14/11/2014 17:55	20
14/11/2014 18:05	20
14/11/2014 18:15	20
14/11/2014 18:34	20
14/11/2014 18:44	20
14/11/2014 18:54	20
14/11/2014 19:04	20
14/11/2014 19:14	20
14/11/2014 19:24	20
14/11/2014 19:33	20
14/11/2014 19:53	20
14/11/2014 20:03	20
14/11/2014 20:12	20
14/11/2014 20:22	20
14/11/2014 20:32	20
14/11/2014 20:42	20
14/11/2014 20:52	20
14/11/2014 21:02	20
14/11/2014 21:21	16
14/11/2014 21:31	0

Table 4-5: Meaco Sensor Readings Sample for Illuminance

4.4. Data Analysis

The data analysis techniques as discussed in Chapter 3 for data pre-processing were utilised, including techniques such as the time-domain statistical technique of calculating mean, and the Euclidean distance formula for the XYZ tristimulus values.

4.4.1. Colour Condition (Measured) Data Analysis

Multiple readings from the colourimeter were obtained in the form of tristimulus values X, Y, Z provided in the Appendix 8.3 and 8.4 for reference. The mean of these values was calculated, in order to get consistent values for the colorimetric data as detailed previously in Table 4-2. The mean averaged tristimulus values XYZ were then calculated by way of Eq. (1) to calculate the colour condition, C of the samples. Table 4-6 details the result of colour condition data points C of the silk samples measured, by way of Euclidean distance. Colour condition C is associated with CIE XYZ non - real primaries, hence do not have any associated units (Brill, 1996).

Silk Sample Reference	Sample Environmental Conditions [k]	C
Sample Reference 1	Silk on display since 1956	281.5
Sample Reference 2	Silk on display since 1991	331.8
Sample Reference 3	Silk kept in storage conditions	362.3
Sample Reference 4	Silk on display since 1993	334.2

Table 4-6: Colourimeter Data (XYZ) Readings converted to single value

Figure 4-7 illustrates the colour condition C for all the four sample references, which are derived from the tristimulus readings, as previously described. The readings reveal that the higher the value of the colour condition C, the better the colour of the silk sample observed. The statical mean of these multiple readings has been plotted in Figure 4-7.

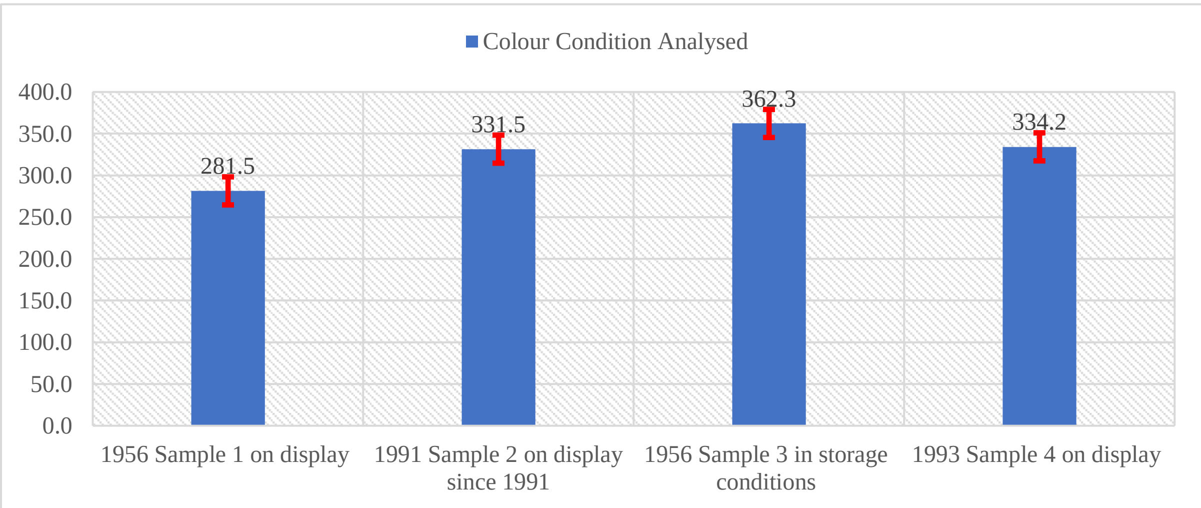

Figure 4-7: CM data - Colour conditions of the samples

have Upon visual inspection and comparison of the condition data, sample reference 3 of the surplus silk, which had been kept in storage conditions, was seen to have better colour condition as compared to the other 3 samples, that had been kept in display conditions for varying time periods.

4.4.2. Environmental Data Analysis

The sensor readings are captured in TimeDate variable format, which are simply records of time and date expressed in a string format. These can vary in their specificity, including hours and seconds. Timestamps are the most common example of TimeDate variable.

4.4.2.1. Temperature Data

To determine the historical temperature in the Great Gallery, data from archives at the Wallace Collection were used, based either on temperature sensor data or historical records of the hygrographs. The museum's monthly and yearly mean temperature was derived from the data. Table 4-7 details the temperature pattern based upon the sensor data collated over the past 10 years, documenting the yearly average of the datasets.

Year	Yearly average temperature (℃)
1996	**19.60**
1997	19.6
1998	19.6
1999	19.6
2000	19.6
2001	19.6
2002	19.6
2003	19.6
2004	19.6
2005	19.6
2006	**20.5**

Year	Yearly average temperature (℃)
2007	**21.0**
2008	**21.6**
2009	**21.0**
2010	**21.2**
2011	**21.0**
2012	**21.0**
2013	**20.1**
2014	**20.3**
2015	**20.6**
2016	**19.7**
2017	**19.8**

Table 4-7: Annual Average Temperature in the Great Gallery

Figure 4-8 illustrates the yearly average temperature pattern based on the sensor data collated over the past ten years using actual readings of the sensors and Hygrothermographs. The average yearly temperature maintained in the Great Gallery over the past 10 years was seen to be at a consistent level of 20℃ $\pm$ 1.5℃.

The values in bold are based on readings from the historic sensor measurements and hygrographs readings from the object archives at the museum. The remaining temperature measurements for the years missing a historical record assume of the best fit to the actual records.

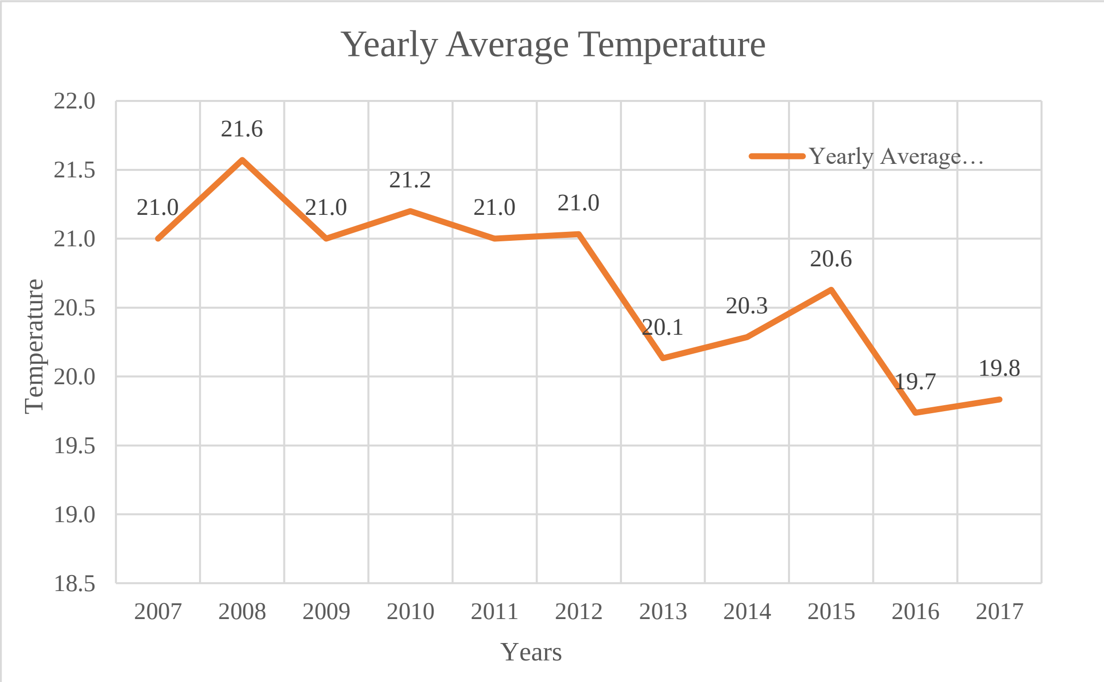

Figure 4-8: Annual Average Temperature at the Great Gallery

4.4.2.2. Relative Humidity Data

The sensor readings of relative humidity for the Great Gallery were gathered. Data inputs taken from the museum object archives in the form of the hygrographs maintained previously in the museum were also used. As with the temperature data, the relative humidity data also suffered from gaps in the archived records.

Table 4-8 shows the yearly average relative humidity maintained in the Great Gallery. The values in bold are based on readings from the historic sensor measurements and hygrographs readings from the object archives at the museum. The remaining relative humidity measurements of the years missing a historical record assume of the best fit to the actual records.

Year	Relative Humidity (%)
2007	**60.0**
2008	**64.0**
2009	55.0
2010	**51.4**
2011	52.0
2012	52.0
2013	52.0
2014	**53.4**
2015	**52.3**
2016	**52.4**
2017	**54.6**

Table 4-8: Annual Average RH in the Great Gallery for the past 10 years

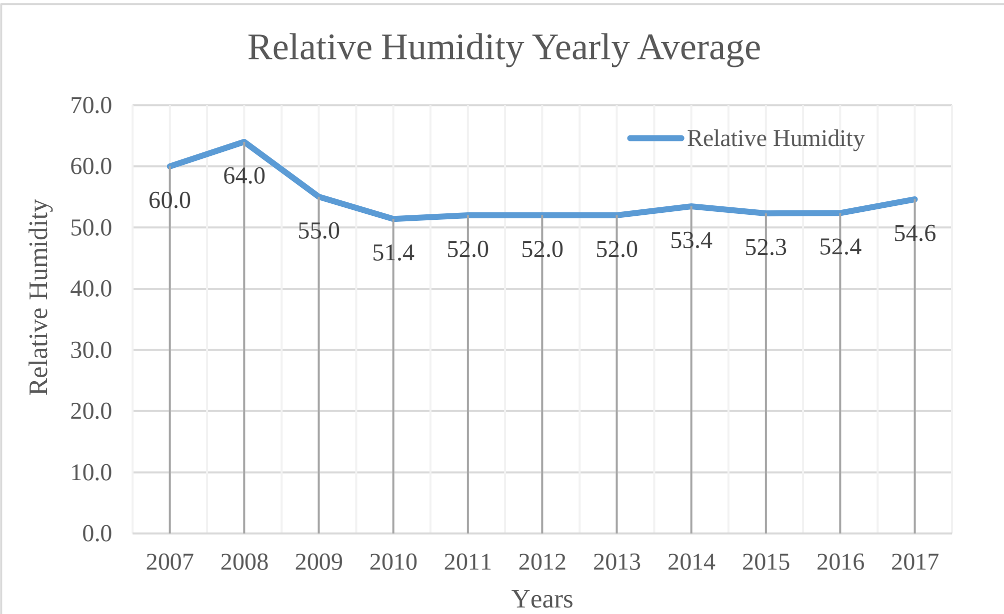

Figure 4-9: Annual Average Relative Humidity Levels at the Great Gallery

The yearly average relative humidity levels maintained in Great Gallery over the past 10 years has seen highest levels at 64% and the lowest at 51.% . This would indicate a 13% fluctuation in the yearly average of relative humidity levels within the last 10 years. The trend also indicates a lowered yearly average of the relative humidity being maintained in recent years.

4.4.2.3. Illuminance Data

The sensor readings for illuminance, (TimeDate format), over recent years was gathered. As with the temperature and relative humidity data, there are gaps in the archived records.

The available sensor data collected from 2014 -2017 for the Great Gallery is utilised as detailed in Table 4-9.

Year	Illuminance (lx) yearly average
2014	49.95
2015	54.33
2016	52.76
2017	55.66

Table 4-9: Annual Average Illuminance Readings at the Great Gallery

The yearly average illuminance based on the available historical sensor data, as measured in the last 4 years, is illustrated in Figure 4-10.

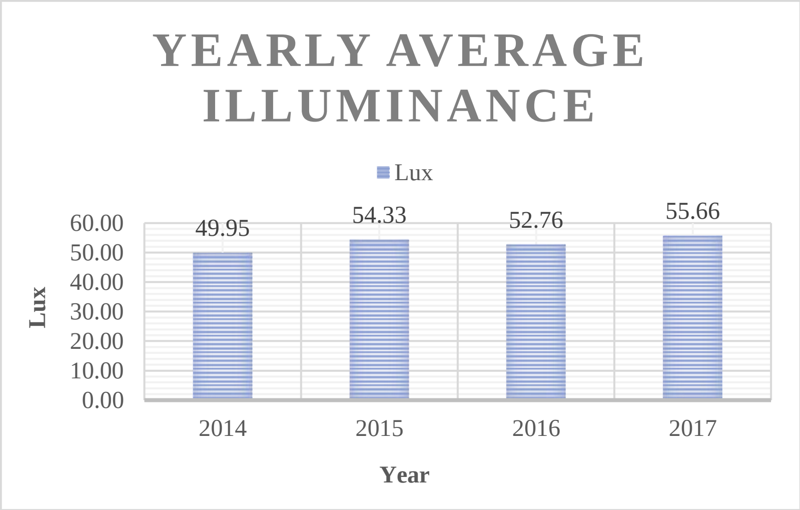

Figure 4-10: Yearly average of Illuminance (lux) sensor data

Illuminance levels are seen to be above the recommended range of 50 lux maximum, (according to the museum standard for textiles), for three out of the four years. The yearly average illuminance levels had seen its highest levels at 55.7lx and the lowest at 50lx. This shows an almost 6% increase in the yearly average for light levels over this 4-year period, based on actual sensor data readings.

4.5. Chapter Summary

This chapter details the primary data collected from the Wallace Collection, and used in the colour fade model. Direct CM data was collected by measuring silk samples from the Shrewsbury Set displayed in the Great Gallery.

Four samples were considered. Sample 1 was the silk sample reference, from the chair that had been on continuous display in the Great Gallery since the chair's restoration in 1956. Museum restoration records suggest that the silk had not been removed from the chair since its restoration. This reference sample had been exposed for the longest period to the open display conditions of the museum. Sample 2 was the silk sample reference, from the chair that had been restored with historically accurate silk, in 1991. Sample 3 was the silk sample reference of the surplus silk kept in storage conditions. This was a surplus offcut from the historically accurate silk fabric roll, that had been kept in storage throughout with a covering protecting it from any exposure to light and minimising the impact of RH. Sample 4 was the silk sample reference, from the chair that had been restored in 1993. Prior to this restoration the silk had been kept in storage, under the same conditions as sample 3, and from the point of its restoration was maintained under the display conditions of sample 2.

Non-invasive, non-destructive measurements of silk were taken with a portable colorimeter in situ. The readings were taken as tristimulus values XYZ, adopting the International Commission of Illumination (CIE) 1931 CIE XYZ colour standard to determine the colour fade. The Euclidian distance formula for colour difference was utilised to determine the colour condition C of each sample reference that had been on museum display for varying periods of time. A specific area of 5 cm in diameter of the silk flower motif, (also known as the Lampas) for each sample was examined. The readings were taken in situ, using a stabilising accessory to keep the instrument in place, at a precise and repeatable distance of 10cm from the surface of the sample to minimise sampling errors, and to provide consistency in the area being analysed. To test the reproducibility of results, three measurements were taken of the same sample. The analysis showed that the higher the value of the colour condition (C) , the better the colour condition of the silk sample observed. An assumption was made that the historically accurate silk replica fabric was kept predominately, either on display, or in museum storage. Hence exposure to any other external environmental conditions cannot be fully accounted for while determining the colour degradation model.

As the CM datapoints were limited, any degradation information such as environmental information, sensors, temperature, moisture, relative humidity, light levels were used to estimate the health. For the scope of this research the environmental sensor data of light levels, relative humidity and temperature were included as indirect CM data. The environmental data of the museum conditions over time was also gathered from museum historical records, for example, archived records for care and restoration, hygrothermographs data, visual inspections data and museum environmental sensor data including temperature, relative humidity, and illuminance. Each environmental sensor measurement had a timestamp record attached and was collected in the form of readings in Time Date variable format. Sensor data was collected every 30 minutes for temperature, every 10 minutes for illuminance and at approximately 20-minute intervals for relative humidity. UV was excluded from the scope of this colour condition model as UV sensor readings were not being picked up by the existing sensors. The deployment of conservation UV filters on windows and low UV from artificial lighting, meant that minimised exposure to almost negligible levels of UV was assumed. Time domain statistical techniques such as the ‘mean’ were calculated to understand the environmental pattern of the Great Gallery.

The average yearly temperature for the past 10 years was seen to be at a consistent $20℃ \mp 1.5℃$. The yearly average relative humidity levels for the past ten years were seen to have its highest annual average levels at 64% and lowest annual average at 51.%, indicating a fluctuation of 13% in the yearly average of RH levels within the last ten years. The yearly average illuminance levels for the past 4 years were seen to have its highest annual average at $55.7lx$ and the lowest annual average at $50lx,$ indicating a 6% increase in the yearly average of light levels over the last 4 years based on actual sensor data readings. The illuminance was maintained at or above the recommended range of 50 lux maximum according to the museum standard for textiles.

The next chapter discusses the application of the data driven prognostic model and the results. Further, demonstration scenarios are developed to determine the predicted RUL of the silk under hypothetical scenarios to aid decision-making.

5. APPLICATIONS OF THE MODEL AND RESULTS

This chapter states the assumptions and limitations encountered in this research project. It goes onto describe the derived prognostic model and its validation. The prognostic model is then used to generate predictions in relation to the remaining useful life of the 1991 restored silk artefact. Finally, the different developed demonstration scenarios are analysed, and the results discussed.

5.1. Limitations and Assumptions

- It is assumed that the fabric was either housed in the museum display or in the museum storage environment. There isn't an accurate historical record of the specific environmental conditions that the silk may have been exposed to outside of these two states, and hence, exposure to any other external environmental conditions has been not considered while determining the fade model.

- The environmental sensor data for the Great Gallery was available for the period 2014 -2017. For the period 1956 to 2014, data points were derived from thermographs or taken from the archives of the Wallace Collection, to establish a complete picture of the historical environmental conditions.

- UV light has not been included in the development of this model as the museum had no errors in the UV light data capture from the sensors. Thd museum had also deployed UV light conservation filters from 2007 onwards, providing near complete elimination of UV light. The impact of UV light prior to 2007, has not been considered, and this missing data may be a significant unknown factor. This is something that can be considered for inclusion in the future modelling.

- The colour condition for the silk fabric was limited to four data points, and it was reasonable to introduce causal information from museum environmental data, as indirect CM data, to postulate an empirical model.

- The colour condition of the original brand-new fabric, woven in 1956 was unknown. The model uses three conditions to derive this unknown constant. Expert opinion of museum professionals was sought to determine the condition of failure of the sample fabric. Sample reference 1, that had been on display in the Great Gallery since 1956, was seen, on visual inspection by the experts to have damage, such as fading and shredding, and was beyond the condition of failure point, with a colour condition value of 281.5. As a result, the lowest acceptable threshold was assumed to be 290. The threshold has been determined based on the measurements of the visually inspected silk on display and in consultation with the subject matter expert.

5.2. Data-driven Diagnostic and Prognostic Modelling

The exponential colour degradation model postulated in Chapter 3, as per Eq. (39), combines the colour of the fabric and the environmental sensor data to determine the sensitivity of the silk samples to the only known factors in the museum controlled environmental conditions.

The methodology adopted utilises the environmental sensor data as detailed in Tables 4-7 to 4-9 of the historical environmental conditions. Additionally, historical records from the museum archives of environmental data in the form of Hygrothermographs output and observational records were considered to determine the conditions of exposure in the periods before sensor data. Further, the gaps in the historical data were filled with best case assumptions from subject matter experts at the Wallace Collection. Appendix 8-1 details the collected environmental data archived records.

The Shrewsbury Set's silk conditions, as detailed in Chapter 4, have four data points in total. The research acknowledges the limited data linking colour condition to time, and so the exponential model utilises three main data points for model building and one condition datapoint is used for validation. As the number of colour condition data points are so few, the simplest possible model is developed, to determine the unknown constants, C_0 $\alpha, \gamma,$ to calibrate the fade model that can be derived, i.e., the number of unknowns in the mathematical model must be equal to, or fewer, than the number of condition data points for a solution to be found. These unknown constants are solved using the measured data in condition 1, 2 and 3. Using optimisation method, the error between the model predictions and the measured values for these three conditions is minimised. The postulated exponential fade model derived (37) - (39) was used to minimise the error between the measured colour values, as detailed in Table 4-6. The notion of using the superscript of (k) was adopted, to associate to the sample being calculated; $k = 1,2,3$. For example, $k = 1$ is the reference to the silk sample being on display since 1956. As a reminder, these three conditions were listed in table 4-6.

Following on from (38), $C(t, T, RH, v) = C_0 e^{-a(T,RH,v)t}$

$$C^{(k)} = C^{(k)}\left(t^{(k)}, T^{(k)}, RH^{(k)}, v^{(k)}\right) = C_0 e^{-a^{(k)} t^{(k)}}, \qquad k=1,2,3 \tag{40}$$

$$\text{where } a^{(k)} = \alpha\left(0.1T^{(k)} - 28.7\right)RH^{(k)} + \gamma v^{(k)} RH^{(k)} \tag{41}$$

The measured value for silk color condition C with the chromometer, for silk exposed to environmental degradation condition $^{(k)}$ is denoted as $M^{(k)}$.

The difference between the measured colour value $M^{(k)}$ for sample conditions 1, 2 and 3, as detailed in Table 4-6, and the associated model predicted values $C^{(k)}$, are used to define an objective function, $F\ (C_0, \alpha,\ \gamma)$, as follows:

$$F\ (C_0, \alpha,\ \gamma) = \left[M^{(1)} - C^{(1)}\right]^2 + \left[M^{(2)} - C^{(2)}\right]^2 + \left[M^{(3)} - C^{(3)}\right]^2 \tag{42}$$

This is a function of the unknown model parameters, $C_0, \alpha,\ \gamma$, that needed to be identified to establish the colour degradation model. By minimising $F\ (C_0, \alpha,\ \gamma)$, the values of the model parameters C_0, α, γ which provide the best fit to the measured data was obtained. This led to a minimisation problem that was solved using non-linear optimisation methods.

$$\min F\ (C_0, \alpha, \gamma) \tag{43}$$

Subject to

$$C_0 > 0, \alpha > 0, \gamma > 0 \tag{44}$$

The positive constraints posed on the three solved variables were required as C_0 is a colourimeter measurement and is always positive, and α and γ are simply weights for the respective model terms.

Optimisation methods to solve the above problem were available with software tools such as Visual Doc (Vrand, 2020) and MATLAB (Mathworks.com, 2020). It should be noted that in general the colour of a brand-new fabric can be measured, assuming such a sample is available, and hence the model parameter C_0 would be known (this would not need to be solved). However, as no brand-new silk sample was available in this case to take this measurement, C_0 was solved for.

Cumulative degradation is the process of systematically analysing and assessing the effect of environmental changes that can accumulate over time. The cumulative effect of the environmental parameters over the time are interactive and additive in manner (Spaling, 1994). The cumulative degradation values, $S1^{(k)}$ and $S2^{(k)}$of the three conditions, were optimized to fit with the model predictions, as illustrated Table 5-1, and further detailed in Appendix 8.5.

Let us consider again $a^{(k)} = \alpha\left(0.1T^{(k)} - 28.7\right)RH^{(k)} + \gamma v^{(k)}RH^{(k)}$, k=1,2,3, and define,

$$S1^{(k)} = \left(0.1T^{(k)} - 28.7\right)RH^{(k)}t^{(k)}, \text{ k=1,2,3} \qquad (45)$$

$$S2^{(k)} = v^{(k)}RH^{(k)}t^{(k)}, \text{ k=1,2,3} \qquad (46)$$

Sample conditions (k)	**Measured value (M)**	**Model Forecast**	**Variance**	$\boldsymbol{S1^{(k)}}$	$\boldsymbol{S2^{(k)}}$
1. On display since 1956 **(k1)**	281.5	282.1	0.6	2392.80	192646.80
2. On display since 1991 **(k2)**	331.5	332	0.5	1033.42	83499.30
3. In storage conditions since 1956 **(k3)**	362.3	362.2	0.1	666.50	15500.00

Table 5-1: Cumulative Colour Degradation Values

Given the limitation in the number of data points for colour condition (over time), the fourth condition k of the measured sample (1993) was used to validate the model, as detailed in Table 5-2.

Sample condition $^{(k)}$	Measured value (M)	Model forecast	Variance	$S1^{(k)}$	$S2^{(k)}$
4. On display since 1993 **(k4)**	334.2	335.1	0.9	955.74	77262.30

Table 5-2: Model validation data inputs and results

By minimising the function, the solution for the three unknown conditions C_0 $\alpha, \gamma,$ was derived. The three solved model parameters for the case study discussed are detailed in Table 5-3.

C_0	α	γ
376.12	3.02E-05	1.12E-06

Table 5-3: Model parameters used to forecast remaining life

With these parameters established, the model could then predict the cumulative damage, in terms of colour degradation, for the silk fabric, and thus, to forecast future fade based on user specified environmental conditions. Figure 5-1 below illustrates the exponential curve of the cumulative degradation of new silk (i.e., assuming $C_0 = 376$). It shows predictions over time (in yearly intervals), for the colour condition. Typical museum display environment conditions (averaged annually) were input into the model and set at; temperature 20.7℃, RH 55%, and illumination $53lx$.

As discussed in the stated assumptions, the minimum threshold for colour fade was assumed to be set at the colour condition value of 290. The exponential colour degradation model as illustrated in Figure 5-1, demonstrates the asymptotic nature of the cumulative decay of the colour loss.

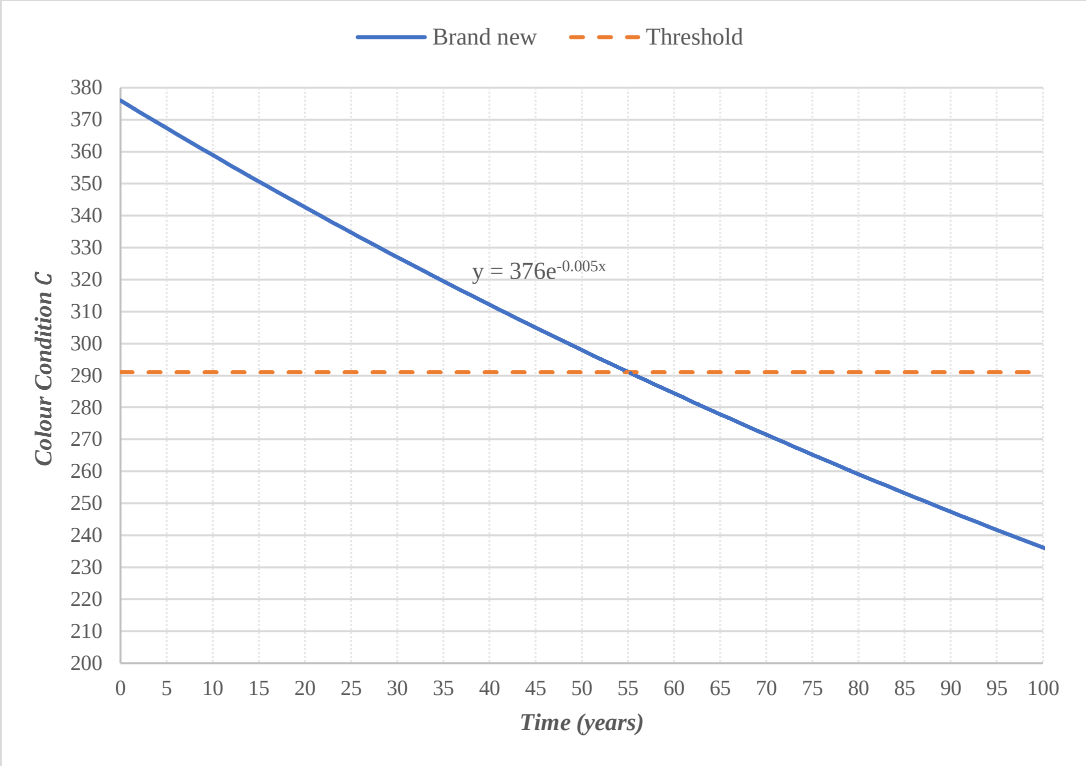

Figure 5-1: Exponential Fade Model (Predicted)

Sensitivity analysis was performed to evaluate the impact of small changes in the colour condition of silk by modelling various future museum environmental scenarios. For the future forecast done at the present time, C_0 was changed to the measured value for the condition of the fabric at the present time.

5.3. Predictions of Fade - Demonstration Scenarios

This section applies the postulated model to the data gathered to determine the sensitivity analysis of the silk degradation to changes in environmental conditions. The sensitivity analysis graphs provide a visual interpretation of the colour degradation forecast results.

Ten scenarios were developed to demonstrate the impact of changes on the remaining life of the silk fabric. The data driven model was used to determine the cumulative impact of the environment on the silk, by performing sensitivity analysis to different scenarios.

For future forecasts done at the present time, C_0 = 331 for sample reference 2 was used. The different scenarios developed are as follows:

5.3.1. Scenario 1 Typical Conditions

Scenario 1 demonstrates typical museum conditions where the parameter inputs to the model of Temperature, RH and illuminance were maintained at $20.7℃$, RH 56.7% and light $55lx$. With these conditions, the model predicts a RUL of approximately 28 years, at the assumed minimum threshold value of 290, as detailed in figure 5-2.

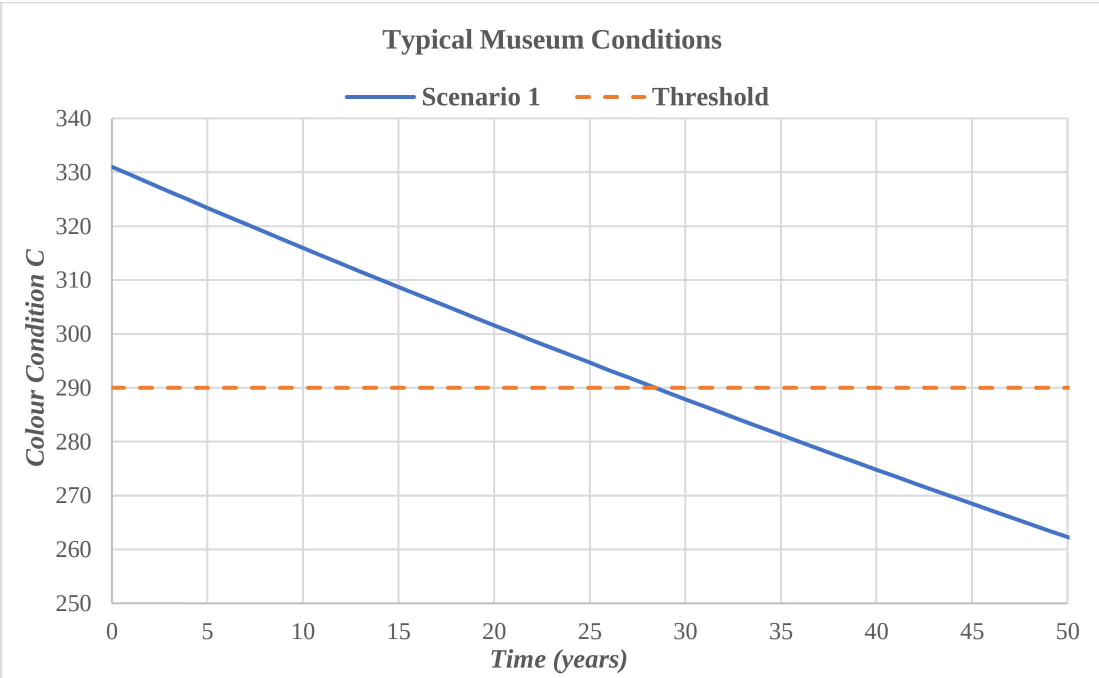

Figure 5-2: Scenario 1 based on existing environmental conditions

5.3.2. Scenario 2 Raised Conditions

Scenario 2 represents a slightly raised condition compared to typical conditions, where environmental conditions parameters in the model were increased by 1 unit (based on yearly averages). Therefore, the temperature was raised to $21.7℃$, RH to 57.7% and illuminance to $56lx$. This demonstration scenario showed a decrease in RUL of 2 years, compared to typical conditions (scenario 1), as detailed in Figure 5-3.

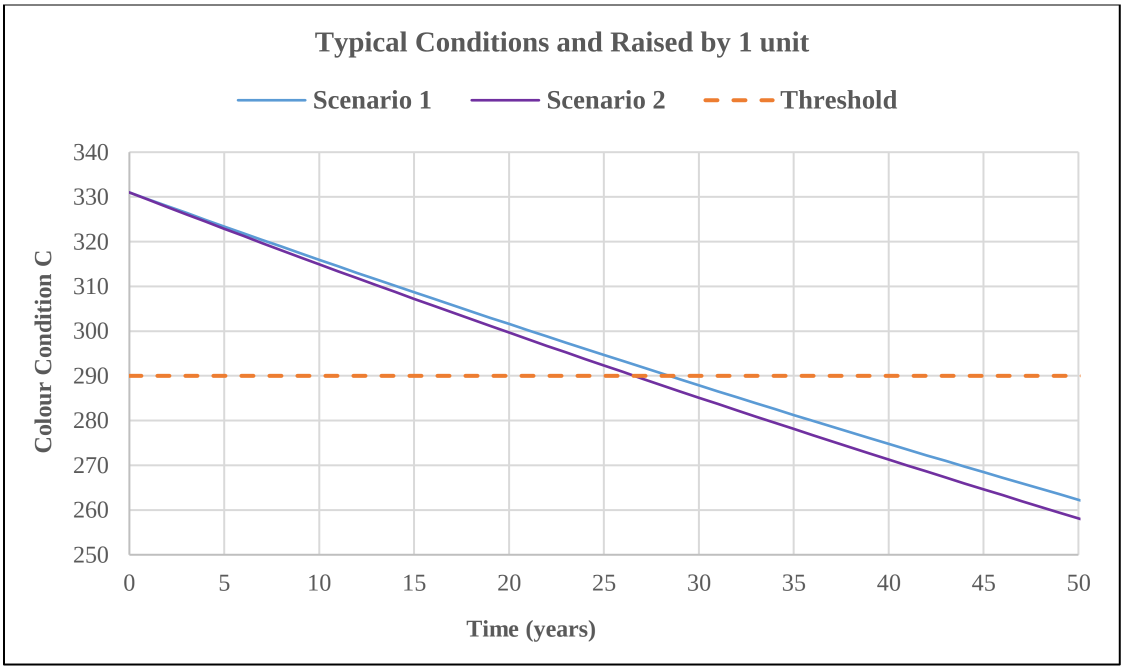

Figure 5-3: Scenario 1 (typical) and Scenario 2 (increase of 1 unit)

5.3.3. Scenario 3 Increased Conditions (10%)

In Scenario 3, environmental conditions parameters were increased by 10% of scenario 1's yearly average, to 22.7℃, RH 62.4% and illuminance to 60.5lx. The model indicates an approximate decrease in the RUL by 6 years, compared to typical conditions (scenario 1), as detailed in Figure 5-4.

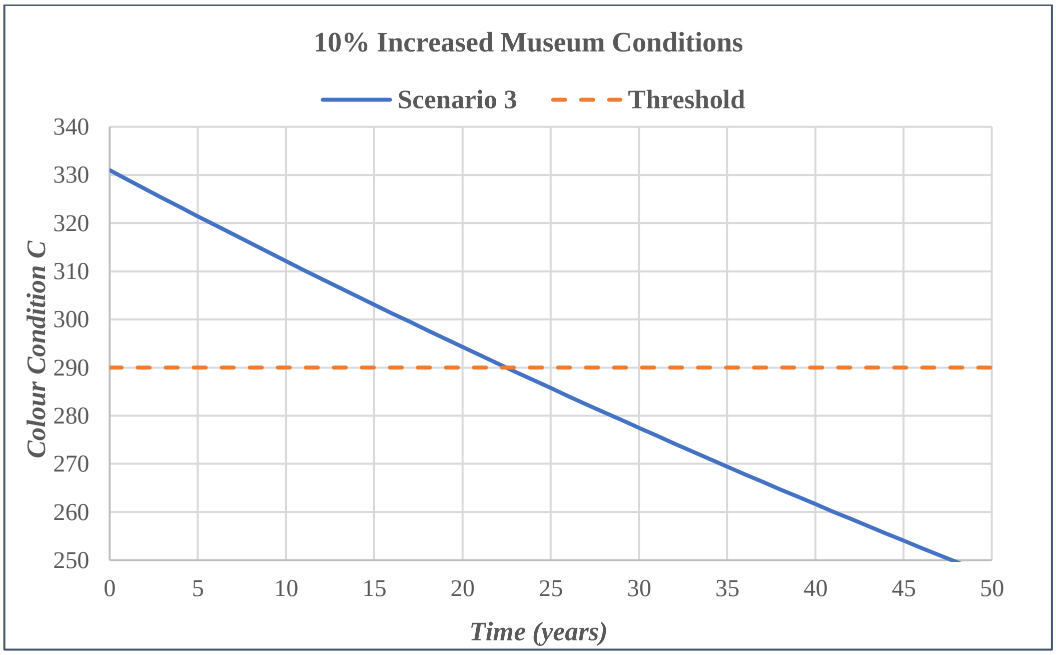

Figure 5-4: Scenario 3 demonstrating 10% increase

5.3.4. Scenario 4 Harsh environmental conditions (15%)

Scenario 4 models harsher conditions compared to Scenario 1, where the environmental condition parameters were increased by approximately 15%. Therefore, the temperature was raised to 23.8℃, RH to 65.2% and illuminance to $63.2lx$. The model indicates a significant decrease in the RUL by 8 years, as is seen in Figure 5-5.

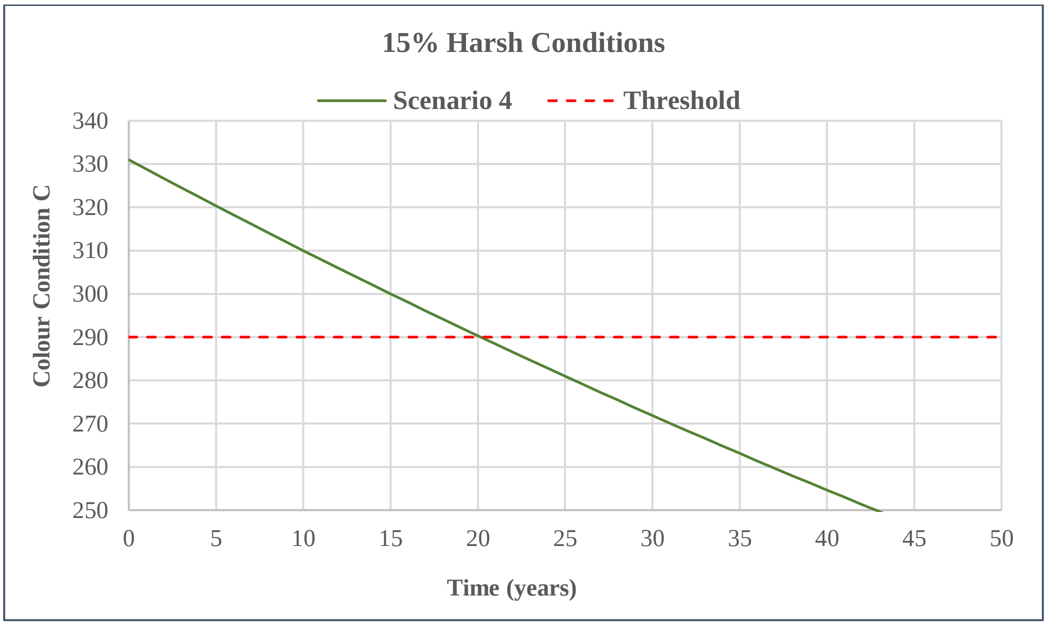

Figure 5-5: Scenario 4 harsh environmental conditions (15% increase)

5.3.5. Scenario 5 Lowered conditions (-5%)

Scenario 5 represents a lowering of the conditions, compared to Scenario 1, by 5%. Therefore, the Temperature was lowered to 19.6℃, $RH\ \ to$ 53.9%, and illuminance to $52.2lux$.

It can be seen in Figure 5-6 that the lowered environmental conditions for all three factors resulted in an increase in the RUL of the silk by almost 4 years.

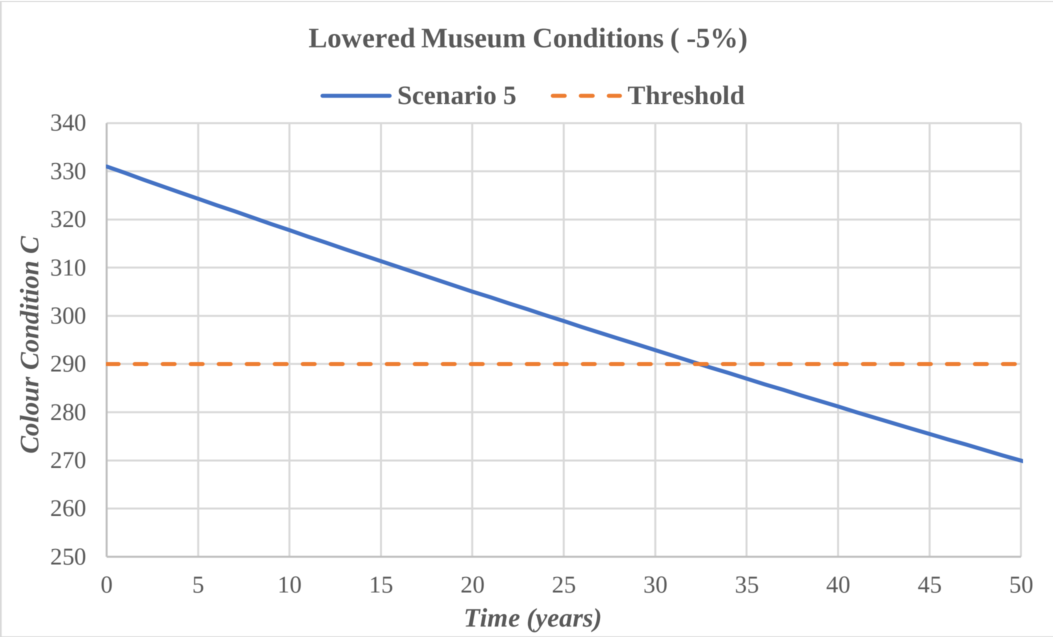

Figure 5-6: Scenario 5 based on lowered environmental conditions

5.3.6. Scenario 6 Reduced conditions (-15%)

Scenario 6 represents further reduced conditions, compared to Scenario 1, where the environmental condition parameters were reduced by 15%, with temperature set to 17.6℃, $RH\ to$ 48%, and illuminance to 46.7lux. Figure 5-7 shows the impact of this change, with the RUL increasing by approximately 15 years, from 28 years under scenario 1 to 43 years under scenario 6.

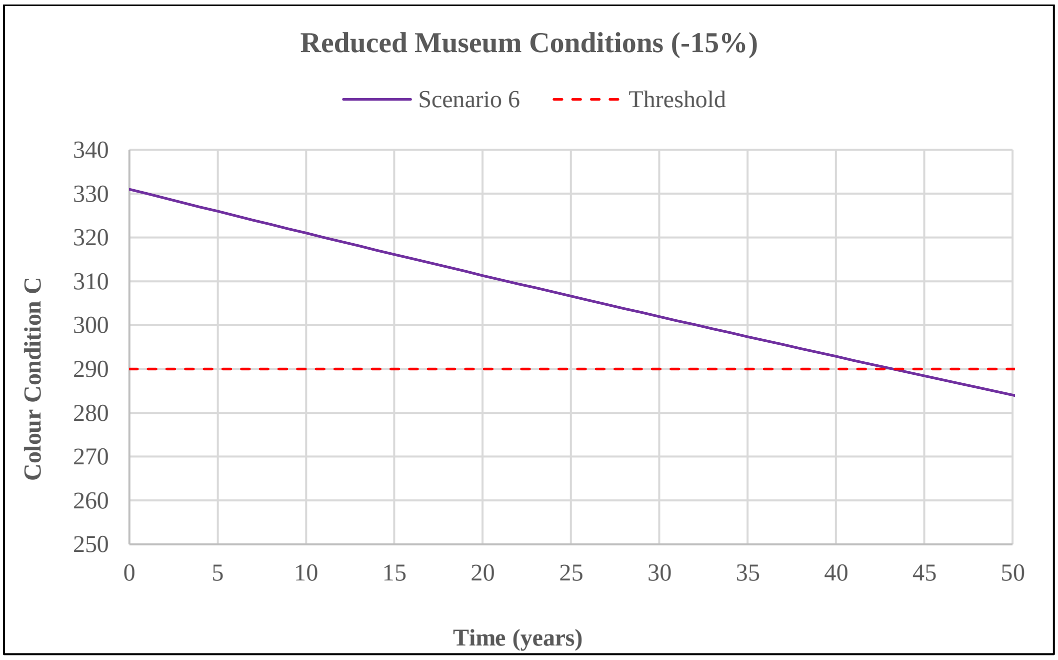

Figure 5-7: Scenario 6 based on 15% lowered environmental conditions

5.3.7. Scenario 7 Lower range of UK Standard 2012 Recommended Range

In Scenario 7, the conditional parameters were set to the lowest range of the UK standard 2012. Temperature was set to 18°C, RH to 50% and illuminance to 50lx. Figure 5-8 illustrates a marked increase in the RUL by 10 years when compared with Scenario 1.

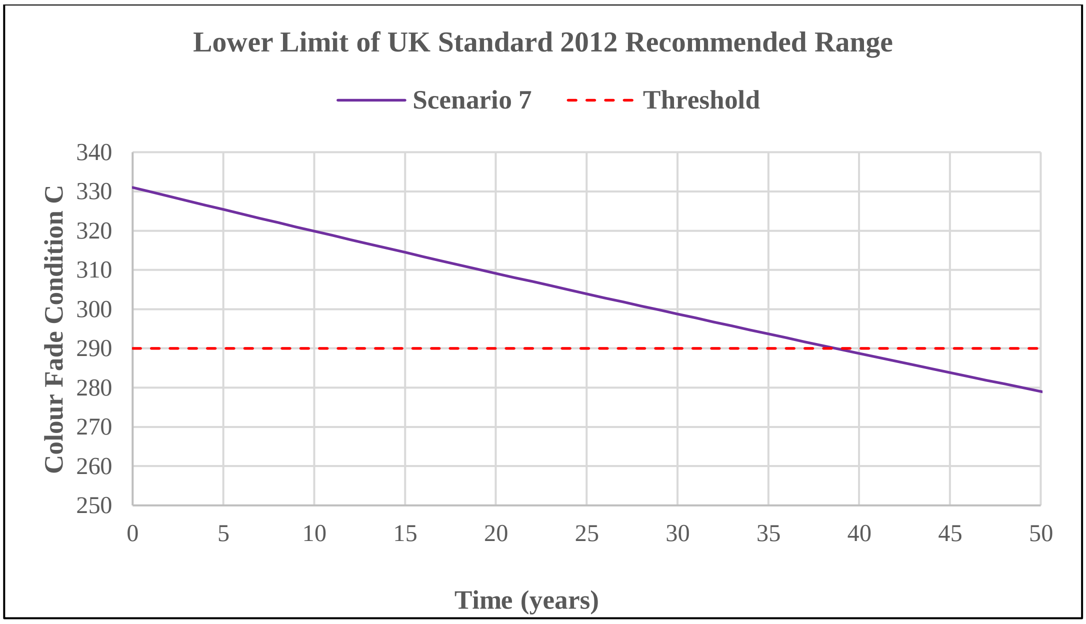

Figure 5-8: Scenario 7 based on minimum UK standard 2012 range

5.3.8. Scenario 8 (a, b, and c) - Each environmental parameter individually increased by 15%

Figure 5-9 Reflects the scenario where the temperature and illuminance were kept at the typical range with RH increased by 15%. Here it can be seen that there is a decrease in RUL by 3 years to 25 years.

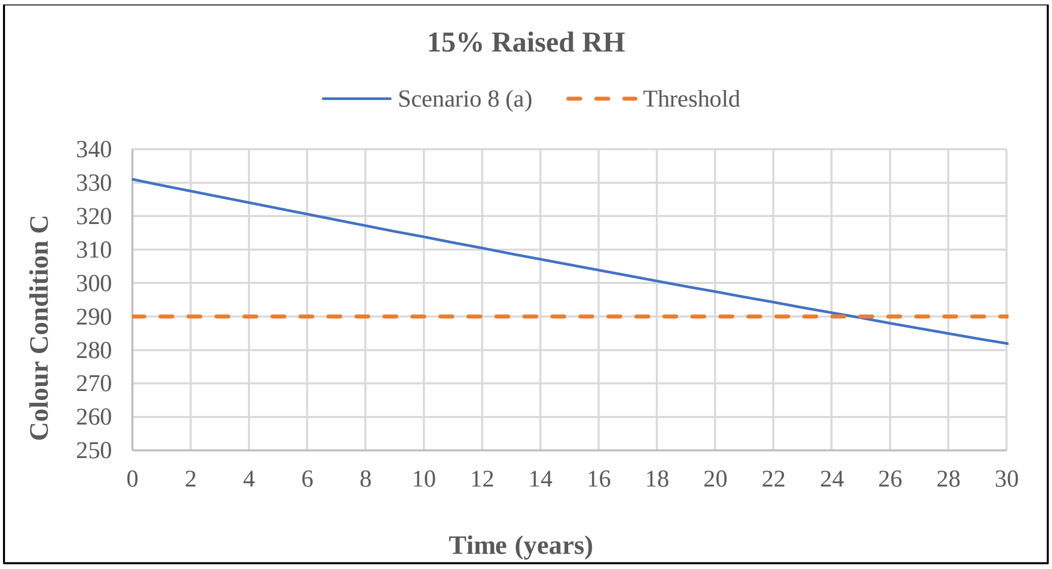

Figure 5-9: Scenario 8a based on RH increase

Similarly, Figure 5-10 demonstrates, the scenario of RH and temperature maintained at the typical range with illuminance levels increased by 15%. Here, it can be seen that there is a decrease in RUL of 2 years, from 28 to 26 years.

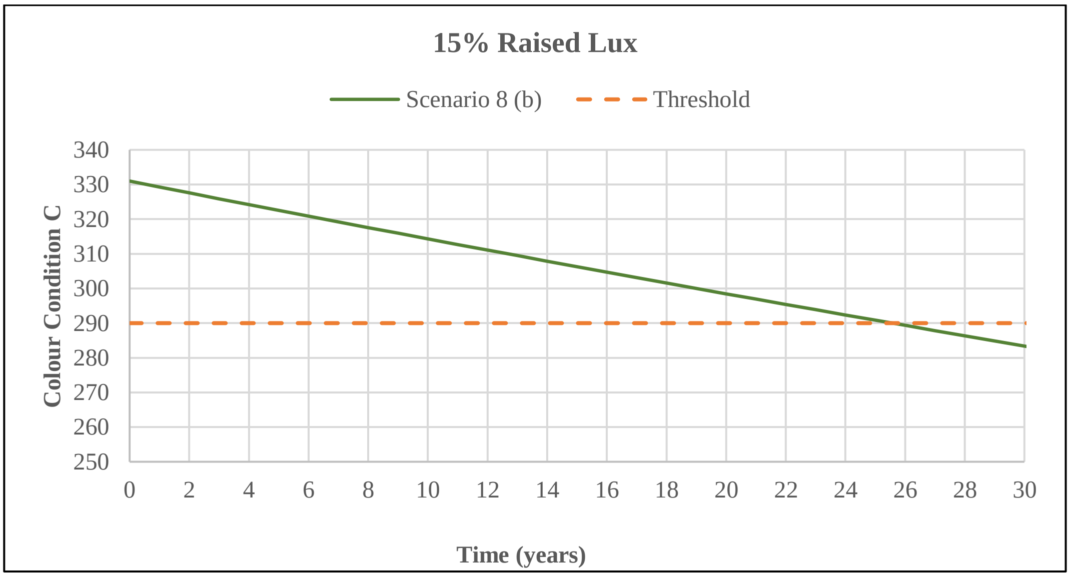

Figure 5-10: Scenario 8b based on 15% increased illuminance

Figure 5-11 demonstrates the scenario in which the temperature is increased by 15% to 23.8C whilst RH and illuminance are maintained at the values seen in scenario 1. There is a decrease in RUL of 2 years, from 28 to 26 years.

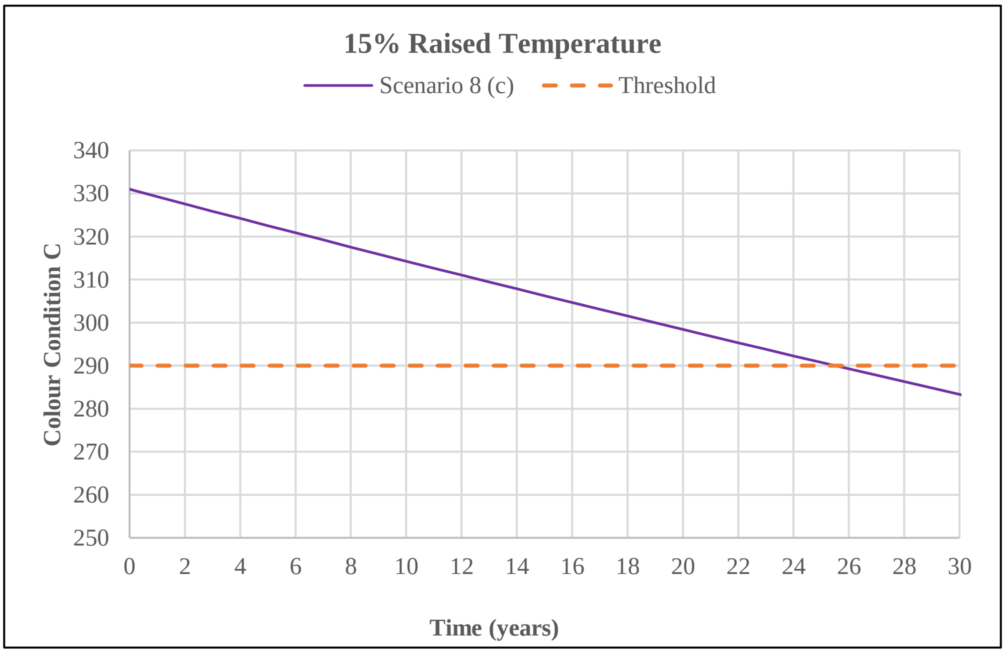

Figure 5-11: Scenario 8c based 15% increase in Temperature

5.3.9. Scenario 9 Alternating Annual Environmental Conditions

To ensure the longevity of the silk under museum environmental conditions, the option to annually rotate the silk, between storage and display was also modelled, as shown in Table 5-4.

Year	Temp (°C)	RH(%)	Lux(lx)
2020	20.7	56.7	55
2021	16	50	5
2022	20.7	56.7	55
2023	16	50	5
2024	20.7	56.7	55
2025	16	50	5
2026	20.7	56.7	55
2027	16	50	5
2028	20.7	56.7	55
2029	16	50	5
2030	20.7	56.7	55

Table 5-4: Sample dataset of the annually alternating environmental conditions

The most significant increase in the RUL of the silk sample can be seen in Figure 5-12, where the sample is modelled to rotate annually from display conditions in the gallery to storage conditions in the museum. Under the conditions of scenario 9, the RUL can be seen to significantly increase from 28 years to approximately 50 years.

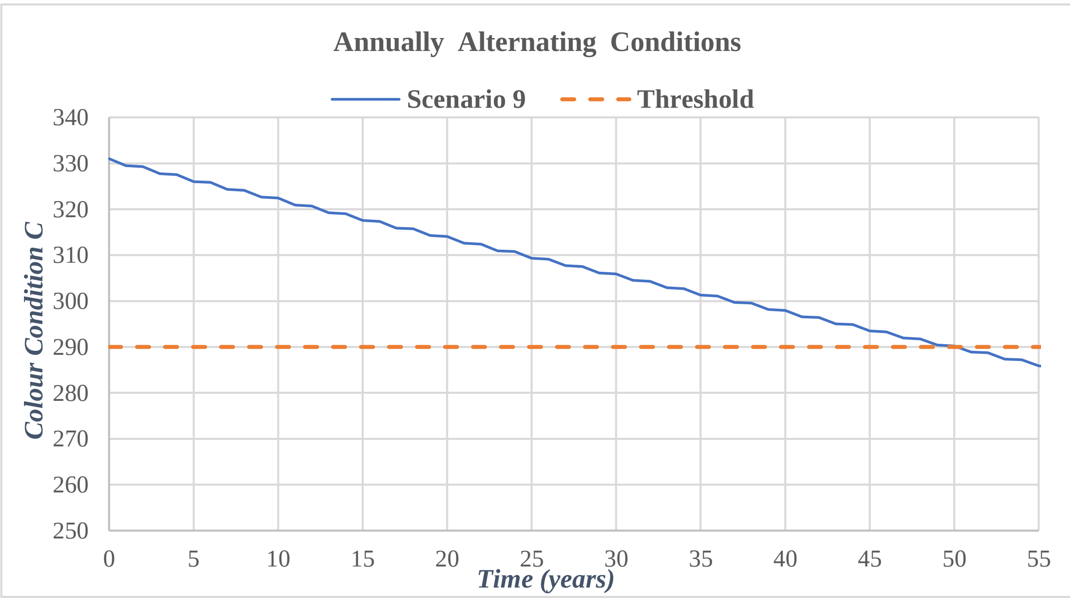

Figure 5-12: Scenario 9 based alternate environmental conditions annually

5.3.10. Scenario 10 Alternating Conditions Every Two Years

Scenario 10 is a variation of Scenario 9, modelling the impact of alternating conditions every two years as opposed to annually under scenario 9, increasing the period under which the silk is displayed, a situation that is possibly more practical for the museum, given the logistical, (and other), challenges of moving the display in and out of storage. Table 5-11 details the environmental conditions for scenario 10.

Year	Temp (°C)	RH(%)	Lux(lx)
2020	16	50	10
2021	20.7	56.7	55
2022	20.7	56.7	55
2023	16	50	10
2024	20.7	56.7	55
2025	20.7	56.7	55

Table 5-5: Sample dataset of alternate (every two years) environmental conditions

Figure 5-13 depicts scenario 10 showing a RUL of 40 years, a reduction of 10 years in the RUL compared with scenario 9.

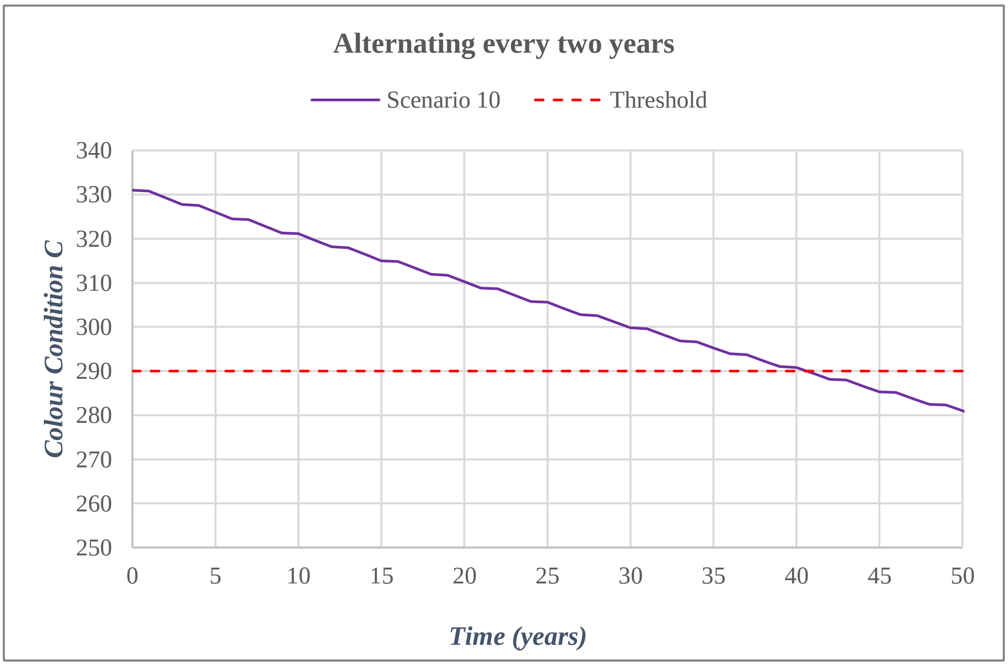

Figure 5-13: Scenario 10 based alternate environmental conditions every two years

5.4. Results

This section discusses the ten different scenarios developed to demonstrate the sensitivity of the silk to the environment in which it is displayed and stored. The scenarios depict the cumulative impact of the three environmental factors being studied, temperature, relative humidity, and light exposure (each measured as a yearly average).

In scenario 1, temperature, RH and illuminance are maintained at typically recommended conditions. It can be observed that the RUL, defined at the point that it has reached the acceptable threshold of 290, (defining the minimum acceptable colour condition of the silk, beyond which point it would require restoration or replacement), within 28 years.

In scenario 2 it can be observed that silk is relatively sensitive to a 1 unit increase for all three environmental conditions and predicts a reduction by approximately two years in the RUL of the silk. This confirms previously published studies (May and Jones 2006) (Muge and Suat, 2016), suggesting the increased fragility of silk fabric to marginal increases in the conditions of temperature, humidity, and illuminance.

Scenario 3 was developed to determine the sensitivity of the silk fabric to an increase of 10% in yearly averages of all three museum environmental conditions. Under this scenario, there is seen to be an adverse impact on the longevity of the silk, reducing the RUL of the fabric by almost 6 years.

In scenario 4 harsher environmental conditions have been developed. The impact was to see a reduction in RUL of the silk by 8 years, confirming that the harsher display conditions have a significantly detrimental impact on the longevity of the silk.

Scenario 5 and 6, reversed the direction in the change of the conditions from the previous scenarios, this time modelling a decrease in the typical museum environmental conditions by 5% and 15% respectively. A 5% reduction leads to a predicted extension by 4 years in the RUL. Lowering all environmental conditions by 15% prolonged the RUL by 15 years from 28 to 43 years.

Scenario 7 looks to predict the RUL based on conditions at the lower end of acceptable museum standards. Under this scenario, the results showed a marked increase in the RUL by 16 years, from 28 to 44 years.

Scenario 8 seeks to model the sensitivity of the silk to individual parameters, increasing each condition by 15%. It can be observed that the impact of harsher RH conditions decreases RUL by 3 years, compared to 2 years for temperature and lux. The result indicates that RH impacts the colour fade more than either temperature or lux separately.

Further, as seen in Scenario 4 where all the parameters combined were raised by 15%, the predicted RUL decreased more significantly by 8 years, thus reflecting the significance of the combined impact of the environmental conditions on the cumulated fade of silk.

Scenario 9 and 10 detail the impact of alternating the silk between the typical environmental display conditions of the gallery, and the environmental conditions in museum storage, on an annual basis or by displaying for 2 years before storing for 1. If the silk is annually rotated from display to storage it seems to have significant impact in prolonging the life of the silk sample fabric from 28 years to approximately 50 years. When the silk is displayed for a longer period, as seen in scenario 10, the silk fabric fades by a greater amount. Whereas scenario 9 shows that the fabric accumulates less damage when it spends greater time under storage conditions.

The most detrimental conditions were demonstrated in scenario 4, which showed a reduction in the RUL to 20 years.

It should also be noted, that during the research, the opinion of subject matter experts was that the fade of the silk become observable at the 12-15-year stage (when under display conditions). Subjectively it can be seen that the RUL is roughly double the point at which fade is observable by experts, and anecdotally, there seems therefore to be some consistency between expert opinion and the predicted model, under typical conditions.

The prognostics for colour degradation can help museums develop mitigation strategies to minimise silk fade; for example, by adopting object rotation or reducing the environmental conditions parameters to the lowest acceptable level in the museum standard range.

Predictive results show the RUL of the fabric in ambient conditions seemed to prolong significantly when the object was moved away from the museum display conditions. If the silk is rotated annually from display to storage, it has an almost doubling effect on the remaining life of the fabric. Although this option would be detrimental to the museum visitor, who, quite reasonably, in the case of the Wallace Collection, may want to see the Shrewsbury Set. Indeed, its movement into storage would involve extra staff time and cost, the inconvenience and cost of which can be compared with associated costs of restoring the chairs more frequently. And so, to aid this complex set of decision making, and insuring it is made on measured evidence as proposed in the methodology, then a systematic approach to object specific conservation can be utilised for informed decision-making and more predictable outcomes.

5.4. Chapter Summary

In this chapter, the diagnostic and the prognostic methodology described in Chapter 3 is applied and evaluated with the help of the data collected from the Wallace Collection, as described in Chapter 4.

The exponential colour degradation model for the silk fabric applied is derived in the format of the model structure provided in chapter 3. The postulated mathematical model derived from the exponential decay model is used to solve the unknown brand-new colour condition of the silk fabric, as well as the unknown model parameters. This is achieved by solving the optimisation problem of minimising the error between the model predictions, and the measured values for these three known conditions. Given the limitation of the availability of linking colour condition data points to time, the fourth condition k of the measured sample (1993) was used to validate the model. The colour condition new (C_0) which was unknown is found through numerical optimisation with a gradient based search algorithm.

The colour fade of the silk as seen in the sample reference, illustrates an asymptotic curve of degradation over time. It demonstrates the overall nature of the cumulative degradation of the silk fabric with a gradual loss of colour in the initial stages, followed by a reduced rate in the later years.

The exponential colour fade model derived can help determine the cumulative colour fade of silk by performing sensitivity analysis to 10 different scenarios. Hypothetical demonstration scenarios ranging from increasing to decreasing museum environmental conditions were developed. Alternate scenarios for object rotation were also developed. It was observed that by adopting a policy of rotation of the silk, the museum can significantly prolong its RUL.

Although recommended museum standards are maintained, there still is significant detrimental effect on the RUL of the silk when displayed. It is also observed that the fabric in the display has the most significant fade as compared to the same fabric kept under storage conditions. The prognostics regarding the colour degradation can potentially help museums mitigate the fade. Minimising deterioration is much more efficient than rectifying the consequent damage to the restored silk.

The next chapter discusses the findings, the recommendations for the Wallace Collection, as well as the future work that can be further explored.

6. DISCUSSION

The primary aim of this research project was to develop a methodology that could be used to predict and enable decision-making to minimise cumulative silk fade in a museum environment. This research has detailed a novel approach, that is non-invasive, non-destructive, data-driven modelling designed to aid the conservation of silk fabrics in situ. The originality of the proposed methodology is a new mathematical model to predict silk fade, built upon the factors of environmental conditions such as lighting, temperature, and humidity.

Current methods for analysing the degradation of silk rely upon accelerated aging techniques. However, these techniques typically entail the need to extract samples from the original artefact, may involve moving fragile artefacts to a laboratory, and can require the use of expensive instruments to conduct the analysis. This study shows that it is feasible to develop a methodology that facilitates non-invasive and non-destructive analysis without removing the silk from the display environment of the museum, thereby establishing a more cost effective and practical approach to silk conservation. Additionally, this research attempts to remove the gap in the conservation literature by providing an empirical method demonstrated through qualitative data relating to the natural aging of silk artefacts, on display under controlled museum environmental conditions. The PHM methodology is applied and demonstrated on three chairs, originally made between 1768 and 1770, and re-upholstered with historically authentic silk in 1956. Although, this methodology has been applied to the chairs that form part of the Shrewsbury Set, displayed in the Great Gallery, at The Wallace Collection in London, it can also be applied to other museums and the protocol of the steps are as detailed.

6.2. Application and Implementation of PHM Methodology for Silk Colour Degradation

6.2.1. Overview

This section summarises the key steps, which provide the protocol of the applied process in developing the PHM methodology.

Several well-established concepts, standards, and techniques, as discussed in detail in Chapter 3, have been adopted to develop this methodology. These include the development of a novel mathematical model to predict the rate of colour degradation, based on historical museum environmental conditions. This model can be utilised to predict the Remaining Useful Life (RUL) of silk, which can inform decision-making relating to the prolongation of the life of the silk, and minimise costly, reactive interventive restorations.

The overall process of the PHM method followed is, identification of the problem definition, condition monitoring data collection, data pre-processing, mathematical modelling, prognostic modelling, demonstration scenarios to determine RUL, and finally the enabling of conservation decision-making. The methodology as discussed in Chapter 3, has the following broad phases, as detailed in Figure 6-1 for managing the silk colour condition.

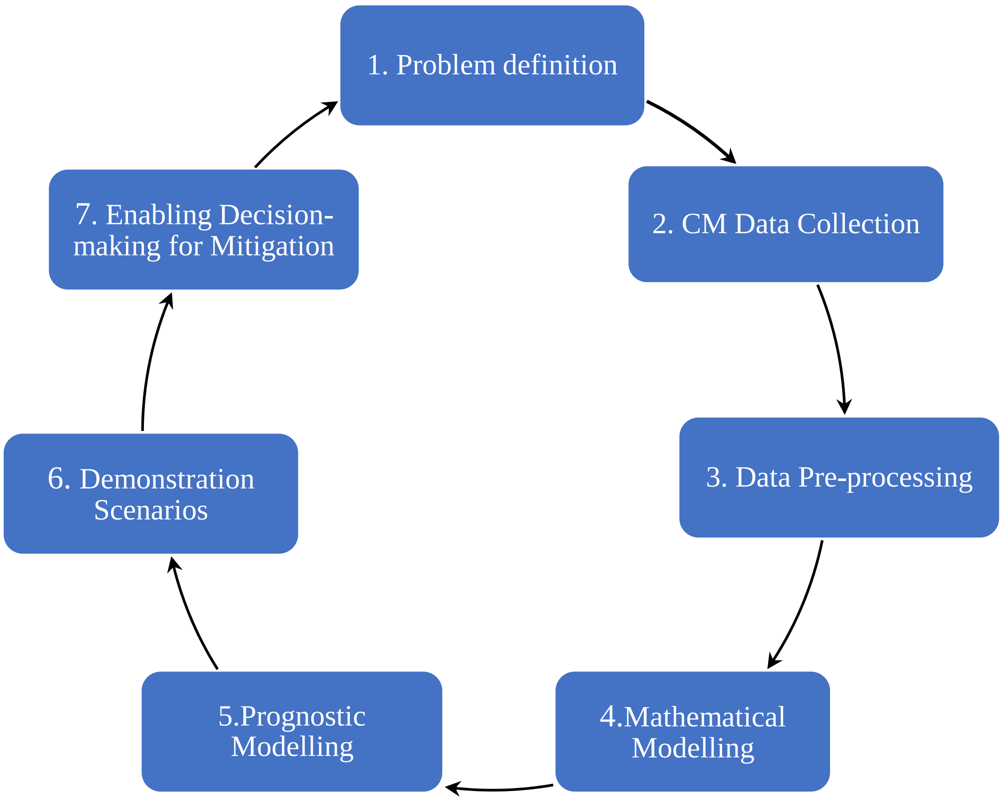

Figure 6-1: Overview of the PHM Methodology

6.2.2. Part 1: Problem Definition

General Application: The Problem Definition stage identifies the core problem, in the case of this research, the issue of silk degradation under museum conditions. Fault detection is defined to be the task of determining if a system or asset is experiencing problems. The condition of the silk must be determined to identify the problem. Health assessment of the asset involves estimating its health by analysing collected data, and if failure data is unavailable, then degradation monitoring or fault detection for abrupt faults can be used.[48] The data can be objective or subjective, depending on the nature of the data and the collections method. If there is an absence of existing condition-based monitoring, the silk on display can be subjectively identified and assessed, through visual inspections. The at-risk silk would start to show physical signs of degradation and/or fading.

Specific application: For the scope of this project, the problem definition was determined subjectively. The subject matter experts' opinion was taken into consideration with the help of visual inspections initially, to identify the lowest acceptable threshold or point of failure of the silk sample on display in the museum's Great Gallery. For example, in the case of the silk in the collection, this related to an unacceptable level of increased fading of the colour of the silk and loss of material in the form of fraying. Such a point of failure represented the point at which the silk had deteriorated to such an extent that it would have been taken away from display to undertake costly restoration. Sample reference 1, that had been on display in the Great Gallery since 1956, was seen, on visual inspection by the experts to have damage, such as fading and shredding, and was beyond the condition of failure point. The areas known as the "lampas" (Flower motif) was selected as it contained in that particular area, all of the coloured threads present in the sample.

6.2.3. Part 2: Data Collection

General Application: Observed health information through constant inspection is often referred to as condition monitoring (CM) data. It can be directly related or indirectly related to the asset health status and can be viewed as its health indicator. The direct CM data is to be gathered with the hand-held colourimeter instrument. This allows measurements to be taken of silk in-situ. The tristimulus values XYZ are to the gathered of the silk samples. If the direct CM data linking the sample to time is limited, degradation information such as environmental information, sensors, temperature, moisture, relative humidity, light levels can be used to estimate the health. Most museums utilise HVAC systems and sensors to maintain and monitor the environment. The historic data needs to be collated both for the direct CM data in the form of Tristimulus values (XYZ) and indirect CM data consisting of temperature, moisture, relative humidity, light levels.

Specific application: For the scope of this research, the direct CM data was collected by measuring the silk with a colorimeter to determine its colour condition using the CIE XYZ colour theory, as discussed in section 2.4.1. The A specific sample area of 5 cm in diameter of the silk flower motif, (also known as the Lampas, and broadly representing all of the colours present in the silk) was examined. The readings were taken in situ, using a stabilising accessory to keep the instrument in place, at a precise and repeatable distance of 10cm from the surface of the sample to minimise sampling errors, and to provide consistency to the area being analysed. To test the reproducibility of results, three measurements were taken of the same sample, as seen in Appendix 8.3. The indirect CM data in the form of environmental sensor data of light levels, relative humidity, and temperature has been included due to the limited historical condition data. The sensor readings of the temperature, light, and relative humidity maintained were collected from the available sensors. Although UV light may be a causal factor, it was not included in this model development for two reasons:

1. Although the museum environmental monitoring system had a provision for measuring ultraviolet rays, the primary sensor dataset provided by the Wallace collection for UV light did not have UV exposure readings. The MEACO sensor system (Meaco, 2020) that had been deployed in the museum had errors in the sensor data capture of UV readings.

2. The museum has deployed UV light conservation filters that provide heat reduction combined with reduced UV light levels. In 2007 museum grade UV light conservation filters, Sun-X MT65 (Sun-X, 2020), were applied and these reduced UV light transmission to <0.1%. In 2012, these filters were supplemented with Sun-MT35, which included heat reduction combined with the reduced UV light transmission. This practically eliminated UV light as a factor for silk colour fade degradation. SUN-X MT90 filters utilised provided 99% UV elimination, hence it was assumed that the UV had been reduced to almost minimal levels such that it could be eliminated as a factor for silk colour fade in the model development.
3. Thus, because of the absence of data and based on the UV elimination measures, UV light has not been included in the reported model development. Although future studies may include it as parameter as shown in the mathematical model.

Figure 6-2 provides an overview of the data inputs.

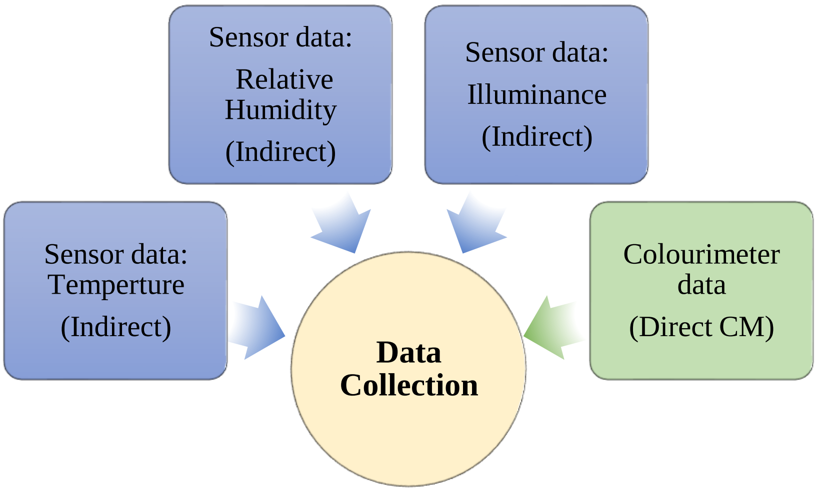

Figure 6-2: Direct and Indirect CM Data Collection

6.2.4. Part 3: Data Pre-processing

Following the data collection, data pre-processing and refinement was undertaken as discussed in Chapter 4.

General Application: Data pre-processing or feature extraction includes data cleaning, data quality evaluation, and segmentation. It helps in identifying valuable parts of data whilst increasing the efficiency of data analysis by removing unwanted segments and redundancy. The data analysis techniques for data pre-processing or signal processing can be generally classified as statistical methods and engineering knowledge-based methods. Some of these techniques, such as distance evaluation techniques (DET) in its various versions, can be applied such as the Euclidean distance evaluation technique (EDET), two-stage feature selection and weighting technique (TFSWT).

The temperature readings measured by the sensors were refined to establish the yearly and monthly averages. Similarly, the sensor measurements for Illuminance, and Relative Humidity (RH) were collated and processed. Time domain statistical techniques such as establishing the Mean, were applied for all the environmental factors and the yearly averages were determined. During this phase, certain indicators of the results began to become apparent.

Specific application: In the case of this study, the data pre-processing indicated that the RH levels in the Great Gallery had fluctuated by approximately 13% over a ten-year period. Published studies reviewed in Chapter 2, have shown fluctuating RH to have a marked detrimental impact on the RUL of silk. The direct colour condition data in the form of XYZ readings was processed to determine colour condition C, as discussed in section 3.2.2. This is derived from the Euclidian distance formula taking the form of equation (1). This was applied to all four samples to determine their colour condition C. Sample reference 1, which was subjectively assessed, by the museum expert to be at the point of failure, was measured to C value, of 281.5. Sample reference 2 was measured to C value, of 331.8. Sample reference 3 was measured to C value, of 362.3 and Sample reference 4 was measured to C value, of 334.2. Therefore, it is seen that the higher the value of the colour condition C, the better the colour of the silk sample observed.

6.2.5. Part 4: Mathematical Model

Chapter 3 details the derivation of the mathematical model.

General Application: The cumulative exponential colour degradation model derived defines temperature and light as sources of energy, that have an additive effect on silk deterioration and RH as a factor that facilitates the photodegradation reaction to occur. For the development of the reaction rate function, which is the exponent in the degradation model, the Arrhenius equation is adopted. The model utilises only the effect of temperature (activation energy and universal gas constants are combined as unknown constants) and linearising the effect of temperature on reaction rates. For most reactions happening at room temperature, the rate of reaction doubles for a $10°C$ rise in temperature (Clark, 2018). To make the mathematical solution of constants easier, the rule proposed for this study, is for the rate to double as room temperature goes from 18℃ to 28℃. Optimisation software tools such as Visual Doc (Vrand, 2020) and MATLAB (Mathworks.com, 2020) was used to solve for the brand-new conditions. It should be noted that in general the colour of a brand-new fabric can be measured, assuming such sample is available, and hence the model parameter C_0 would be known and would not need to be solved. In the case of historic silk, where the new condition was not possible to measure, C_0 was be treated as an unknown parameter and estimated along with unknown α *and* γ. An empirical exponential decay model is derived as an optimal fit for the silk colour degradation as detailed,

$$C(t,T,RH,v) = C_0 e^{-a(T,RH,v)t} \qquad (47)$$

Where,

C = condition at time t

C_0 : the condition at time $t = 0$

where a = a constant which is a function of mean temperature $T°K$ linearised, relative humidity (RH), v = light levels (*lx*) over time t.

Specific Application: The Shrewsbury Set's silk conditions, as detailed in Chapter 4, have four data points in total, corresponding to the period when the chairs were restored with historically accurate silk in 1956, 1991, 1993 and with reference to surplus silk from the same fabric roll, which was kept in environmentally controlled storage conditions. The research acknowledges the limited data linking colour condition to time, and so the exponential model utilises three main data points for model building and one condition datapoint is used for validation. As the data points which link colour condition to time are limited, the reference to causal information to published silk studies, as well as, to subject matter experts in the museums, helped to inform the models development. Thus, the simplest empirical exponential decay model is derived as an optimal fit for the silk fade.

The final colour degradation model, as per Eq. (37) – Eq. (39) is:

$$C_0 e^{-at} = C_0 e^{-[\alpha(0.1T-28.7)+\gamma v]RH]t}$$

$$C(t, T, RH, v) = C_0 e^{-a(T,RH,v)t}$$

$$\text{Discretised } \; C = C_0 e^{\sum_{i=1}^{n}(-\alpha(0.1T_i-28.7)RH_i\Delta t_i-\gamma(v_i RH_{i)}\Delta t_i)}$$

$\sum_{i=1}^{n} \Delta t_i = t$ (Forecasting time horizon in unit of years)

T_i, RH_i, Lv_i = Averaged values of temperature (in Kelvin), relative humidity (in %), and light (in lux) for the time period Δt_i

C = condition at time t

C_0 : the condition at time $t = 0$

$\alpha, \ \gamma$ = model constants

Time intervals utilised for this model were in the unit of years, but could also be in the unit of months, weeks, or days. The unknown constants $\alpha, \ \gamma,$ which calibrate the model were generated. These unknowns were solved using the measured data in silk conditions by minimising the model prediction error for the model expression (equation 39). Using numerical optimization with a gradient based search algorithm, the error between the model predictions and the measured values for these three conditions was minimised, as detailed in Chapter 4 Table 4-6 and in Appendix 8.5 and 8.6. Optimisation methods to solve the above problem were available with software tools such as Visual Doc (Vrand, 2020) and MATLAB (Mathworks.com, 2020). However, for the scope of this study, as no brand-new silk sample could have been measured, C_0 was solved mathematically. By minimising the function, the solution for the three unknown conditions $C_0 \ \alpha, \gamma,$ was derived. The three solved model parameters for the case study as discussed previously are detailed in Table 5-3.

6.2.6. Part 5: Prognostic Colour Degradation Model

General application: The exponential decay model provides the structural underpinnings of the developed prognostic modelling. It enables the utilisation of the existing sensor-based environmental data and correlates colourimeter data with the use of optimisation. With the parameters established in Table 5-3 in Chapter 5, the model can help predict the cumulative degradation, in terms of colour change, for a silk fabric. The cumulative degradation values $S1^{(k)}$ and $S2^{(k)}$ would be derived as per Eq. (45) and Eq. (46) for each of the environmental conditions denoted by superscript of (k).
Where,

$$S1^{(k)} = \left(0.1T^{(k)} - 28.7\right)RH^{(k)}t^{(k)}, \text{ k=1,2,3, *} \quad (45)$$

$$S2^{(k)} = v^{(k)}RH^{(k)}t^{(k)}, \text{ k=1,2,3, *} \quad (46)$$

The notion of using the superscript of (k) is adopted, to associate to the sample being calculated; $k = 1,2,3$. For example, $k = 1$ is the reference to the silk sample on display. These values relate to cumulative colour degradation. Time horizon can be changed to days, weeks, or months. For this research the time horizon is taken in years. The exponential curve would display the predictions over time (at a yearly interval) for the cumulative colour degradation of silk. Expert opinion of museum professionals would need to be sought to determine the condition of failure of the sample fabric, to determine the lowest acceptable threshold.

Specific application: The exponential curve displays the predictions over time (at a yearly interval) for the cumulative colour degradation. The degradation values are derived as per Eq. (47) and Eq. (48) for three environmental conditions (1956 sample 1 ,1991 sample 2, 1956 storage sample 3) utilised as illustrated in Table 5-1 and further detailed in Appendix 8.5.
where, $S1^{(k)}$ and $S2^{(k)}$ are the cumulative degradation values for each environmental condition, denoted by superscript of (k)

$$S1^{(k)} = \left(0.1T^{(k)} - 28.7\right)RH^{(k)}t^{(k)}, \text{ k=1,2,3} \quad (47)$$

$$S2^{(k)} = v^{(k)}RH^{(k)}t^{(k)}, \text{ k=1,2,3} \quad (48)$$

The exponential decay model of colour fade is illustrated in Figure 6-3, showing an asymptotic curve of degradation over time, based on the mathematically derived colour condition value $C_0 = 376$.

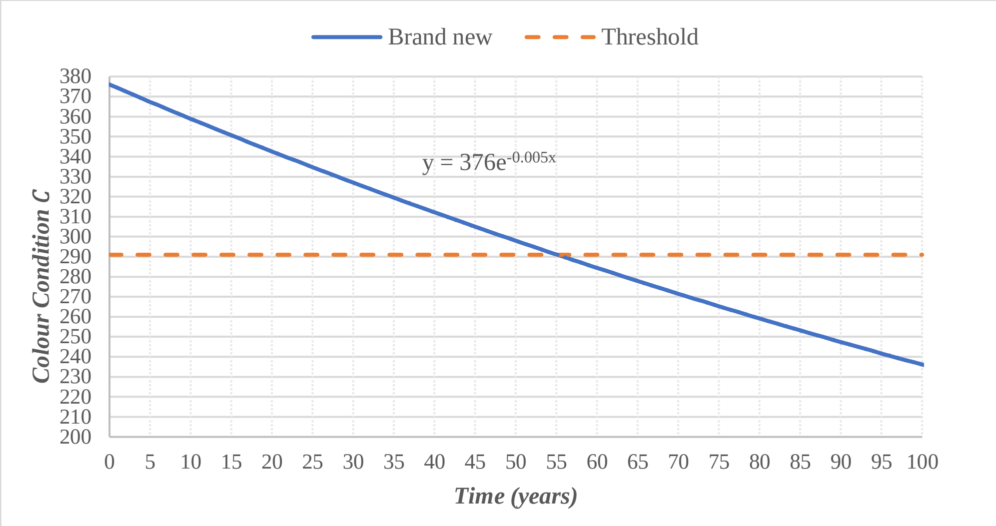

Figure 6-3: Exponential Model of Silk Colour Condition

Hence, this illustrates the overall nature of the cumulative degradation of the silk fabric with a gradual loss of colour in the initial stages, followed by a reduced rate in the later years. Expert opinion of museum professionals was sought to determine the condition of failure of the sample fabric. Sample reference 1, that had been on display in the Great Gallery since 1956, was seen, on visual inspection by the experts to have damage, such as fading and shredding, and was beyond the condition of failure point, with a colour condition value of 281.5. As a result, the lowest acceptable threshold was assumed to be 290. Based upon this point of failure threshold, it can be estimated that the brand-new silk would have a life of 55 years, when maintained in the typical museum environmental conditions. To add more data points of the measured value for silk color condition C with the chromometer, for silk exposed to environmental degradation condition $^{(k)}$ denoted as $M^{(k)}$. Thus, the measured colour value $M^{(k)}$ for sample conditions 1, 2 and 3, as detailed in Table 4-6 can be further added to annually as per equation 40.

6.2.7. Part 6: Forecasting Demonstration Scenarios

General application: This novel non-invasive and non-destructive, data driven prognostic modelling for the silk colour condition in-situ can be used to predict the cumulative damage to silk fabric over different time horizons and under different museum environmental conditions. These scenarios can be custom developed as per the needs of the museum's conservators, to predict the sensitivity of the environment and the colour condition of silk.

Specific application: The 10 demonstration scenarios, as detailed in Chapter 5 assessed the sensitivity of the silk sample 2 in its environmental conditions. This enables the RUL prediction of silk sample 2, that has been on display since 1991. It was measured and analysed as exhibiting, colour condition value C_0 331.The prognostic degradation data of the 10 scenarios modelled can be found in Appendix 8.8. The results are summarised in Table 6-1.

Scenario	Museums Environmental Conditions	RUL (years)
Scenario 1 Typical	Typically maintained yearly average temperature 20.7°C, RH 56.7(%) and illuminance 55lx	28
Scenario 2 Raised	Marginally raised by 1-unit, yearly average in temperature to 21.7°C, RH to 57.7% and illuminance to 56lx	27
Scenario 3 Increased	10% increase in the yearly average temperature to 22.7°C, RH 62.37% and illuminance to 60.5lx	22
Scenario 4 Harsh	15% increase approximately in the yearly average of temperature to 23.8°C, RH 65.2% and illuminance to 63.2lx	20
Scenario 5 Lowered	5% decrease in the yearly average of temperature 19.6°C, RH 53.7% and illuminance 52.2lx	32
Scenario 6 Reduced	15% decrease in the yearly average of temperature (17.6°C), RH (48.2%) and illuminance (46.7lx)	43
Scenario 7	Lower range of the UK standard guidelines temperature 18°C, RH 50% and illuminance 50lx	38
Scenario 8 (a,b,c)	Only one environmental condition increased by 15% a) RH (15%) increased to 65.2%	25
	b) Light (15%) increased 63.2lx	26
	c)Temperature (15%) increased 23.8°C	26
Scenario 9 Alternate	Alternating typical display conditions of temp 20.7°C, RH 56.7(%), 55lx with storage conditions of 16°C, RH 50(%), and max 10lx	50
Scenario 10 Alternate every 2 years	Alternating display conditions every two years with storage conditions of 16°C, RH 50(%), and max 10lx	40

Table 6.1: Summary of Demonstration Scenarios Results

Scenario1 predicted the RUL of silk sample 2 to be 28 years under current environmental conditions. In scenario 2 it was observed that silk is relatively sensitive to a marginal increase such as a 1 unit increase in yearly averages of all three environmental conditions. This increase predicted a reduction by one year in the *RUL* of the silk. This confirms previously published studies (Muge and Suat, 2016) (May and Jones (2006), suggesting the increased fragility of silk fabric to marginal increases in the conditions of temperature, humidity, and illuminance.

Scenario 8 which models the sensitivity of each individual parameter, by increasing each by 15% independently of the others, showed that harsher RH conditions decreased RUL by 3 years, compared to 2 years for temperature and lux. The result indicating that RH impacts the colour fade more than either temperature or lux separately, confirming previously published studies by Saunders and Kirby (2004), who used accelerated aging to understand photodegradation of pigments, and concluded that increased RH at a constant temperature caused greater colour change, in dyed silk. Scenario 8 also indicated that the severity of impact, from the combined cumulative damage of raised conditions for all three parameters, was found to be far more damaging, than each individual condition separately, introducing an additive effect on colour fade.

The best-case scenario for prolonging the RUL of the silk was based on the scenarios involving object rotation, namely scenarios 9 and 10. It was observed that rotation from display to storage prolonged the RUL by almost 22 years. If the object was rotated annually from display to storage, it had an almost doubling effect on the RUL. In the same regard, scenario 7, establishes the fact that the RUL can be significantly improved by setting the environmental conditions, towards the lower end of the spectrum of museum guidance standards. Under this scenario, the results predicted a marked increase in the RUL by 18 years, from 27 to 44 years.
Whilst the previous scenarios revealed the best predictive outcomes, Scenario 4, highlighted the worst, showing clearly, that increases in the factors, resulted in a significant degradation in the colour of the silk. For all the analysis conducted, the overwhelming conclusion was that the demonstration scenarios clearly exhibited their value in the process of museum decision making, in establishing the predicted outcomes, to support the museums preservation objectives.

6.2.8. Part 7: Health Management by enabling decision-making with mitigation strategies.

The main purpose of the general conservation process is to stabilise the artefacts in their care. The rate of deterioration may be slowed until a critical point is reached, when an equilibrium is disturbed, and the reaction gathers momentum (Bradley, 1994). According to the literature reviewed in Chapter 2, the tendency to make standards an end in themselves, instead of a means to improve the preservation of collections has been challenging. Atkinson, (2014) and Alcántara, (2002) have iterated that the best method of improvement should be based on the continuous unique study of individual collections. Minimising deterioration, under the specific conditions of its situation, is much more efficient than rectifying the consequent damage to the restored silk.

Prognostic modelling has indicated that silk rotation away from display conditions to storage conditions, prolongs the RUL of the silk fabric most significantly. Although object rotation would involve extra staff and time thus introducing additional cost, this can be compared with the typically high costs associated with the restoration of the silk. The prognostics method could help museums develop mitigation strategies to minimise silk fade by adopting object rotation or reducing the environmental conditions parameters to the lowest thresholds in the museum standard range. The sensitivity analysis of these scenarios depicts a clear correlation between a longer exposure to the environmental display conditions, and a greater impact on the colour fade of the silk. This is true for all three parameters (light, RH, Temp). Although increased RH conditions alone decrease RUL by 3 years, as compared to the same level of increase for light or temperature reducing the RUL by two years.

The degradation model detailed with Equations 37 and 38 (Section 3.2.4) is derived in the form to predict the colour level of the silk fabric after a certain period and environmental conditions. However, the model can be inversed and expressed as a model that solves for temperature (similarly humidity or light) that will provide a certain level of degradation, respectively colour condition (C) of the fabric, over a pre-defined time.

Inversing the models requires a simple transformation. In the case of solving for the environmental parameters, the model is manipulated as follows:

$$\mathrm{C(t, T, RH, v) = C_0 e^{-a(T,RH,v)t}}$$

Denote $C(t, T, RH, v)$ with a simple notation C

$$Then\ \frac{C}{C_0} = e^{-a(T,RH,v)t} \tag{49}$$

$$\ln\left(\frac{C}{C_0}\right) = \ln\left[e^{-a(T,RH,v)t}\right] \tag{50}$$

$$\ln\left(\frac{C}{C_0}\right) = -a(T,RH,v)t \tag{51}$$

Per equation Equations 37 (Section 3.2.4),

$$a(T,RH,v)t = [\alpha(0.1T - 28.7) + \gamma v]RH \tag{52}$$

Therefore,

$$[\alpha(0.1T - 28.7) + \gamma v]RH = -\frac{\ln C - ln\, C_0}{t} \tag{53}$$

With eq. (53) it is possible to express and solve for T, RH, and light. For example, to solve for temperature (T):

$$\alpha.RH(0.1T - 28.7) + \gamma vRH = \frac{\ln C_0 - \ln C}{t} \tag{54}$$

$$0.1T - 28.7 = \frac{1}{\alpha.RH}\left[\frac{\ln C - \ln C_0}{t} - \gamma vRH\right] \tag{55}$$

$$T = 10\left(28.7 + \frac{1}{\alpha.RH}\left[\frac{\ln C - \ln C_0}{t} - \gamma vRH\right]\right) \tag{56}$$

The inverse modelling calculations may be required in instances when the museum may want to establish environmental parameter values that result in a predefined level of degradation of a given period, thus helping to inform the decisions and control of the museum environment. For example, if the requirement for the silk is to last approximately 40 years (i.e., colour degrades to the threshold value), and the RH is 50% and illuminance is $50lx$±2, solving for the temperature point that it should be maintained at 18C. In this case such conditions are feasible, falling within the lower range of the UK standard guidelines.

This methodology can also provide the museum with the prognostics to make informed practical decisions about the silk being monitored. For example, concerns relating to the impact on artifacts, from their lending to other museums, may be partly or wholly resolved using this model.

6.3. Specific Recommendations for The Wallace Collection

Based on the research work, the following recommendations are proposed for the Wallace Collection:

- Improving the accuracy of the Modelled predictions, through more regular Colorimetric Data Collection: Further development of the PHM model for Shrewsbury Set could be beneficial. Recommendation for additional annual data points relating colour condition be recorded. This would provide a continual representation of the cumulative colour loss over time, thus evolving the predictive model. Although annual data points for colour condition C for the Shrewsbury set are required, but for any new study this can be changed to months, weeks, or days.
- Building Colorimetric Condition Database: Data relating to colour condition can be extended to other collections of silk as well. This can help build a repository for the museum of the changing colour conditions of silk. This can include new fabric samples from recent restorations, as well as old historical samples.
- Documentation: It is assumed that the fabric was either housed in the museum display or in the museum storage environment. There isn't an accurate historical record of the specific environmental conditions that the silk may have been exposed to outside of these two states, and hence, exposure to any other external environmental conditions has been not considered while determining the fade model. The archives documenting restoration or repair could benefit from further details regarding environmental exposure. For example, stating the length of time silk was kept out of the controlled museum environmental conditions, and the level of exposure to light levels, relative humidity fluctuation and temperature levels during the period of restoration.
- Silk Rotation based on PHM modelling: Predictive results (as detailed in chapter 5) show the RUL of the silk in ambient conditions seemed to prolong significantly if it were moved away from the display conditions. Rotating the silk annually had an almost doubling effect on the RUL of the silk fabric being studied, suggesting that limiting the time on exhibition could reduce the cumulative damage to the silk.
- Alternative Option for Rotation: If the annual silk rotation is logistically difficult, the museum may prefer to rotate them every two years. For example, exhibiting under display conditions for two years and then under storage conditions for one year. This can be seen (in chapter 5) significantly prolong the life of the silk.

- Existing environmental conditions: It has also been observed in the demonstration scenario in chapter 5 that if the environmental conditions (Temperature, relative humidity, and light) were reduced to the lower extent of the museum standard guidelines, there was a noticeable prolongation in the RUL of the silk fabric.

6.3. Areas for Future Research

Further research could build upon this work in the following areas:

- Further Development of a Diagnostic and Prognostic Tool: A web-enabled database management system using Visual Studio and complementary visualisation tool, Tableau is recommended. This could enable user-friendly on-site data collection, and aid pre-processing, and prognostic modelling.

- Extension of the PHM Method: Colour condition data from other silk collections can collected and similarly documented. This would establish a repository of colour condition data correlated to environmental conditions. This could include new fabric samples from recent restorations, or original samples of historical significance. This could help in adapting and evolving this model for use in the conservation of other artefacts, for example, coloured silks and textiles, the fade of paint on wood objects or marquetry, (such as on the current Reisner's collection housed at the Wallace Collection).

- UV Sensor Data: Although ultraviolet (UV) light has been discounted from this model, its inclusion in the future would be beneficial such as a NIR spectrophotometer to measure potential UV damage.

- Other Considerations: Pollutants in the form of gases can increase acidity, thus extending the causal parameters leading to deterioration of silk. Therefore, the PHM model could be extended to include these parameters (and others, for example, the impact of footfall).

7. CONCLUSION

Silk artefacts represent an important part of our civilisational heritage, often being conserved in museums for the purposes of education, tourism, and research. Conservation of silk artefacts represents a significant challenge for museums housing such collections. Often, in spite of having expensive environmental systems, silk artefacts remain prone to continual degradation.

Restoring silk, comes at a significant cost to museums, and therefore a more cost-effective and less interventive approach to conservation is needed. To assist conservators in their efforts to prolong the Remaining Useful Life of such artefacts, museum standards exist, which, based on broad categorisations of materials, provide guidelines for the range of conditions under which the artefacts should be maintained on display. However, more specific guidance to conservators is absent, as there is a general lack of literature and analysis relating to the natural aging of silk artefacts under certain environmental conditions.

Studies relating to silk conservation have tended towards the use of accelerated aging methods, which have required the use of micro samples, (fibres, threads, materials), from the original silk, or require the movement of the artefact, from its place of display to a laboratory, for analysis. The conclusion from the literature review is that there has been limited comprehensive study into non-invasive and non-destructive in situ techniques. Therefore, there is a need to accurately predict the extent of silk's degradation, without damage to the silk in the process of this analysis, within the context of the museum's' environmental conditions, and with the goal of aiding its conservation.

The research detailed here, brings together the methodology of Prognostic Health Management (PHM), as applied in fields such as aerospace engineering, built environments and nuclear sciences, to this area of silk conservation. Prognostic Health Management (PHM) establishes an efficient management process, relating to the conditions under which machines and materials are maintained, to extend their life and avoid the need for unpredictable and costly repairs. PHM entails both diagnostics and prognostics. Diagnostics are based on knowledge about the current operation and environmental system through observed data. Prognostics involve the assessment of actual health conditions and the use of degradation modelling to derive remaining useful life (RUL) predictions. Where there is limited conditional data, the prognostic method can use statistical, data-driven approaches for this derivation.

Silk conservation studies have typically used instruments such as colourimeters and spectrophotometers. Although, the latter are more sophisticated and have a wider spectral range, they are also more expensive and have limited portability. Unlike spectrophotometers, techniques such as XRF and near-infrared (NIR) spectroscopy are more portable, however, NIR spectroscopy requires a suitable reference dataset for comparison. The issue here is that most silk datasets are based on newly woven silk samples, not data derived from heritage, aged silk, and therefore comparisons cannot be extrapolated. Colourimeters, on the other hand, have proven to be accessible, portable, accurate and affordable. Colourimetry measurements can be applied to the CIE international standards to determine colour of the samples.

To achieve the desired prognostic modelling, a new mathematical fade model is postulated, using a derived exponential decay model to predict cumulative colour degradation. This model adapts a linearised Arrhenius reaction rate, to predict the fading, (colour degradation) of the silk, based upon its exposure to environmental conditions, such as temperature, light levels, and relative humidity. It is the first time such a model has been presented that seeks to combine these factors with colorimetric data.

A relatively inexpensive portable instrument was used to take in situ measurements of silk samples, from chairs, forming part of the Shrewsbury Set, displayed at the Wallace Collection in London. The data driven diagnostic technique adopted the international colour standard, such as CIE XYZ, with Euclidian distance analysis to identify the colour condition of the silk. Statistical data-driven prognostic techniques were utilised to model the cumulative degradation of the colorimetric condition data of the silk and to predict its remaining useful life. The diagnostic and prognostic tools presented in this research were validated though numerical optimisation and through demonstration examples.

Data was collected by measuring four silk samples. Sample 1 was the silk sample reference, from a chair that had been on continuous display in the Great Gallery since its restoration in 1956. This reference sample had been exposed for the longest period to the open display conditions of the museum. Sample 2 was from the chair that had been restored with historically accurate silk in 1991. Sample 3 was a surplus offcut from the 1956 fabric roll, that had been kept in storage with a protective covering limiting its exposure to light and minimising the impact of relative humidity. Sample 4 was from the chair that had been restored in 1993.

The readings were measured as tristimulus values XYZ, adopting the International Commission of Illumination (CIE) 1931 CIE XYZ colour standard to determine the colour fade. The Euclidian distance formula for colour difference was utilised to determine the colour condition C of each sample reference. The analysis indicated that the higher the value of the colour condition (C), the better the colour condition of the silk sample observed. An assumption was made that the historically accurate silk replica fabric was kept predominately, either on display, or in museum storage. The environmental data of the museum conditions was gathered from museum historical records, such as the archived records for care and restoration, hygrothermographs, visual inspection and sensor data including temperature, relative humidity, and illuminance.

The actual sensor data for the previous 10 years showed an average annual temperature of $20℃ \mp 1.5℃$. Over the same period, the average annual relative humidity was seen to peak at 64% and decline to 51%, fluctuating by 13%. The yearly average illuminance levels, based on 4 years of data, was seen to have a highest annual average at $55.7lx$ and lowest annual average at $50lx$, indicating a 6% increase.

The postulated mathematical model derived the exponential decay model that solved for the unknown brand-new colour condition (C_0) of the silk fabric, and two unknown model parameters. The unknown colour condition new (C_0) was found through numerical optimisation using a gradient based search algorithm. The brand-new colour condition was determined to be 376.12 and based on this the brand-new silk was derived to have a life of 55 years, under the maintained museum environmental conditions. Given the limitation of colour condition data relative to time, the fourth condition k of the measured sample (1993) was used to validate the model. The variance between the measured value and the model prediction was 0.9.

The colour fade of the silk illustrates an asymptotic curve of degradation over time. It demonstrates the overall nature of the cumulative degradation of the silk fabric with a gradual loss of colour in the initial stages, followed by a reduced rate in the later years. There remains the possibility of reversing the model in which the remaining useful life years are predetermined, and the environmental parameters calculated to reach the time-based objective.

Ten different hypothetical sensitivity scenarios were developed to demonstrate colour degradation. Overall, sensitivity analysis depicted a clear correlation between a longer exposure to the environmental display conditions, and a greater impact on the colour degradation of the silk. The scenarios showed that the silk samples were relatively sensitive to marginal increases in all three parameters (Light, Relative Humidity, Temperature). However, it was seen that Relative Humidity impacted the colour fade more than either temperature or Light separately. The combined cumulative damage of all three parameters, was found to be more damaging, than each individual condition separately. The best-case scenario for prolonging the RUL of the silk was based on scenarios involving object rotation, (moving the silk from display into storage for a period of time), in which the RUL was seen to increase from a typical 28 years to approximately 50 years. These modelled predictions were seen to be useful in informing decision-making relating to the prolongation of the RUL of the Silk chairs, minimising costly reactive interventive restorations.

Future recommendations include, the further adoption by the Wallace Collection of this condition-based conservation methodology and its derived modelled output for the Shrewsbury Set; Greater emphasis on the collection of additional annual or monthly condition data points using a colorimeter; Expanding the methodology and its application to other other silk based artefacts in the Wallace Collection; Creating a colourimeter database for silk artefacts with a view towards enabling further research, and aiding long-term conservation more generally within the broader community of museums. Whilst the impact of UV light prior to 2007, was not considered in this modelling, primarily because there was an absence of suitable data, it was seen that the deployment from 2007 onwards, of conservation UV filters on windows and low UV from artificial lighting, meant that the silks exposure to UV was minimised to almost negligible levels during this time. However, the missing data is an unknown factor, and so it is recommended that the impact of this could be further investigated to determine its significance to the conservation recommendations. Future development of a diagnostic and prognostic tool could be developed within a mobile based application, codifying the PHM method, and combining the function of the colourimeter. Finally, this novel interdisciplinary research can be extended, practically, for use in the conservation of other artefacts, for example, other textiles, the fade of paint on wood artefacts, or marquetry.

8. REFERENCES

Agnew, N. (2010) *Conservation of the Ancient Sites on the Silk Road.* Proceedings of the Second International Conference on the Conservation of Grotto Sites, Mogao Grottoes, Dunhuang, People's Republic of China, June 28–July 3, 2004. Los Angeles: Getty Publication.

Ahn, C., Zeng, X., Li, L. & Obendorf, S.K. (2014) '*Thermal Degradation of Natural Dyes and their Analysis using HPLC-DAD-MS', Fashion and Textiles*, 1, 22 (2014). doi: https://doi.org/10.1186/s40691-014-0022-5

Alcántara, R. (2002) Standards in Preventive Conservation: Meanings and Applications, Methods, (June), p. 47, [online] Available at: http://www.iccrom.org/pdf/ICCROM_04_StandardsPreventiveConser_en.pdf. (Accessed: 22 August 2020)

Alexandrakis, G., Manasakis, C. & Kampanis, N. A. (2019) '*Economic and Societal Impacts on Cultural Heritage Sites, Resulting from Natural Effects and Climate Change',* Heritage 2019, (2), pp. 279–305. doi: https://doi.org/10.3390/heritage2010019

An, D., Kim, N. H. and Choi, J.-H. (2015) Practical options for selecting data-driven or physics-based prognostics algorithms with reviews, *Reliability Engineering & System Safety*, 133, pp. 223–236, [online] Available at: http://www.sciencedirect.com/science/article/pii/S0951832014002245.

Ashley-Smith, J. (2018) *Challenges of Managing Collection Environment*, Conservation Perspectives, The GCI Newsletter, (33.2) Fall 2018. Available at: http://www.getty.edu/conservation/publications_resources/newsletters/33_2/feature.html (Accessed: 19 August 2020).

Atakul, N., Thaheem, M. J. and De Marco, A. (2014) Risk management for sustainable restoration of immovable cultural heritage, part 1: PRM framework, *Journal of Cultural Heritage Management and Sustainable Development*, 4(2), pp. 149–165.

Atkinson, J. Kirby. (2014) '*Environmental Conditions for the Safeguarding of Collections: A background to the current debate on the control of relative humidity and temperature',* Studies in Conservation, 59(4), pp. 205-212. doi: https://doi.org/10.1179/2047058414Y.0000000141

Avison, D., Shah, H. U., Powell, R. S. and Uppal, P. S. (1992) 'Applying methodologies for information systems development', *Journal of Information Technology*, pp. 127–140.

Avrami, E., Mason, R. and Tore, M.D.L. (2000) *Values and Heritage Conservation: A Research Report.* Los Angeles: The Getty Conservation Museum. Available at:https://www.getty.edu/conservation/publications_resources/pdf_publications/pdf/valuesrpt.pdf. (Accessed: 22 April 2017).

Badillo-Sanchez, D., Chelazzi, D., Giorgi, R., Cincinelli, A. and Baglioni, P. (2019) '*Understanding the structural degradation of South American historical silk: A Focal Plane Array (FPA) FTIR and multivariate analysis'*, Scientific Reports, 9(1), p. 17239, [online] Available at: https://doi.org/10.1038/s41598-019-53763-5.

Bakker, F. T., Antonelli, A., Clarke, J. A., Cook, J. A., Edwards, S. V., Ericson, P. G. P., Faurby, S., Ferrand, N., Gelang, M., Gillespie, R. G., Irestedt, M., Lundin, K., Larsson, E., Matos-Maraví, P., Müller, J., von Proschwitz, T., Roderick, G. K., Schliep, A., Wahlberg, N., Wiedenhoeft, J. and Källersjö, M. (2020) The global museum: Natural history collections and the future of evolutionary science and public education, *PeerJ*, 8, pp. 1–40. Available at: https://doi.org/10.7717/peerj.8225

Baraldi, P., Cadini, F., Mangili, F. and Zio, E. (2013) 'Model-based and data-driven prognostics under different available information', *Probabilistic Engineering Mechanics*, 32, pp. 66–79, [online] Available at: http://www.sciencedirect.com/science/article/pii/S0266892013000143. (Accessed: 24 June 2020)

Baraldi, P., Mangili, F. and Zio, E. (2015) A prognostics approach to nuclear component degradation modeling based on Gaussian Process Regression, Progress in Nuclear Energy, 78, pp. 141–154, [online] Available at: http://www.sciencedirect.com/science/article/pii/S0149197014002431. (Accessed: 05 June 2020)

Beć, K. B. and Huck, C. W. (2019) *‘Breakthrough Potential in Near-Infrared Spectroscopy: Spectra Simulation. A Review of Recent Developments*’, Frontiers in Chemistry, 7, pp. 48, [online] Available at: https://www.frontiersin.org/article/10.3389/fchem.2019.00048. (Accessed: 16 June 2020)

Benden, D.M and Taft, M.C. (2019) ‘A Long View of Archaeological Collections Care, Preservation, and Management’, *Advances in Archaeological Practice*, 7(3), pp. 217-223.

Bennett, F. (2019) *"Climate Control in the Face of Climate Change: Reducing Carbon Footprints in Museums"*. Seton Hall University Dissertations and Theses (ETDs). 2674. Available at: https://scholarship.shu.edu/dissertations/2674 (Accessed: 4 June 2020)

Boersma, F., Taylor, J., Dardes, K., and Lumkomski, M. (2018) *The Managing Collection Environments Initiative*. Conservation Perspectives, The GCI Newsletter, (33.2) Fall 2018. Available at: http://www.getty.edu/conservation/publications_resources/newsletters/33_2/managing.html (Accessed: 19 August 2020).

Bolewski, A., Matosz, M., Pohorecki, W., del Hoyo-Meléndez, J.M. (2020) ‘*Comparison of neutron activation analysis (NAA) and energy dispersive X-ray fluorescence (XRF) spectrometry for the non-destructive analysis of coins minted under the early Piast dynasty’,* Radiat. Phys. Chem. 171, 108699. https://doi.org/https://doi.org/10.1016/j.radphyschem.2020.108699

Boulet-Audet, M., Lefèvre, T., Buffeteau, T., & Pézolet, M. (2008) ‘*Attenuated total reflection infrared spectroscopy: an efficient technique to quantitatively determine the orientation and conformation of proteins in single silk fibers’*, Applied spectroscopy, 62(9), pp. 956–962. https://doi.org/10.1366/000370208785793380

Bradley, S.M. (1994) Do objects have a finite lifetime? *Care of Collections: Leicester Readers in Museum Studies*. Oxford: Routledge.

Brill, M. H. (1996) Do tristimulus values have units? *Color: Research and applications*, 21(4), pp. 310–313.

Brzozowska, I., Bogdanowicz, A., Szczęsny, P., Zielenkiewicz, U. and Laudy, A. (2018) Evaluation of bacterial diversity on historical silk velvet textiles from the Museum of King John III's Palace at Wilanów, Poland, *International Biodeterioration & Biodegradation*, 131, pp. 78–87, [online] Available at: http://www.sciencedirect.com/science/article/pii/S0964830516305662.

Cąkici, N., Aksu, M. I. and Erdemir, E. (2015) '*A survey of the physico-chemical and microbiological quality of different pastirma types: A dry-cured meat product', CYTA - Journal of Food*, Taylor & Francis, 13(2), pp. 196–203, [online] Available at: https://doi.org/10.1080/19476337.2014.938123.

Caple, C. (2012) *Preventative Conservation in Museums: Leicester Readers in Museum Studies.* Oxford: Routledge.

Cao, Y. and Wang, B. (2009) '*Biodegradation of Silk Biomaterials'*, International Journal of Molecular Sciences, 10(4), pp. 1514-1524.

Carter, D. J. and Walker, A. K. (1999) Collection environment, *Care and conservation of natural history collections*, pp. 139–151. Available at: https://www.natsca.org/sites/default/files/publications/books/Environment.pdf (Accessed: 21 October 2020)

CCI. (2017) *Agents of Deterioration, Canadian Conservation Institute*. Available at: https://www.canada.ca/en/conservation-institute/services/agents-deterioration.html (Accessed: 28 April 2020)

Chakraborty, J.N. (2015) *Fundamental and Practices in Colouration of Textiles.* 2nd edition. India: CRC Press. pp. 453.

Choudhary, A.K.R. (2015) Colour-Difference Assessment: Principles of Colour and Appearance Measurement. Available at: https://www.sciencedirect.com/topics/engineering/colour-difference-formula (Accessed: 17 May 2020)

Choudhary, A.K.R. (2014) *Principles of Colour and Appearance Measurement*: Object Appearance, Colour Perception and Instrumental Measurement. Available at: https://www.sciencedirect.com/topics/engineering/colorimeter (Accessed: 8 June 2020)

Chu, S. J., Trushkowsky, R.D. and Paravina, R.D. (2010) *'Dental Colour Matching Instruments and Systems. Review of Clinical and Research aspects',* Journal of dentistry, 38, supplement 2(2010), pp. e2–e16. doi: https://doi.org/10.1016/j.jdent.2010.07.001

CIE (2020) *About CIE.* International Commission of Illumination. Available at: http://cie.co.at/about-cie(Accessed: 14 June 2020)

CIE (2020B). Colorimetry – Part 2: CIE Standard Illuminants. International Commission of Illumination. Available at: http://cie.co.at/publications/colorimetry-part-2-cie-standard-illuminants (Accessed: 14 November 2020)

CIE (2020C). Colorimetry – Part 3: CIE Tristimulus Values. International Commission of Illumination. Available at: http://cie.co.at/publications/colorimetry-part-6-ciede2000-colour-difference-formula-0 (Accessed: 14 November 2020)

CIE (2020D). Colorimetry – Part 3: CIE Tristimulus Values. International Commission of Illumination. Available at: http://cie.co.at/publications/colorimetry-part-3-cie-tristimulus-values-2 (Accessed: 14 November 2020)

Clark, J. (2018) The Effect of Temperature on Reaction Rates. Available at: https://www.chemguide.co.uk/physical/basicrates/temperature.html (Accessed: 03 November 2017)

Clementi, C., Miliani, C., Romani, G. & Favaro, G. (2006) '*In Situ Fluorimetry: A Powerful non-invasive Diagnostic Technique for Natural Dyes used in Artefacts: Part 1. Spectral Characterization of Orcein in Solution, on Silk and Wool Laboratory-Standards and a Fragment of Renaissance Tapestry',* Spectrochimica Acta Part A: Molecular and Biomolecular Spectroscopy, 64(4), pp. 906-912.

Colombini, M. P., Andreotti, A., Baraldi, C., Degano, I. and Łucejko, J. J. (2007) Colour fading in textiles: A model study on the decomposition of natural dyes, Microchemical Journal, 85(1 SPEC. ISS.), pp. 174–182.

Colourphil - Graphic Quality Consultancy (2020) *Introduction to Colour Models (Spaces).* Available at: https://www.colourphil.co.uk/xyz_colour_space.shtml (Accessed:15 June 2020)

Couteau, C., Philippe, A., Vibet, M.-A., Paparis, E., Coiffard, L. (2018) '*Study of the influence of substrate and spectrophotometer characteristics on the in vitro measurement of sunscreens efficiency*', Eur. J. Pharm. Sci. 121, pp. 210–217. https://doi.org/https://doi.org/10.1016/j.ejps.2018.05.010

Craic Technologies (2019) What is a Spectrophotometer? Available at: http://www.microspectra.com/support/learn/what-is-a-spectrophotometer (Accessed: 8 June 2020)

Cristina Heras, V., Wijffels, A., Cardoso, F., Vandesande, A., Santana, M., Van Orshoven, J., Steenberghen, T. and van Balen, K. (2013) *A value-based monitoring system to support heritage conservation planning*, Journal of Cultural Heritage Management and Sustainable Development, 3(2) 130–147. DOI: https://doi.org/10.1108/jchmsd-10-2012-005

Dahlin, E. (1995) *Preventive conservation strategies for organic objects in museums*, historic buildings and archives Plenary sessions, Buildings, pp. 57–60, [online] Available at: http://www.cyfronet.krakow.pl/~ncbratas/pdf/full_dahlin.pdf.

De la Torre, M., (2013). *Values and Heritage Conservation*. Heritage & Society, 6(2), pp.155–166. Available at: http://www.maneyonline.com/doi/abs/10.1179/2159032X13Z.00000000011.

Degano, I., Biesaga M.P., Colombini M.P, Trojanowicz, M. (2011) '*Historical and archaeological textiles: an insight on degradation products of wool and silk yarns',* Journal of Chromatography A. 2011 Aug 26;1218(34):5837-47. DOI: https://doi.org/10.1016/j.chroma.2011.06.095.

Del Hoyo-Melendez, J.M. and Mecklenburg, M.F. (2012) '*Micro-fading Spectrometry: A Tool for Real-Time Assessment of the Light Fastness of Dye/Textile Systems'*, Fibres and Polymers, 13(8), pp. 1079-1085.

De la Torre, M. (2013) '*Values and Heritage Conservation*', *Heritage & Society*, 6(2), pp.155–166. Available at https://doi.org/10.1179/2159032X13Z.00000000011

Depcinski, M. C. (2014) *'Conservation in Museums, In Smith, C. (ed.), Encyclopedia of Global Archaeology'*, New York, NY, Springer New York, pp. 1656–1659, [online] Available at: https://doi.org/10.1007/978-1-4419-0465-2_796.

Drury, P., & McPherson, A. (2008) *Conservation Principles, Policies and Guidance*, In English Heritage.

Duxbury, D. F. (1994) The sensitized fading of triphenylmethane dyes in polymer films: Part 1, *Dyes and Pigments*, 25(2), pp. 131–166, [online] Available at: http://www.sciencedirect.com/science/article/pii/0143720894850445.

Eastern Applied (2018) *The Cost of XRF Analyzers (both short and long term*). Available at: http://www.easternapplied.com/blog/xrf-sales/xrf-analyzers- (Accessed: 16 June 2020)

Edwards, J. (2019) What is Predictive Analytics? Transforming data into future insights. Available at:https://www.cio.com/article/3273114/what-is-predictive-analytics-transforming-data-into-future-insights.html (Accessed: 4 June 2020)

Erhardt, D., & Mecklenburg, M. (1995) '*Accelerated VS Natural Aging: Effect of Aging Conditions on the Aging Process of Cellulose'*, *Materials Research Society Symposia Proceedings*, 352 (1995), pp. 247-270. doi:10.1557/PROC-352-247

European Network for Conservation-Restoration Education. (2002) *ECCO Professional Guidelines*. Available at: http://www.encore-edu.org/ecco1.html (Accessed: 22 April 2020).

Fan, T. and Zhao, W. (2017) ‘Ensemble of model-based and data-driven prognostic approaches for reliability prediction,’ *Prognostics and System Health Management Conference* (PHM-Harbin), Harbin, 2017, pp. 1-6, doi: 10.1109/PHM.2017.8079114.

Fink, O., Wang, Q., Svensén, M., Dersin, P., Lee, W. J. and Ducoffe, M. (2020) Potential, challenges and future directions for deep learning in prognostics and health management applications, *Engineering Applications of Artificial Intelligence*, 92, p. 103678, [online] Available at: http://www.sciencedirect.com/science/article/pii/S0952197620301184.

Fisher Scientific (2020) *Spectrophotometers*. Available at: https://www.fishersci.co.uk/gb/en/products/I9C8L6BV/spectrophotometers.html (Accessed: 16 June 2020)

Ford, A. and Roberts, A. (1998) Colour Space Conversions, 1998, pp. 1–31.[online] Available at: https://poynton.ca/PDFs/coloureq.pdf (Accessed: 18 May 2020)

Forrester, J. V., Dick, A. D., McMenamin, P. G., Roberts, F. and Pearlman, E. (2016) *Chapter 5 - Physiology of vision and the visual system*, In Forrester, J. V, Dick, A. D., McMenamin, P. G., Roberts, F., and Pearlman, E. B. T.-T. E. (Fourth E. (eds.), W.B. Saunders, pp. 269-337.e2, [online] Available at: http://www.sciencedirect.com/science/article/pii/B9780702055546000058.

Forster, A.M. and Kayan, B. (2009) ‘*Maintenance for historic buildings: A current perspective*’, Structural Survey, 27(3), pp. 210–229. doi: 10.1108/02630800910971347.

Gebraeel, N., Elwany, A. and Pan, J. (2009) ‘*Residual Life Predictions in the Absence of Prior Degradation Knowledge*,’ in IEEE Transactions on Reliability, vol. 58, no. 1, pp. 106-117, doi: 10.1109/TR.2008.2011659.

Garside, P., Lahlil, S. and Wyeth, P. (2005) *‘Characterization of Historic Silk by Polarized Attenuated Total Reflectance Fourier Transform Infrared Spectroscopy for Informed Conservation,’* Applied Spectroscopy, 59(10), pp.1242-1247. https://doi.org/10.1366/000370205774430855

Garziera, R., Amabili, M. and Collini, L. (2007) Structural health monitoring techniques for historical buildings, *IV Conferencia Panamericana de END*, pp. 1–12, [online] Available at: http://www.aaende.org.ar/aaende_end/material/141-Garziera.pdf.

Geisler, J. (2015) *Choosing the Best Detection Method: Absorbance vs. Fluorescence*. Available at: https://www.biocompare.com/Bench-Tips/173963-Choosing-the-Best-Detection-Method-Absorbance-vs-Fluorescence/ (Accessed: 11 June 2020)

Gilchrist, A and Nobbs, J. (2000) '*Colorimetry Theory'*, Encyclopaedia of Spectroscopy and Spectrometry, 1(21 Jan 2000). Available at: 35https://www.researchgate.net/profile/James_Nobbs/publication/331159636_Colorimetry_Theory/links/5c69437e92851c1c9de62cfb/Colorimetry-Theory.pdf (Accessed: 11 June 2020)

Goh, K. M., Tjahjono, B., Baines T. and Subramaniam, S. (2006)"*A Review of Research in Manufacturing Prognostics*," 4th IEEE International Conference on Industrial Informatics, Singapore, 2006, pp. 417-422, doi: 10.1109/INDIN.2006.275836.

Gutarowska, B., Pietrzak, K., Machnowski, W., and Miczarek, J.K. (2017) *'Historical Textiles – A review of Microbial Deterioration Analysis and Disinfection Methods, Textile Research Journal,'* 87(19), pp. 2388-2406.

Heras, C.V., Wijffels, A., Cardoso, F., Vandesande, A., Santana, M., Orshoven, V. J., Steenberghen, T. and Balen, V. K. (2013) '*A value-based monitoring system to support heritage conservation planning*', Journal of Cultural Heritage Management and Sustainable Development, 3(2), pp. 130–147. doi: 10.1108/jchmsd-10-2012-005

Heritage Fund (2013) *New Research Reveals heritage tourism boosts UK economy in tough times.* Available at: https://www.heritagefund.org.uk/news/new-research-reveals-heritage-tourism-boosts-uk-economy-tough-times (Accessed: 12 May 2020)

Historic England (2019) *Heritage and the Economy*. Available at: https://historicengland.org.uk/research/heritage-counts/heritage-and-economy/ (Accessed: 12 May 2020)

Hoffman, D. (2007) 'Prognostics and Health Management (PHM) / Condition Based Maintenance', *IEEE Reliability Society 2007 Annual Technology Report*, pp. 1–7.

HSE Health and Safety Executive. (1992) *Temperature: What the law says.* Available at: https://www.hse.gov.uk/temperature/law.htm (Accessed: 28 April 2020).

Hu, C., Youn, B. D., Wang, P. and Taek Yoon, J. (2012) 'Ensemble of data-driven prognostic algorithms for robust prediction of remaining useful life', *Reliability Engineering & System Safety*, 103, pp. 120–135, [online] Available at: http://www.sciencedirect.com/science/article/pii/S0951832012000427.

ICOM International Community of Museums. (2008) *Museum Definition*. Available at: http://www.icom-cc.org/242/about/terminology-for-conservation/ (Accessed: 27 April 2020).

ICOM-CC International Community of Museums – Committee for Conservation. (2008) *What is conservation*. Available at: http://www.icom-cc.org/330/about-icom-cc/what-is-conservation/conservation:-who,-what-amp;-why/ (Accessed: 27 April 2020).

ICOMOS (2013) *The Australia ICOMOS Charter for Places of Cultural Significance, The Burra Charter*. Available at: https://australia.icomos.org/wp-content/uploads/The-Burra-Charter-2013-Adopted-31.10.2013.pdf (Accessed: 28 April 2020)

Idrus, A., Khamidi, F. & Sodangi, M., 2010. *Maintenance management framework for conservation of heritage buildings in Malaysia.* Modern Applied Science, 4(11), pp.66–77. Available at: http://ccsenet.org/journal/index.php/mas/article/view/8040.

Image Permanence Institute (IPI). (2019) *Collections Environmental Monitoring.* Available at: https://www.imagepermanenceinstitute.org/research/environmental.html (Accessed: 22 April 2020).

Jain, R., Young, M., Dogra, S., Kennedy, H., Nguyen, V., Jones, S., Bilaloglu, S., Hochman, K., Raz, E., Galetta, S. and Horwtiz, L. (2020) COVID-19 related neuroimaging findings: A signal of thromboembolic complications and a strong prognostic marker of poor patient outcome, *Journal of the Neurological Sciences*, 414, p. 116923, [online] Available at: http://www.sciencedirect.com/science/article/pii/S0022510X20302604.

Jinzenji, K., Hoshino, T., Williams, L. and Takahashi, K. (2013) An experience report for software quality evaluation in highly iterative development methodology using traditional metrics, *2013 IEEE 24th International Symposium on Software Reliability Engineering, ISSRE 2013*, pp. 310–319.

Just Science. (2017) *What is Photodegradation.* Available at: http://www.justscience.in/articles/what-is-photodegradation/2017/07/26 (Accessed: 30 April 2020).

Kamal, H. M., Elkhial, M. M. and Tawfik, T. S. (2018) *'The Role of Preventive Conservation in Designing King Tutankhamun Galleries in the Grand Egyptian Museum*', Studies in Conservation, Taylor & Francis, 63(sup1), pp. 138–145. DOI: https://doi.org/10.1080/00393630.2018.1504453

Kasajima, I. (2019). '*Measuring plant colours'*, Plant biotechnology (Tokyo, Japan), 36(2), 63–75. https://doi.org/10.5511/plantbiotechnology.19.0322a

Karlsson, M.C.F., Álvarez-Asencio, R., Bordes, R. et al. (2019) '*Characterization of paint formulated using secondary TiO2 pigments recovered from waste paint',* J Coat Technol Res 16, pp. 607–614 https://doi.org/10.1007/s11998-018-0132-x

Keene, S. (2002) *Managing Conservation.* 2nd Edition. Oxford: Butterworth-Heinemann.

Kim, G., Kim, H., Zio, E. and Heo, G. (2018) Application of particle filtering for prognostics with measurement uncertainty in nuclear power plants, *Nuclear Engineering and Technology*, 50(8), pp. 1314–1323, [online] Available at: http://www.sciencedirect.com/science/article/pii/S1738573318302742.

Kirby, J. and Saunders, D. (2004) *Fading and Colour Change of Prussian Blue: Methods of Manufacture and the Influence of Extenders*, National Gallery Technical Bulletin 25 Figure 4. Pg.66. https://www.nationalgallery.org.uk/technical-bulletin/kirby_saunders2004

Kirkland, J.D. (2009) '*Identification of changes in the surface of textiles subjected to plasma chemical treatment using attenuated total reflectance-fourier transform infrared spectroscopy'*. Master's Theses and Doctoral Dissertations. 252. https://commons.emich.edu/theses/252

Klein, L. J., Bermudez, S. A., Schrott, A. G., Tsukada, M., Dionisi-Vici, P., Kargere, L., Marianno, F., Hamann, H. F., López, V. and Leona, M. (2017) '*Wireless sensor platform for cultural heritage monitoring and modeling system',* Sensors (Switzerland), 17(9), pp. 1–21.

Klisińska-Kopacz, A., Łydżba-Kopczyńska, B., Czarnecka, M., Koźlecki, T., del Hoyo Mélendez, J., Mendys, A., Kłosowska-Klechowska, A., Obarzanowski, M. and Frączek, P. (2019) '*Raman spectroscopy as a powerful technique for the identification of polymers used in cast sculptures from museum collections'*, Journal of Raman Spectroscopy, 50(2), pp. 213–221.

Knell, S. (1994) *Care of Collections*: Leicester Readers in Museum Studies. Oxford: Routledge.

Konica Minolta (2020A) *Products: Introduction*. Available at: https://www5.konicaminolta.eu/en/measuring-instruments/products/colour-measurement/chroma-meters/cr-400-410/introduction.html (Accessed: 8 June 2020)

Konica Minolta (2019B) *Measuring Fundamentals*: *Comparing Colourimeters and Spectrophotometer*. Available at: https://www.konicaminolta.com/instruments/knowledge/color/part3/01.html (Accessed: 11 June 2020)

Konica Minolta (2020C) *Products: Spectrophotometer*. Available at: https://sensing.konicaminolta.asia/product/spectrophotometer-cm-3610a/ (Accessed: 15 June 2020)

Koperska, M. A., Pawcenis, D., Bagniuk, J., Zaitz, M. M., Missori, M., Łojewski, T. and Łojewska, J. (2014) Degradation markers of fibroin in silk through infrared spectroscopy, *Polymer Degradation and Stability*, 105, pp. 185–196, [online] Available at: http://linkinghub.elsevier.com/retrieve/pii/S0141391014001542 (Accessed 24 July 2017).

Koperska, M.A., Lojewski, T. & Lowjewska, J. (2015) '*Evaluating Degradation of Silk's Fibroin by Attenuated total Reflectance Infrared Spectroscopy: Case study of ancient banners from Polish Collections'*, Spectrochimica Acta Part A: Molecular Biomolecular Spectroscopy, 135 (2015), pp. 576-582.

Koussoulou, T., (1999) '*Photodegradation and photostabilization of historic silks in the museum environment – evaluation of a new conservation treatment',* Papers from the Institute of Archaeology, 10, pp.75–88. DOI: http://doi.org/10.5334/pia.135

Kozlowski, R. (2018) *Collection environments and evidence-based decision-making*. Conservation Perspectives, The GCI Newsletter, (33.2) Fall 2018. Available at: http://www.getty.edu/conservation/publications_resources/newsletters/33_2/evidence_based.html (Accessed: 19 August 2020).

Kroslowtitz, K., 2012. *Computer History Museum.* Available at: https://computerhistory.org/blog/preservation-conservation-restoration-whats-the-difference/ (Accessed: 4 November 2019).

Kumar, S. and Pecht, M. (2010) Modeling approaches for prognostics and health management of electronics, *International Journal of Performability Engineering*, 6(5), pp. 467–476.

Le Pevelen, D.D., Tranter, G.E. (2017) *'FT-IR and Raman Spectroscopies, Polymorphism Applications'*, in: Lindon, J.C., Tranter, George E, Koppenaal, D.W.B.T.-E. of S. and S. (Third E.

(Eds.), . Academic Press, Oxford, pp. 750–761. https://doi.org/https://doi.org/10.1016/B978-0-12-409547-2.12161-4

Leenson, I. A. (1999) Old Rule of Thumb and the Arrhenius Equation, *Journal of Chemical Education*, American Chemical Society, 76(10), p. 1459, [online] Available at: https://doi.org/10.1021/ed076p1459.

Lee, J., Jin, C., Liu, Z. and Davari, H. (2017) Introduction to Data-Driven Methodologies for Prognostics and Health Management, In *Probabilistic Prognostics and Health Management of Energy Systems*, pp. 9–32.

Li, L., Decai, G., Zhengyuan, Y. and Jie, W. (2019) *'A preliminary study of the decline in solubility of ancient silk protein, Polymer Degradation and Stability'*, 169, pp. 108988, [online] Available at: http://www.sciencedirect.com/science/article/pii/S0141391019303167.

Li, R., Verhagen, W. J. C. and Curran, R. (2020) A systematic methodology for Prognostic and Health Management system architecture definition, *Reliability Engineering & System Safety*, 193, p. 106598, [online] Available at: http://www.sciencedirect.com/science/article/pii/S0951832018315084.

Liu, H., Zhao, S., Zhang, Q., Yeerken, T. and Yu, W. (2019) *'Secondary structure transformation and mechanical properties of silk fibres by ultraviolet irradiation and water'*, Textile Research Journal, 89(14), pp. 2802–2812. [online] Available at: https://doi.org/10.1177/0040517518803788

Lu, C., Bera, K., Wang, X., Prasanna, P., Xu, J., Janowczyk, A., Beig, N., Yang, M., Fu, P., Lewis, J., Choi, H., Schmid, R. A., Berezowska, S., Schalper, K., Rimm, D., Velcheti, V. and Madabhushi, A. (2020) A prognostic model for overall survival of patients with early-stage non-small cell lung cancer: a multicentre, retrospective study, *The Lancet Digital Health*, 2(11), pp. e594–e606, [online] Available at: http://www.sciencedirect.com/science/article/pii/S2589750020302259.

Lumenlearningcom. (2019) *Activation Energy and Temperature Dependence*. Available at: https://courses.lumenlearning.com/trident-boundless-chemistry/chapter/activation-energy-and-temperature-dependence/ (Accessed: 11 February 2019).

Luxford, N. and Thickett, D. (2011*) 'Designing accelerated ageing experiments to study silk deteriorating in historic houses',* Journal of the Institute of Conservation, 34(1), pp. 115-127.

Luxford, N. Thickett, D. and Wyeth, P. (2019) *Non-Destructive Testing of Silk: Problems and Possibilities.* [online] Available at: https://www.researchgate.net/profile/Naomi_Luxford/publication/333565828_Non-destructive_testing_of_silk_problems_and_possibilities/links/5cf4cf9c299bf1fb18531a8d/Non-destructive-testing-of-silk-problems-and-possibilities.pdf (Accessed: 6 May 2020).

Luxford, N. Thickett, D. and Wyeth, P. (2009) '*Preserving Silk: Reassessing Deterioration factors for historic silk artefacts', Proceedings of the Combined Conference of the Textile Institute*, Dunedin, New Zealand, 15-17 April 2009, pp. 151-156.

Malvern Panalytical, (2020) Products: XRF |X-ray fluorescence. Available at: https://www.malvernpanalytical.com/en/products/technology/xray-analysis/x-ray-fluorescence (Accessed: 8 June 2020)

Martínez, M. A., Calero, A. I. and Valero, E. M. (2020) '*Colorimetric and Spectral Data Analysis of Consolidants used for Preservation of Medieval Plasterwork'*, Journal of Cultural Heritage 42(2020), pp. 64–71.

Masciotta, M. G., Morais, M. J., Ramos, L. F., Oliveira, D. V., Sánchez-Aparicio, L. J. and González-Aguilera, D. (2019) *'A Digital-based Integrated Methodology for the Preventive Conservation of Cultural Heritage: The Experience of HeritageCare Project'*, International Journal of Architectural Heritage, Taylor & Francis, 00(00), pp. 1–20, [online] Available at: https://doi.org/10.1080/15583058.2019.1668985.

MathWorks (2020) *MATLAB.* Available at https://uk.mathworks.com/products/matlab.html (Accessed: 04 August 2020).

May, E. and Jones, M. (2006) *Conservation Science: Heritage Materials.* Cambridge: RSC Publishing, pp. 73-83.

Meaco (2020) *Measurement and Control*. [online] Available at https://meaco.co.uk (Accessed: 04 August 2020).

Meister, N.B. (2019) '*A Guide to the Preventative Care of Archaeological Collections', Advances in Archaeological Practice*, 7(3), pp. 267-273.

Minakshi, P., Ghosh, M., Kumar, R., Patki, H.S., Saini, H.M., Ranjan, K., Brar, B., Prasad, G. (2019) Chapter 15 - *Single-Cell Metabolomics: Technology and Applications*, in: Barh, D., Azevedo, V.B.T.-S.-C.O. (Eds.), . Academic Press, pp. 319–353. [online] Available at https://doi.org/10.1016/B978-0-12-814919-5.00015-4

Mahmud, M. A., Bates, A. K., Wood, T., Abdelgawad, A. and Yelamarthi, K. (2018) 'A complete Internet of Things (IoT) platform for Structural Health Monitoring (SHM)', *IEEE 4th World Forum on Internet of Things (WF-IoT),* Singapore, 2018, pp. 275-279, doi: 10.1109/WF-IoT.2018.8355094.

Muge, Y. S. & Suat, C. (2016) '*Silk fibre degradation and Analysis by Proteomics', Annals of the University of Oradea. Fascicle of Textiles*, 17(1), pp. 137-142(6).

Murata, H. Saitoh, K. and Sumida, Y. (2018) *True Colour Imagery Rendering for Himawari-8 with a colour reproduction Approach based on the CIE XYZ colour System,* Journal of Meteorological Society of Japan. Vol. 96B, 211-238.

Museums and Galleries Commission. (1992) *Standards in the Museum Care of Archaeological Collections*. [online] Available at: https://326gtd123dbk1xdkdm489u1q-wpengine.netdna-ssl.com/wp-content/uploads/2016/11/Standards-in-the-museum-care-of-archaeological-collections.pdf (Accessed: 22 January 2018).

Museums and Galleries Scotland. (2020a) *Caring for Textile Collections in Museums*. [online] Available at: https://collectionstrust.org.uk/resource/caring-for-textile-collections-in-museums/ (Accessed: 30 April 2020)

Museums and Galleries Scotland. (2020b) *Temperature and Humidity in Museums*. [online] Available at: https://www.museumsgalleriesscotland.org.uk/advice/collections/temperature-and-humidity-in-museums/ (Accessed: 30 April 2020).

Nasrazadani, S and Hassani, S. (2016) *Modern analytical techniques in failure analysis of aerospace, chemical, and oil and gas industries*. Handbook of materials failure analysis with case studies from the oil and gas industry. [online] Available at: https://www.sciencedirect.com/topics/chemistry/fourier-transform-infrared-spectroscopy (Accessed: 30 April 2020).

National Park Service (2002) Curatorial Care of Textile Objects, *NPS Museum Handbook, Part I: Museum Collections*, p. 50, [online] Available at: https://www.nps.gov/museum/publications/MHI/Appendix K.pdf. (Accessed: 22 August 2020)

National Park Service (2002b) Curatorial Care of Textile Objects - Appendix K, *NPS Museum Handbook, Part I: Museum Collections*, p. K:1-K46. [online] Available at: https://www.nps.gov/museum/publications/MHI/Appendix%20K.pdf (Accessed: 22 August 2020)

NEDCC (2012). *Monitoring Temperature and Relative Humidity*. [online] Available at: https://www.nedcc.org/free-resources/preservation-leaflets/2.-the-environment/2.2-monitoring-temperature-and-relative-humidity (Accessed: 21April 2020).

Neuhaus, E. (2012) *A critical look at the use of HVAC systems in the museum environment*, Climate for Collections, Standards and uncertainties, Munich 2012. [online] Available at: https://physitec.nl/publicaties/2012_A_critical_look_at_the_use_of_HVAC_systems_in_the_museum_environment.pdf (Accessed: 4 June 2020)

Nishimura, D. (2011) *Understanding Preservation Metrics*, Image Permanence Institute, Rochester Institute of Technology. [online] Available at: http://www.imagepermanenceinstitute.org/webfm_send/316 (Accessed: 08 September 2015).

NPS (1993)Calibration of Hygrometers and Hygrothermographs. [online] Available at: https://www.nps.gov/museum/publications/conserveogram/03-02.pdf (Accessed: 9 November 2020)

Padfield, Tim & Landi, Sheila. (1966). The Light-Fastness of the Natural Dyes. Studies in Conservation. 11. 10.1179/sic.1966.022.

Padfield, T. (2004) *The TWPI in action.* Creative Commons Attribution. [online] Available at: http://www.conservationphysics.org/twpi (Accessed: 08 September 2015).

Pagliarino, A (2019) AICCM Environmental Guidelines 2018. [online] Available at: https://aiccm.org.au/conservation/environmental-guidelines/ (Accessed:19 August 2020).

Patil, M. (2019) *What are the types of colorimeter?* [online] Available at: https://chrominfo.blogspot.com/2019/09/what-are-types-of-colorimeter.html (Accessed: 11 June 2020)

Peets, P., Kaupmees, K., Vahur, S. et al. (2019) *'Reflectance FT-IR spectroscopy as a viable option for textile fiber identification'*, Heritage Science, 7(93). [online] Available at: https://doi.org/10.1186/s40494-019-0337-z

Pecht, M. G. (2008) Prognostics and Health Management of Electronics, Prognostics and Health Management of Electronics, pp. 1–315.

Pospíšilová, D., Pech, M., Kotyk, M. (2016) '*The Use of Non-Destructive Instrumental Methods in the Determination of Metal Objects from the Asian Collection of the Náprstek Museum',* Ann. Náprstek Museum 37, pp. 93–102. https://doi.org/10.1515/anpm-2017-0007

Ramanathan, G (2016) Colorimeter vs. Spectrophotometer: What's the Difference? [online] Available at: https://blog.hunterlab.com/blog/color-measurement-2/colorimeter-vs-spectrophotometer-knowing-the-differences-among-color-measurement-technologies/ (Accessed: 08 June 2020).

Ramgopal, G., Ramani, R., Ramachandra, P. & Ranganathaiah, C. (1998) '*UV Degradation of Bivoltine Silk Fibre: A Positron Annihilation Study',* European Polymer Journal, 34(10), pp. 1423-1427.

Randall, D. L. (1997) '*Instruments for the Measurement of Color'*, Color Technology in the Textile Industry, Second Edition, AATCC, (1997), pp. 9–17. [online] Available at: https://pdfs.semanticscholar.org/4ee7/5a94f974d2c0dbf142151fb2f888df90d96d.pdf (Accessed: 337 June 2020)

Rezaeianjouybari, B. and Shang, Y. (2020) Deep learning for prognostics and health management: State of the art, challenges, and opportunities, *Measurement*, 163, p. 107929, [online] Available at: http://www.sciencedirect.com/science/article/pii/S026322412030467X.

Rosunally, Y., Z. (2012) 'Diagnostic and Prognostic Analysis Tools for Monitoring Degradation in Aged Structures', PhD thesis, University of Greenwich, London.

Rosunally, Y. Z., Stoyanov, S., Bailey, C., Mason, P., Campbell, S., Monger, G. and Bell, I. (2011) 'Fusion Approach for Prognostics Framework of Heritage Structure', in *IEEE Transactions on Reliability*, 60(1), pp. 3-13, March 2011, doi: 10.1109/TR.2011.2104451.

Ruga, L., Orlandi, F. & Fornaciari, M. (2019) *'Preventive Conservation of Cultural Heritage: Biodeteriogens Control by Aerobiological Monitoring'* Sensors 2019, 19(17), 3647; https://doi.org/10.3390/s19173647

Salonen, A. & Deleryd, M. (2011) *Cost of poor maintenance: A concept for maintenance performance improvement*, Journal of Quality in Maintenance Engineering, 17(1), pp. 63–73

Samanali, G.A.P., Paasi, I., Lowe, B.J., Smith, C.A., Fraser-Miller, S.J. and Gordon, K.C. (2020) *'Understanding Consolidants on Harakeke Fibres using Raman Micsrocopy: Implication for Conservation',* Journal of Cultural Heritage, (2020). DOI: https://doi.org/10.1016/j.culher.2020.03.005

Saranga, H. (2002) *Relevant condition-parameter strategy for an effective condition-based maintenance*, Journal of Quality in Maintenance Engineering, 8(1) 92–105. DOI: https://doi.org/10.1108/13552510210420612.

Sargazi, M., Kaykhaii, M., (2020) *'Application of a smartphone-based spectrophotometer for rapid in-field determination of nitrite and chlorine in environmental water samples*', Spectrochimica Acta Part A: Mol. Biomol. Spectrosc. 227(15 Feb 2020), pp. 117672. https://doi.org/https://doi.org/10.1016/j.saa.2019.117672

Saunders, D., and Kirby, J. (2004) *The effect of Relative Humidity on Artists' Pigments'*, National Gallery Technical Bulletin, 25, pp. 62-72. Available at: http://www.nationalgallery.org.uk/technical-bulletin/saunders_kirby2004 (Accessed: 13 February 2019)

Saxena, A., Celaya, J., Balaban, E., Goebel, K., Saha, B., Saha, S. and Schwabacher, M. (2008) 'Metrics for evaluating performance of prognostic techniques,' *2008 International Conference on Prognostics and Health Management*, Denver, CO, 2008, pp. 1-17, doi: 10.1109/PHM.2008.4711436.

Schlanger, S., Wilshusen, R. and Roberts, H. (2015) From Mining Sites to Mining Data: Archaeology's Future, Kiva, Taylor & Francis, 81(1–2), pp. 80–99. doi: 10.1080/00231940.2015.1118739

Shahid, M.,Wertz, J., Degano, I., Aceto, M., Khan, M.I. & Quye, A.(2019) '*Analytical Methods for Determination of Anthraquinone Dyes in Historical Textiles: A Review',* Analytica Chimica Acta, 1083(2019), pp.58-87. Doi: https://doi.org/10.1016/j.aca.2019.07.009

Sharif-Askari, H. and Abu-Hijleh, B. (2018) '*Reviews of Museums' Indoor Environment Conditions Studies and Guidelines and Their Impact on the Museums' Artifacts and Energy Consumption', Building and Environment*, 143(2018), pp. 186 -195.

Sharif, S. and Esmaeli, V. (2017) *'Effects of temperature and relative humidity on permanence of Buyid silk'*, *Journal of Cultural Heritage*, 27(2017), pp. 72-79.

Simpson, M. L. and Jansen, J. F. (1991) '*Imaging colorimetry: a new approach'*, Applied Optics, 30(32), pp. 4666-4671.https://doi.org/10.1364/AO.30.004666.

Si, X.-S., Wang, W., Hu, C.-H. and Zhou, D.-H. (2011) Remaining useful life estimation – A review on the statistical data driven approaches, *European Journal of Operational Research*, 213(1), pp. 1–14, [online] Available at: http://www.sciencedirect.com/science/article/pii/S0377221710007903.

Smith, M.J. and Thomson, K. (2017a) *Forensic analysis of textile degradation and natural damage, Forensic Textile Science*. *Series: The Textile Institute Book Series*. Woodhead Publishing: Duxford, pp. 41-69.

Smith, M., Thompson, K. and Lennard, F. (2017b) A literature review of analytical techniques for materials characterisation of painted textiles—Part 2: spectroscopic and chromatographic analytical instrumentation, *Journal of the Institute of Conservation*, 40(3), pp. 252–266.

Smithsonian National Postal Museum. (undated) *Agents of Degradation*. Available at: https://postalmuseum.si.edu/collections/preservation/agents-of-deterioration.html (Accessed: 28 April 2020)

Spaling, H. (1994) Cumulative effects assessment: Concepts and principles, *Impact Assessment*, 12(3), pp. 231–251.

Sun, B., Zeng, S., Kang., R and Pecht, M. (2010) 'Benefits analysis of prognostics in systems', *Prognostics and System Health Management Conference*, Macao, 2010, pp. 1-8, doi: 10.1109/PHM.2010.5413503.

Sun-X (n.d) Conservation Window films and Blinds. Available at: https://www.sun-x.co.uk/conservation (Accessed: 17 June 2018)

Tamburini, D. and Dyer, J. (2019) '*Fibre optic reflectance spectroscopy and multispectral imaging for the non-invasive investigation of Asian colourants in Chinese textiles from Dunhuang (7th-10th century AD), Dyes and Pigments*', 162, pp. 494–511, [online] Available at: http://www.sciencedirect.com/science/article/pii/S0143720818317716.

TES Electrical Electronic Corporation (2014) Product Information. Available at: http://www.tes.com.tw/en/product_detail.asp?seq=363 (Accessed: 8 June 2020).

The Council for Museums, Libraries and Archives. (2002) *Benchmarks in Collection Care for Museums, Archives and Libraries, a self-assessment checklist*. London, Resource. Available at: https://collectionstrust.org.uk/wp-content/uploads/2016/08/Benchmarks2_updated__Oct_2014-3.compressed.pdf
(Accessed: 22 April 2020).

The Field Museum. (2020) *Preventative Conservation*. Available at: https://www.fieldmuseum.org/science/research/area/conserving-collections/preventive-conservation (Accessed: 27 April 2020).

Thompson, K., Smith, M. and Lennard, F. (2017) A literature review of analytical techniques for materials characterisation of painted textiles—Part 1: categorising painted textiles, sampling and the use of optical tools, *Journal of the Institute of Conservation*, Taylor & Francis, 40(1), pp. 64–82, [online] Available at: https://doi.org/10.1080/19455224.2016.1269355.

Tkalcic, M. and Tasic J. F. "Colour spaces: perceptual, historical and applicational background," The IEEE Region 8 EUROCON 2003. Computer as a Tool., Ljubljana, Slovenia, 2003, pp. 304-308 vol.1, doi: 10.1109/EURCON.2003.1248032.

Tsui, K. L., Chen, N., Zhou, Q., Hai, Y. and Wang, W. (2015) Prognostics and Health Management: A Review on Data Driven Approaches, Wu, S. (ed.), *Mathematical Problems in*

Engineering, Hindawi Publishing Corporation, 2015, p. 793161, [online] Available at: https://doi.org/10.1155/2015/793161.

Valach, J., Juliš, K., Štefcová, P., Pech, M., Wolf, B., Kotyk, M. and Frankl, J. (2015) '*Everything is data - Overview of modular system of sensors for museum environment', International Archives of the Photogrammetry, Remote Sensing and Spatial Information Sciences - ISPRS Archives*, 40(5W7), pp. 439–442.

Vasileiadou, A., Karapanagiotis, I. and Zotou, A. (2019) '*UV-induced degradation of wool and silk dyed with shellfish purple, Dyes and Pigments'*, 168(April), pp. 317–326. Available at: https://doi.org/10.1016/j.dyepig.2019.04.068

Vilaplana, F., Nilsson, J., Sommer, D.V.P, & Karlsson, S. (2014) '*Analytical Markers for Silk Degradation: Comparing Historic Silk and Silk Artificially Aged in Different Environments*', Anal Bioanal Chemistry, 2015 (407), pp. 1433-1449. Doi 10.1007/s00216-014-8361-z

Vogl, G. W., Weiss, B. A. and Helu, M. (2019) A review of diagnostic and prognostic capabilities and best practices for manufacturing, *Journal of Intelligent Manufacturing*, Springer US, 30(1), pp. 79–95.

VR&D (2020) *VisualDoc.* Available at: http://www.vrand.com/products/visualdoc/ (Accessed: 04 July 2019)

Wallace Collection (2020) *History of the Collection*. Available at https://www.wallacecollection.org/art/collection/history-collection/ (Accessed: 04 Feb 2019)

Wang, J. and Wong, W. (2019) '*Unravelling the Conservation History of silk faced ancient Dunhuang Manuscripts in the British Library'*, Studies in Conservation, 64(3), pp. 125–137.

Wang, Z., Wang, H., Zhang, T., Xu, C. (2017) *'Investigation on absorption performance between cement and emulsified asphalt with UV–Vis spectrophotometer*', Constr. Build. Mater. 136, pp. 256–264. https://doi.org/https://doi.org/10.1016/j.conbuildmat.2017.01.016

Wiltshire County Council, (2006) Preventative conservation: *Signposts Factsheet 4*'. *Museums, Libraries, and Archives Council.* Available at: https://collectionstrust.org.uk/resource/preventive-conservation/ (Accessed: 4 November 2019)

Wolthuis, R., Schut, T.C.B., Caspers, P.J., Buschman, H.P.J., Romer, T.J., Bruining, H.A., Puppels, G.J. (1999) CHAPTER THIRTY-TWO - *Raman Spectroscopic Methods for In Vitro and In Vivo Tissue Characterization*, in: MASON, W.T.B.T.-F. and L.P. for B.A. (Second E. (Ed.), Biological Techniques Series. Academic Press, London, pp. 433–455. https://doi.org/10.1016/B978-012447836-7/50034-8

Xu, B. (2010) *11 - Grading of cotton by color measurement*, In Gulrajani, M. L. B. T.-C. M. (ed.), *Woodhead Publishing Series in Textiles*, Woodhead Publishing, pp. 253–278, [online] Available at: http://www.sciencedirect.com/science/article/pii/B9781845695590500108. (Accessed: 15 June 2020)

Xu, J.-L., Thomas, K. V, Luo, Z., Gowen, A.A. (2019) *'FTIR and Raman imaging for microplastics analysis: State of the art, challenges and prospects'*, TrAC Trends Anal. Chem. 119, 115629. https://doi.org/https://doi.org/10.1016/j.trac.2019.115629

Yao, H., Lin, K., Ungurean, I. and Yang, Y.(2019) 'Constrained Relay Node Deployment in Wireless Sensor Network for Structural Health Monitoring', *International Conference on Sensing and Instrumentation in IoT Era (ISSI)*, Lisbon, Portugal, 2019, pp. 1-5, doi: 10.1109/ISSI47111.2019.9043653.

Yang, J., Liao, X., Yin, W., Wang, B., Yue, J., Bai, L., Liu, D., Zhu, T., Huang, Z. and Kang, Y. (2020) Elevated cardiac biomarkers may be effective prognostic predictors for patients with COVID-19: A multicenter, observational study, *The American Journal of Emergency Medicine*, [online] Available at: http://www.sciencedirect.com/science/article/pii/S0735675720308998.

Zhang S., Kang, R., He, X. and Pecht, M. G. (2008) 'China's Efforts in Prognostics and Health Management', in *IEEE Transactions on Components and Packaging Technologies*, 31(2), pp. 509-518, doi: 10.1109/TCAPT.2008.925702

Zhang, H., Kang, R. and Pecht, M. (2009) A hybrid prognostics and health management approach for condition-based maintenance, *IEEM 2009 - IEEE International Conference on Industrial Engineering and Engineering Management*, IEEE, pp. 1165–1169.
Zhang, X., Berghe, I.V. & Wyeth, P. (2011*) 'Heat and moisture promoted deterioration of raw silk estimated by amino acid analysis*', Journal of Cultural Heritage, 12(4), pp. 408-41.

Zhang, X. and Wyeth, P. (2007) Moisture Sorption as a Potential Condition Marker for Historic Silks: Noninvasive Determination by Near-Infrared Spectroscopy, *Applied Spectroscopy*, OSA, 61(2), pp. 218–222, [online] Available at: https://www.osapublishing.org/as/abstract.cfm?uri=as-61-2-218. (Accessed: 8 June 2020)

Zhang, X. and Yuan, S. (2010) *"Measuring Quantitatively the Deterioration Degree of Ancient Silk Textiles by Viscometry', Chinese Journal of Chemistry,* 28 (4), pp. 656-662.

Zhao, Y. and Li, L. (2019) 'Colorimetric properties and application of temperature indicator thermochromic pigment for thermal woven textile', *Textile Research Journal*, 89(15), pp. 3098–3111. doi: 10.1177/0040517518805390.

Zinchenko, T., Pecherskaya, E., Golubkov, P., Artamonov, D., Kozlov, G. and Shepeleva, Y. (2020) Automated Spectrophotometer Control System, *Procedia Computer Science*, 167, pp. 477–486, [online] Available at: http://www.sciencedirect.com/science/article/pii/S1877050920307286.

8. APPENDIX

8.1. Additional Historic Environmental Data Samples

8.1.1. Temperature and Humidity Charts

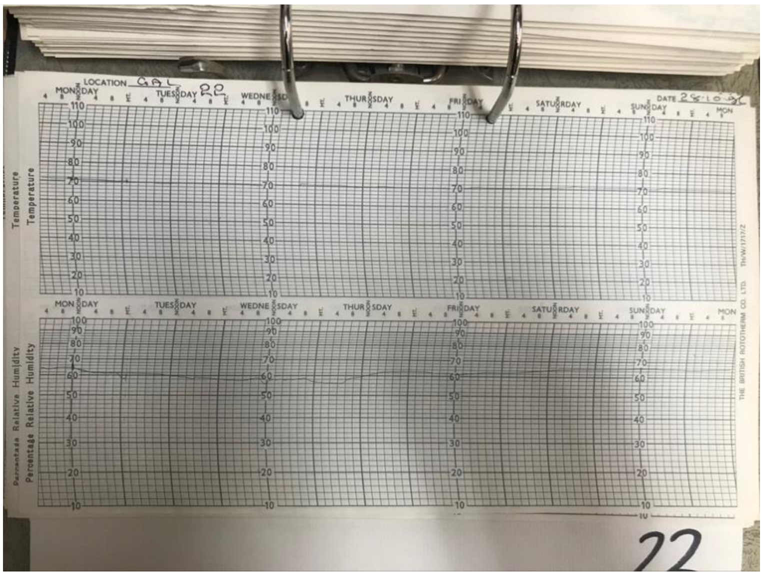

Figure 8-1: Weekly Temperature and Relative Humidity Charts

8.1.2. Archived Historical Temperature and Humidity Readings

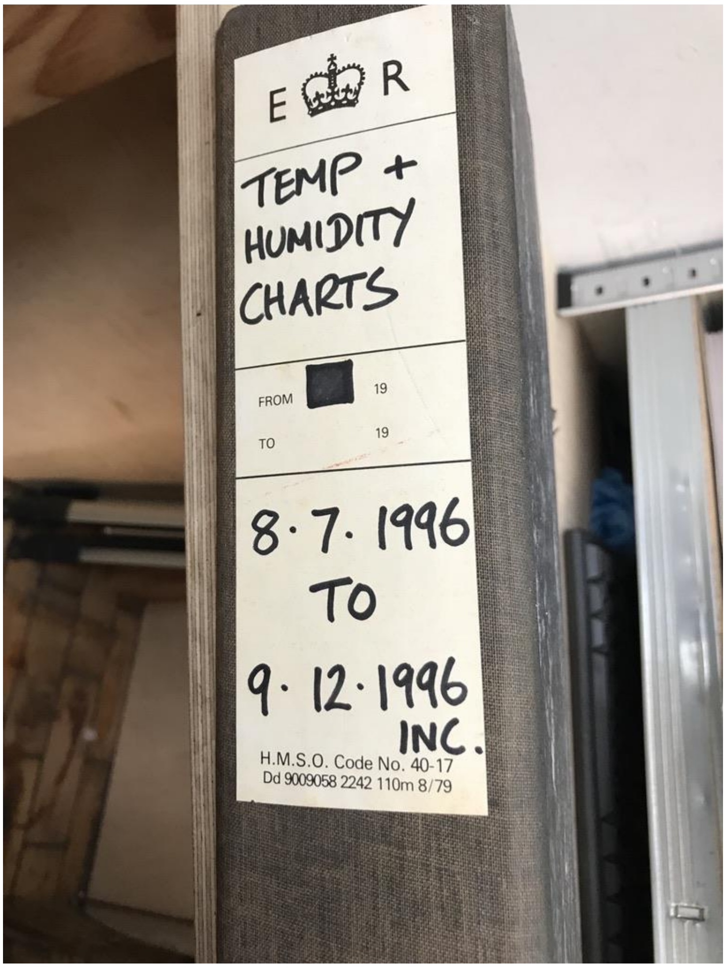

Figure 8-2: Record of Temperature and Relative Humidity Charts archived

8.1.3. Sample Hygrothermographs Readings

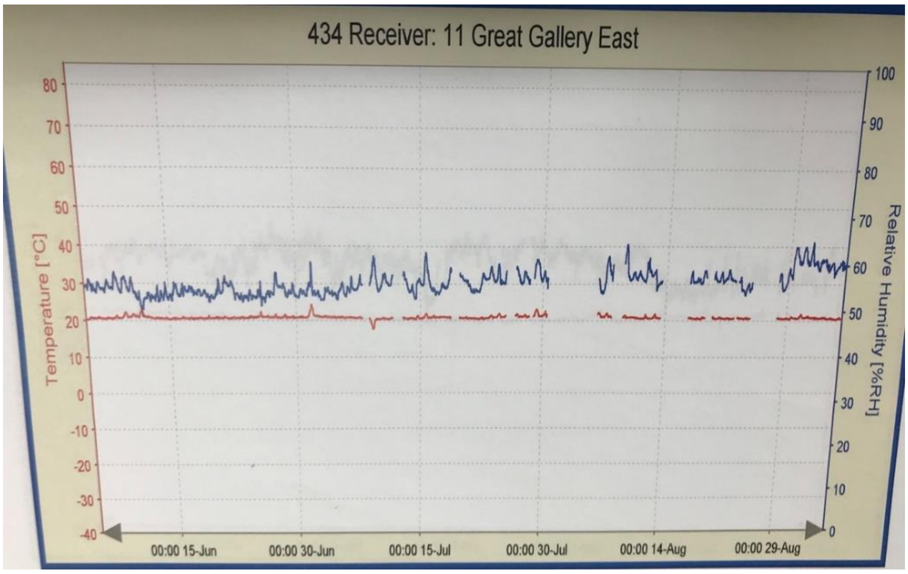

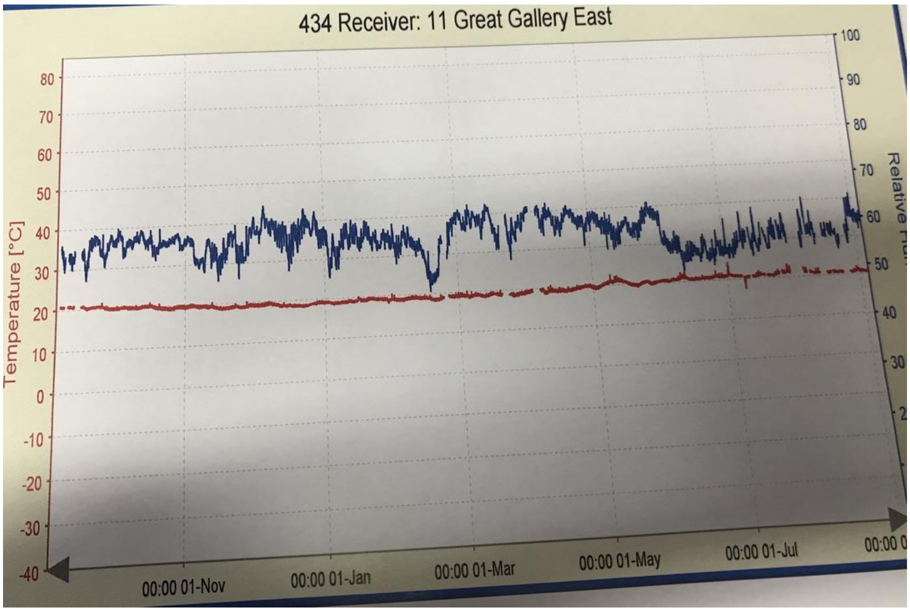

Figure 8-3: Hygrothermograph Sample Readings of Temperature and RH

8.1.4. Historical Temperature and Humidity Readings

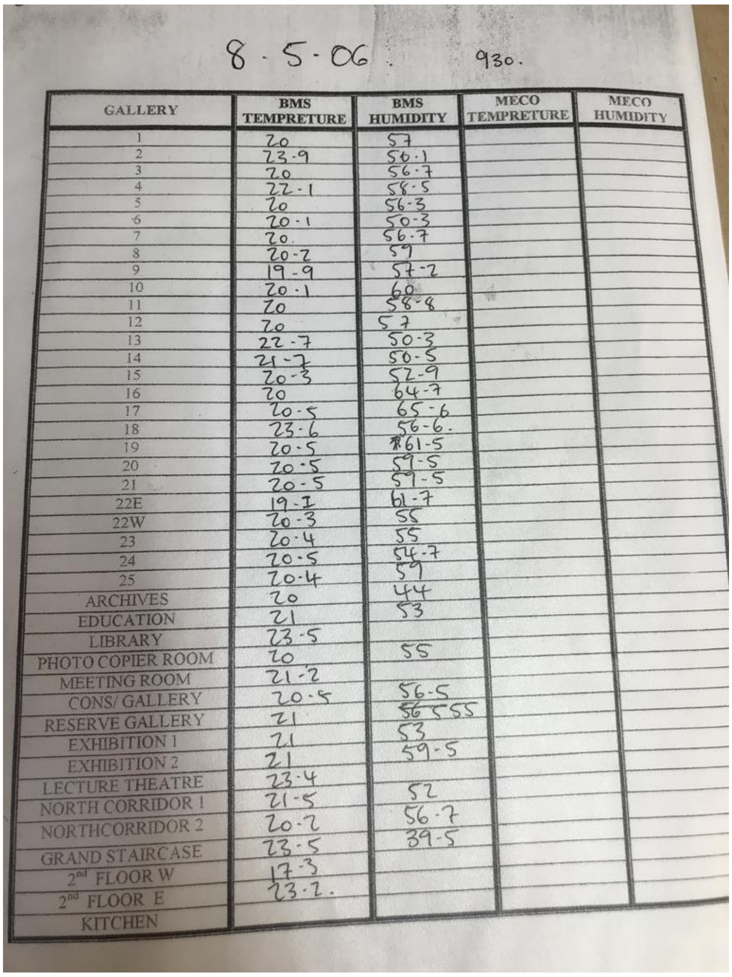

8.5.06. 930.

GALLERY	BMS TEMPRETURE	BMS HUMIDITY	MECO TEMPRETURE	MECO HUMIDITY
1	20	57		
2	23.9	56.1		
3	20	56.7		
4	22.1	58.5		
5	20	56.3		
6	20.1	50.3		
7	20.	56.7		
8	20.2	59		
9	19.9	57.2		
10	20.1	60		
11	20	58.8		
12	20	57		
13	22.7	50.3		
14	21.7	50.5		
15	20.3	52.9		
16	20	64.7		
17	20.5	65.6		
18	23.6	56.6.		
19	20.5	61.5		
20	20.5	59.5		
21	20.5	59.5		
22E	19.1	61.7		
22W	20.3	55		
23	20.4	55		
24	20.5	54.7		
25	20.4	59		
ARCHIVES	20	44		
EDUCATION	21	53		
LIBRARY	23.5			
PHOTO COPIER ROOM	20	55		
MEETING ROOM	21.2			
CONS/ GALLERY	20.5	56.5		
RESERVE GALLERY	21	~~56.5~~ 55		
EXHIBITION 1	21	53		
EXHIBITION 2	21	59.5		
LECTURE THEATRE	23.4			
NORTH CORRIDOR 1	21.5	52		
NORTHCORRIDOR 2	20.2	56.7		
GRAND STAIRCASE	23.5	39.5		
2nd FLOOR W	17.3			
2nd FLOOR E	23.2.			
KITCHEN				

Figure 8-4: Sample of manual record keeping of temperature and RH readings

8.1.5. Historical Temperature and Humidity Readings

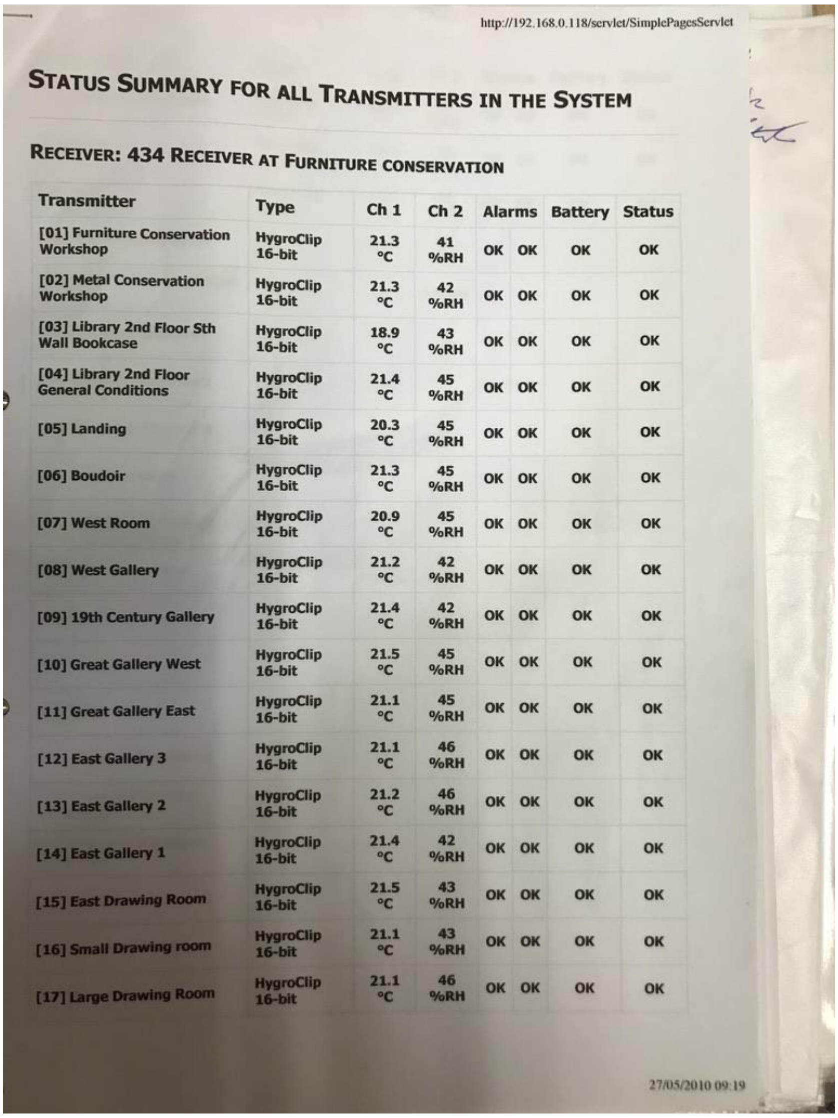

http://192.168.0.118/servlet/SimplePagesServlet

STATUS SUMMARY FOR ALL TRANSMITTERS IN THE SYSTEM

RECEIVER: 434 RECEIVER AT FURNITURE CONSERVATION

Transmitter	Type	Ch 1	Ch 2	Alarms		Battery	Status
[01] Furniture Conservation Workshop	HygroClip 16-bit	21.3 °C	41 %RH	OK	OK	OK	OK
[02] Metal Conservation Workshop	HygroClip 16-bit	21.3 °C	42 %RH	OK	OK	OK	OK
[03] Library 2nd Floor Sth Wall Bookcase	HygroClip 16-bit	18.9 °C	43 %RH	OK	OK	OK	OK
[04] Library 2nd Floor General Conditions	HygroClip 16-bit	21.4 °C	45 %RH	OK	OK	OK	OK
[05] Landing	HygroClip 16-bit	20.3 °C	45 %RH	OK	OK	OK	OK
[06] Boudoir	HygroClip 16-bit	21.3 °C	45 %RH	OK	OK	OK	OK
[07] West Room	HygroClip 16-bit	20.9 °C	45 %RH	OK	OK	OK	OK
[08] West Gallery	HygroClip 16-bit	21.2 °C	42 %RH	OK	OK	OK	OK
[09] 19th Century Gallery	HygroClip 16-bit	21.4 °C	42 %RH	OK	OK	OK	OK
[10] Great Gallery West	HygroClip 16-bit	21.5 °C	45 %RH	OK	OK	OK	OK
[11] Great Gallery East	HygroClip 16-bit	21.1 °C	45 %RH	OK	OK	OK	OK
[12] East Gallery 3	HygroClip 16-bit	21.1 °C	46 %RH	OK	OK	OK	OK
[13] East Gallery 2	HygroClip 16-bit	21.2 °C	46 %RH	OK	OK	OK	OK
[14] East Gallery 1	HygroClip 16-bit	21.4 °C	42 %RH	OK	OK	OK	OK
[15] East Drawing Room	HygroClip 16-bit	21.5 °C	43 %RH	OK	OK	OK	OK
[16] Small Drawing room	HygroClip 16-bit	21.1 °C	43 %RH	OK	OK	OK	OK
[17] Large Drawing Room	HygroClip 16-bit	21.1 °C	46 %RH	OK	OK	OK	OK

27/05/2010 09:19

Figure 8-5: Sample temperature and humidity HygroClip readings

8.2. Shrewsbury Set: Sourced from The Wallace Collection Archives

Figure 8-6: Shrewsbury Set armchair c.1890

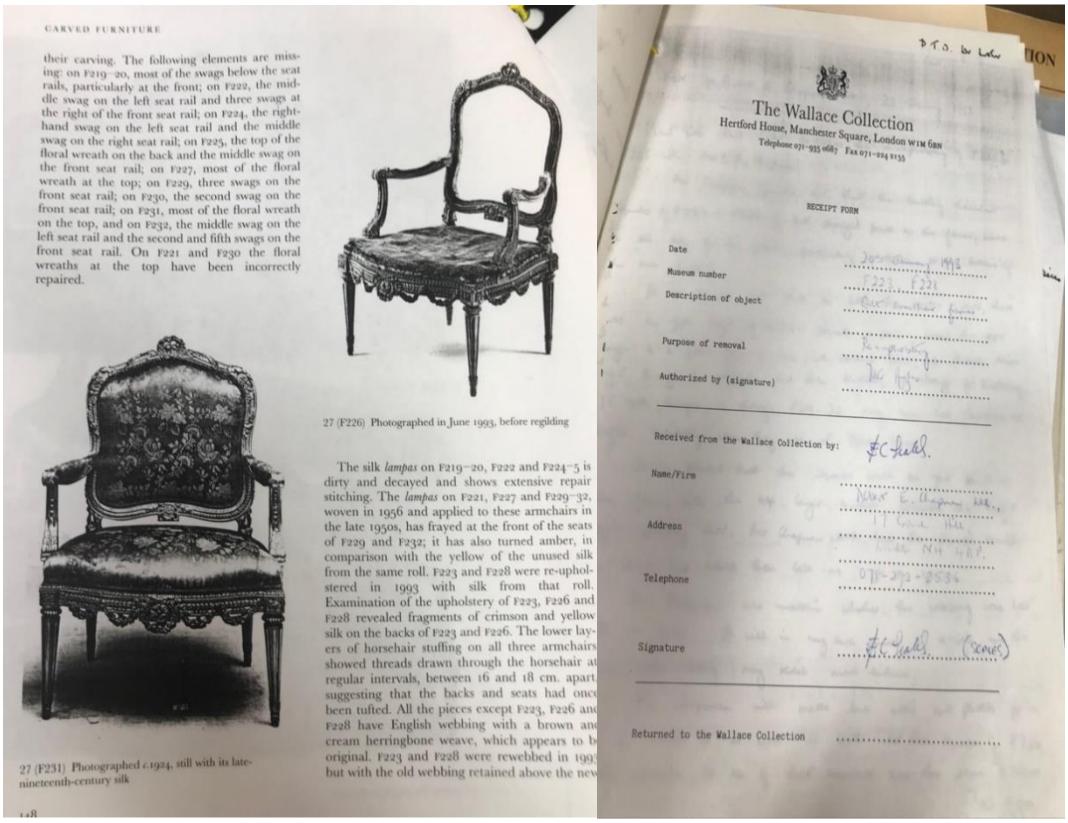

CARVED FURNITURE

their carving. The following elements are missing: on F219–20, most of the swags below the seat rails, particularly at the front; on F222, the middle swag on the left seat rail and three swags at the right of the front seat rail; on F224, the right-hand swag on the left seat rail and the middle swag on the right seat rail; on F225, the top of the floral wreath on the back and the middle swag on the front seat rail; on F227, most of the floral wreath at the top; on F229, three swags on the front seat rail; on F230, the second swag on the front seat rail; on F231, most of the floral wreath on the top, and on F232, the middle swag on the left seat rail and the second and fifth swags on the front seat rail. On F221 and F230 the floral wreaths at the top have been incorrectly repaired.

27 (F231) Photographed c.1924, still with its late-nineteenth-century silk

27 (F226) Photographed in June 1993, before regilding

The silk *lampas* on F219–20, F222 and F224–5 is dirty and decayed and shows extensive repair stitching. The *lampas* on F221, F227 and F229–32, woven in 1956 and applied to these armchairs in the late 1950s, has frayed at the front of the seats of F229 and F232; it has also turned amber, in comparison with the yellow of the unused silk from the same roll. F223 and F228 were re-upholstered in 1993 with silk from that roll. Examination of the upholstery of F223, F226 and F228 revealed fragments of crimson and yellow silk on the backs of F223 and F226. The lower layers of horsehair stuffing on all three armchairs showed threads drawn through the horsehair at regular intervals, between 16 and 18 cm. apart, suggesting that the backs and seats had once been tufted. All the pieces except F223, F226 and F228 have English webbing with a brown and cream herringbone weave, which appears to be original. F223 and F228 were rewebbed in 199[3] but with the old webbing retained above the new

148

The Wallace Collection
Hertford House, Manchester Square, London W1M 6BN
Telephone 071-935 0687 Fax 071-224 2155

RECEIPT FORM

Date ....
Museum number F223, F228
Description of object ....
Purpose of removal ....
Authorized by (signature) ....

Received from the Wallace Collection by:
Name/Firm ....
Address ....
Telephone ....
Signature ....

Returned to the Wallace Collection ....

Figure 8-7: Shrewsbury Set Silk Restoration details

8.3 TES 136 Chroma Meter Tristimulus measurements (in-situ)

Silk Sample Reference	X	Y	Z
1. Sample 1 on Display since 1956			
Reading 1	190.9	179.1	105.1
Reading 2	190	178.1	105.1
Average	**190.5**	**178.6**	**105.1**
2. Sample 2 on display since 1991 and kept in storage conditions before that			
Reading 1	226.2	218.7	117.3
Reading 2	220.8	212.2	113.8
Reading 3	226.4	214.1	114.6
Average	**224.5**	**215.0**	**115.2**
3. Silk Sample 3 in storage since 1956			
Reading 1	242.4	232.1	140.1
Reading 2	240.2	230.2	137.6
Reading 3	242.4	231.7	139.6
Sample 4 on display since 1993 and kept in storage conditions before that			
Reading 1	227.2	213.1	119.1
Reading 2	222	212.9	118.8
Reading 3	228.9	214.9	120
Average	**227.7**	**213.6**	**119.3**

Table 8-1: Primary Condition Data - Chromameter multiple readings

8.4. Chromameter Data Analysed

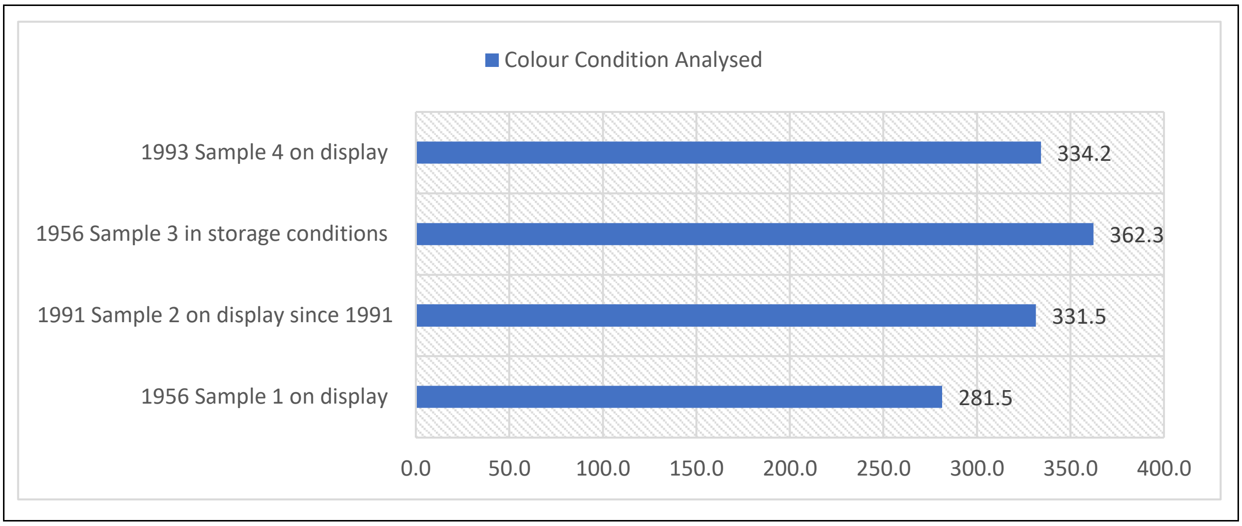

Figure 8-8: Chromameter data analysed for the four silk conditions

8.5. Effect of the environmental parameters

8.5.1 For Sample Reference 1 (Display Since 1956)

Year	Temp (°C)	RH (%)	Lux (lx)	Temp (K)	(0.1T-28.7)	alpha[(0.1T-28.7)RH]Δt	gamma(lv * RH)Δt	Δt
1956	20.7	56.7	55	293.9	0.68	38.84	3118.50	1
1957	20.7	56.7	55	293.9	0.68	38.84	3118.50	1
1958	20.7	56.7	55	293.9	0.68	38.84	3118.50	1
1959	20.7	56.7	55	293.9	0.68	38.84	3118.50	1
1960	20.7	56.7	55	293.9	0.68	38.84	3118.50	1
1961	20.7	56.7	55	293.9	0.68	38.84	3118.50	1
1962	20.7	56.7	55	293.9	0.68	38.84	3118.50	1
1963	20.7	56.7	55	293.9	0.68	38.84	3118.50	1
1964	20.7	56.7	55	293.9	0.68	38.84	3118.50	1
1965	20.7	56.7	55	293.9	0.68	38.84	3118.50	1
1966	20.7	56.7	55	293.9	0.68	38.84	3118.50	1
1967	20.7	56.7	55	293.9	0.68	38.84	3118.50	1
1968	20.7	56.7	55	293.9	0.68	38.84	3118.50	1
1969	20.7	56.7	55	293.9	0.68	38.84	3118.50	1
1970	20.7	56.7	55	293.9	0.68	38.84	3118.50	1
1971	20.7	56.7	55	293.9	0.68	38.84	3118.50	1
1972	20.7	56.7	55	293.9	0.68	38.84	3118.50	1
1973	20.7	56.7	55	293.9	0.68	38.84	3118.50	1
1974	20.7	56.7	55	293.9	0.68	38.84	3118.50	1
1975	20.7	56.7	55	293.9	0.68	38.84	3118.50	1
1976	20.7	56.7	55	293.9	0.68	38.84	3118.50	1
1977	20.7	56.7	55	293.9	0.68	38.84	3118.50	1
1978	20.7	56.7	55	293.9	0.68	38.84	3118.50	1
1979	20.7	56.7	55	293.9	0.68	38.84	3118.50	1
1980	20.7	56.7	55	293.9	0.68	38.84	3118.50	1
1981	20.7	56.7	55	293.9	0.68	38.84	3118.50	1
1982	20.7	56.7	55	293.9	0.68	38.84	3118.50	1
1983	20.7	56.7	55	293.9	0.68	38.84	3118.50	1
1984	20.7	56.7	55	293.9	0.68	38.84	3118.50	1
1985	20.7	56.7	55	293.9	0.68	38.84	3118.50	1
1986	20.7	56.7	55	293.9	0.68	38.84	3118.50	1
1987	20.7	56.7	55	293.9	0.68	38.84	3118.50	1
1988	20.7	56.7	55	293.9	0.68	38.84	3118.50	1
1989	20.7	56.7	55	293.9	0.68	38.84	3118.50	1
1990	20.7	56.7	55	293.9	0.68	38.84	3118.50	1
1991	20.7	56.7	55	293.9	0.68	38.84	3118.50	1
1992	20.7	56.7	55	293.9	0.68	38.84	3118.50	1
1993	20.7	56.7	55	293.9	0.68	38.84	3118.50	1
1994	20.7	56.7	55	293.9	0.68	38.84	3118.50	1
1995	20.7	56.7	55	293.9	0.68	38.84	3118.50	1
1996	**19.60**	**58.50**	55	**292.8**	0.58	33.64	3217.50	1
1997	20.7	56.7	55	293.9	0.68	38.84	3118.50	1
1998	20.7	56.7	55	293.9	0.68	38.84	3118.50	1
1999	20.7	56.7	55	293.9	0.68	38.84	3118.50	1
2000	20.7	56.7	55	293.9	0.68	38.84	3118.50	1
2001	20.7	56.7	55	293.9	0.68	38.84	3118.50	1
2002	20.7	56.7	55	293.9	0.68	38.84	3118.50	1
2003	20.7	56.7	55	293.9	0.68	38.84	3118.50	1
2004	20.7	56.7	55	293.9	0.68	38.84	3118.50	1
2005	20.7	56.7	55	293.9	0.68	38.84	3118.50	1
2006	**20.5**	**58.0**	55	293.7	0.66	38.57	3190.00	1
2007	**21.0**	**60.0**	55	294.2	0.72	42.90	3300.00	1
2008	**21.6**	**64.0**	55	294.7	0.77	49.42	3520.00	1
2009	20.7	56.7	55	293.9	0.68	38.84	3118.50	1
2010	**21.2**	**51.4**	55	294.4	0.73	37.78	2827.00	1
2011	20.7	56.7	55	293.9	0.68	38.84	3118.50	1
2012	**21.0**	56.7	55	294.2	0.72	40.73	3118.50	1
2013	**20.1**	56.7	55	293.3	0.63	35.62	3118.50	1
2014	**20.3**	**53.4**	49.95	293.4	0.64	34.40	2669.45	1
2015	**20.6**	**52.3**	54.33	293.8	0.68	35.44	2840.57	1
2016	**19.7**	**52.4**	52.76	292.9	0.59	30.83	2762.65	1
2017	**19.8**	**54.6**	55.66	293.0	0.60	32.66	3039.13	1
			54.9			2392.80	192646.80	

Table 8-2: Environmental conditions (k1)

8.5.2. Sample Condition 2 (on Display since 1991)

Year	Temp (℃)	RH (%)	Lux (lx)	Temp (K)	(0.1T-28.7)	alpha[(0.1T-28.7)RH]Δt	gamma(lv * RH)Δt	Δt
1991	20.7	56.7	55	293.9	0.685	38.84	3118.50	1
1992	20.7	56.7	55	293.9	0.685	38.84	3118.50	1
1993	20.7	56.7	55	293.9	0.685	38.84	3118.50	1
1994	20.7	56.7	55	293.9	0.685	38.84	3118.50	1
1995	20.7	56.7	55	293.9	0.685	38.84	3118.50	1
1996	**19.60**	**58.50**	55	292.8	0.575	33.64	3217.50	1
1997	20.7	56.7	55	293.9	0.685	38.84	3118.50	1
1998	20.7	56.7	55	293.9	0.685	38.84	3118.50	1
1999	20.7	56.7	55	293.9	0.685	38.84	3118.50	1
2000	20.7	56.7	55	293.9	0.685	38.84	3118.50	1
2001	20.7	56.7	55	293.9	0.685	38.84	3118.50	1
2002	20.7	56.7	55	293.9	0.685	38.84	3118.50	1
2003	20.7	56.7	55	293.9	0.685	38.84	3118.50	1
2004	20.7	56.7	55	293.9	0.685	38.84	3118.50	1
2005	20.7	56.7	55	293.9	0.685	38.84	3118.50	1
2006	**20.5**	**58.0**	55	293.7	0.665	38.57	3190.00	1
2007	**21.0**	**60.0**	55	294.2	0.715	42.90	3300.00	1
2008	**21.6**	**64.0**	55	294.7	0.772	49.42	3520.00	1
2009	20.7	56.7	55	293.9	0.685	38.84	3118.50	1
2010	**21.2**	**51.4**	55	294.4	0.735	37.78	2827.00	1
2011	20.7	56.7	55	293.9	0.685	38.84	3118.50	1
2012	**21.0**	56.7	55	294.2	0.718	40.73	3118.50	1
2013	**20.1**	56.7	55	293.3	0.628	35.62	3118.50	1
2014	**20.3**	**53.4**	**49.9**	293.4	0.644	34.40	2669.45	1
2015	**20.6**	**52.3**	**54.3**	293.8	0.678	35.44	2840.57	1
2016	**19.7**	**52.4**	**52.8**	292.9	0.589	30.83	2762.65	1
2017	**19.8**	**54.6**	**55.7**	293.0	0.598	32.66	3039.13	1
						1033.42	83499.30	

Table 8-3: Environmental conditions [k2]

8.5.3. Sample Condition 3 (In Storage Since 1956)

Year	Temp (°C)	RH (%)	Lux (lx)	Temp (K)	(0.1T-28.7)	alpha[(0.1T-28.7)RH]Δt	gamma(V x RH)Δt	Δt
1956	16	50	5	289.2	0.22	10.75	250.00	1
1957	16	50	5	289.2	0.22	10.75	250.00	1
1958	16	50	5	289.2	0.22	10.75	250.00	1
1959	16	50	5	289.2	0.22	10.75	250.00	1
1960	16	50	5	289.2	0.22	10.75	250.00	1
1961	16	50	5	289.2	0.22	10.75	250.00	1
1962	16	50	5	289.2	0.22	10.75	250.00	1
1963	16	50	5	289.2	0.22	10.75	250.00	1
1964	16	50	5	289.2	0.22	10.75	250.00	1
1965	16	50	5	289.2	0.22	10.75	250.00	1
1966	16	50	5	289.2	0.22	10.75	250.00	1
1967	16	50	5	289.2	0.22	10.75	250.00	1
1968	16	50	5	289.2	0.22	10.75	250.00	1
1969	16	50	5	289.2	0.22	10.75	250.00	1
1970	16	50	5	289.2	0.22	10.75	250.00	1
1971	16	50	5	289.2	0.22	10.75	250.00	1
1972	16	50	5	289.2	0.22	10.75	250.00	1
1973	16	50	5	289.2	0.22	10.75	250.00	1
1974	16	50	5	289.2	0.22	10.75	250.00	1
1975	16	50	5	289.2	0.22	10.75	250.00	1
1976	16	50	5	289.2	0.22	10.75	250.00	1
1977	16	50	5	289.2	0.22	10.75	250.00	1
1978	16	50	5	289.2	0.22	10.75	250.00	1
1979	16	50	5	289.2	0.22	10.75	250.00	1
1980	16	50	5	289.2	0.22	10.75	250.00	1
1981	16	50	5	289.2	0.22	10.75	250.00	1
1982	16	50	5	289.2	0.22	10.75	250.00	1
1983	16	50	5	289.2	0.22	10.75	250.00	1
1984	16	50	5	289.2	0.22	10.75	250.00	1
1985	16	50	5	289.2	0.22	10.75	250.00	1
1986	16	50	5	289.2	0.22	10.75	250.00	1
1987	16	50	5	289.2	0.22	10.75	250.00	1
1988	16	50	5	289.2	0.22	10.75	250.00	1
1989	16	50	5	289.2	0.22	10.75	250.00	1
1990	16	50	5	289.2	0.22	10.75	250.00	1
1991	16	50	5	289.2	0.22	10.75	250.00	1
1992	16	50	5	289.2	0.22	10.75	250.00	1
1993	16	50	5	289.2	0.22	10.75	250.00	1
1994	16	50	5	289.2	0.22	10.75	250.00	1
1995	16	50	5	289.2	0.22	10.75	250.00	1
1996	16	50	5	289.2	0.22	10.75	250.00	1
1997	16	50	5	289.2	0.22	10.75	250.00	1
1998	16	50	5	289.2	0.22	10.75	250.00	1
1999	16	50	5	289.2	0.22	10.75	250.00	1
2000	16	50	5	289.2	0.22	10.75	250.00	1
2001	16	50	5	289.2	0.22	10.75	250.00	1
2002	16	50	5	289.2	0.22	10.75	250.00	1
2003	16	50	5	289.2	0.22	10.75	250.00	1
2004	16	50	5	289.2	0.22	10.75	250.00	1
2005	16	50	5	289.2	0.22	10.75	250.00	1
2006	16	50	5	289.2	0.22	10.75	250.00	1
2007	16	50	5	289.2	0.22	10.75	250.00	1
2008	16	50	5	289.2	0.22	10.75	250.00	1
2009	16	50	5	289.2	0.22	10.75	250.00	1
2010	16	50	5	289.2	0.22	10.75	250.00	1
2011	16	50	5	289.2	0.22	10.75	250.00	1
2012	16	50	5	289.2	0.22	10.75	250.00	1
2013	16	50	5	289.2	0.22	10.75	250.00	1
2014	16	50	5	289.2	0.22	10.75	250.00	1
2015	16	50	5	289.2	0.22	10.75	250.00	1
2016	16	50	5	289.2	0.22	10.75	250.00	1
2017	16	50	5	289.2	0.22	10.75	250.00	1
						666.50	15500.00	

Table 8-4: Environmental storage conditions [k3]

8.5.4. Sample Reference 4 (Display since 1993) for Model Validation (S1 and S2)

Year	Temp (℃)	RH (%)	Lux (lx)	Temp (K)	(0.1T-28.7)	alpha[(0.1T-28.7)RH]Δt	gamma(lv * RH)Δt	Δt
1993	20.7	56.7	55	293.9	0.685	38.84	3118.50	1
1994	20.7	56.7	55	293.9	0.685	38.84	3118.50	1
1995	20.7	56.7	55	293.9	0.685	38.84	3118.50	1
1996	**19.60**	**58.50**	55	292.8	0.575	33.64	3217.50	1
1997	20.7	56.7	55	293.9	0.685	38.84	3118.50	1
1998	20.7	56.7	55	293.9	0.685	38.84	3118.50	1
1999	20.7	56.7	55	293.9	0.685	38.84	3118.50	1
2000	20.7	56.7	55	293.9	0.685	38.84	3118.50	1
2001	20.7	56.7	55	293.9	0.685	38.84	3118.50	1
2002	20.7	56.7	55	293.9	0.685	38.84	3118.50	1
2003	20.7	56.7	55	293.9	0.685	38.84	3118.50	1
2004	20.7	56.7	55	293.9	0.685	38.84	3118.50	1
2005	20.7	56.7	55	293.9	0.685	38.84	3118.50	1
2006	**20.5**	**58.0**	55	293.7	0.665	38.57	3190.00	1
2007	**21.0**	**60.0**	55	294.2	0.715	42.90	3300.00	1
2008	**21.6**	**64.0**	55	294.7	0.772	49.42	3520.00	1
2009	20.7	56.7	55	293.9	0.685	38.84	3118.50	1
2010	**21.2**	**51.4**	55	294.4	0.735	37.78	2827.00	1
2011	20.7	56.7	55	293.9	0.685	38.84	3118.50	1
2012	**21.0**	56.7	55	294.2	0.718	40.73	3118.50	1
2013	**20.1**	56.7	55	293.3	0.628	35.62	3118.50	1
2014	**20.3**	**53.4**	**49.9**	293.4	0.644	34.40	2669.45	1
2015	**20.6**	**52.3**	**54.3**	293.8	0.678	35.44	2840.57	1
2016	**19.7**	**52.4**	**52.8**	292.9	0.589	30.83	2762.65	1
2017	**19.8**	**54.6**	**55.7**	293.0	0.598	32.66	3039.13	1
						955.74	77262.30	

Table 8-5: Environmental conditions (k4)

8.6. Colour Fade Model Parameters derived through Optimisation

VISUAL DOC RESULTS	
fr	fr1
1.00E-06	1.00E-06
alpha Vdoc	gamma Vdoc
3.021227E+01	1.115565E+00
alpha model	gamma model
3.02E-05	1.12E-06

Table 8-6: Visual Doc optimisation results

α	γ	C_0
3.02E-05	1.12E-06	376.12

Table 8-7: Results of model unknown parameters derived mathematically

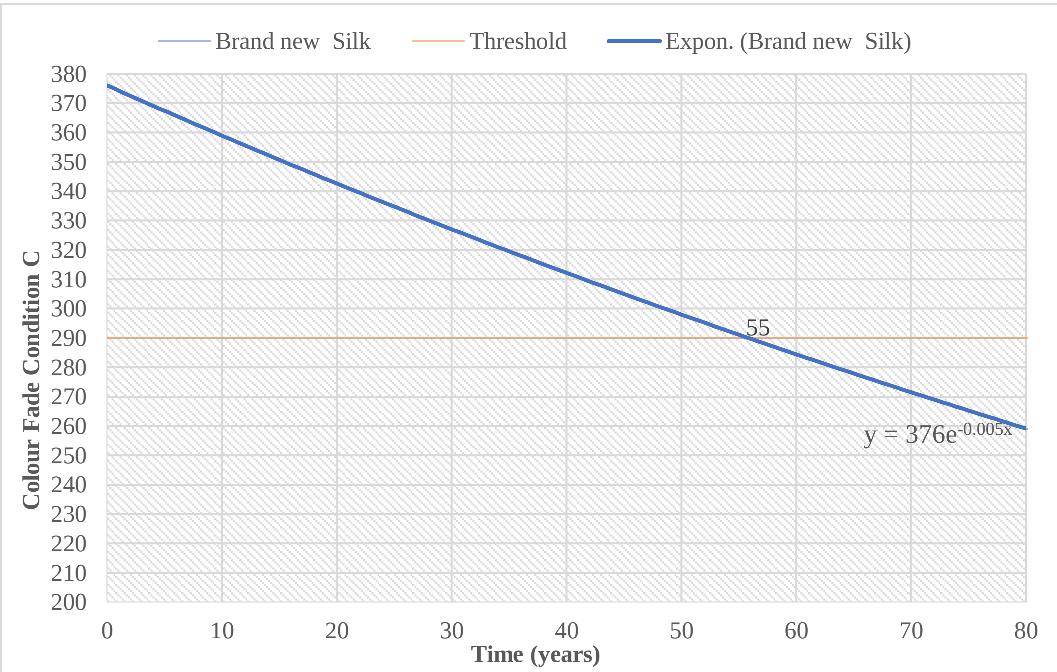

Figure 8-9: Exponential Silk Colour Fade Model

8.7 Model Validation with Sample Condition 4 – On display 1993

Sample environmental conditions $^{(k)}$	$S1^{(k)}$	$S2^{(k)}$
4. On display since 1993	955.74	77262.30

Table 8-8: Cumulative environmental damage for sample condition 4

Year	Temp (°C)	RH(%)	Lux(lx)	Temp (K)	(0.1T-28.7)	[(0.1T-28.7)RH]Δt	(v × RH)Δt	Δt	S1	S2	376.00
2020	20.7	56.7	55	293.9	0.68	38.84	3118.50	1	955.74	77262.30	335.13

Table 8-9: Model Prediction of test sample condition 4

Sample env. conditions $^{(k)}$	Measured value (M)	Model forecast	Variance	$S1^{(k)}$	$S2^{(k)}$
4. On display since 1993	334.2	335.1	0.9	955.74	77262.30

Table 8-10: Model validation of test sample condition 4

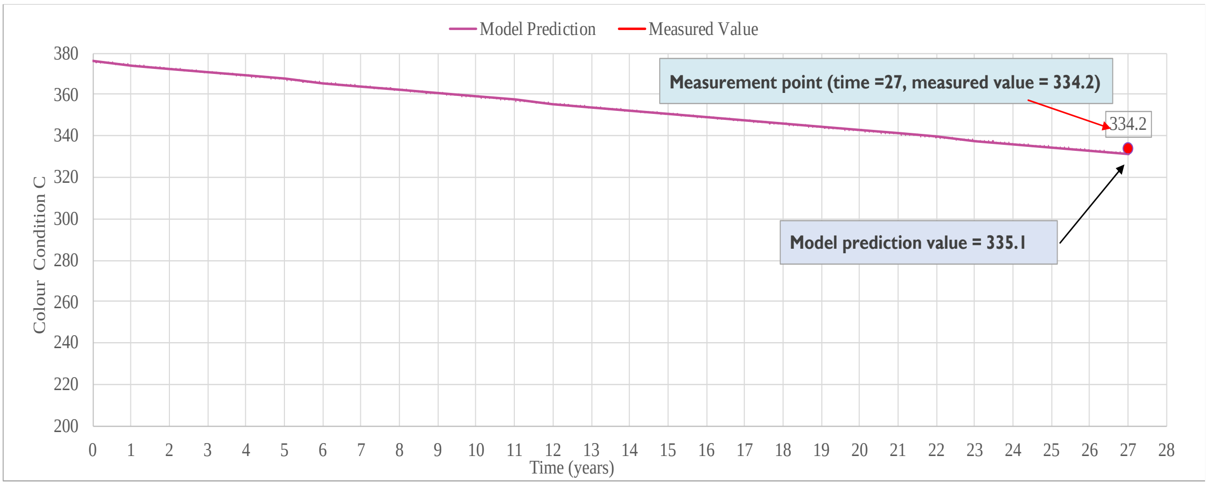

Figure 8-10: Model validation of test sample condition 4

8.8. Prognostic Modelling for Silk Sample Reference 2 (1991)

8.8.1. Scenario 1 Typical Conditions

Year	Temp (℃)	RH(%)	Lux(lx)	Temp (K)	(0.1T-28.7)	[(0.1T-28.7)RH]Δt	(v × RH)Δt	Δt	S1	S2	331.00	0
2020	20.7	56.7	55	293.9	0.68	38.84	3118.50	1	38.84	3118.50	329.46	1
2021	20.7	56.7	55	293.9	0.68	38.84	3118.50	1	77.68	6237.00	327.93	2
2022	20.7	56.7	55	293.9	0.68	38.84	3118.50	1	116.52	9355.50	326.41	3
2023	20.7	56.7	55	293.9	0.68	38.84	3118.50	1	155.36	12474.00	324.90	4
2024	20.7	56.7	55	293.9	0.68	38.84	3118.50	1	194.20	15592.50	323.39	5
2025	20.7	56.7	55	293.9	0.68	38.84	3118.50	1	233.04	18711.00	321.89	6
2026	20.7	56.7	55	293.9	0.68	38.84	3118.50	1	271.88	21829.50	320.39	7
2027	20.7	56.7	55	293.9	0.68	38.84	3118.50	1	310.72	24948.00	318.91	8
2028	20.7	56.7	55	293.9	0.68	38.84	3118.50	1	349.56	28066.50	317.43	9
2029	20.7	56.7	55	293.9	0.68	38.84	3118.50	1	388.39	31185.00	315.95	10
2030	20.7	56.7	55	293.9	0.68	38.84	3118.50	1	427.23	34303.50	314.49	11
2031	20.7	56.7	55	293.9	0.68	38.84	3118.50	1	466.07	37422.00	313.03	12
2032	20.7	56.7	55	293.9	0.68	38.84	3118.50	1	504.91	40540.50	311.57	13
2033	20.7	56.7	55	293.9	0.68	38.84	3118.50	1	543.75	43659.00	310.13	14
2034	20.7	56.7	55	293.9	0.68	38.84	3118.50	1	582.59	46777.50	308.69	15
2035	20.7	56.7	55	293.9	0.68	38.84	3118.50	1	621.43	49896.00	307.26	16
2036	20.7	56.7	55	293.9	0.68	38.84	3118.50	1	660.27	53014.50	305.83	17
2037	20.7	56.7	55	293.9	0.68	38.84	3118.50	1	699.11	56133.00	304.41	18
2038	20.7	56.7	55	293.9	0.68	38.84	3118.50	1	737.95	59251.50	303.00	19
2039	20.7	56.7	55	293.9	0.68	38.84	3118.50	1	776.79	62370.00	301.59	20
2040	20.7	56.7	55	293.9	0.68	38.84	3118.50	1	815.63	65488.50	300.19	21
2041	20.7	56.7	55	293.9	0.68	38.84	3118.50	1	854.47	68607.00	298.80	22
2042	20.7	56.7	55	293.9	0.68	38.84	3118.50	1	893.31	71725.50	297.41	23
2043	20.7	56.7	55	293.9	0.68	38.84	3118.50	1	932.15	74844.00	296.03	24
2044	20.7	56.7	55	293.9	0.68	38.84	3118.50	1	970.99	77962.50	294.66	25
2045	20.7	56.7	55	293.9	0.68	38.84	3118.50	1	1009.83	81081.00	293.29	26
2046	20.7	56.7	55	293.9	0.68	38.84	3118.50	1	1048.67	84199.50	291.93	27
2047	20.7	56.7	55	293.9	0.68	38.84	3118.50	1	1087.51	87318.00	290.57	28
2048	20.7	56.7	55	293.9	0.68	38.84	3118.50	1	1126.35	90436.50	289.22	29
2049	20.7	56.7	55	293.9	0.68	38.84	3118.50	1	1165.19	93555.00	287.88	30
2050	20.7	56.7	55	293.9	0.68	38.84	3118.50	1	1204.02	96673.50	286.55	31
2051	20.7	56.7	55	293.9	0.68	38.84	3118.50	1	1242.86	99792.00	285.22	32
2052	20.7	56.7	55	293.9	0.68	38.84	3118.50	1	1281.70	102910.50	283.89	33
2053	20.7	56.7	55	293.9	0.68	38.84	3118.50	1	1320.54	106029.00	282.57	34
2054	20.7	56.7	55	293.9	0.68	38.84	3118.50	1	1359.38	109147.50	281.26	35

Table 8-11: Cumulative degradation data (Scenario 1)

8.8.2. Scenario 2 Raised Museum Conditions (1 unit)

Year	Temp (℃)	RH(%)	Lux(lx)	Temp (K)	(0.1T-28.7)	[(0.1T-28.7)RH]Δt	(v x RH)Δt	Δt	S1	S2	331.00	0
2020	21.7	57.70	56.00	294.9	0.79	45.29	3231.20	1	45.29	3231.20	329.36	1
2021	21.7	57.70	56.00	294.9	0.79	45.29	3231.20	1	90.59	6462.40	327.72	2
2022	21.7	57.70	56.00	294.9	0.79	45.29	3231.20	1	135.88	9693.60	326.10	3
2023	21.7	57.70	56.00	294.9	0.79	45.29	3231.20	1	181.18	12924.80	324.48	4
2024	21.7	57.70	56.00	294.9	0.79	45.29	3231.20	1	226.47	16156.00	322.87	5
2025	21.7	57.70	56.00	294.9	0.79	45.29	3231.20	1	271.77	19387.20	321.27	6
2026	21.7	57.70	56.00	294.9	0.79	45.29	3231.20	1	317.06	22618.40	319.68	7
2027	21.7	57.70	56.00	294.9	0.79	45.29	3231.20	1	362.36	25849.60	318.09	8
2028	21.7	57.70	56.00	294.9	0.79	45.29	3231.20	1	407.65	29080.80	316.51	9
2029	21.7	57.70	56.00	294.9	0.79	45.29	3231.20	1	452.95	32312.00	314.94	10
2030	21.7	57.70	56.00	294.9	0.79	45.29	3231.20	1	498.24	35543.20	313.38	11
2031	21.7	57.70	56.00	294.9	0.79	45.29	3231.20	1	543.53	38774.40	311.82	12
2032	21.7	57.70	56.00	294.9	0.79	45.29	3231.20	1	588.83	42005.60	310.28	13
2033	21.7	57.70	56.00	294.9	0.79	45.29	3231.20	1	634.12	45236.80	308.74	14
2034	21.7	57.70	56.00	294.9	0.79	45.29	3231.20	1	679.42	48468.00	307.21	15
2035	21.7	57.70	56.00	294.9	0.79	45.29	3231.20	1	724.71	51699.20	305.68	16
2036	21.7	57.70	56.00	294.9	0.79	45.29	3231.20	1	770.01	54930.40	304.17	17
2037	21.7	57.70	56.00	294.9	0.79	45.29	3231.20	1	815.30	58161.60	302.66	18
2038	21.7	57.70	56.00	294.9	0.79	45.29	3231.20	1	860.60	61392.80	301.16	19
2039	21.7	57.70	56.00	294.9	0.79	45.29	3231.20	1	905.89	64624.00	299.66	20
2040	21.7	57.70	56.00	294.9	0.79	45.29	3231.20	1	951.18	67855.20	298.18	21
2041	21.7	57.70	56.00	294.9	0.79	45.29	3231.20	1	996.48	71086.40	296.70	22
2042	21.7	57.70	56.00	294.9	0.79	45.29	3231.20	1	1041.77	74317.60	295.23	23
2043	21.7	57.70	56.00	294.9	0.79	45.29	3231.20	1	1087.07	77548.80	293.76	24
2044	21.7	57.70	56.00	294.9	0.79	45.29	3231.20	1	1132.36	80780.00	292.30	25
2045	21.7	57.70	56.00	294.9	0.79	45.29	3231.20	1	1177.66	84011.20	290.85	26
2046	21.7	57.70	56.00	294.9	0.79	45.29	3231.20	1	1222.95	87242.40	289.41	27
2047	21.7	57.70	56.00	294.9	0.79	45.29	3231.20	1	1268.25	90473.60	287.97	28
2048	21.7	57.70	56.00	294.9	0.79	45.29	3231.20	1	1313.54	93704.80	286.55	29
2049	21.7	57.70	56.00	294.9	0.79	45.29	3231.20	1	1358.84	96936.00	285.12	30
2050	21.7	57.70	56.00	294.9	0.79	45.29	3231.20	1	1404.13	100167.20	283.71	31
2051	21.7	57.70	56.00	294.9	0.79	45.29	3231.20	1	1449.42	103398.40	282.30	32
2052	21.7	57.70	56.00	294.9	0.79	45.29	3231.20	1	1494.72	106629.60	280.90	33
2053	21.7	57.70	56.00	294.9	0.79	45.29	3231.20	1	1540.01	109860.80	279.51	34

Table 8-12: Cumulative degradation data (Scenario 2)

8.8.3. Scenario 3 Increased Conditions (10%)

Year	Temp (℃)	RH(%)	Lux(lx)	Temp (K)	(0.1T-28.7)	[(0.1T-28.7)RH]Δt	(v × RH)Δt	Δt	S1	S2	331.00	0
2020	22.7	62.4	60.5	295.9	0.88	55.22	3775.20	1	55.22	3775.20	329.06	1
2021	22.7	62.4	60.5	295.9	0.88	55.22	3775.20	1	110.45	7550.40	327.13	2
2022	22.7	62.4	60.5	295.9	0.88	55.22	3775.20	1	165.67	11325.60	325.21	3
2023	22.7	62.4	60.5	295.9	0.88	55.22	3775.20	1	220.90	15100.80	323.31	4
2024	22.7	62.4	60.5	295.9	0.88	55.22	3775.20	1	276.12	18876.00	321.41	5
2025	22.7	62.4	60.5	295.9	0.88	55.22	3775.20	1	331.34	22651.20	319.53	6
2026	22.7	62.4	60.5	295.9	0.88	55.22	3775.20	1	386.57	26426.40	317.65	7
2027	22.7	62.4	60.5	295.9	0.88	55.22	3775.20	1	441.79	30201.60	315.79	8
2028	22.7	62.4	60.5	295.9	0.88	55.22	3775.20	1	497.02	33976.80	313.94	9
2029	22.7	62.4	60.5	295.9	0.88	55.22	3775.20	1	552.24	37752.00	312.10	10
2030	22.7	62.4	60.5	295.9	0.88	55.22	3775.20	1	607.46	41527.20	310.27	11
2031	22.7	62.4	60.5	295.9	0.88	55.22	3775.20	1	662.69	45302.40	308.45	12
2032	22.7	62.4	60.5	295.9	0.88	55.22	3775.20	1	717.91	49077.60	306.64	13
2033	22.7	62.4	60.5	295.9	0.88	55.22	3775.20	1	773.14	52852.80	304.84	14
2034	22.7	62.4	60.5	295.9	0.88	55.22	3775.20	1	828.36	56628.00	303.06	15
2035	22.7	62.4	60.5	295.9	0.88	55.22	3775.20	1	883.58	60403.20	301.28	16
2036	22.7	62.4	60.5	295.9	0.88	55.22	3775.20	1	938.81	64178.40	299.51	17
2037	22.7	62.4	60.5	295.9	0.88	55.22	3775.20	1	994.03	67953.60	297.76	18
2038	22.7	62.4	60.5	295.9	0.88	55.22	3775.20	1	1049.26	71728.80	296.01	19
2039	22.7	62.4	60.5	295.9	0.88	55.22	3775.20	1	1104.48	75504.00	294.28	20
2040	22.7	62.4	60.5	295.9	0.88	55.22	3775.20	1	1159.70	79279.20	292.55	21
2041	22.7	62.4	60.5	295.9	0.88	55.22	3775.20	1	1214.93	83054.40	290.84	22
2042	22.7	62.4	60.5	295.9	0.88	55.22	3775.20	1	1270.15	86829.60	289.13	23
2043	22.7	62.4	60.5	295.9	0.88	55.22	3775.20	1	1325.38	90604.80	287.44	24
2044	22.7	62.4	60.5	295.9	0.88	55.22	3775.20	1	1380.60	94380.00	285.75	25
2045	22.7	62.4	60.5	295.9	0.88	55.22	3775.20	1	1435.82	98155.20	284.08	26
2046	22.7	62.4	60.5	295.9	0.88	55.22	3775.20	1	1491.05	101930.40	282.41	27
2047	22.7	62.4	60.5	295.9	0.88	55.22	3775.20	1	1546.27	105705.60	280.75	28
2048	22.7	62.4	60.5	295.9	0.88	55.22	3775.20	1	1601.50	109480.80	279.11	29

Table 8-13: Cumulative degradation data (Scenario 3)

8.8.4. Scenario 4 Harsh Conditions (15%)

Year	Temp (℃)	RH(%)	Lux(lx)	Temp (K)	(0.1T-28.7)	[(0.1T-28.7)RH]Δt	(v × RH)Δt	Δt	S1	S2	331.00	0
2020	23.8	65.20	63.20	297.0	1.00	64.87	4120.64	1	64.87	4120.64	328.84	1
2021	23.8	65.20	63.20	297.0	1.00	64.87	4120.64	1	129.75	8241.28	326.69	2
2022	23.8	65.20	63.20	297.0	1.00	64.87	4120.64	1	194.62	12361.92	324.55	3
2023	23.8	65.20	63.20	297.0	1.00	64.87	4120.64	1	259.50	16482.56	322.43	4
2024	23.8	65.20	63.20	297.0	1.00	64.87	4120.64	1	324.37	20603.20	320.32	5
2025	23.8	65.20	63.20	297.0	1.00	64.87	4120.64	1	389.24	24723.84	318.23	6
2026	23.8	65.20	63.20	297.0	1.00	64.87	4120.64	1	454.12	28844.48	316.15	7
2027	23.8	65.20	63.20	297.0	1.00	64.87	4120.64	1	518.99	32965.12	314.09	8
2028	23.8	65.20	63.20	297.0	1.00	64.87	4120.64	1	583.87	37085.76	312.03	9
2029	23.8	65.20	63.20	297.0	1.00	64.87	4120.64	1	648.74	41206.40	309.99	10
2030	23.8	65.20	63.20	297.0	1.00	64.87	4120.64	1	713.61	45327.04	307.97	11
2031	23.8	65.20	63.20	297.0	1.00	64.87	4120.64	1	778.49	49447.68	305.95	12
2032	23.8	65.20	63.20	297.0	1.00	64.87	4120.64	1	843.36	53568.32	303.95	13
2033	23.8	65.20	63.20	297.0	1.00	64.87	4120.64	1	908.24	57688.96	301.97	14
2034	23.8	65.20	63.20	297.0	1.00	64.87	4120.64	1	973.11	61809.60	300.00	15
2035	23.8	65.20	63.20	297.0	1.00	64.87	4120.64	1	1037.98	65930.24	298.03	16
2036	23.8	65.20	63.20	297.0	1.00	64.87	4120.64	1	1102.86	70050.88	296.09	17
2037	23.8	65.20	63.20	297.0	1.00	64.87	4120.64	1	1167.73	74171.52	294.15	18
2038	23.8	65.20	63.20	297.0	1.00	64.87	4120.64	1	1232.61	78292.16	292.23	19
2039	23.8	65.20	63.20	297.0	1.00	64.87	4120.64	1	1297.48	82412.80	290.32	20
2040	23.8	65.20	63.20	297.0	1.00	64.87	4120.64	1	1362.35	86533.44	288.42	21
2041	23.8	65.20	63.20	297.0	1.00	64.87	4120.64	1	1427.23	90654.08	286.54	22
2042	23.8	65.20	63.20	297.0	1.00	64.87	4120.64	1	1492.10	94774.72	284.66	23
2043	23.8	65.20	63.20	297.0	1.00	64.87	4120.64	1	1556.98	98895.36	282.80	24
2044	23.8	65.20	63.20	297.0	1.00	64.87	4120.64	1	1621.85	103016.00	280.96	25

Table 8-14: Cumulative degradation data (Scenario 4)

8.8.5. Scenario 5 Lowered Conditions (-5%)

Year	Temp (℃)	RH(%)	Lux(lx)	Temp (K)	(0.1T-28.7)	[(0.1T-28.7)RH]Δt	(v × RH)Δt	Δt	S1	S2	331.00	0
2020	19.6	53.9	52.25	292.8	0.58	30.99	2816.28	1	30.99	2816.28	329.65	1
2021	19.6	53.9	52.25	292.8	0.58	30.99	2816.28	1	61.99	5632.55	328.31	2
2022	19.6	53.9	52.25	292.8	0.58	30.99	2816.28	1	92.98	8448.83	326.98	3
2023	19.6	53.9	52.25	292.8	0.58	30.99	2816.28	1	123.97	11265.10	325.64	4
2024	19.6	53.9	52.25	292.8	0.58	30.99	2816.28	1	154.96	14081.38	324.32	5
2025	19.6	53.9	52.25	292.8	0.58	30.99	2816.28	1	185.96	16897.65	323.00	6
2026	19.6	53.9	52.25	292.8	0.58	30.99	2816.28	1	216.95	19713.93	321.68	7
2027	19.6	53.9	52.25	292.8	0.58	30.99	2816.28	1	247.94	22530.20	320.38	8
2028	19.6	53.9	52.25	292.8	0.58	30.99	2816.28	1	278.93	25346.48	319.07	9
2029	19.6	53.9	52.25	292.8	0.58	30.99	2816.28	1	309.93	28162.75	317.77	10
2030	19.6	53.9	52.25	292.8	0.58	30.99	2816.28	1	340.92	30979.03	316.48	11
2031	19.6	53.9	52.25	292.8	0.58	30.99	2816.28	1	371.91	33795.30	315.19	12
2032	19.6	53.9	52.25	292.8	0.58	30.99	2816.28	1	402.90	36611.58	313.91	13
2033	19.6	53.9	52.25	292.8	0.58	30.99	2816.28	1	433.90	39427.85	312.63	14
2034	19.6	53.9	52.25	292.8	0.58	30.99	2816.28	1	464.89	42244.13	311.36	15
2035	19.6	53.9	52.25	292.8	0.58	30.99	2816.28	1	495.88	45060.40	310.09	16
2036	19.6	53.9	52.25	292.8	0.58	30.99	2816.28	1	526.87	47876.68	308.83	17
2037	19.6	53.9	52.25	292.8	0.58	30.99	2816.28	1	557.87	50692.95	307.57	18
2038	19.6	53.9	52.25	292.8	0.58	30.99	2816.28	1	588.86	53509.23	306.32	19
2039	19.6	53.9	52.25	292.8	0.58	30.99	2816.28	1	619.85	56325.50	305.07	20
2040	19.6	53.9	52.25	292.8	0.58	30.99	2816.28	1	650.84	59141.78	303.83	21
2041	19.6	53.9	52.25	292.8	0.58	30.99	2816.28	1	681.84	61958.05	302.60	22
2042	19.6	53.9	52.25	292.8	0.58	30.99	2816.28	1	712.83	64774.33	301.37	23
2043	19.6	53.9	52.25	292.8	0.58	30.99	2816.28	1	743.82	67590.60	300.14	24
2044	19.6	53.9	52.25	292.8	0.58	30.99	2816.28	1	774.81	70406.88	298.92	25
2045	19.6	53.9	52.25	292.8	0.58	30.99	2816.28	1	805.81	73223.15	297.70	26
2046	19.6	53.9	52.25	292.8	0.58	30.99	2816.28	1	836.80	76039.43	296.49	27
2047	19.6	53.9	52.25	292.8	0.58	30.99	2816.28	1	867.79	78855.70	295.28	28
2048	19.6	53.9	52.25	292.8	0.58	30.99	2816.28	1	898.78	81671.98	294.08	29
2049	19.6	53.9	52.25	292.8	0.58	30.99	2816.28	1	929.78	84488.25	292.88	30
2050	19.6	53.9	52.25	292.8	0.58	30.99	2816.28	1	960.77	87304.53	291.69	31
2051	19.6	53.9	52.25	292.8	0.58	30.99	2816.28	1	991.76	90120.80	290.50	32
2052	19.6	53.9	52.25	292.8	0.58	30.99	2816.28	1	1022.75	92937.08	289.32	33
2053	19.6	53.9	52.25	292.8	0.58	30.99	2816.28	1	1053.75	95753.35	288.14	34
2054	19.6	53.9	52.25	292.8	0.58	30.99	2816.28	1	1084.74	98569.63	286.97	35
2055	19.6	53.9	52.25	292.8	0.58	30.99	2816.28	1	1115.73	101385.90	285.80	36
2056	19.6	53.9	52.25	292.8	0.58	30.99	2816.28	1	1146.72	104202.18	284.64	37
2057	19.6	53.9	52.25	292.8	0.58	30.99	2816.28	1	1177.72	107018.45	283.48	38
2058	19.6	53.9	52.25	292.8	0.58	30.99	2816.28	1	1208.71	109834.73	282.33	39
2059	19.6	53.9	52.25	292.8	0.58	30.99	2816.28	1	1239.70	112651.00	281.18	40
2060	19.6	53.9	52.25	292.8	0.58	30.99	2816.28	1	1270.69	115467.28	280.04	41

Table 8-15: Cumulative degradation data (Scenario 5)

8.8.6. Scenario 6 Reduced Conditions (-15%)

Year	Temp (℃)	RH(%)	Lux(lx)	Temp (K)	(0.1T-28.7)	[(0.1T-28.7)RH]Δt	(v × RH)Δt	Δt	S1	S2	331.00	0
2020	17.6	48.20	46.75	290.8	0.38	18.08	2253.35	1	18.08	2253.35	329.99	1
2021	17.6	48.20	46.75	290.8	0.38	18.08	2253.35	1	36.15	4506.70	328.98	2
2022	17.6	48.20	46.75	290.8	0.38	18.08	2253.35	1	54.23	6760.05	327.98	3
2023	17.6	48.20	46.75	290.8	0.38	18.08	2253.35	1	72.30	9013.40	326.97	4
2024	17.6	48.20	46.75	290.8	0.38	18.08	2253.35	1	90.38	11266.75	325.97	5
2025	17.6	48.20	46.75	290.8	0.38	18.08	2253.35	1	108.45	13520.10	324.98	6
2026	17.6	48.20	46.75	290.8	0.38	18.08	2253.35	1	126.53	15773.45	323.99	7
2027	17.6	48.20	46.75	290.8	0.38	18.08	2253.35	1	144.60	18026.80	323.00	8
2028	17.6	48.20	46.75	290.8	0.38	18.08	2253.35	1	162.68	20280.15	322.01	9
2029	17.6	48.20	46.75	290.8	0.38	18.08	2253.35	1	180.75	22533.50	321.03	10
2030	17.6	48.20	46.75	290.8	0.38	18.08	2253.35	1	198.83	24786.85	320.04	11
2031	17.6	48.20	46.75	290.8	0.38	18.08	2253.35	1	216.90	27040.20	319.07	12
2032	17.6	48.20	46.75	290.8	0.38	18.08	2253.35	1	234.98	29293.55	318.09	13
2033	17.6	48.20	46.75	290.8	0.38	18.08	2253.35	1	253.05	31546.90	317.12	14
2034	17.6	48.20	46.75	290.8	0.38	18.08	2253.35	1	271.13	33800.25	316.15	15
2035	17.6	48.20	46.75	290.8	0.38	18.08	2253.35	1	289.20	36053.60	315.19	16
2036	17.6	48.20	46.75	290.8	0.38	18.08	2253.35	1	307.28	38306.95	314.22	17
2037	17.6	48.20	46.75	290.8	0.38	18.08	2253.35	1	325.35	40560.30	313.26	18
2038	17.6	48.20	46.75	290.8	0.38	18.08	2253.35	1	343.43	42813.65	312.31	19
2039	17.6	48.20	46.75	290.8	0.38	18.08	2253.35	1	361.50	45067.00	311.35	20
2040	17.6	48.20	46.75	290.8	0.38	18.08	2253.35	1	379.58	47320.35	310.40	21
2041	17.6	48.20	46.75	290.8	0.38	18.08	2253.35	1	397.65	49573.70	309.45	22
2042	17.6	48.20	46.75	290.8	0.38	18.08	2253.35	1	415.73	51827.05	308.51	23
2043	17.6	48.20	46.75	290.8	0.38	18.08	2253.35	1	433.80	54080.40	307.56	24
2044	17.6	48.20	46.75	290.8	0.38	18.08	2253.35	1	451.88	56333.75	306.62	25
2045	17.6	48.20	46.75	290.8	0.38	18.08	2253.35	1	469.95	58587.10	305.69	26
2046	17.6	48.20	46.75	290.8	0.38	18.08	2253.35	1	488.03	60840.45	304.75	27
2047	17.6	48.20	46.75	290.8	0.38	18.08	2253.35	1	506.10	63093.80	303.82	28
2048	17.6	48.20	46.75	290.8	0.38	18.08	2253.35	1	524.18	65347.15	302.89	29
2049	17.6	48.20	46.75	290.8	0.38	18.08	2253.35	1	542.25	67600.50	301.97	30
2050	17.6	48.20	46.75	290.8	0.38	18.08	2253.35	1	560.33	69853.85	301.05	31
2051	17.6	48.20	46.75	290.8	0.38	18.08	2253.35	1	578.40	72107.20	300.13	32
2052	17.6	48.20	46.75	290.8	0.38	18.08	2253.35	1	596.48	74360.55	299.21	33
2053	17.6	48.20	46.75	290.8	0.38	18.08	2253.35	1	614.55	76613.90	298.30	34
2054	17.6	48.20	46.75	290.8	0.38	18.08	2253.35	1	632.63	78867.25	297.38	35
2055	17.6	48.20	46.75	290.8	0.38	18.08	2253.35	1	650.70	81120.60	296.48	36
2056	17.6	48.20	46.75	290.8	0.38	18.08	2253.35	1	668.78	83373.95	295.57	37
2057	17.6	48.20	46.75	290.8	0.38	18.08	2253.35	1	686.85	85627.30	294.67	38
2058	17.6	48.20	46.75	290.8	0.38	18.08	2253.35	1	704.93	87880.65	293.77	39
2059	17.6	48.20	46.75	290.8	0.38	18.08	2253.35	1	723.00	90134.00	292.87	40
2060	17.6	48.20	46.75	290.8	0.38	18.08	2253.35	1	741.08	92387.35	291.97	41
2061	17.6	48.20	46.75	290.8	0.38	18.08	2253.35	1	759.15	94640.70	291.08	42
2062	17.6	48.20	46.75	290.8	0.38	18.08	2253.35	1	777.23	96894.05	290.19	43
2063	17.6	48.20	46.75	290.8	0.38	18.08	2253.35	1	795.30	99147.40	289.31	44
2064	17.6	48.20	46.75	290.8	0.38	18.08	2253.35	1	813.38	101400.75	288.42	45
2065	17.6	48.20	46.75	290.8	0.38	18.08	2253.35	1	831.45	103654.10	287.54	46
2066	17.6	48.20	46.75	290.8	0.38	18.08	2253.35	1	849.53	105907.45	286.66	47
2067	17.6	48.20	46.75	290.8	0.38	18.08	2253.35	1	867.60	108160.80	285.79	48
2068	17.6	48.20	46.75	290.8	0.38	18.08	2253.35	1	885.68	110414.15	284.91	49
2069	17.6	48.20	46.75	290.8	0.38	18.08	2253.35	1	903.75	112667.50	284.04	50
2070	17.6	48.20	46.75	290.8	0.38	18.08	2253.35	1	921.83	114920.85	283.18	51
2071	17.6	48.20	46.75	290.8	0.38	18.08	2253.35	1	939.90	117174.20	282.31	52
2072	17.6	48.20	46.75	290.8	0.38	18.08	2253.35	1	957.98	119427.55	281.45	53
2073	17.6	48.20	46.75	290.8	0.38	18.08	2253.35	1	976.05	121680.90	280.59	54

Table 8-16: Cumulative degradation data (Scenario 6)

8.8.7. Scenario 7 Lower limit of the recommended museum standard

Year	Temp (℃)	RH(%)	Lux(lx)	Temp (K)	(0.1T-28.7)	[(0.1T-28.7)RH]Δt	(v × RH)Δt	Δt	S1	S2	331.00	0
2020	19	45	45	292.2	0.52	23.18	2025.00	1	23.18	2025.00	330.02	1
2021	19	45	45	292.2	0.52	23.18	2025.00	1	46.35	4050.00	329.05	2
2022	19	45	45	292.2	0.52	23.18	2025.00	1	69.53	6075.00	328.07	3
2023	19	45	45	292.2	0.52	23.18	2025.00	1	92.70	8100.00	327.11	4
2024	19	45	45	292.2	0.52	23.18	2025.00	1	115.88	10125.00	326.14	5
2025	19	45	45	292.2	0.52	23.18	2025.00	1	139.05	12150.00	325.17	6
2026	19	45	45	292.2	0.52	23.18	2025.00	1	162.23	14175.00	324.21	7
2027	19	45	45	292.2	0.52	23.18	2025.00	1	185.40	16200.00	323.26	8
2028	19	45	45	292.2	0.52	23.18	2025.00	1	208.58	18225.00	322.30	9
2029	19	45	45	292.2	0.52	23.18	2025.00	1	231.75	20250.00	321.35	10
2030	19	45	45	292.2	0.52	23.18	2025.00	1	254.93	22275.00	320.40	11
2031	19	45	45	292.2	0.52	23.18	2025.00	1	278.10	24300.00	319.45	12
2032	19	45	45	292.2	0.52	23.18	2025.00	1	301.28	26325.00	318.51	13
2033	19	45	45	292.2	0.52	23.18	2025.00	1	324.45	28350.00	317.57	14
2034	19	45	45	292.2	0.52	23.18	2025.00	1	347.63	30375.00	316.63	15
2035	19	45	45	292.2	0.52	23.18	2025.00	1	370.80	32400.00	315.69	16
2036	19	45	45	292.2	0.52	23.18	2025.00	1	393.98	34425.00	314.76	17
2037	19	45	45	292.2	0.52	23.18	2025.00	1	417.15	36450.00	313.83	18
2038	19	45	45	292.2	0.52	23.18	2025.00	1	440.33	38475.00	312.90	19
2039	19	45	45	292.2	0.52	23.18	2025.00	1	463.50	40500.00	311.98	20
2040	19	45	45	292.2	0.52	23.18	2025.00	1	486.68	42525.00	311.06	21
2041	19	45	45	292.2	0.52	23.18	2025.00	1	509.85	44550.00	310.14	22
2042	19	45	45	292.2	0.52	23.18	2025.00	1	533.03	46575.00	309.22	23
2043	19	45	45	292.2	0.52	23.18	2025.00	1	556.20	48600.00	308.31	24
2044	19	45	45	292.2	0.52	23.18	2025.00	1	579.38	50625.00	307.40	25
2045	19	45	45	292.2	0.52	23.18	2025.00	1	602.55	52650.00	306.49	26
2046	19	45	45	292.2	0.52	23.18	2025.00	1	625.73	54675.00	305.58	27
2047	19	45	45	292.2	0.52	23.18	2025.00	1	648.90	56700.00	304.68	28
2048	19	45	45	292.2	0.52	23.18	2025.00	1	672.08	58725.00	303.78	29
2049	19	45	45	292.2	0.52	23.18	2025.00	1	695.25	60750.00	302.88	30
2050	19	45	45	292.2	0.52	23.18	2025.00	1	718.43	62775.00	301.99	31
2051	19	45	45	292.2	0.52	23.18	2025.00	1	741.60	64800.00	301.09	32
2052	19	45	45	292.2	0.52	23.18	2025.00	1	764.78	66825.00	300.20	33
2053	19	45	45	292.2	0.52	23.18	2025.00	1	787.95	68850.00	299.32	34
2054	19	45	45	292.2	0.52	23.18	2025.00	1	811.13	70875.00	298.43	35
2055	19	45	45	292.2	0.52	23.18	2025.00	1	834.30	72900.00	297.55	36
2056	19	45	45	292.2	0.52	23.18	2025.00	1	857.48	74925.00	296.67	37
2057	19	45	45	292.2	0.52	23.18	2025.00	1	880.65	76950.00	295.80	38
2058	19	45	45	292.2	0.52	23.18	2025.00	1	903.83	78975.00	294.92	39
2059	19	45	45	292.2	0.52	23.18	2025.00	1	927.00	81000.00	294.05	40
2060	19	45	45	292.2	0.52	23.18	2025.00	1	950.18	83025.00	293.18	41
2061	19	45	45	292.2	0.52	23.18	2025.00	1	973.35	85050.00	292.32	42
2062	19	45	45	292.2	0.52	23.18	2025.00	1	996.53	87075.00	291.45	43
2063	19	45	45	292.2	0.52	23.18	2025.00	1	1019.70	89100.00	290.59	44
2064	19	45	45	292.2	0.52	23.18	2025.00	1	1042.88	91125.00	289.73	45
2065	19	45	45	292.2	0.52	23.18	2025.00	1	1066.05	93150.00	288.88	46
2066	19	45	45	292.2	0.52	23.18	2025.00	1	1089.23	95175.00	288.02	47
2067	19	45	45	292.2	0.52	23.18	2025.00	1	1112.40	97200.00	287.17	48
2068	19	45	45	292.2	0.52	23.18	2025.00	1	1135.58	99225.00	286.32	49
2069	19	45	45	292.2	0.52	23.18	2025.00	1	1158.75	101250.00	285.48	50
2070	19	45	45	292.2	0.52	23.18	2025.00	1	1181.93	103275.00	284.63	51
2071	19	45	45	292.2	0.52	23.18	2025.00	1	1205.10	105300.00	283.79	52
2072	19	45	45	292.2	0.52	23.18	2025.00	1	1228.28	107325.00	282.95	53
2073	19	45	45	292.2	0.52	23.18	2025.00	1	1251.45	109350.00	282.12	54
2074	19	45	45	292.2	0.52	23.18	2025.00	1	1274.63	111375.00	281.28	55

Table 8-17: Cumulative degradation data (Scenario 7)

8.8.8. Scenario 8 (a, b, c) Each environmental parameter individually increased by 15%

Year	Temp (℃)	RH(%)	Lux(lx)	Temp (K)	(0.1T-28.7)	[(0.1T-28.7)RH]Δt	(v × RH)Δt	Δt	S1	S2	331.00	0
2020	20.7	65.20	55.00	293.9	0.68	44.66	3586.00	1	44.66	3586.00	329.23	1
2021	20.7	65.20	55.00	293.9	0.68	44.66	3586.00	1	89.32	7172.00	327.48	2
2022	20.7	65.20	55.00	293.9	0.68	44.66	3586.00	1	133.99	10758.00	325.73	3
2023	20.7	65.20	55.00	293.9	0.68	44.66	3586.00	1	178.65	14344.00	323.99	4
2024	20.7	65.20	55.00	293.9	0.68	44.66	3586.00	1	223.31	17930.00	322.26	5
2025	20.7	65.20	55.00	293.9	0.68	44.66	3586.00	1	267.97	21516.00	320.54	6
2026	20.7	65.20	55.00	293.9	0.68	44.66	3586.00	1	312.63	25102.00	318.83	7
2027	20.7	65.20	55.00	293.9	0.68	44.66	3586.00	1	357.30	28688.00	317.13	8
2028	20.7	65.20	55.00	293.9	0.68	44.66	3586.00	1	401.96	32274.00	315.44	9
2029	20.7	65.20	55.00	293.9	0.68	44.66	3586.00	1	446.62	35860.00	313.76	10
2030	20.7	65.20	55.00	293.9	0.68	44.66	3586.00	1	491.28	39446.00	312.08	11
2031	20.7	65.20	55.00	293.9	0.68	44.66	3586.00	1	535.94	43032.00	310.42	12
2032	20.7	65.20	55.00	293.9	0.68	44.66	3586.00	1	580.61	46618.00	308.76	13
2033	20.7	65.20	55.00	293.9	0.68	44.66	3586.00	1	625.27	50204.00	307.11	14
2034	20.7	65.20	55.00	293.9	0.68	44.66	3586.00	1	669.93	53790.00	305.48	15
2035	20.7	65.20	55.00	293.9	0.68	44.66	3586.00	1	714.59	57376.00	303.85	16
2036	20.7	65.20	55.00	293.9	0.68	44.66	3586.00	1	759.25	60962.00	302.23	17
2037	20.7	65.20	55.00	293.9	0.68	44.66	3586.00	1	803.92	64548.00	300.61	18
2038	20.7	65.20	55.00	293.9	0.68	44.66	3586.00	1	848.58	68134.00	299.01	19
2039	20.7	65.20	55.00	293.9	0.68	44.66	3586.00	1	893.24	71720.00	297.41	20
2040	20.7	65.20	55.00	293.9	0.68	44.66	3586.00	1	937.90	75306.00	295.83	21
2041	20.7	65.20	55.00	293.9	0.68	44.66	3586.00	1	982.56	78892.00	294.25	22
2042	20.7	65.20	55.00	293.9	0.68	44.66	3586.00	1	1027.23	82478.00	292.68	23
2043	20.7	65.20	55.00	293.9	0.68	44.66	3586.00	1	1071.89	86064.00	291.12	24
2044	20.7	65.20	55.00	293.9	0.68	44.66	3586.00	1	1116.55	89650.00	289.56	25
2045	20.7	65.20	55.00	293.9	0.68	44.66	3586.00	1	1161.21	93236.00	288.02	26
2046	20.7	65.20	55.00	293.9	0.68	44.66	3586.00	1	1205.87	96822.00	286.48	27
2047	20.7	65.20	55.00	293.9	0.68	44.66	3586.00	1	1250.54	100408.00	284.95	28
2048	20.7	65.20	55.00	293.9	0.68	44.66	3586.00	1	1295.20	103994.00	283.43	29
2049	20.7	65.20	55.00	293.9	0.68	44.66	3586.00	1	1339.86	107580.00	281.92	30
2050	20.7	65.20	55.00	293.9	0.68	44.66	3586.00	1	1384.52	111166.00	280.42	31

Table 8-18: Cumulative degradation data (15% Raised RH)

Year	Temp (℃)	RH(%)	Lux(lx)	Temp (K)	(0.1T-28.7)	[(0.1T-28.7)RH]Δt	(v × RH)Δt	Δt	S1	S2	331.00	0
2020	23.8	56.70	55.00	297.0	1.00	56.42	3118.50	1	56.42	3118.50	329.29	1
2021	23.8	56.70	55.00	297.0	1.00	56.42	3118.50	1	112.83	6237.00	327.59	2
2022	23.8	56.70	55.00	297.0	1.00	56.42	3118.50	1	169.25	9355.50	325.89	3
2023	23.8	56.70	55.00	297.0	1.00	56.42	3118.50	1	225.67	12474.00	324.21	4
2024	23.8	56.70	55.00	297.0	1.00	56.42	3118.50	1	282.08	15592.50	322.53	5
2025	23.8	56.70	55.00	297.0	1.00	56.42	3118.50	1	338.50	18711.00	320.86	6
2026	23.8	56.70	55.00	297.0	1.00	56.42	3118.50	1	394.92	21829.50	319.21	7
2027	23.8	56.70	55.00	297.0	1.00	56.42	3118.50	1	451.33	24948.00	317.56	8
2028	23.8	56.70	55.00	297.0	1.00	56.42	3118.50	1	507.75	28066.50	315.91	9
2029	23.8	56.70	55.00	297.0	1.00	56.42	3118.50	1	564.17	31185.00	314.28	10
2030	23.8	56.70	55.00	297.0	1.00	56.42	3118.50	1	620.58	34303.50	312.66	11
2031	23.8	56.70	55.00	297.0	1.00	56.42	3118.50	1	677.00	37422.00	311.04	12
2032	23.8	56.70	55.00	297.0	1.00	56.42	3118.50	1	733.41	40540.50	309.43	13
2033	23.8	56.70	55.00	297.0	1.00	56.42	3118.50	1	789.83	43659.00	307.83	14
2034	23.8	56.70	55.00	297.0	1.00	56.42	3118.50	1	846.25	46777.50	306.24	15
2035	23.8	56.70	55.00	297.0	1.00	56.42	3118.50	1	902.66	49896.00	304.66	16
2036	23.8	56.70	55.00	297.0	1.00	56.42	3118.50	1	959.08	53014.50	303.08	17
2037	23.8	56.70	55.00	297.0	1.00	56.42	3118.50	1	1015.50	56133.00	301.51	18
2038	23.8	56.70	55.00	297.0	1.00	56.42	3118.50	1	1071.91	59251.50	299.96	19
2039	23.8	56.70	55.00	297.0	1.00	56.42	3118.50	1	1128.33	62370.00	298.40	20
2040	23.8	56.70	55.00	297.0	1.00	56.42	3118.50	1	1184.75	65488.50	296.86	21
2041	23.8	56.70	55.00	297.0	1.00	56.42	3118.50	1	1241.16	68607.00	295.33	22
2042	23.8	56.70	55.00	297.0	1.00	56.42	3118.50	1	1297.58	71725.50	293.80	23
2043	23.8	56.70	55.00	297.0	1.00	56.42	3118.50	1	1354.00	74844.00	292.28	24
2044	23.8	56.70	55.00	297.0	1.00	56.42	3118.50	1	1410.41	77962.50	290.77	25
2045	23.8	56.70	55.00	297.0	1.00	56.42	3118.50	1	1466.83	81081.00	289.27	26
2046	23.8	56.70	55.00	297.0	1.00	56.42	3118.50	1	1523.25	84199.50	287.77	27
2047	23.8	56.70	55.00	297.0	1.00	56.42	3118.50	1	1579.66	87318.00	286.28	28
2048	23.8	56.70	55.00	297.0	1.00	56.42	3118.50	1	1636.08	90436.50	284.80	29
2049	23.8	56.70	55.00	297.0	1.00	56.42	3118.50	1	1692.50	93555.00	283.33	30
2050	23.8	56.70	55.00	297.0	1.00	56.42	3118.50	1	1748.91	96673.50	281.87	31
2051	23.8	56.70	55.00	297.0	1.00	56.42	3118.50	1	1805.33	99792.00	280.41	32

Table 8-19: Cumulative degradation data (15% Raised Temperature)

Year	Temp (℃)	RH(%)	Lux(lx)	Temp (K)	(0.1T-28.7)	[(0.1T-28.7)RH]Δt	(v × RH)Δt	Δt	S1	S2	331.00	0
2020	20.7	56.70	63.25	293.9	0.68	38.84	3586.28	1	38.84	3586.28	329.29	1
2021	20.7	56.70	63.25	293.9	0.68	38.84	3586.28	1	77.68	7172.55	327.59	2
2022	20.7	56.70	63.25	293.9	0.68	38.84	3586.28	1	116.52	10758.83	325.90	3
2023	20.7	56.70	63.25	293.9	0.68	38.84	3586.28	1	155.36	14345.10	324.22	4
2024	20.7	56.70	63.25	293.9	0.68	38.84	3586.28	1	194.20	17931.38	322.55	5
2025	20.7	56.70	63.25	293.9	0.68	38.84	3586.28	1	233.04	21517.65	320.88	6
2026	20.7	56.70	63.25	293.9	0.68	38.84	3586.28	1	271.88	25103.93	319.23	7
2027	20.7	56.70	63.25	293.9	0.68	38.84	3586.28	1	310.72	28690.20	317.58	8
2028	20.7	56.70	63.25	293.9	0.68	38.84	3586.28	1	349.56	32276.48	315.94	9
2029	20.7	56.70	63.25	293.9	0.68	38.84	3586.28	1	388.39	35862.75	314.31	10
2030	20.7	56.70	63.25	293.9	0.68	38.84	3586.28	1	427.23	39449.03	312.69	11
2031	20.7	56.70	63.25	293.9	0.68	38.84	3586.28	1	466.07	43035.30	311.07	12
2032	20.7	56.70	63.25	293.9	0.68	38.84	3586.28	1	504.91	46621.58	309.47	13
2033	20.7	56.70	63.25	293.9	0.68	38.84	3586.28	1	543.75	50207.85	307.87	14
2034	20.7	56.70	63.25	293.9	0.68	38.84	3586.28	1	582.59	53794.13	306.28	15
2035	20.7	56.70	63.25	293.9	0.68	38.84	3586.28	1	621.43	57380.40	304.70	16
2036	20.7	56.70	63.25	293.9	0.68	38.84	3586.28	1	660.27	60966.68	303.13	17
2037	20.7	56.70	63.25	293.9	0.68	38.84	3586.28	1	699.11	64552.95	301.56	18
2038	20.7	56.70	63.25	293.9	0.68	38.84	3586.28	1	737.95	68139.23	300.01	19
2039	20.7	56.70	63.25	293.9	0.68	38.84	3586.28	1	776.79	71725.50	298.46	20
2040	20.7	56.70	63.25	293.9	0.68	38.84	3586.28	1	815.63	75311.78	296.92	21
2041	20.7	56.70	63.25	293.9	0.68	38.84	3586.28	1	854.47	78898.05	295.39	22
2042	20.7	56.70	63.25	293.9	0.68	38.84	3586.28	1	893.31	82484.33	293.86	23
2043	20.7	56.70	63.25	293.9	0.68	38.84	3586.28	1	932.15	86070.60	292.35	24
2044	20.7	56.70	63.25	293.9	0.68	38.84	3586.28	1	970.99	89656.88	290.84	25
2045	20.7	56.70	63.25	293.9	0.68	38.84	3586.28	1	1009.83	93243.15	289.34	26
2046	20.7	56.70	63.25	293.9	0.68	38.84	3586.28	1	1048.67	96829.43	287.84	27
2047	20.7	56.70	63.25	293.9	0.68	38.84	3586.28	1	1087.51	100415.70	286.36	28
2048	20.7	56.70	63.25	293.9	0.68	38.84	3586.28	1	1126.35	104001.98	284.88	29
2049	20.7	56.70	63.25	293.9	0.68	38.84	3586.28	1	1165.19	107588.25	283.41	30
2050	20.7	56.70	63.25	293.9	0.68	38.84	3586.28	1	1204.02	111174.53	281.95	31
2051	20.7	56.70	63.25	293.9	0.68	38.84	3586.28	1	1242.86	114760.80	280.49	32

Table 8-20: Cumulative degradation data (15% Raised Lux)

8.8.9. Scenario 9 Alternating Annual Environmental Conditions

Year	Temp (℃)	RH(%)	Lux(lx)	Temp (K)	(0.1T-28.7)	[(0.1T-28.7)RH]Δt	(v × RH)Δt	Δt	S1	S2	331.00	0
2020	20.7	56.7	55	293.9	0.68	38.84	3118.50	1	38.84	3118.50	329.46	1
2021	16	50	5	289.2	0.22	10.75	250.00	1	49.59	3368.50	329.26	2
2022	20.7	56.7	55	293.9	0.68	38.84	3118.50	1	88.43	6487.00	327.74	3
2023	16	50	5	289.2	0.22	10.75	250.00	1	99.18	6737.00	327.54	4
2024	20.7	56.7	55	293.9	0.68	38.84	3118.50	1	138.02	9855.50	326.02	5
2025	16	50	5	289.2	0.22	10.75	250.00	1	148.77	10105.50	325.82	6
2026	20.7	56.7	55	293.9	0.68	38.84	3118.50	1	187.61	13224.00	324.31	7
2027	16	50	5	289.2	0.22	10.75	250.00	1	198.36	13474.00	324.11	8
2028	20.7	56.7	55	293.9	0.68	38.84	3118.50	1	237.20	16592.50	322.61	9
2029	16	50	5	289.2	0.22	10.75	250.00	1	247.95	16842.50	322.41	10
2030	20.7	56.7	55	293.9	0.68	38.84	3118.50	1	286.79	19961.00	320.92	11
2031	16	50	5	289.2	0.22	10.75	250.00	1	297.54	20211.00	320.72	12
2032	20.7	56.7	55	293.9	0.68	38.84	3118.50	1	336.38	23329.50	319.24	13
2033	16	50	5	289.2	0.22	10.75	250.00	1	347.13	23579.50	319.04	14
2034	20.7	56.7	55	293.9	0.68	38.84	3118.50	1	385.97	26698.00	317.56	15
2035	16	50	5	289.2	0.22	10.75	250.00	1	396.72	26948.00	317.37	16
2036	20.7	56.7	55	293.9	0.68	38.84	3118.50	1	435.56	30066.50	315.90	17
2037	16	50	5	289.2	0.22	10.75	250.00	1	446.31	30316.50	315.71	18
2038	20.7	56.7	55	293.9	0.68	38.84	3118.50	1	485.14	33435.00	314.24	19
2039	16	50	5	289.2	0.22	10.75	250.00	1	495.89	33685.00	314.05	20
2040	20.7	56.7	55	293.9	0.68	38.84	3118.50	1	534.73	36803.50	312.59	21
2041	16	50	5	289.2	0.22	10.75	250.00	1	545.48	37053.50	312.41	22
2042	20.7	56.7	55	293.9	0.68	38.84	3118.50	1	584.32	40172.00	310.96	23
2043	16	50	5	289.2	0.22	10.75	250.00	1	595.07	40422.00	310.77	24
2044	20.7	56.7	55	293.9	0.68	38.84	3118.50	1	633.91	43540.50	309.33	25
2045	16	50	5	289.2	0.22	10.75	250.00	1	644.66	43790.50	309.14	26
2046	20.7	56.7	55	293.9	0.68	38.84	3118.50	1	683.50	46909.00	307.70	27
2047	16	50	5	289.2	0.22	10.75	250.00	1	694.25	47159.00	307.52	28
2048	20.7	56.7	55	293.9	0.68	38.84	3118.50	1	733.09	50277.50	306.09	29
2049	16	50	5	289.2	0.22	10.75	250.00	1	743.84	50527.50	305.91	30
2050	20.7	56.7	55	293.9	0.68	38.84	3118.50	1	782.68	53646.00	304.49	31
2051	16	50	5	289.2	0.22	10.75	250.00	1	793.43	53896.00	304.30	32
2052	20.7	56.7	55	293.9	0.68	38.84	3118.50	1	832.27	57014.50	302.89	33
2053	16	50	5	289.2	0.22	10.75	250.00	1	843.02	57264.50	302.71	34
2054	20.7	56.7	55	293.9	0.68	38.84	3118.50	1	881.86	60383.00	301.30	35
2055	16	50	5	289.2	0.22	10.75	250.00	1	892.61	60633.00	301.12	36
2056	20.7	56.7	55	293.9	0.68	38.84	3118.50	1	931.45	63751.50	299.72	37
2057	16	50	5	289.2	0.22	10.75	250.00	1	942.20	64001.50	299.54	38
2058	20.7	56.7	55	293.9	0.68	38.84	3118.50	1	981.04	67120.00	298.15	39
2059	16	50	5	289.2	0.22	10.75	250.00	1	991.79	67370.00	297.97	40
2060	20.7	56.7	55	293.9	0.68	38.84	3118.50	1	1030.63	70488.50	296.59	41
2061	16	50	5	289.2	0.22	10.75	250.00	1	1041.38	70738.50	296.41	42
2062	20.7	56.7	55	293.9	0.68	38.84	3118.50	1	1080.22	73857.00	295.03	43
2063	16	50	5	289.2	0.22	10.75	250.00	1	1090.97	74107.00	294.86	44
2064	20.7	56.7	55	293.9	0.68	38.84	3118.50	1	1129.81	77225.50	293.49	45
2065	16	50	5	289.2	0.22	10.75	250.00	1	1140.56	77475.50	293.31	46
2066	20.7	56.7	55	293.9	0.68	38.84	3118.50	1	1179.40	80594.00	291.95	47
2067	16	50	5	289.2	0.22	10.75	250.00	1	1190.15	80844.00	291.77	48
2068	20.7	56.7	55	293.9	0.68	38.84	3118.50	1	1228.99	83962.50	290.42	49
2069	16	50	5	289.2	0.22	10.75	250.00	1	1239.74	84212.50	290.24	50
2070	20.7	56.7	55	293.9	0.68	38.84	3118.50	1	1278.58	87331.00	288.90	51
2071	16	50	5	289.2	0.22	10.75	250.00	1	1289.33	87581.00	288.72	52
2072	20.7	56.7	55	293.9	0.68	38.84	3118.50	1	1328.17	90699.50	287.38	53
2073	16	50	5	289.2	0.22	10.75	250.00	1	1338.92	90949.50	287.21	54
2074	20.7	56.7	55	293.9	0.68	38.84	3118.50	1	1377.76	94068.00	285.87	55
2075	16	50	5	289.2	0.22	10.75	250.00	1	1388.51	94318.00	285.70	56
2076	20.7	56.7	55	293.9	0.68	38.84	3118.50	1	1427.35	97436.50	284.38	57
2077	16	50	5	289.2	0.22	10.75	250.00	1	1438.10	97686.50	284.20	58
2078	20.7	56.7	55	293.9	0.68	38.84	3118.50	1	1476.94	100805.00	282.89	59
2079	16	50	5	289.2	0.22	10.75	250.00	1	1487.69	101055.00	282.71	60
2080	20.7	56.7	55	293.9	0.68	38.84	3118.50	1	1526.52	104173.50	281.40	61

Table 8-21: Cumulative degradation data (Scenario 9)

8.8.10. Scenario 10 Alternating Conditions Every Two Years

Year	Temp (℃)	RH(%)	Lux(lx)	Temp (K)	(0.1T-28.7)	[(0.1T-28.7)RH]Δt	(v × RH)Δt	Δt	S1	S2	331.00	0
2020	16	50	5	289.2	0.22	10.75	250.00	1	10.75	250.00	330.80	1
2021	20.7	56.7	55	293.9	0.68	38.84	3118.50	1	49.59	3368.50	329.26	2
2022	20.7	56.7	55	293.9	0.68	38.84	3118.50	1	88.43	6487.00	327.74	3
2023	16	50	5	289.2	0.22	10.75	250.00	1	99.18	6737.00	327.54	4
2024	20.7	56.7	55	293.9	0.68	38.84	3118.50	1	138.02	9855.50	326.02	5
2025	20.7	56.7	55	293.9	0.68	38.84	3118.50	1	176.86	12974.00	324.51	6
2026	16	50	5	289.2	0.22	10.75	250.00	1	187.61	13224.00	324.31	7
2027	20.7	56.7	55	293.9	0.68	38.84	3118.50	1	226.45	16342.50	322.80	8
2028	20.7	56.7	55	293.9	0.68	38.84	3118.50	1	265.29	19461.00	321.31	9
2029	16	50	5	289.2	0.22	10.75	250.00	1	276.04	19711.00	321.11	10
2030	20.7	56.7	55	293.9	0.68	38.84	3118.50	1	314.88	22829.50	319.62	11
2031	20.7	56.7	55	293.9	0.68	38.84	3118.50	1	353.72	25948.00	318.14	12
2032	16	50	5	289.2	0.22	10.75	250.00	1	364.47	26198.00	317.95	13
2033	20.7	56.7	55	293.9	0.68	38.84	3118.50	1	403.31	29316.50	316.47	14
2034	20.7	56.7	55	293.9	0.68	38.84	3118.50	1	442.14	32435.00	315.00	15
2035	16	50	5	289.2	0.22	10.75	250.00	1	452.89	32685.00	314.81	16
2036	20.7	56.7	55	293.9	0.68	38.84	3118.50	1	491.73	35803.50	313.35	17
2037	20.7	56.7	55	293.9	0.68	38.84	3118.50	1	530.57	38922.00	311.90	18
2038	16	50	5	289.2	0.22	10.75	250.00	1	541.32	39172.00	311.71	19
2039	20.7	56.7	55	293.9	0.68	38.84	3118.50	1	580.16	42290.50	310.26	20
2040	20.7	56.7	55	293.9	0.68	38.84	3118.50	1	619.00	45409.00	308.82	21
2041	16	50	5	289.2	0.22	10.75	250.00	1	629.75	45659.00	308.63	22
2042	20.7	56.7	55	293.9	0.68	38.84	3118.50	1	668.59	48777.50	307.20	23
2043	20.7	56.7	55	293.9	0.68	38.84	3118.50	1	707.43	51896.00	305.78	24
2044	16	50	5	289.2	0.22	10.75	250.00	1	718.18	52146.00	305.59	25
2045	20.7	56.7	55	293.9	0.68	38.84	3118.50	1	757.02	55264.50	304.17	26
2046	20.7	56.7	55	293.9	0.68	38.84	3118.50	1	795.86	58383.00	302.76	27
2047	16	50	5	289.2	0.22	10.75	250.00	1	806.61	58633.00	302.58	28
2048	20.7	56.7	55	293.9	0.68	38.84	3118.50	1	845.45	61751.50	301.17	29
2049	20.7	56.7	55	293.9	0.68	38.84	3118.50	1	884.29	64870.00	299.78	30
2050	16	50	5	289.2	0.22	10.75	250.00	1	895.04	65120.00	299.60	31
2051	20.7	56.7	55	293.9	0.68	38.84	3118.50	1	933.88	68238.50	298.20	32
2052	20.7	56.7	55	293.9	0.68	38.84	3118.50	1	972.72	71357.00	296.82	33
2053	16	50	5	289.2	0.22	10.75	250.00	1	983.47	71607.00	296.64	34
2054	20.7	56.7	55	293.9	0.68	38.84	3118.50	1	1022.31	74725.50	295.26	35
2055	20.7	56.7	55	293.9	0.68	38.84	3118.50	1	1061.15	77844.00	293.89	36
2056	16	50	5	289.2	0.22	10.75	250.00	1	1071.90	78094.00	293.72	37
2057	20.7	56.7	55	293.9	0.68	38.84	3118.50	1	1110.74	81212.50	292.35	38
2058	20.7	56.7	55	293.9	0.68	38.84	3118.50	1	1149.58	84331.00	291.00	39
2059	16	50	5	289.2	0.22	10.75	250.00	1	1160.33	84581.00	290.82	40
2060	20.7	56.7	55	293.9	0.68	38.84	3118.50	1	1199.17	87699.50	289.47	41
2061	20.7	56.7	55	293.9	0.68	38.84	3118.50	1	1238.01	90818.00	288.13	42
2062	16	50	5	289.2	0.22	10.75	250.00	1	1248.76	91068.00	287.95	43
2063	20.7	56.7	55	293.9	0.68	38.84	3118.50	1	1287.60	94186.50	286.62	44
2064	20.7	56.7	55	293.9	0.68	38.84	3118.50	1	1326.44	97305.00	285.29	45
2065	16	50	5	289.2	0.22	10.75	250.00	1	1337.19	97555.00	285.11	46
2066	20.7	56.7	55	293.9	0.68	38.84	3118.50	1	1376.02	100673.50	283.79	47
2067	20.7	56.7	55	293.9	0.68	38.84	3118.50	1	1414.86	103792.00	282.47	48
2068	16	50	5	289.2	0.22	10.75	250.00	1	1425.61	104042.00	282.30	49
2069	20.7	56.7	55	293.9	0.68	38.84	3118.50	1	1464.45	107160.50	280.99	50

Table 8-22: Cumulative degradation data (Alternating Two Years)